PHOTOCATALYTIC C-S BOND FORMATION USING *N*-THIO AND *N*-PERTHIO PHTHALIMIDE DERIVATIVES

Hsin-Ju Huang

A thesis submitted to the Department of Chemistry and Biomolecular Sciences in conformity with the requirements for the degree of Master of Science in Chemistry

University of Ottawa
Ottawa, Ontario, Canada
January 2024

Abstract

A method for unsymmetric disulfide synthesis from carboxylic acids under photoredox conditions has been developed. *N*-Perthiophthalimide derivatives (Harpp reagents) are used as disulfurating reagents in a decarboxylative disulfuration. Though significant sulfide formation was observed when using less sterically-hindered (primary and secondary) Harpp reagents, tertiary Harpp reagents affording corresponding disulfides in good yields. At first glance, the reaction was expected to go through radical substitution directly on the Harpp reagent to obtain the observed disulfide and a phthalimidyl radical that would reoxidize the reduced photocatalyst. However, computational studies suggest a high barrier and endergonic reaction for such a mechanism due to the high energy of the liberated phthalimidyl radical (N-H BDE in phthalimide is predicted to be ~120 kcal/mol). Supported by calculation and experiments, an alternative mechanism was proposed: perthyl radicals generated from single electron reduction of Harpp reagent dimerized to form tetrasulfides, which are known to undergo efficient radical substitution to afford disulfides. Mechanistic studies on previously reported sulfurations using *N*-thiophthalimide derivatives suggested a similar mechanism - specifically that disulfides generated in situ undergo radical substitution to provide the sulfide products. Direct C-H disulfuration using Harpp reagents under a variety of conditions was also investigated, but found to have very limited substrate scope. It would appear that the instability of the disulfurating reagents, be they Harpp reagents or tetrasulfides generated therefrom, under the various oxidative conditions prevented the development of a general approach.

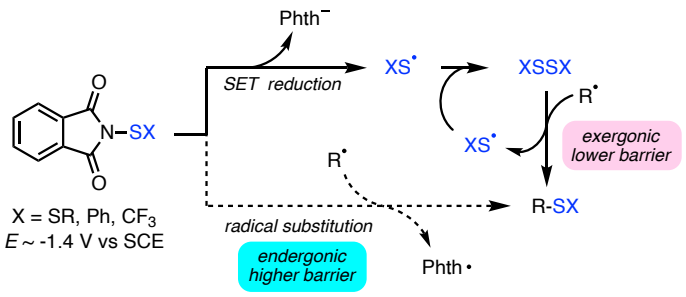
Phth⁻
SET reduction
XS•
XSSX
R•
XS•
exergonic
lower barrier
R•
R-SX
radical substitution
endergonic
higher barrier
Phth•
N–SX
O
O
X = SR, Ph, CF3
E ~ -1.4 V vs SCE

Acknowledgement

First and foremost, I am grateful to my supervisors, Prof. Derek Pratt for his invaluable advice, continuous support, and patience during my PhD study. With his immense knowledge and plentiful experience, he guided me along the way to logically solve the mechanism puzzle. I thank him for always easy to reach out whenever I was stuck in the research or filled with piles of questions about chemistry.

I would also like to express my deepest appreciation to Dr. Zijun Wu for his guidance and help along the way. Discussion about organic synthesis with him always inspired me and excited me.

I would like to thank all the members in the Pratt's group. It is their kind help and mentally support that made my study a lot easier and full of joy. Special thanks to Dr. Luke Farmer for his generosity in sharing knowledge especially for CV measurement and computation. I also appreciate Dr. Julian Helberg for his humorous and entertaining talk that lighten up the beginning/the most stressful period of this journey. I am also thankful to Alireza Dehdari, Eda Kilic and Dr. Aditya Upadhyay, the joy we made together always mentally support me.

Lastly, I would like to express my gratitude to my family in Taiwan, including my parents, uncle, aunts and cousins for always support and take care of each other. It provides me the comfort when pursuing the degree. I thank my husband with all my heart for always being so understanding and supportive and accompany me through this agonizing period in the most positive way.

Statement of Originality

I certify that all the work described in this thesis is the original work of the author with the exception of that performed by my co-worker as noted in the statement of contribution. The work in this thesis draws upon a great deal of previously published research. Any published work by others is cited in the references.

Hsin-Ju Huang

Statement of Contribution

The research in this thesis was carried out by the author, with the exception of the calculations shown in Figure 1 and the synthesis of compounds **1e**, **1f** and **1g**, which were carried out by Dr. Zijun Wu.

Table of Contents

List of Schemes

List of Tables

List of Figures

List of Abbreviations

Ac	acetyl
Acr	acridinium
Ar	aryl
BDE	bond dissociation energy
Bn	benzyl
bpy	2,2’-bipyridine
Bu	butyl
Bz	benzoyl
CV	cyclic voltammetry
Cy	cyclohexyl
DABCO	1,4-diazabicyclo[2.2.2]octane
DCE	dichloroethane
DCM	dichloromethane
DDQ	2,3-dichloro-5,6-dicyano-1,4-benzoquinone
DEAD	diethyl azodicarboxylate
DMAP	4-dimethylaminopyridine
DMF	dimethylformamide
dtbbpy	4,4’-di-tert-butyl-2,2’-dipyridyl
Et	ethyl
GC	gas chromatography
HAT	hydrogen atom transfer
Me	methyl
Mes	mesityl
MeCN	acetonitrile
NMR	nuclear magnetic resonance
PC	photocatalyst

Ph	phenyl
ppy	2-phenylpyridine
Pr	propyl
py	pyridine / pyridyl
SCE	saturated calomel electrode
S_N2	substitution nucleophilic bimolecular
SET	single electron transfer
TBADT	tetra-n-butylammonium decatungstate
TBAF	tetra-n-butylammonium fluoride
THF	tetrahydrofuran

1. Introduction

1.1 Unsymmetric disulfides and their synthesis through polar chemistry

The sulfur atom, which is accessible to various oxidation state ranging from –2 to +6, can be present in wide variety of functional groups from low valent thiol, thioether, disulfide, and sulfoxide to high valent sulfone, sulfate and sulfite. In comparison with oxygen, sulfur has a larger atomic size, more diffuse orbitals, and lower electronegativity. Consequently, the versatile characteristics and properties of organosulfur compounds make them ubiquitous in nature and possess broad applications in materials,[1,2] food and agricultural chemistry[3] and pharmaceuticals.[4,5]

In pharmaceutical chemistry particularly, since the first discovery of 'Prontosil' as an antibacterial compound with a sulfonamide group in 1930s, the versatility of sulfur compounds in drugs has been demonstrated in all classes of therapeutic agents ranging from antiviral, antibacterial, antitumoral, antifungal, antiparasitic, anti-glaucoma, etc.[6] Nowadays, sulfur is one of the most frequently found heteroatoms in U.S. Food and Drug Administration (FDA) approved drugs (behind only oxygen and nitrogen). More than 30% of the top 200 small molecule pharmaceuticals by retail sales in 2022 contain functional groups with a sulfur atom,[7] highlighting the importance of this element in drug design.

Among the wide variety of organosulfur functional groups, disulfide, which is well known to be constructed by oxidation of thiols, is an important and versatile category. With its cleavage and reformation properties between thiols under redox conditions, the sulfur-sulfur bond plays an important role in biology, for cell signaling functions as well as contributing to the tertiary and quaternary structures of proteins. Formation of the disulfide bond in proteins is catalyzed by thiol-disulfide oxidoreductases, such as protein disulfide isomerase (PDI). The process involves two

consecutive thiol/disulfide exchange reactions.[8] At first, a nucleophilic protein thiolate attacks the disulfide of the enzyme. The resulting disulfide then undergoes nucleophilic attack by a second protein thiolate. The mechanism is illustrated below using glutathione disulfide (GS-SG) as the oxidant (Scheme 1).

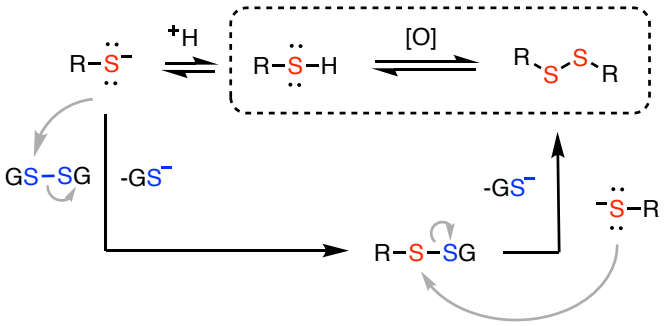

Scheme 1. Mechanism for disulfide formation through oxidation of thiols

The unique reactivity of the disulfide motif also provides some disulfide compounds with specific biological activities including anti-bacterial and anti-viral (Scheme 2).[9] For example, allium species, which contain disulfide and higher (polysulfide) linkages, are inhibitory against microorganisms such as bacteria, fungi, viruses and parasites.[10] Disulfides have also been used in pharmaceutical applications such as anti-cancer or anti-tumor drugs,[5] including 4 of 200 top selling drugs which are cysteine derivatives, for example, Lanreotide has been used to slow or stop tumor growth in patients with neuroendocrine tumors and to treat carcinoid syndrome.[11]

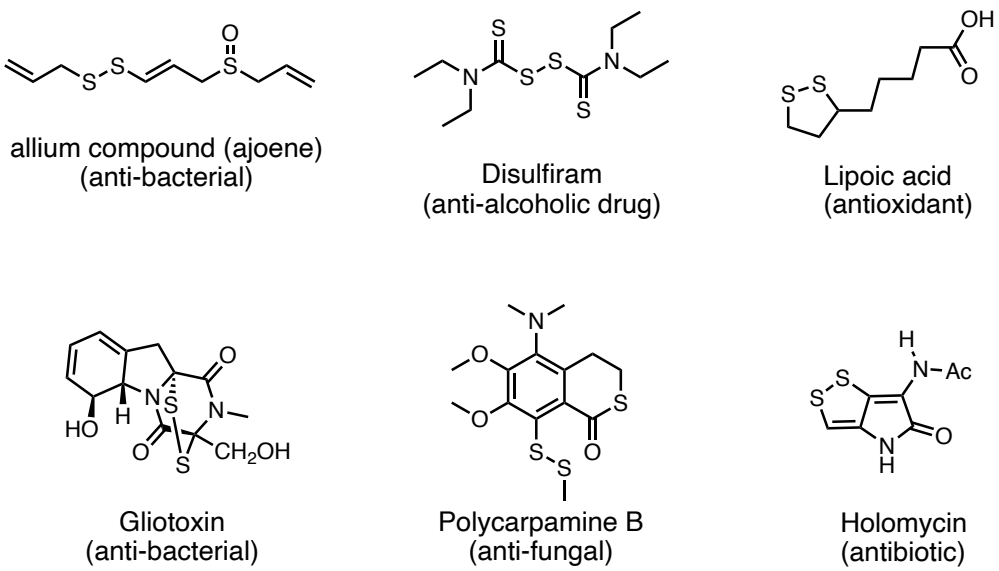

Scheme 2. Representative bio-active disulfides

Given the importance of the disulfide moiety, chemists have long endeavoured to develop efficient ways to construct disulfides. A general method to construct symmetric disulfides is simply through oxidation of thiols. However, unsymmetric disulfides are obviously more of a challenge. The classic methods affording unsymmetrical disulfides involve S_N2 processes, in which a pre-functionalized thiol with a leaving group is utilized as an electrophile to react with a second thiol as the nucleophile.[12] Selective formation of unsymmetric disulfide through oxidative coupling between two different thiols is another typical pathway.[13,14] Directly employing commercially available thiols without pre-functionalization makes this method relatively simple and has high atom economy. Various oxidants have been used for this strategy, such as sodium tellurite,[15] iodine,[16] peroxides,[17] DDQ,[18,19] DEAD,[20] electrode,[21] oxygen,[22] etc. One main type of mechanism starts from the activation of the more reactive thiol through nucleophilic substitution on the oxidant followed by the second substitution from the less reactive thiol (illustrated in Scheme 3 using I_2 as oxidant[16]). Though the high selectivity of the unsymmetric disulfide

formation can be achieved by different reactivity of thiols toward oxidant, symmetric disulfide byproduct by thiol-disulfide exchange is unavoidable.

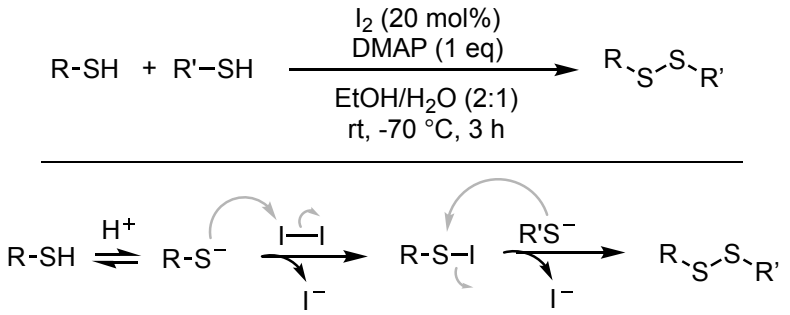

Scheme 3. Unsymmetric disuflide formation via oxidation of thiols.

In recent years, several efficient protocols for the synthesis of unsymmetrical disulfides by S–S bond formation other than oxidative coupling / nucleophilic substitution have been reported. In 2003, the group of Yamaguchi developed an exchange protocol between two distinct symmetrical disulfides with the assistance of a rhodium(I) catalyst. In this reaction, exchange between di(*n*-butyl) disulfide and several symmetrical dialkyl disulfides or diaryl disulfides is rapid, completing within 15 min in refluxing acetone. With a four-fold excess of one symmetrical disulfide the equilibrium is shifted sufficiently to provide the unsymmetrical disulfide in good yield (Scheme 4). Compared with conventional exchange reactions, this reaction takes place rapidly under mild conditions and is applicable to peptide disulfide exchange.[23]

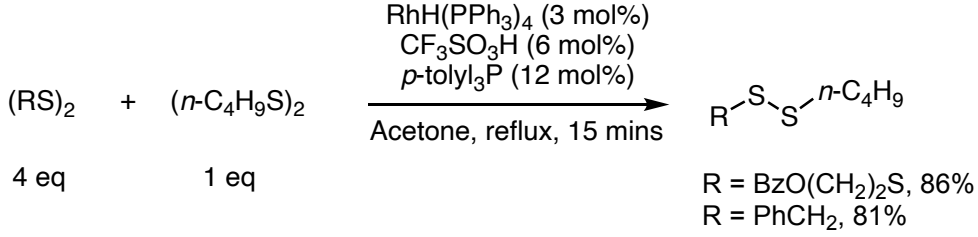

Scheme 4. Representative cases for disulfide exchange reaction under Rh catalysis

Inorganic sulfur salts such as sodium thiosulfate ($Na_2S_2O_3$) have also been utilized as the sulfur source to introduce sulfur moieties on alkyl halides. For example, the group of Pan has developed unsymmetrical disulfide synthesis by Cs_2CO_3 catalyzed coupling reactions of thioacetate, sodium thiosulfate and benzyl halides in water (Scheme 5). Mechanistically, thioacetate is hydrolyzed to generate RS^- in the presence of base and water and then $BnSSO_3Na$ generated from benzyl chloride and $Na_2S_2O_3$ undergoes nucleophilic attack by RS^- to provide the disulfide product.[24]

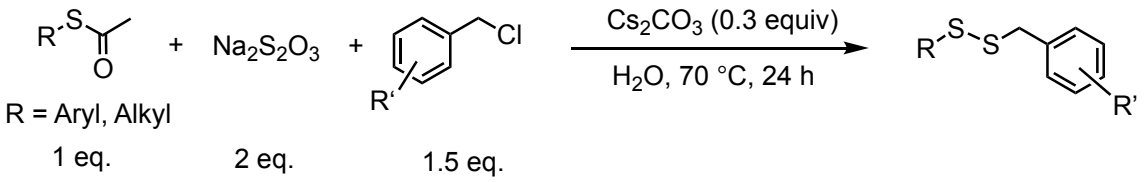

Scheme 5. Cs_2CO_3 catalyzed unsymmetric disulfide formation with acetyl sulfide and sodium thiosulfate.

A novel method developed by the group of Jiang uses comproportionation between two inorganic sulfur salts of different oxidation states on S – sulfinates and thiosulfates – to construct unsymmetric disulfides (Scheme 6). Mechanistically, sulfinates were first dimerized and reduced into sulfonothioate under acidic conditions (due to the sulfur trioxide generation from substitution of the alkyl thiosulfate). The resulting sulfonothioate was then attacked by alkyl thiosulfate generated from alkyl halide and sodium thiosulfate. Neither extra oxidant nor reductant was needed in this transition metal free reaction. Though this reaction can also be applied in the late stage disulfuration of pharmaceuticals and natural products, offering a convenient method for drug

modification, introduction of inorganic sulfur to organic molecules restricts the application in organic synthesis.[25]

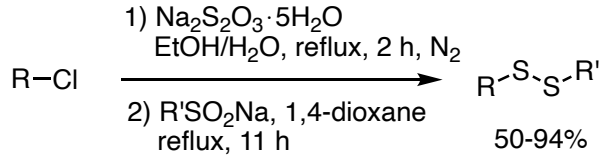

Scheme 6. Unsymmetric disulfide formation from comproportionation between sulfinates and thiosulfates

Due to the unavoidable thiol-disulfide exchange and symmetric disulfide formation in the construction of S–S bonds, recent efforts have focused more on C–S bond formation for unsymmetric disulfide formation. Generally, this type of reaction goes through polar mechanisms by cross-coupling or nucleophilic substitution with electrophilic disulfurating reagent to introduce "RSS" moieties.

The group of Jiang viewed hydropersulfides (RSSH), the key intermediates in the cell killing action of an anticancer nature product,[26] as potential disulfurating reagent. With the concern about the short lifetime of RSSH due to the high sensitivity and activity, easily forming mixture of (poly)sulfides by substitution with themselves, a 'mask' was designed for this disulfurating reagent. In 2016 they disclosed the reactions of acetyl persulfides with boronic acids to construct disulfide under copper-catalyzed oxidative cross-coupling conditions (Scheme 7). This approach can be applied with arylboronic acids bearing various electron withdrawing and donating functional groups or fused rings. Examples of late-stage modification of a pharmaceutical and natural product with this approach were also provided.[27]

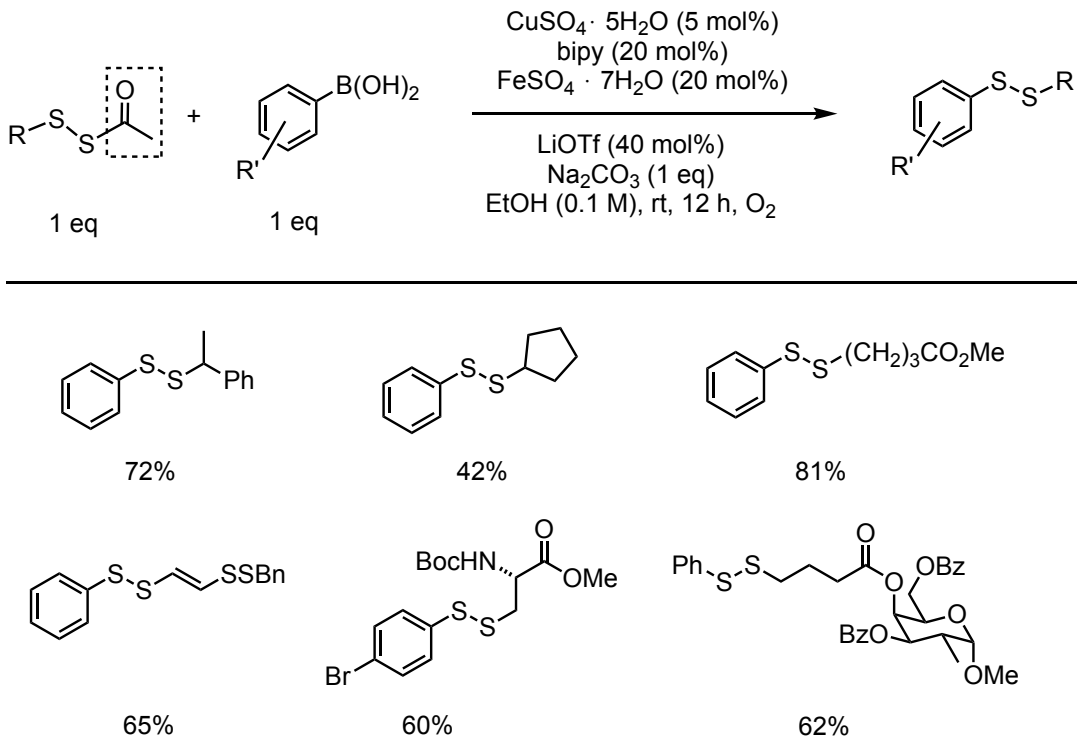

Scheme 7. Unsymmetric disulfide formation from acetyl disulfurating reagent

In 2018, the same group developed another masked disulfurating reagent. While acetyl persulfides yielded nucleophiles in situ (persulfide anion, RSS^-) in the above conditions, by exchanging the acetyl group for a methoxyl group, a persulfide cation equivalent (RSS^+) can be used as an electrophilic disulfurating reagent. To selectively activate the S–O bond over the S–S bond, the hard acid tris(perfluorophenyl)borane was used as a catalyst for coupling between the methoxyl disulfurating reagent and nucleophile. This protocol was applied with a wide variety of nucleophiles from carbon, nitrogen to sulfide resulting in disulfides and trisulfides (Scheme 8).[28]

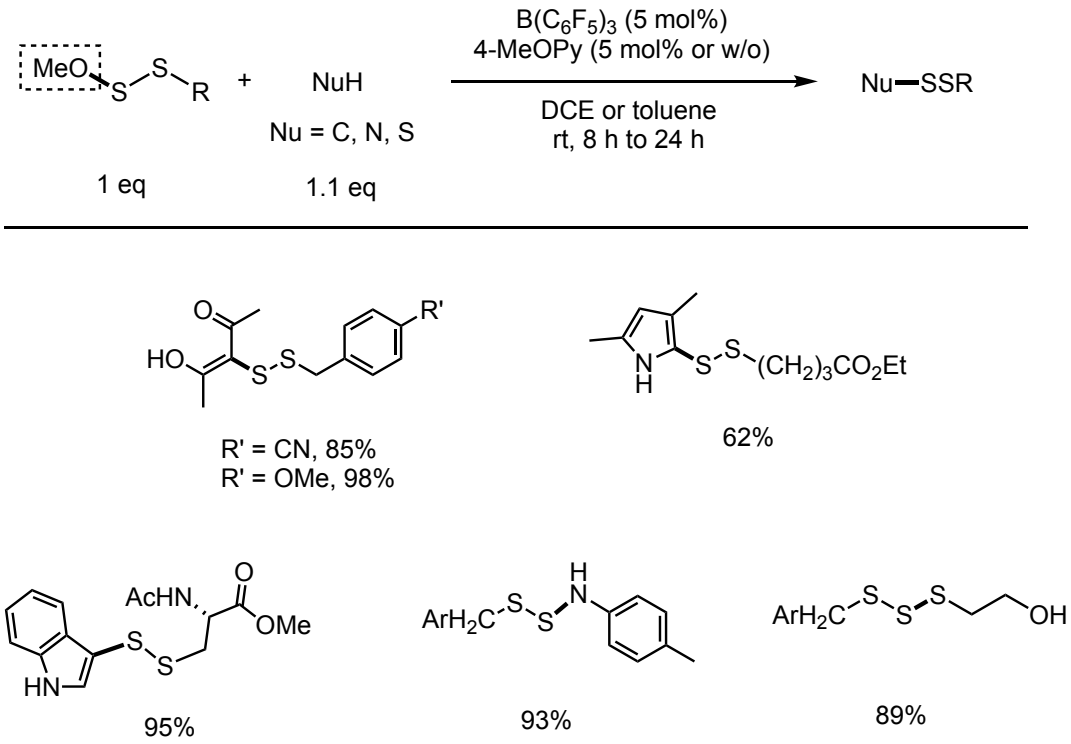

Scheme 8. Unsymmetric disulfide formation from methoxyl disulfurating reagent

The same year, *tert*-butyl 1-(*p*-tolyl) trisulfide-1,1-dioxide was developed as an electrophilic disulfurating reagent by the group of Xu.[29] Under copper-catalyzed conditions, various aryl boronic acids could be transformed into corresponding disulfides (Scheme 9). This electrophilic disulfuration reaction can also be extended to react with nucleophile such as β-keto ester and thiol in presense of DMAP as base.

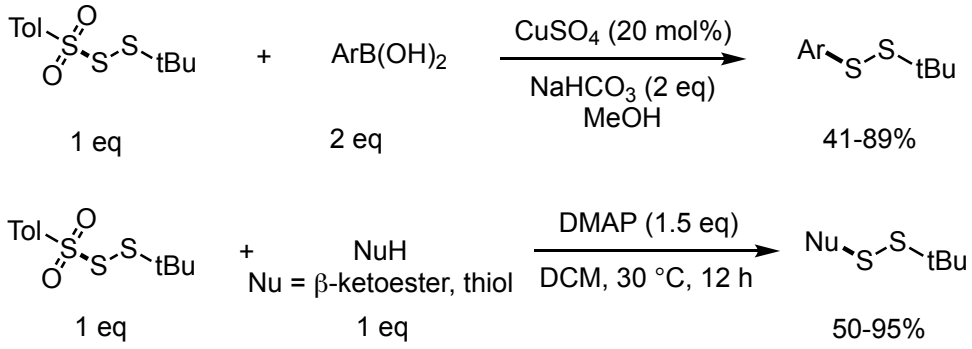

Scheme 9. Unsymmetric disulfide formation by using *SS-tert*-butyl *p*-toluenesulfone as disulfurating reagent

Similarly, Wang[30] and co-workers disclosed a versatile Cu-catalyzed cross-coupling disulfuration reaction from phthalimide-derived disulfurating reagents, *N*-perthiophthalimides (sometimes called Harpp reagents[30–32]) and commercially available boronic acids under mild and practical conditions (Scheme 10A). The authors surmised that weak coordination between oxygen in the Harpp reagent and copper induced the selective oxidative insertion of copper into the N−S bond to enable disulfide formation. This reaction showed excellent compatibility with diversely sensitive functional groups in study of the substrate scope and its robust nature was demonstrated by late-stage modification of natural products and pharmaceuticals. Since this pioneering work using phthalimide derivatives as disulfurating reagents, metal-free disulfuration using this reagent with different nucleophiles have subsequently been developed by Jiang group (β-keto ester as nucleophile, with limited ester variation)[32] and Pan group (indole as nucleophile)[33] (Scheme 10B, C).

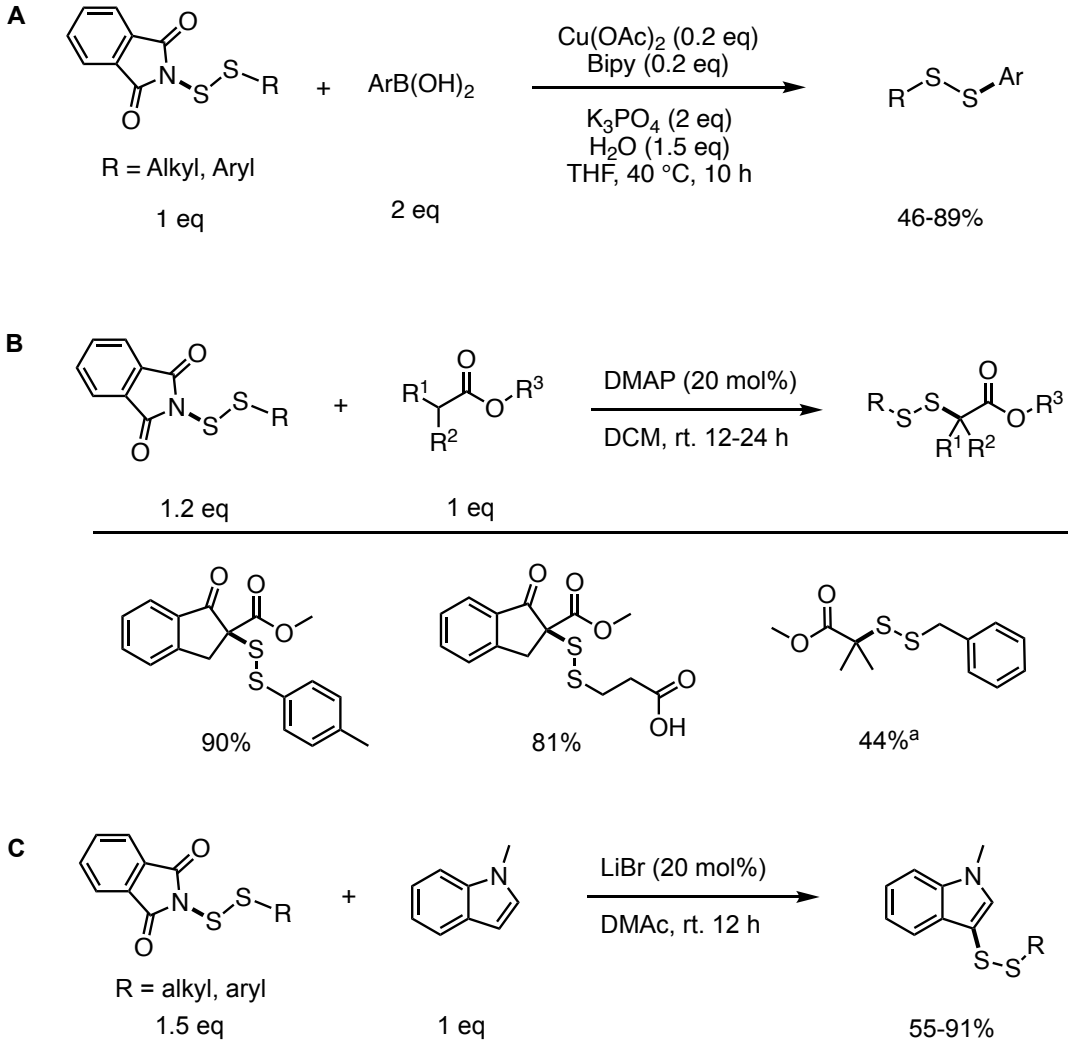

Scheme 10. Phthalimide derivatives as disulfurating reagents

1.2 Unsymmetric disulfide formation through radical pathway

While several 'masked' disulfurating reagents were developed to furnish unsymmetric disulfides, limited nucleophilic reaction partners (mostly aryl boronic acids, heteroatom-centered nucleophiles or 1,3-dicarbonyl substrates) for these strategies restrict their scopes. More recently, our group disclosed that tetrasulfides are excellent disulfurating reagents for unsymmetric disulfide

formation by homolytic substitution of thermally or photochemically generated alkyl and aryl radicals (Scheme 11).[34] In this method, after direct substitution by alkyl or aryl radical on the tetrasulfide, liberated thermodynamically stable perthiyl radicals are able to recombine at near diffusion-controlled rates ($k = 6 \times 10^9$ $M^{-1}s^{-1}$ at 25 °C)[35] to regenerate starting material for further substitution. A radical clock experiment revealed that alkyl radical substitution on tetrasulfides is a rapid reaction with a rate constant of $k_{sub} = 5.8 \times 10^5$ M^{-1} s^{-1}. Attributed to the low energy of the central S–S bond (BDE ~ 36 kcal/mol)[35] in the tetrasulfide, calculations also suggested a low energy barrier of 11.6 kcal/mol and highly exergonic reaction ($\Delta G° = -21.0$ kcal/mol) for the substitution of a model alkyl (ethyl) radical with *t*-BuSSSS*t*-Bu. Primary, secondary, tertiary, as well as aryl and benzyl substituted tetrasulfides provide good to excellent yields of corresponding disulfides.

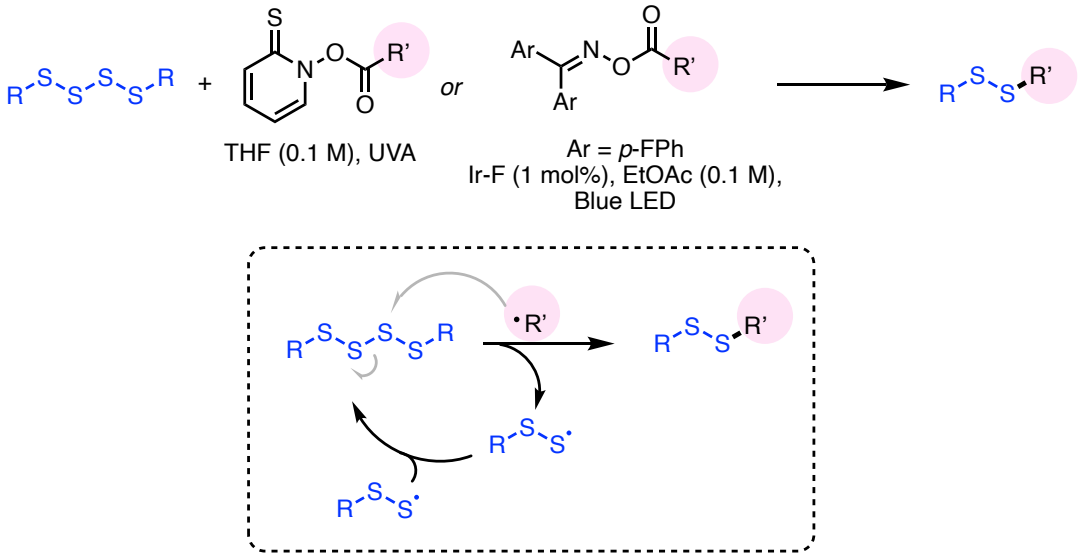

Scheme 11. Unsymmetric disulfide formation by radical substitution with tetrasulfides

In this reaction, pre-functionalization of carboxylic acids to afford Barton esters or acyl oximes as alkyl radical precursors was required. Simple carboxylic acids were not applicable due to the instability of the tetrasulfide under the oxidative conditions for decarboxylation. To address this issue, the following year[36] our group developed trisulfide-1,1-dioxides as an alternative disulfurating reagent to convert carboxylic acids directly into disulfides (Scheme 12). This approach relies on reductive quenching cycle of excited photocatalyst (acridinium salt) to oxidize carboxylic acid to form alkyl radical. Similarly to the tetrasulfide, the generated alkyl radical undergoes homolytic substitution on trisulfide-1,1-dioxide to afford unsymmetric disulfides, meanwhile, the resulting sulfonyl radical are capable of re-oxidized the reduced photocatalyst to complete the catalytic cycle (Scheme 13). A radical clock experiment provided k_{sub} = 6.5 × 10^5 M^{-1} s^{-1} for the reaction of a primary alkyl radical with cumyl substituted trisulfide dioxide.

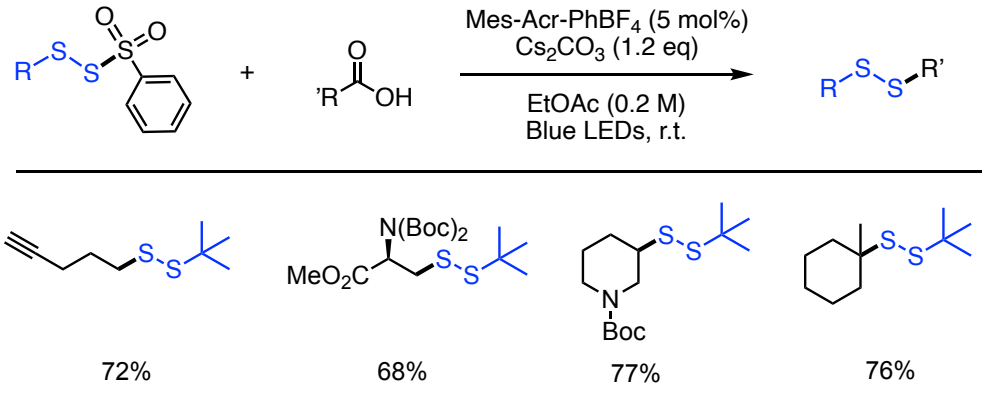

Scheme 12. Unsymmetric disulfide formation using trisulfide-1,1-dioxides as disulfurating reagents

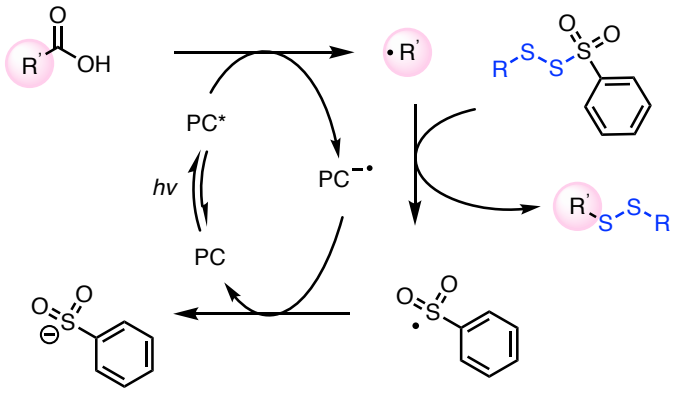

Scheme 13. Mechanism of disulfuration using trisulfide-1,1-dioxide

By applying *N*-allylsulfonamide, this method was further extended into remote site-selective C-H disulfuration. Mechanistically, the liberated sulfonyl radical would add to the terminal alkene of *N*-allylsulfonamide and liberate an amidyl radical that subsequently undergoes 1,5-hydrogen atom transfer to generate an alkyl radical, and by substitution on another trisulfide-1,1-dioxide, introduces a disulfide moiety at the γ-position of the amide (Scheme 14).

It is noteworthy that, unlike tetrasulfides – wherein primary and secondary substituents are applicable to afford disulfide – when primary and secondary trisulfide dioxides are used, substitution to afford sulfide becomes competitive, providing sulfide as predominant product instead of disulfide.

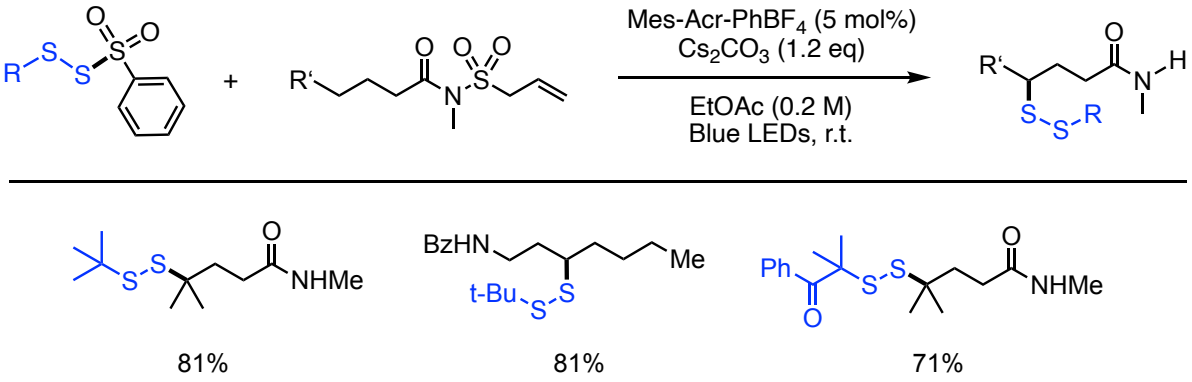

Scheme 14. C-H disulfuration by using trisulfide-1,1-dioxide with *N*-allylsulfonamide

In recent years, photocatalysis has been successfully applied for hydrogen-atom transfer (HAT) mediated radical functionalization of C-H bonds. Among them, decatungstate anion ($[W_{10}O_{32}]^{4-}$), a transition metal oxygen–anion cluster, has been widely used as a powerful photocatalyst for direct HAT.[37] With irradiation, it is capable of hydrogen atom abstraction from unactivated C-H bonds of up to 100 kcal/mol in bond dissociation energy.[38]

In 2022, Studer established the method of using TBADT (tetra-*n*-butylammonium decatungstate, $(n\text{-}Bu_4N)_4[W_{10}O_{32}]$) as photocatalyst for C-H disulfuraion with tetrasulfide.[39] Under their conditions, $Na_2S_2O_8$ is used as stoichiometric oxidant to re-oxidize the photocatalyst to complete the catalytic cycle (Scheme 15).

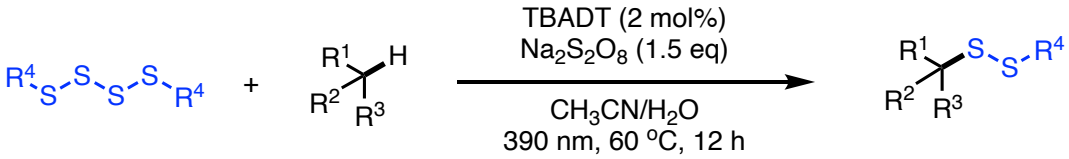

Scheme 15. C-H disulfuration of using TBADT and sodium persulfate with tetrasulfide

1.3 Phthalimide derivatives and the initial hypothesis

While developing trisulfide-1,1-dioxides as disulfurating reagents (Scheme 11), we discovered that this reagent could be easily prepared from *N*-perthiophthalimides (Harpp reagent).[36] In the 1970s, these types of reagents were introduced by David N. Harpp as an alternative (di)sulfur transfer reagent to unstable sulfur monochloride. In their studies, they focused on the reaction between thiol as nucleophile to afford trisulfide (Scheme 16). As mentioned in Section 1.1, not until recently did Wang, Jiang and Pan groups demonstrate the utility of this reagent more generally as a disulfurating reagent to introduce disulfide moiety to carbon center nucleophile. However, to our knowledge there have been no applications or discussion about the radical reactivity of this reagent.

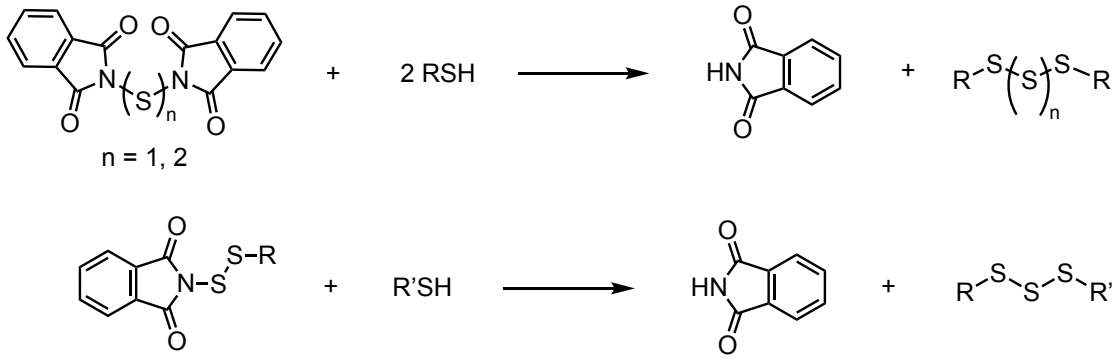

Scheme 16. Phthalimide derivatives as (di)sulfur transfer reagents

In contrast to *N*-perthiophthalimide derivatives, *N*-thiophthalimide derivatives have previously been reported to undergo radical substitution to afford sulfides – particularly trifluoromethylsulfides[40–45] (Scheme 17A-C) and phenylsulfides[46] (Scheme 17D).

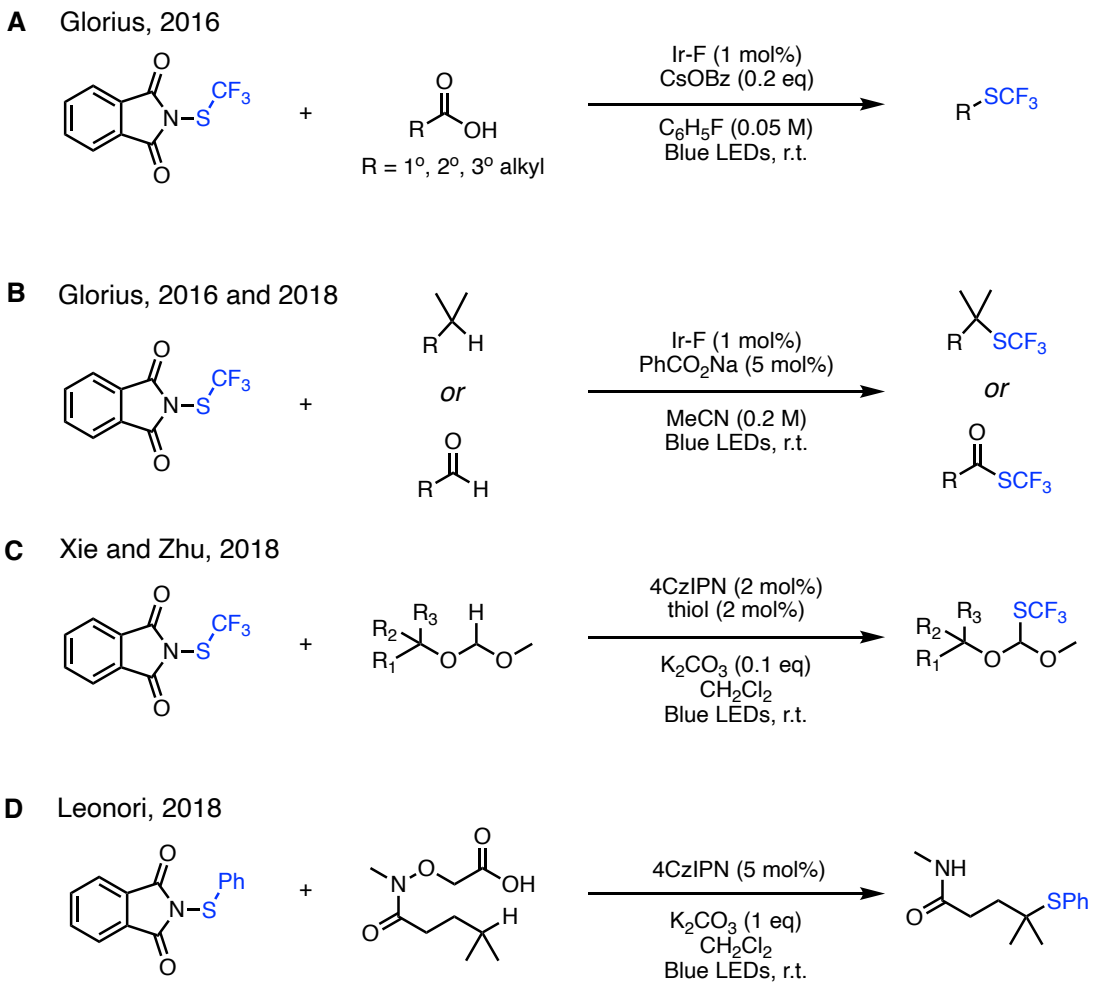

Scheme 17. Previous works using *N*-thiophthalimide derivatives as sulfurating reagents

In general, for these types of reactions, the mechanism shown in Scheme 18 has been proposed wherein the phthalimidyl radical liberated upon substitution was able to re-oxidize the reduced photocatalyst, functioning the same way as the sulfonyl radical formed when the trisulfide-1,1-dioxide is used as disulfurating reagent (Scheme 12). As such, we envisioned that the Harpp reagents could be used directly for disulfuration through the same mechanism, by which we could bypass the step of activating carboxylic acids for use with tetrasulfides or converting the Harpp reagent into trisulfide-1,1-dioxides for use with carboxylic acids directly.

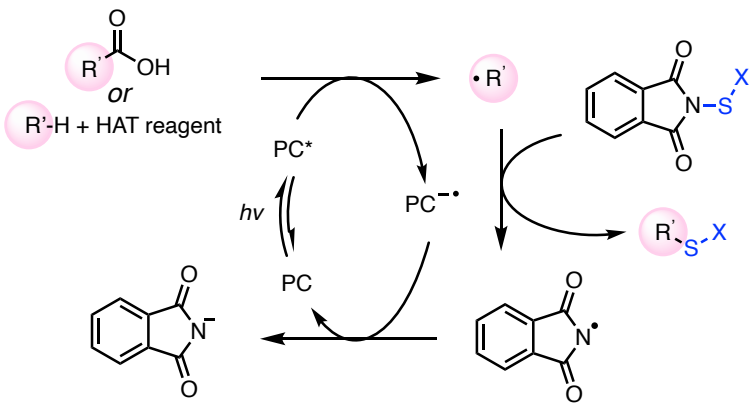

Scheme 18. Proposed mechanism for sulfuration using *N*-thiophthalimide derivatives

2. Results and Discussion

The following research was published in ACS Catalysis in October 2023, under the same title. Reprinted (adapted) with permission from *ACS Catalysis* **2023**, *13*, 21, 13912–13919. Copyright © 2023 American Chemical Society.

2.1 Proof of concept and optimization

In our group's previous research using trisulfide-1,1-dioxides as disulfurating reagents, the strongly oxidizing excited state of an acridinium photocatalyst (Mes-Acr-PhBF$_4$, $E_{1/2}^{red}$ (Mes-Acr-Ph^{+*}/Mes-Acr-Ph^{+}) = +2.15 V vs. SCE)[47] was used to oxidize carboxylates to afford alkyl radicals for substitution. Building on this concept, we envisioned that the alkyl radical generated from the above combination could react with the Harpp reagent directly to form the disulfide product along with the phthalimidyl radical. Oxidation of the reduced acridinium catalyst with phthalimidyl radical via single electron transfer (SET) would regenerate the photocatalyst to complete the catalytic cycle, producing phthalimide as a byproduct. In a preliminary attempt, we followed our

previously optimized conditions, but replaced the disulfurating reagent with the *tert*-butyl Harpp reagent **1a**. We combined Harpp reagent **1a** (1.5 equiv) and carboxylic acid **2a** (1 equiv) in the presence of 5 mol% acridinium photocatalyst (Mes-Acr-PhBF$_4$) and CsF (1 equiv) in ethyl acetate and irradiated the mixture with blue LEDs at room temperature. To our delight, 63% of the corresponding disulfide was isolated. Later, for our own convenience, we switched the excess reagent from the synthesized Harpp reagent **1a** to the commercially available carboxylic acid **2a**. Gratifyingly, the isolated yield of **3a** increased to 72%, though 95% of disulfide product **3a** was observed by ^{1}H NMR (see Section 4.3 for experimental details).

Other changes to the reaction conditions are shown in Table 1. By replacing the Mes-Acr-PhBF$_4$ photocatalyst with the Ir-F complex ([Ir(dF(CF$_3$)ppy)$_2$(dtbbpy)]PF$_6$, $E_{1/2}^{red}$ [Ir(lll)*/Ir(ll)] = +1.21 V vs. SCE)[48], the desired product was obtained in similar yields. However, use of the more common Ru(ll) complex (Ru(bpy)$_3$Cl$_2$) instead, did not provide any product, probably due to the insufficient ability to oxidize a carboxylate ($E_{1/2}^{red}$ [Ru(ll)*/Ru(l)] = +0.77 V vs. SCE, versus $E_{1/2}^{red}$ (hexanoate) = +1.16 V vs. SCE)[48] (entry 3, 4). While carbonates (Cs$_2$CO$_3$ and K$_2$CO$_3$) and TBAF as alternatives to CsF provided good yields, the stronger base *t*-BuOK led to poorer results. NaOAc failed to provide the desired product, probably due to the oxidation of the acetate under the reaction conditions (entry 5 – 9). Though the reaction could be carried out in various solvents, ethyl acetate proved optimal. Control experiments were also performed to confirm the necessity of each component. Inert atmosphere was also crucial for the reaction, as no product was formed without exchanging air with nitrogen as the atmosphere.

Table 1. Reaction optimization of decarboxylative disulfuration.

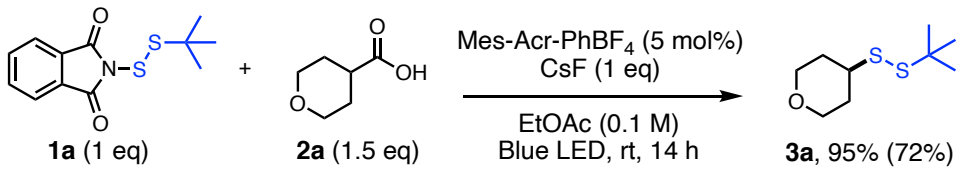

1a (1 eq) + **2a** (1.5 eq) → **3a**, 95% (72%)

Entry	Deviation from above condition	Yield of **3a** [%][b.c]
1	none	95 (72)
2	With Acr-Mes$^+$ ClO_4^- as photocatalyst	59
3	$[Ir(dF(CF_3)ppy)_2(dtbbpy)]PF_6$ (1 mol%) as photocatalyst	91
4	With $Ru(bpy)_3Cl_2$ (1 mol%) as photocatalyst	NP
5	With Cs_2CO_3 as base	74
6	With K_2CO_3 as base	81
7	With *t*BuOK as base	8
8	With NaOAc as base	NP
9	With TBAF as base	86
10	With MeCN as solvent	80
11	With THF as solvent	36
12	With DCE as solvent	85
13	With *t*BuOH as solvent	67
14	With $PhCF_3$ as solvent	37
15	With DMF as solvent	70
16	Without base	< 5
17	Without light	NP
18	Without Acr-Mes$^+$ BF_4^-	NP
19	Without degassing	NP

[a] Reaction conditions: **1a** (0.2 mmol), **2** (0.3 mmol), photocatalyst (5 mol%), base (1 equiv), EtOAc (2 mL), RT, blue LEDs, 14 h. [b] Yields were determined by ^{1}H NMR spectroscopy using mesitylene as internal standard. Isolated yield are given in parentheses. [c] NP = no product.

2.2 Substrate scope of decarboxylative disulfuration

With the optimized condition in hand, we investigated the generality with which the Harpp reagents could be employed for disulfuration (Table 2). The reaction was found to proceed well using each of primary, secondary, and tertiary carboxylic acids. Substrates bearing alkene (**3t**), alkyne (**3k**), bromide (**3n**), and protected amine functionalities (**3c**, **3m**, **3p**) were tolerated, providing corresponding disulfide products in moderate to good yields. Although low conversion was observed for phthalimide protected amines in ethyl acetate, probably due to the poor solubility of the substrate, changing to DMF significantly improved the outcome of the reaction (**3f**, **3g**). Potassium trifluoroborate salts could also be used as substrates, without the need for added base (**3q**, **3r**). Harpp reagents with cumyl, propiophenone, pulegone and dimethyl butanone groups could also be used to obtain the corresponding disulfides (**3s** – **3w**).

Table 2. Substrate scope of decarboxylative disulfuration.

1a (1 eq) + **2** (1.5 eq) → **3**

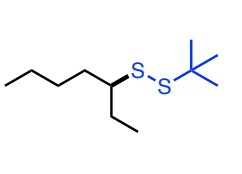

3b, 84%

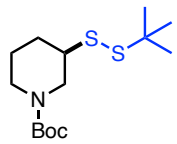

3c, 64%

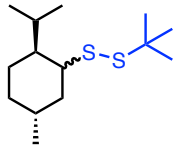

3d, 69%

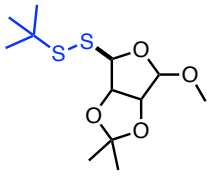

3e, 65%

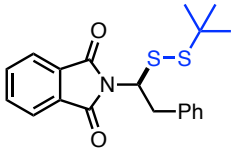

3f, 59%[c]

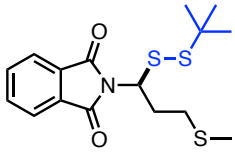

3g, 55%[c]

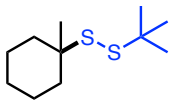

3h, 75%

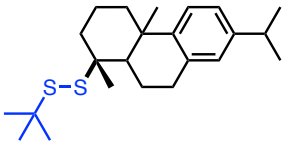

3i, 53%

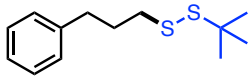

3j, 65%

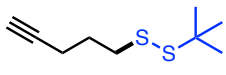

3k, 44%

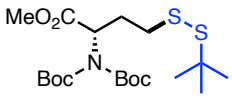

3m, 57%

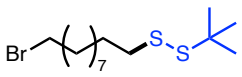

3n, 51%

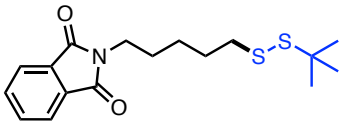

3p, 55%

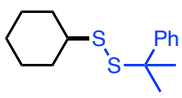

3q, 73%[b]

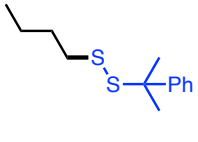

3r, 50%[b]

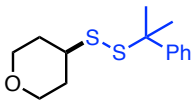

3s, 74%
(1 mmol : 74%)

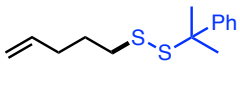

3t, 56%

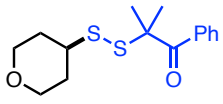

3u, 52%

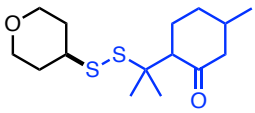

3v, 66%

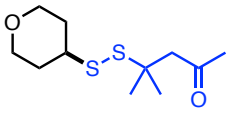

3w, 51%

[a] Reaction conditions : **2** (0.3 mmol), **1a** (0.2 mmol), photocatalyst (5 mol%), base (0.2 mmol), ethyl acetate (2 mL), room temperature, blue LEDs, 14 h. Indicated yields following isolated and

purification. [b] From potassium trifluoroborate salts instead of carboxylic acids, under the same conditions as in [a], but without base. [c] Reaction carried out in DMF.

2.3 Substituent effects on disulfuration

As we expanded our scope investigations to include Harpp reagents with non-tertiary alkyl substitution, we found a significant decrease in the yield of disulfide (Scheme 19). While the *i*-propyl Harpp reagent still provided disulfide product in 56% yield, the *n*-propyl Harpp reagent afforded only a trace amount of disulfide. Meanwhile, the sulfide product was obtained in 26% yield as the predominant product while using the *n*-propyl Harpp reagent.

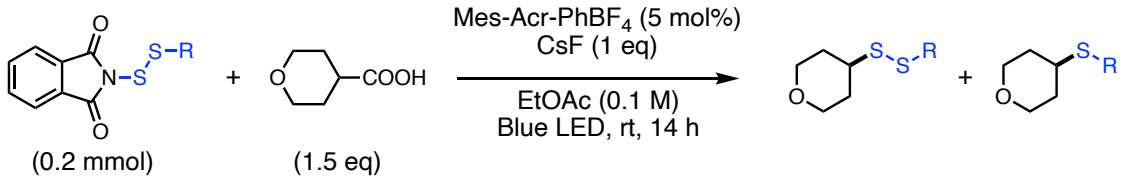

R	Disulfide (%)	Sulfide (%)
t-Bu	72	0
i-Pr	56	trace
n-Pr	trace	26

Scheme 19. Substituent effects on the regioselectivity of decarboxylative disulfuration.

To provide more insight into the regioselectivity of substitution on the Harpp reagent, we computed the barriers and energetics of these reactions using CBS-QB3[49] with methyl radical as a model alkyl radical (Figure 1).[49] The calculations predict a lower energy barrier for substitution on the terminal sulfur atom than the central sulfur atom on the *n*-propyl Harpp reagent (13.6 kcal/mol *vs* 18.5 kcal/mol). This supports the predominant amount of sulfide formation from *n*-

propyl Harpp reagent. The same trend holds true for reactions on the *i*-propyl Harpp reagent (15.4 *vs* 20.1 kcal/mol) and the *t*-butyl Harpp reagent (18.1 *vs* 18.7 kcal/mol). Moreover, in all cases, substitution on the terminal sulfur atom to obtain sulfide was predicted to be an exergonic reaction (from −10.5 to −11.8 kcal/mol), while substitution on the inner sulfur atom to obtained disulfide was predicted to be an endergonic reaction (from +10.7 to +11.8 kcal/mol). These energy differences can be attributed to the instability of the departing phthalimidyl radical (the N-H BDE of phthalimide is predicted to be 120.5 kcal/mol by CBS-QB3) compared to the more stable phthalimide-*N*-thiyl radical (the S-H BDE of N-sulfhydrylphthalimide is predicted to be 79.2 kcal/mol by CBS-QB3). The high energy of the phthalimidyl radical implies that it is a very poor leaving group in homolytic substitution reactions, in general.

With the above results, it is clear that homolytic substitution to yield sulfide over disulfide is both thermodynamically and kinetically preferred. We then concluded that another pathway instead of the direct substitution is responsible for the exclusive disulfide formation from the *tert*-butyl Harpp reagent.

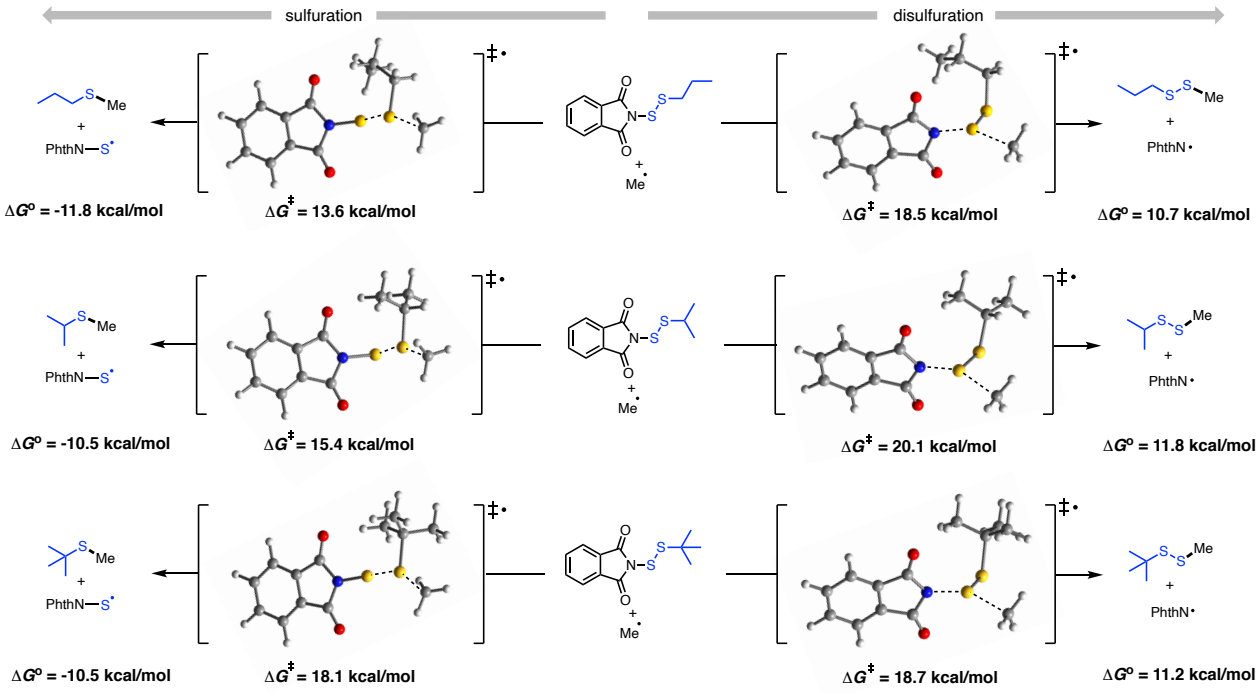

Figure 1. Lowest energy transition state structures and corresponding reaction energetics as determined by CBS-QB3 (at 298 K) for substitution of a model alkyl radical (methyl) on 1°, 2° and 3° Harpp reagents

2.4 Alternative mechanism

Given that the phthalimide anion is a good leaving group (pK_a = 8.3 in water for phthalimide)[31], *N*-thiophthalimide and *N*-perthiophthalimide derivatives have been developed as sulfurating[31, 50] and disulfurating reagents in polar reactions[33, 32] and transition metal catalyzed cross-coupling reactions[30] (as introduced in Section 1.1). With this in mind, we carried out the reaction using 6-heptenoic acid (**2w**) as substrate to confirm that the reaction went through a radical pathway instead of nucleophilic substitution. We obtained **3y**, which derives from the 5-exo cyclization of the initially formed terminal radical, in 66% yield (Scheme 20). Moreover, as we increased the equivalents of the Harpp reagent used to trap the alkyl radical, the ratio of the

cyclized product and the linear product remained the same (**3x** : **3y** ~ 7 : 1). This result further suggests that the Harpp reagent does not trap the generated alkyl radical directly.

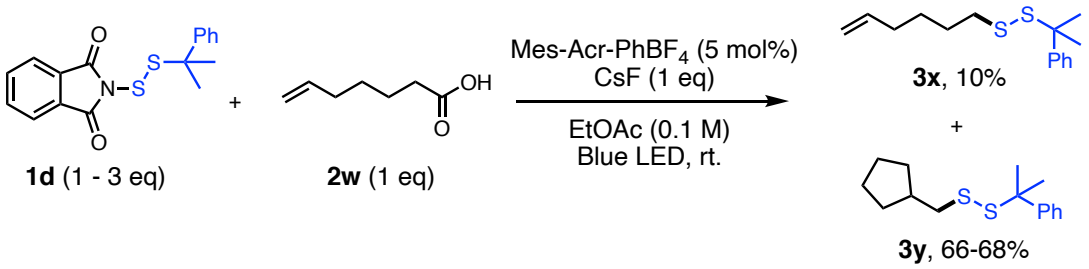

Scheme 20. Attempted radical clock experiment

As we considered other reasonable mechanisms for this disulfuration, methodologies utilizing *N*-(acyloxy)phthalimides (NHP) ester[51,52] as radical precursors provided us some insight into an alternative reactivity of phthalimide derivatives (Scheme 21). As a redox-active ester, NHP ester is predisposed to accept an electron and undergo fragmentation to yield the phthalimide anion and the corresponding radical for further transformation.

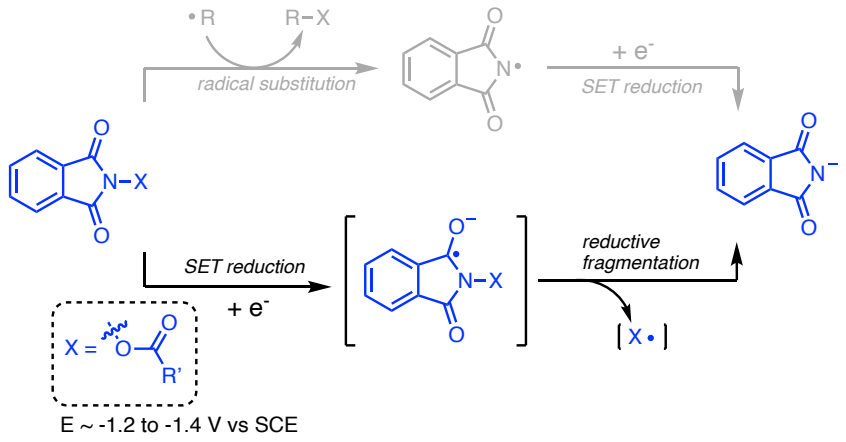

Scheme 21. Alternative mechanism inspired by alkyl radical generation from an NHP ester.

Given that the reduction potential of the Harpp reagent (*tert*-butyl Harpp reagent, E_{pc} = −1.36 V vs. SCE) is close to that of NHP ester (E_{pc} = −1.28 to −1.39 V vs. SCE in MeCN),[53] we surmised that the reduction followed by fragmentation might be involved in our disulfuration. The perthiyl radical, which would form upon fragmentation, would be expected to dimerize into tetrasulfide ($k = 6 \times 10^9$ $M^{-1}s^{-1}$),[35] which our group has shown to be an excellent disulfurating reagent (see section 1.2). This would account for the irreversible voltammagram we obtained in our electrochemical studies of Harpp reagents (see Section 4.8 for experimental detail).

The alternative mechanism is depicted in Scheme 22. It is noteworthy that although the acridine radical ($E^{red}_{1/2}$ = –0.59 V vs. SCE)[54] formed following oxidation of the substrate cannot reduce the Harpp reagent, it can be further excited to become a more potent reductant (Mes-Acr-$PhBF_4$, E^*_{ox} = –3.36 V vs. SCE).[47]

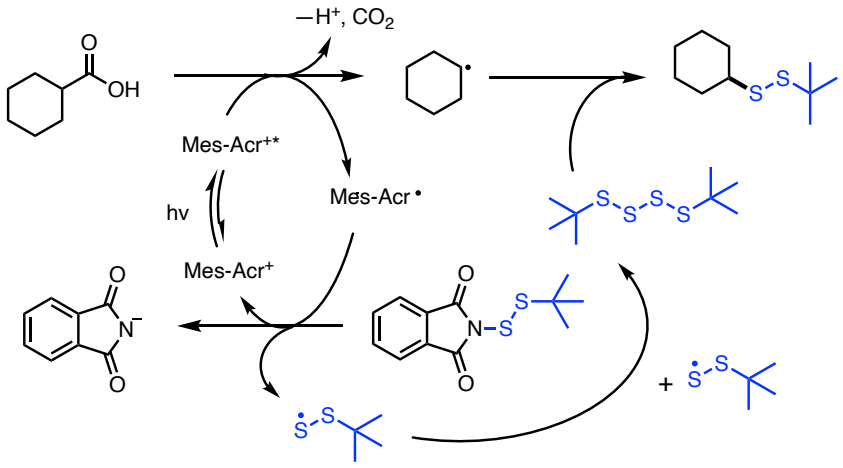

Scheme 22. Alternative mechanism for decarboxylative disulfuration.

This alternative mechanism, rather than direct radical substitution on the Harpp reagent, was further supported experimentally by our observations for reactions carried out with alkyl

radical precursors generated under non-redox conditions (Scheme 23). Undecyl radicals generated from thermolysis of lauroyl peroxide at 80°C yielded no disulfide in the presence of either *n*-propyl or tert-butyl Harpp reagents. Instead, 21% of sulfide was formed in the presence of the *n*-propyl Harpp reagent, but only trace sulfide was detected in the presence of the tert-butyl Harpp reagent, consistent with the higher calculated activation energy (13.6 kcal/mol *vs.* 18.1 kcal/mol) for sulfide formation. In sharp contrast, replacing Harpp reagents with tetrasulfide or trisulfide-1,1-dioxide, both of which were previously reported as excellent disulfurating reagents with alkyl radical via direct substitution, provided corresponding disulfides in good yield (81% and 62% for the tetrasulfide and trisulfide-1,1-dioxides respectively). This was consistent with relatively low energy barrier and exergonic reaction to generate disulfide by direct substitution on the tetrasulfide and trisulfide-1,1-dioxides (for tetrasulfide, $\Delta G^{\ddagger}$ = 11.4 kcal/mol and ΔG^{o} = –23.0 kcal/mol; for trisulfide-1,1-dioxide, $\Delta G^{\ddagger}$ = 12.2 kcal/mol, ΔG^{o} = –17.3 kcal/mol).

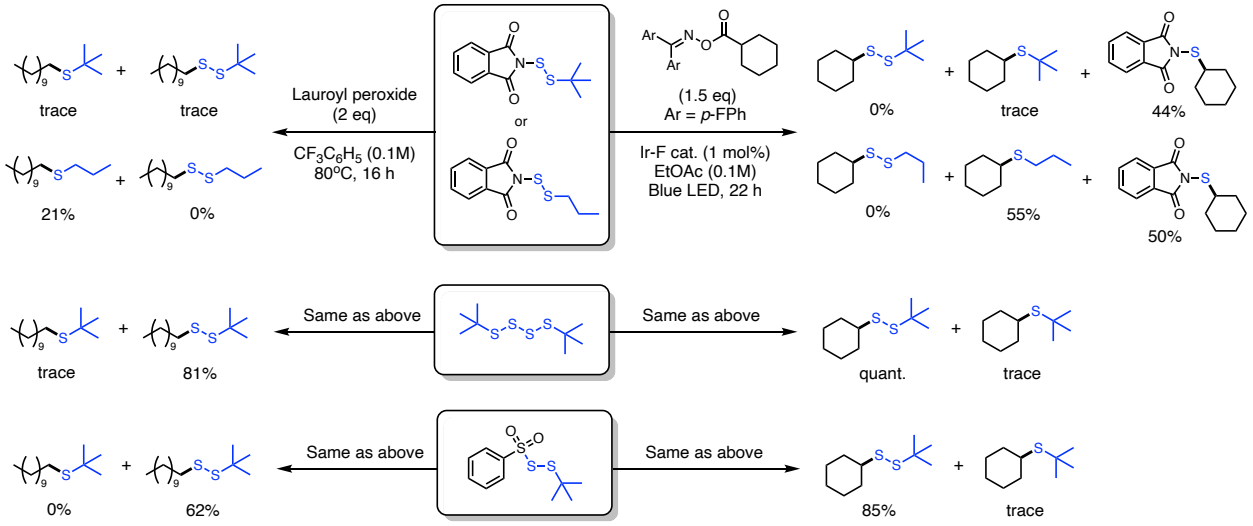

Scheme 23. Alkyl radical substitution with alkyl radicals generated under non-redox conditions.

Similar results were obtained by using cyclohexyl radicals generated from energy transfer photocatalysis, using the cyclohexyl acyloxime and the iridium photocatalyst [Ir(dF(CF_3)ppy)$_2$(dtbbpy)] under blue LED irradiation.[55] Reactions with the *tert*-butyl Harpp reagent or *n*-propyl Harpp reagent failed to yield disulfides, while replacing them with tetrasulfide and trisulfide-1,1-dioxide afforded corresponding disulfide in high yields.

It is noteworthy that under both conditions, alkyl substitution on the inner sulfur atom of the Harpp reagent did not occur and instead of N–S bond cleavage, the weaker S–S bond was cleaved to obtain *N*-cyclohexylthiophthalimide (compare CBS-QB3-calculated BDEs: S–S = 64.4 kcal/mol *vs* N–S = 71.7 kcal/mol in PhthSS^{t}Bu; S–S = 62.3 kcal/mol *vs* BDE of N–S = 71.8 kcal/mol in PhthSS^{n}Bu).

To further delineate the roles of the Harpp reagent and the tetrasulfide, which is an unavoidable (non-negligible) byproduct of photolysis of the Harpp reagent, we carried out reactions with varying amounts of each from the outset (Scheme 24), but with different terminal substituents (*t*-butyl on the Harpp reagent and cumyl on the tetrasulfide).

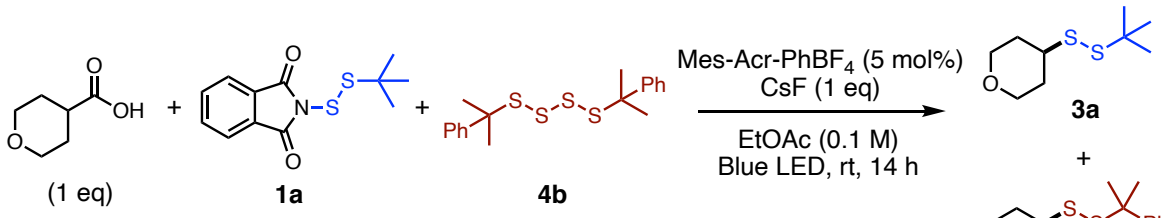

reagents (eq)		products (%)	
1a	**4b**	**3a**	**3s**
0	1	-	trace
0.5	1	13	42
1	1	29	71
1	0.75	28	67
1	0.5	38	63
1	0.25	53	41

Scheme 24. Control reactions with varying *t*-butyl Harpp reagent and dicumyl tetrasulfide.

In the reaction with only dicumyl tetrasulfide (**4b**), in the absence of the Harpp reagent, a trace amount of **3s** was obtained. This indicated that the substitution occurred on the tetrasulfide, but without the Harpp reagent to turn over the photocatalyst, the reaction ceased. This necessity of the Harpp reagent to regenerate the oxidized photocatalyst was further demonstrated when only 0.5 equivalent of the Harpp reagent was initially added as the reactant, which resulted in a combined 55% yield of disulfide products (**3a** + **3s**). Furthermore, with addition of dicumyl tetrasulfide (**4b**) as a competing reaction partner, we observed that the disulfide derived from tetrasulfide, **3s**, was always the dominant product. Though reducing the amount of tetrasulfide gradually decreased the proportion of the disulfide derived from it (**3s**), not until it was reduced to 0.25 eq, was **3s** no longer the dominant product. This preference resulted from the larger amount of added dicumyl tetrasulfide (**4b**) than di-*tert*-butyl tetrasulfide formed from the Harpp reagent *in situ* present in solution. Moreover, the presence of cumyl,*tert*-butyl tetrasulfide, formed from cross

combination of cumylperthiyl radical and *tert*-butylperthiyl radical also supported the generation of *tert*-butylperthiyl radical from the Harpp reagent during the reaction.

Given the realization that tetrasulfide must be formed in situ for the disulfiration to occur, we wondered if the low yield observed for some substrates were due to the low steady-state concentration of tetrasulfide that must exist during the reaction. We then revisited disulfuration of *N*-phthalimide protected phenylalanine, which had yielded only 5% and wherein only a tiny amount of the Harpp reagent was consumed. Indeed, we found that by adding a small amount of tetrasulfide from the outset resulted in significant yield improvement — up to 74% when 20 mol% of tetrasulfide was added (Scheme 25).

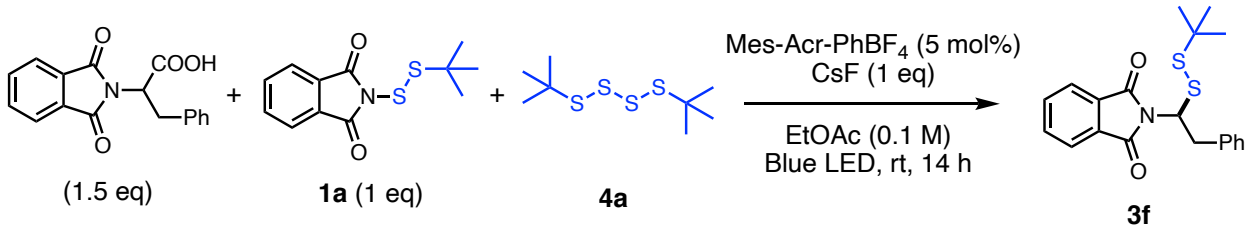

added **4a** (mol%)	recovered **1a** (%)	product **3f** (%)
0	95	4
5	92	13
10	73	16
20	14	74

Scheme 25. Effect of added tetrasulfide on the disulfuration of a challenging substrate with a Harpp reagent.

With the results of the calculations and experiments provide above, we have effectively ruled out direct substitution of alkyl radicals on the Harpp reagents to afford disulfides and instead, provided evidence in favour of the direct substitution of alkyl radicals on tetrasulfides which are formed from the Harpp reagents in situ.

2.5 Mechanistic studies of reaction with N-thiophthalimide derivatives

With the alternative mechanism for disulfuration in mind, we wondered if this mechanism holds true for previously reported methodologies using *N*-(trifluoromethylthio) phthalimide (hereafter PhthSCF$_3$) and *N*-(phenylthio)-phthalimide (hereafter PhthSPh) as sulfurating reagents. Analogous CBS-QB3 calculations predict that substitutions on PhthSCF$_3$ and PhthSPh are endergonic reactions (ΔG^o = 5.4 and 10.2 kcal/mol, respectively) (Figure 2). Though they showed lower energy barrier than direct substitution on the Harpp reagent ($\Delta G^‡$ = 16.3 and 16.7 kcal/mol for PhthSCF$_3$ and PhthSPh *vs* 18.5 and 18.7 for PhthSS^{n}Pr and PhthSS^{t}Bu), they were still higher than those reagents which work well in radical substitution (e.g. sulfide formation from PhthSS^{n}Pr, $\Delta G^‡$ = 13.6 kcal/mol and disulfide formation from either ^{t}BuSSSS^{t}Bu, $\Delta G^‡$ = 11.6 kcal/mol, or PhSO$_2$SS*t*-Bu, $\Delta G^‡$ = 12.2 kcal/mol).

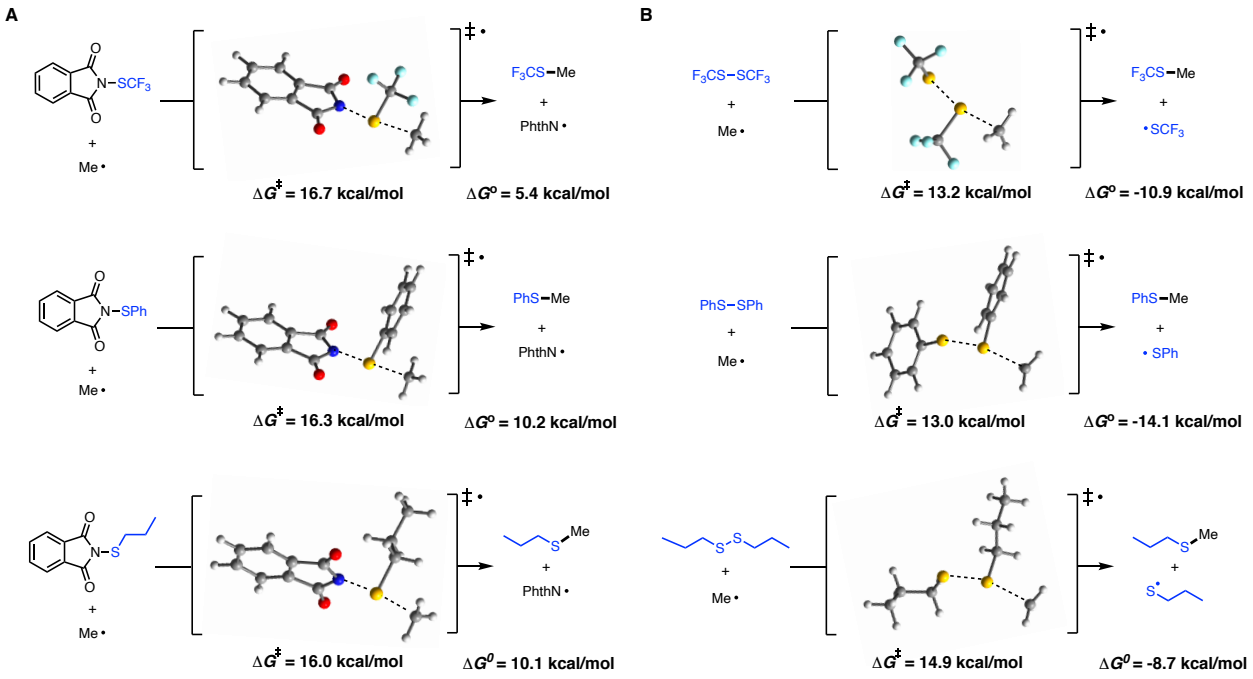

Figure 2. Lowest energy transition state structures and corresponding reaction energetics determined by CBS-QB3 (at 298 K) for substitution of a model alkyl radical (methyl) on N-thiophthalimide derivatives and corresponding disulfides

Thus, it seems reasonable to consider the alternative mechanism wherein a disulfide is formed *in situ* from the reduction of the *N*-thiophthalimides. In this scenario, the substitutions are predicted to be exergonic (ΔG^{o} = –10.9 and –14.1 kcal/mol for CF_3SSCF_3 and PhSSPh, respectively) and to proceed with barriers similar to those predicted for the successful direct substitutions ($\Delta G^{\ddagger}$ ~ 13 kcal/mol). Later, reduction potentials of $PhthSCF_3$ and PhthSPh were measured by cyclic voltammetry to be E_{pc} = –1.34 and –1.37 V vs. SCE respectively, which were similar in magnitude and irreversibility to those of PhthSS^{t}Bu (E_{pc} = –1.36 V vs. SCE). Thus, single electron reduction from reduced photocatalyst to $PhthSCF_3$ and PhthSPh, same as to PhthSS^{t}Bu, is feasible and is expected to occur with subsequent N-S bond fragmentation.

Next, similarly to our experiments with the Harpp reagents, alkyl radicals were generated under non-redox conditions in the presence of PhthSCF$_3$ and PhthSPh to figure out the feasibility of radical substitution on both substrates. Before doing so, for comparison, we repeated Glorius' remote C-H functionalization using PhthSCF$_3$ as trifluoromethylthiolation reagent and obtained 76% of the corresponding sulfide **11** (Scheme 26A, reported yield: 73%[40]). Similarly, PhthSPh was used as the phenylthiolation reagent under Leonori's conditions, which provided us 64% of the expected product **8** (Scheme 26B, reported yield: 69%[46]). One may expect that, if the reaction goes through radical substitution directly to PhthSCF$_3$ or PhthSPh, even though the alkyl radical was generated by other means, substitution on these *N*-thiophthalimide derivatives should occur similarly. However, under energy transfer photocatalytic conditions (Scheme 27), the sulfides were obtained in 41% and 30% yield from PhthSCF$_3$ and PhthSPh respectively, around 30% lower than the yields obtained under the original photoredox conditions. By replacing PhthSPh with PhSSPh, the yield of sulfide could be increased to 77% under energy transfer photocatalytic conditions. It is also noteworthy that CF$_3$SSCF$_3$ was clearly observed in crude ^{19}F NMR spectra of reactions with PhthSCF$_3$. Although the results suggested that the radical substitution on *N*-thiophthalimide derivative seemed feasible, given the observation of CF$_3$SSCF$_3$ in the reaction, the mechanism of sulfide formation was still ambiguous.

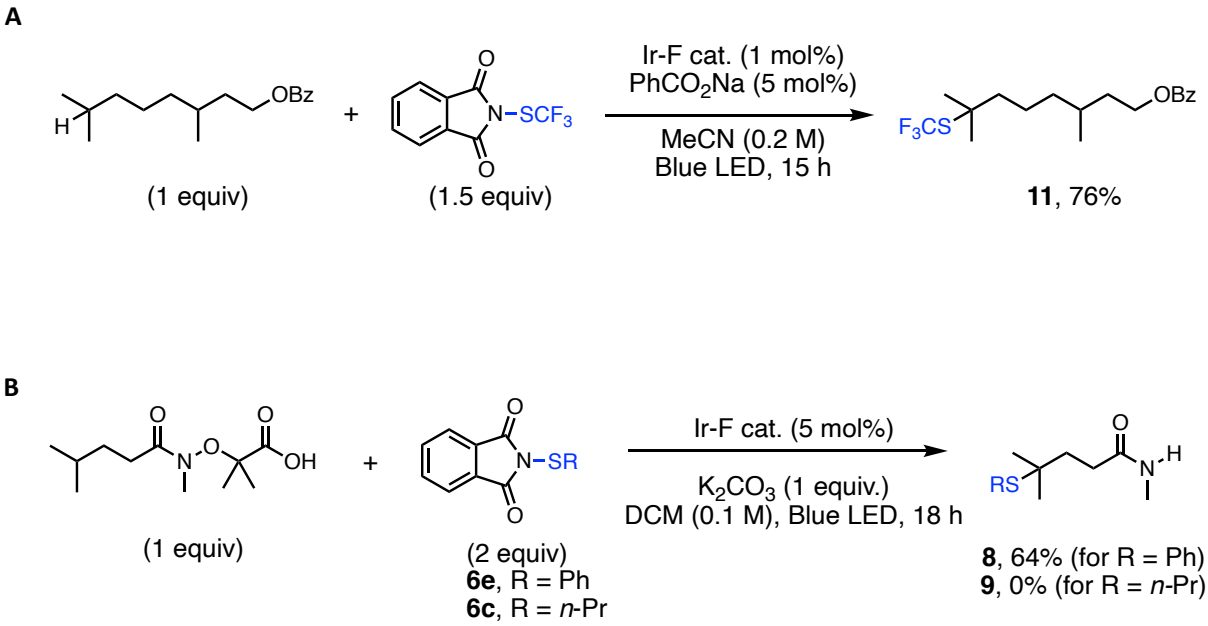

Scheme 26. Reported methods of using *N*-thiophthalimide derivatives as sulfurating reagents

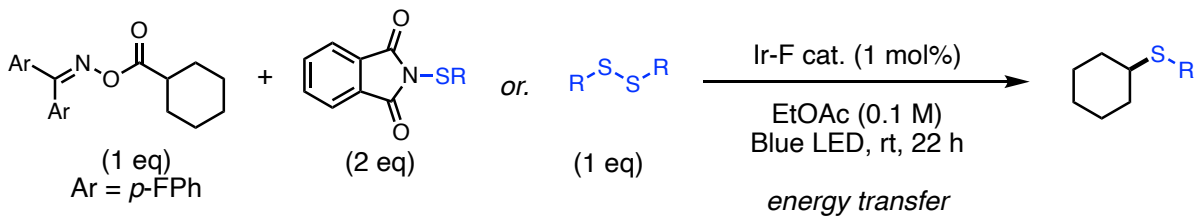

R	Yield of sulfide (%)	
	from PhthSR	from RSSR
CF_3	41	n.d.
Ph	30	77
n-Pr	25	52

Scheme 27. Radical substitution on *N*-thiophthalimide derivatives under non-redox condtitions.

For further investigation of the mechanism, we prepared *N*-(*n*-propylthio)phthalimide (PhthS^{n}Pr) for comparison. CBS-QB3 calculations predicted that the energy barrier and the reaction free energy for radical substitution on PhthS^{n}Pr was similar to PhthSPh ($\Delta G^{\ddagger}$ = 16.0 and 16.3 kcal/mol, and ΔG^{o} = 10.1 and 10.2 kcal/mol for PhthS^{n}Pr and PhthSPh, respectively). Indeed, under energy transfer photocatalytic conditions, PhthS^{n}Pr underwent homolytic substitution similarly to PhthSPh (30% *vs* 25% yield). Under photoredox conditions (Scheme 26B), however, PhthS^{n}Pr failed to provide the corresponding product. The observation of large amounts of ^{n}PrSS^{n}Pr from reductive fragmentation of Phth^{n}Pr (E_{pc} = –1.47 V *vs* SCE in CH_3CN) indicated that the redox cycle had actually occurred. The failure then provided us with compelling evidence that the substitution occurs on ^{n}PrSS^{n}Pr instead of PhthS^{n}Pr. Indeed, rate constants for undecyl radical to undergo substitution on dialkyl disulfide (MeSSMe) and diaryl disulfide (PhSSPh) in benzene at 25°C have been reported to be 6 × 10^4 and 2 × 10^5 $M^{-1}s^{-1}$, respectively. Our calculated difference of 1.9 kcal/mol higher in energy barrier for substitution on ^{n}PrSS^{n}Pr than on PhSSPh (by a methyl radical at 25 °C in the gas phase) ($\Delta G^{\ddagger}$ = 14.9 *vs* 13.0 kcal/mol) makes a ~25-fold difference in rate that suppressed the reaction.

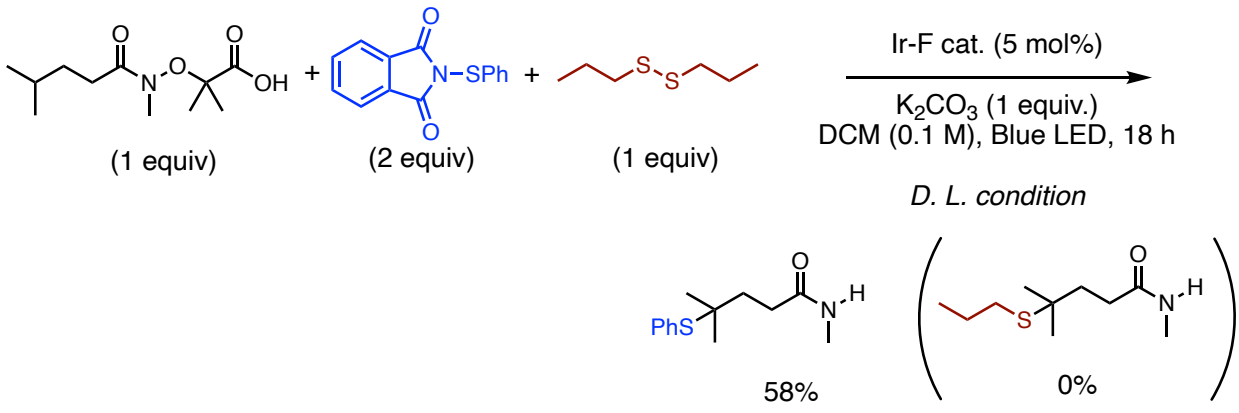

Scheme 28. Reaction of phthSPh under photoredox condition with additional dialkyl disulfide.

The ease of substitution on PhSSPh compared to ^{n}PrSS^{n}Pr, as predicted from the literature precedent, is very obvious from the results of the experiment shown in Scheme 28. We conducted a reaction under photoredox conditions with an additional equivalent of ^{n}PrSS^{n}Pr. As such, if direct substitution on *N*-thiophthalimide derivative was operative, given the preference for radical substitution on ^{n}PrSS^{n}Pr over PhthSPh shown in the calculation, we surmised that an additional equivalent of ^{n}PrSS^{n}Pr might be compatible with PhthSPh. However, to our surprise, the thiophenylation product, derived from PhthSPh, was obtained in 58% yield without obvious observation of sulfide derived from ^{n}PrSS^{n}Pr. This results again supported that PhSSPh was formed *in situ* and acting as the key reagent for the substitution, which outcompeted ^{n}PrSS^{n}Pr.

2.6 From decarboxylation to C-H functionalization

With more insight of the reaction mechanism of our decarboxylative disulfuration, in which Harpp reagent plays important roles as both oxidant to re-oxidize the photocatalyst and precursor to the disulfurating reagent, we then attempted to apply this unique reactivity of the Harpp reagent in C-H disulfuration.

2.6.1 Utilizing direct hydrogen atom transfer reagent — TBADT

Being inspired by Studer's work of using THADT as a HAT reagent for C-H disulfuration with tetrasulfide (shown in Section 1.2), together with our understanding of the reactivity of Harpp reagent, we surmised that Harpp reagent could be a replacement for tetrasulfide and $Na_2S_2O_8$ to accomplish the work (Scheme 29).

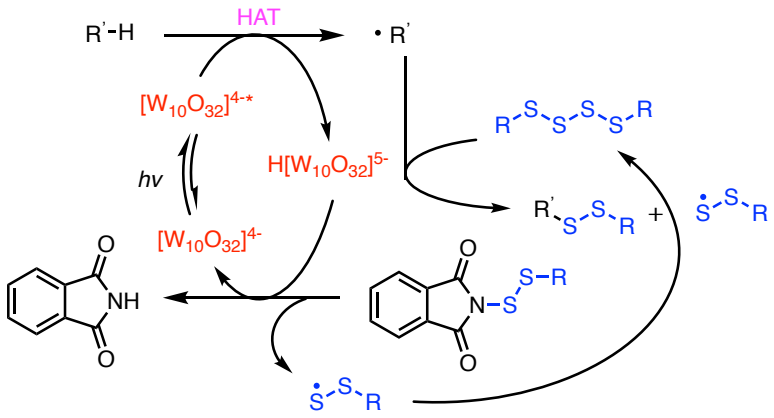

Scheme 29. TBADT as photocatalyst for C-H disulfuration

We began to investigate the proposed transformation by exposing the *tert*-butyl Harpp reagent and cyclohexane to 390 nm Kessil lamp overnight in the presence of TBADT. Indeed, the desired disulfide product was formed in a significant amount (Scheme 30). However, dialkyl trisulfide was formed as a non-separable byproduct by column chromatography, and was indistinguishable by ^{1}H NMR— with combined 37% NMR yield (disulfide and trisulfide). Increasing the reaction temperature to 60ºC, without fan cooling, did not make much of an improvement in selectivity or combined yield. Though it wasn't mentioned in their publication, the same mixture was observed while we conducted the experiment under Studer's disulfuration conditions with tetrasulfides.

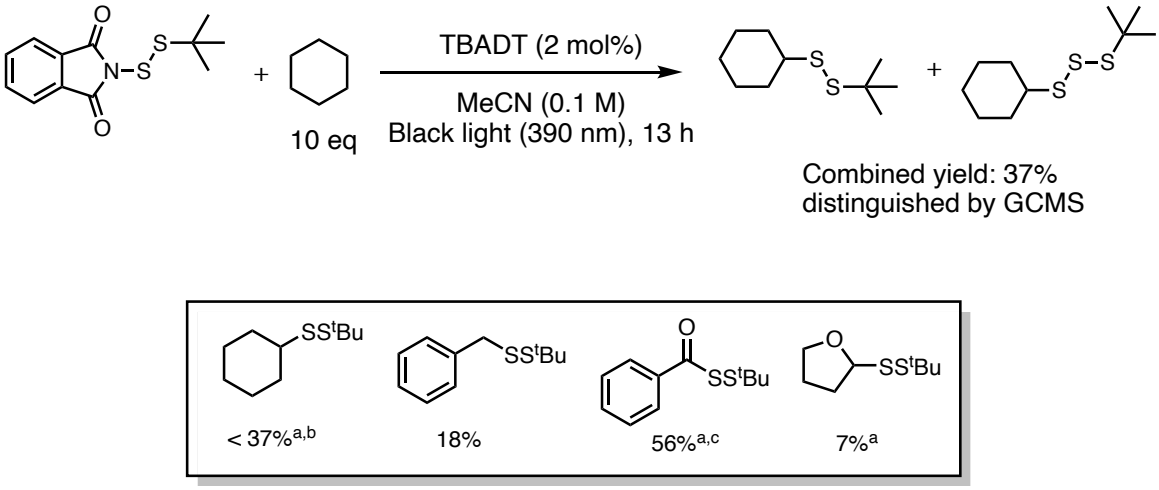

Scheme 30. Substrates of C-H disulfuration using TBADT

(a) NMR yields; (b) Yield including trisulfide;
(c) Irradiated under 365 nm using photoreactor, and MeCN/H_2O = 2/1 as solvent.

Substrates other than cyclohexane were subsequently tested. Toluene, which possesses a weaker C-H bond (BDE = 88 kcal/mol *vs* 99 kcal/mol in cyclohexane), provided only 18% of the desired product. Benzaldehyde seemed to be more suitable under these conditions, and provided a 56% yield of corresponding disulfide, with 13% of trisulfide byproduct. The higher reactivity of benzaldehyde might be attributed to the polarity match between the C-H bond in benzaldehyde and TBADT, the photocatalyst which preferably abstracts more hydridic H-atoms due to its electrophilic nature from electron deficient oxygen atom.[56] However, the same trend did not show on THF, from which only 7% of the corresponding disulfide was obtained.

With low yields but full consumption of Harpp reagent in most cases, we wondered if the low yields were caused by the instability of the Harpp reagent under near ultraviolet light irradiation and/or the presence of TBADT. Several control experiments in the absence of cyclohexane were conducted. We then surprisingly found that although the Harpp reagent itself

was stable upon irradiation (390 nm), it was consumed within 4h in the presence of TBADT (Scheme 31).

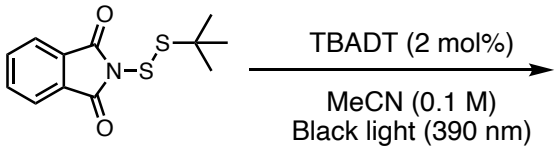

Entry	Harpp reagent	TBADT	Light	Results (remaining Harpp reagent)
1	V	V		> 90% (4 h)
2	V		V	> 90% (4 h)
3	V	V	V	8% (2 h); 0% (4 h)

Scheme 31. Harpp reagent stability in presence of TBADT

With the observation of significant blue color in entry 3, which corresponds to the reduced tungsten center, we surmised that consumption of the Harpp reagent was attributed to single electron transfer mechanism (SET) shown in Scheme 32. To start, light excited TBADT may undergo HAT from the solvent (MeCN, $k = 6.5 \times 10^4$ $M^{-1}s^{-1}$ for HAT from MeCN to TBADT)[56] to afford singly reduced decatungstate ($H^+[W_{10}O_{32}]^{5-}$). Disproportion of singly reduced decatungstate would generate the active decatungstate and doubly reduced decatungstate.[56] By re-oxidizing this doubly reduced decatungstate, Harpp reagent was reduced into phthalimidyl anion and perthiyl radical. Since we did not observe a significant amount of HAT product from polarity unmatched acetonitrile, we surmised that tetrasulfide, which generated from rapid self-recombination of perthiyl radical, was the one which further reduced active decatungstate. Indeed, cyclic voltammetry measurement on tetrasulfide showed an oxidation potential at 1.89 V vs. SCE which indicated tetrasulfide is oxidizable by irradiated TBADT ($E_{1/2}^{red}$ $[W_{10}O_{32}]^{4-*}/[W_{10}O_{32}]^{5-}$ = +2.44 V vs. SCE).

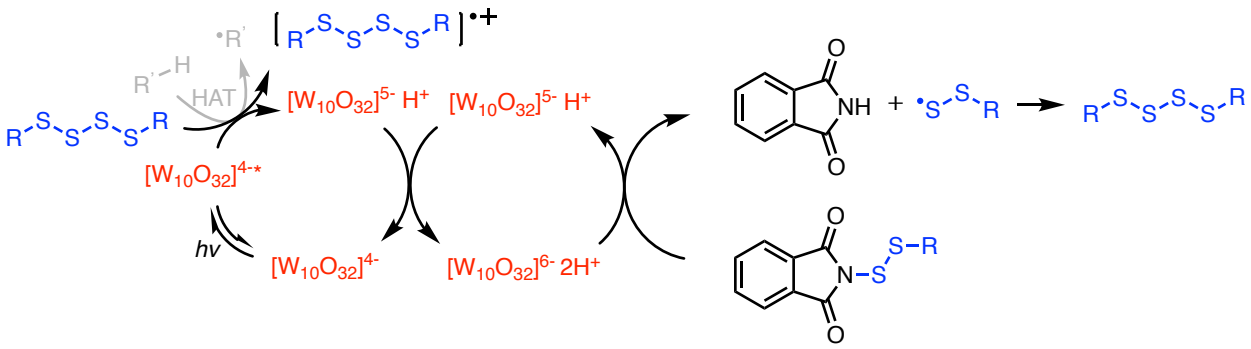

Scheme 32. Mechanism of Harpp reagent consumption in presence of TBADT

Realizing the obvious instability of the Harpp reagent under TBADT/ 390 nm system, we halted our investigation into using TBADT as HAT reagent in our C-H disulfuration and sought another suitable system.

2.6.3 Indirect hydrogen atom transfer reagents — Quinuclidine radical cation

We then sought an indirect hydrogen atom transfer system for the C-H disulfuration (Scheme 33). Among them, the aminium radical cation derived from quinuclidine has been widely used as a photocatalytic HAT reagent.[57] We envisioned that with lower oxidation potential of quinuclidine, the system may accomplish the C-H disulfuration under milder oxidative conditions by preventing the oxidation of tetrasulfide generated in situ. As proposed mechanism, Ir catalyst ($Ir[dF(CF_3)ppy]_2(dtbbpy)PF_6$) would undergo reductive quenching cycle ($E_{1/2}^{red}$ [Ir(lll)*/Ir(ll)] = +1.21 V vs. SCE) through oxidation of quinuclidine ($E_{1/2}^{ox}$ = +1.1 V vs. SCE).[58] The quinuclidinium radical cation (BDE of $H\text{-}N^+$ = 100 kcal/mol) can then abstract an H-atom from $C(sp^3)$-H bond in the substrate to provide an alkyl radical.

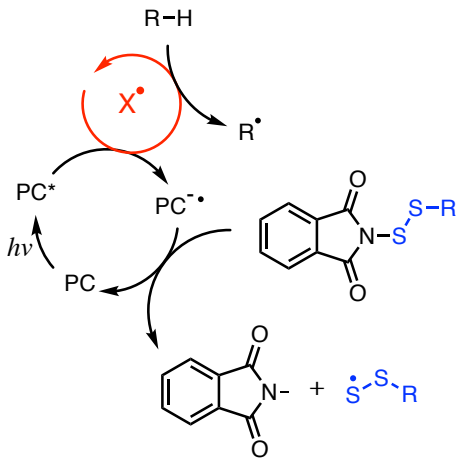

Scheme 33. Proposed mechanism for C-H disulfuration under indirect HAT catalysis

As proof of concept, we combined Harpp reagent **1d** (1 equiv) and THF (10 equiv) in the presence of 1 mol% Ir catalyst (Ir[dF(CF_3)ppy]$_2$(dtbbpy)PF_6), quinuclidine (20 mol%) and K_2CO_3 (0.5 equiv) in acetonitrile under irradiation overnight with blue LEDs (Scheme 34). To our delight, the desired product was obtained in 58% purified yield (65% NMR yield). The effects of different equivalents of THF, amount of quinuclidine catalyst, Ir catalyst, base, and solvent were investigated in our optimization process (see experimental details in section 4.7).

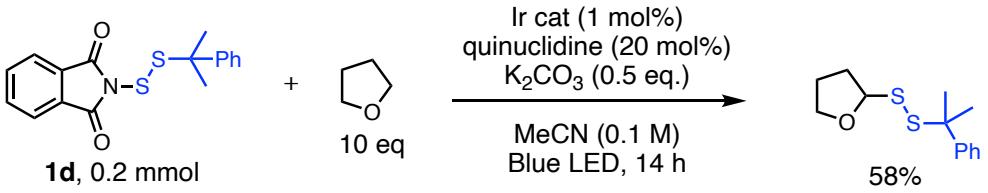

Scheme 34. Proof of concept of using Ir/quinuclidine as photocatalytic HAT system

During our control experiments, we found that, similarly to our observations in the presence of TBADT, the Harpp reagent was consumed in the absence of substrate (THF) within

7h. With this in mind, time dependent experiments were conducted and we surprisingly found the full conversion of Harpp reagent within an hour — with 70% NMR yield of disulfide.

With the optimized condition in hand, the substrate scope of this efficient transformation was investigated. However, they turned out to be limited (Scheme 35). Though tetrahydrothiophene and ambroxide still provided 54% and 32% yields respectively, six membered rings which possess slightly higher α–(C-H) BDEs (92 kcal/mol in THF; 96 kcal/mol in tetrahydropyran)[59] dramatically decreased the yield to 12%. Ethylbenzene and benzaldehyde, which possess even weaker C-H bonds then THF (~88 kcal/mol for both benzylic and formyl C-H bond)[59] were not applicable to the transformation, presumably due to the less hydridic character of the C-H bond that reduced the efficiency of HAT process with the electrophilic quinuclidinium radical.

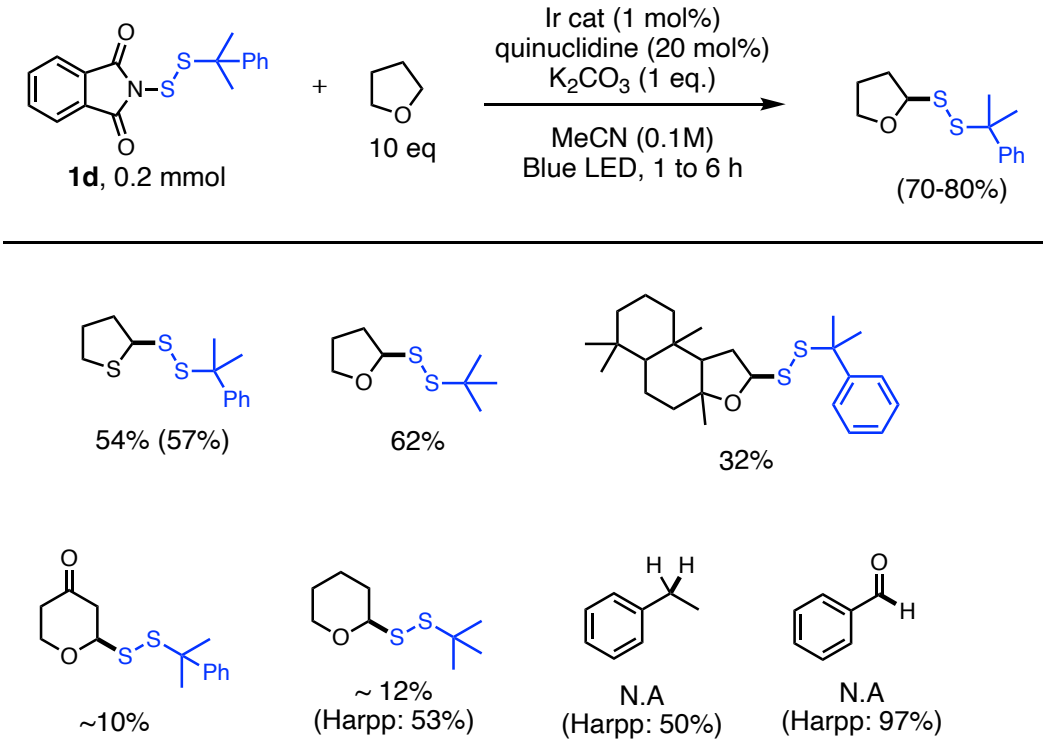

Scheme 35. Substrates of using Ir/quinuclidine as photocatalytic HAT system

While searching for a more potent HAT reagent that could activate a wider variety of substrates, we were inspired by Maruoka's recent publication of using cationic DABCO-based catalyst as a HAT reagent for C-H alkylation with alkene.[60] The dicationic aminium radical generated under photoredox conditions has greater reactivity than the quinuclidinium radical, due to its higher electrophilicity and stronger N^+-H bond (BDE ~ 106 kcal/mol *vs*. BDE ~ 100 kcal/mol in the quinuclidinium ion) (Scheme 36). Thus, we presumed that this DABCO-based HAT reagent would be able to abstract H-atoms from C-H bonds that were difficult to activate using quinuclidine.

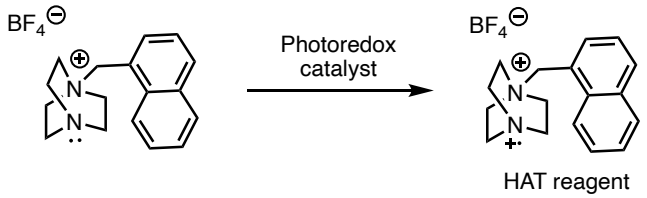

Scheme 36. Cationic DABCO-based HAT reagent

However, we found that neither unactivated C-H bonds from cyclohexane nor hydridic C-H bonds from THF provided the desired disulfide products using this reagent. We further found that the otherwise successful C-H functionalization with dimethyl fumarate was unsuccessful upon addition of the Harpp reagent (Scheme 37). In this case, the alkene remained intact while the Harpp reagent was fully consumed. This indicated that reduction of the Harpp reagent by photocatalyst happened, however, the formation of alkyl radical was impeded. The problem might come from the generated tetrasulfide undergoing redox reaction with either acridinium photocatalyst or dicationic aminium radical. Thus, we surmised that the failure of our C-H disulfurations, in general, might be attributed to the instability of tetrasulfide under these strongly oxidizing conditions.

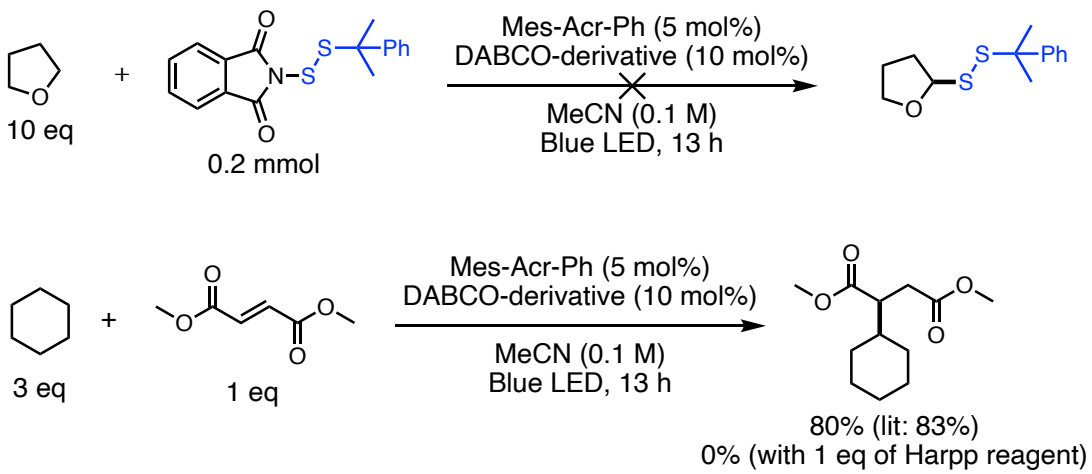

Scheme 37. C-H functionalization by using DABCO-derivative as HAT reagent

2.6.2 Indirect hydrogen atom transfer reagents — Benzoyl radical

With the similarity of involving phthalimide derivative, Glorius' condition of using sodium benzoate as indirect HAT reagent was another promising system to try on (Scheme 16B). By the success of using Ir catalyst ($[Ir(dF(CF_3)ppy)_2(dtbbpy)]PF_6$) in our decarboxylative disulfuration (Table 1, Entry 3), we have already known that the reduced Ir catalyst are capable of reducing Harpp reagent. We envision that benzoyloxy radical ($PhCO_2\cdot$), generated by reductive quenching of Ir catalyst, could perform hydrogen atom abstraction from C(sp^3)-H bonds of alkane substrates.[40]

Cyclohexane was first used as a substrate to test out hypothesis. However, only a small amount of Harpp reagent was consumed with none of the desired disulfuration product being observed. To our disappointment, neither moving to a substrate with more hydridic C-H bonds (THF) nor using the reported model substrate provided the corresponding products (Scheme 38). To rule out the potential problem from low steady state concentration of tetrasulfide, the same reaction with an additional equivalent of tetrasulfide was conducted. Similarly, most of the Harpp

reagent survived with no disulfide product being formed. This implied that the initial generation of alkyl radical was not efficient. Furthermore, we found that the addition of Harpp reagent poisoned the otherwise successful reaction with $PhthSCF_3$ (Scheme 39). Therefore, we surmised that the presence of Harpp reagent suppressed the alkyl radical formation probably by reacting with the key HAT reagent.

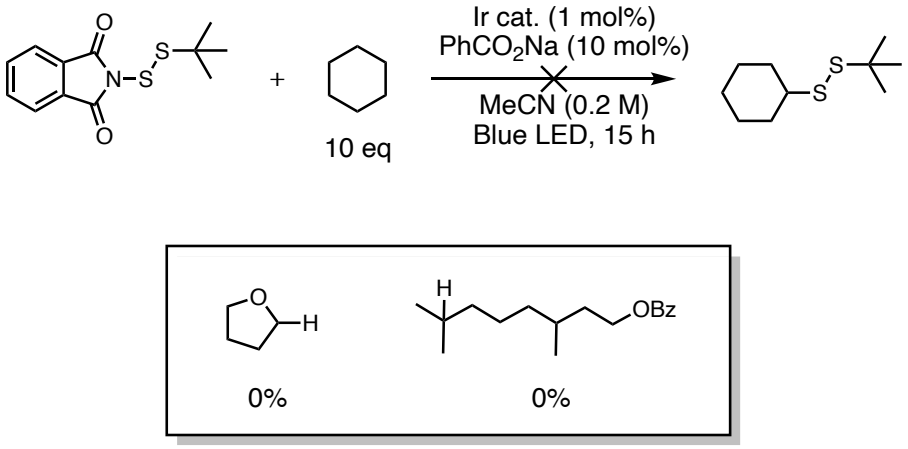

Scheme 38.Trials of C-H disulfuration with benzoate as HAT reagent

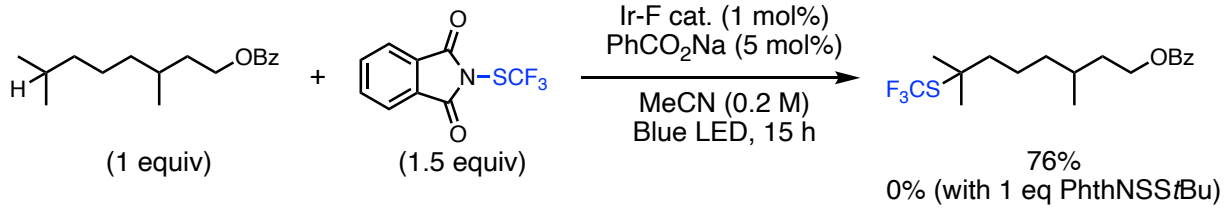

Scheme 39. Proposed mechanism for C-H disulfuration under indirect HAT catalysis

3. Conclusion

Harpp reagents have been found to be effective disulfurating reagents for the decarboxylative disulfuration with carboxylic acids under photoredox conditions. The reaction was initially expected to go through radical substitution directly on the Harpp reagent, however, calculations and reactions with non-redox (either thermally or photochemically) generated alkyl radicals both suggested that sulfide formation was favored (kinetically and thermodynamically) over disulfide formation in direct substitution on the Harpp reagents. Thus it was unlikely to be the mechanism for the exclusive formation of disulfide.

Our extensive mechanistic studies suggested that instead of radical substitution on the Harpp reagents, the reactions are likely to go through single electron reduction of the Harpp reagent by the reduced photocatalyst followed by fragmentation and dimerization to generate tetrasulfide as the active disulfurating reagent, which was previously reported by our group to be an excellent disulfurating reagent through radical substitution. The mechanism was not only supported by the observation of tetrasulfide as byproduct, but also supported by competition experiments which show preferential radical substitution on tetrasulfide over Harpp reagent and a massive increase in product formation by initial addition of sub-stoichiometric tetrasulfide for challenging substrates.

A similar mechanism is also proposed to account for previously reported sulfurations using *N*-thiophthalimide derivatives. Thiyl radicals generated from reduction of *N*-thiophthalimide derivatives can dimerize to form symmetric disulfides which undergo radical substitution by alkyl radicals to afford the observed sulfides. This mechanistic proposal was logically supported by calculation and the outcomes of reactions carried out under both redox and non-redox conditions.

Direct C-H disulfuration using the Harpp reagents under a variety of conditions were tried, however the Harpp reagent was observed to be self-consumed in these redox conditions and provided very limited substrate scope.

With more understanding into the reactivity of phthalimide derivatives, we believe this type of reagent can have broader application in organic synthesis in the future. By changing the substituent on phthalimide derivative, other than disulfide moiety, we may be able to introduce other functionalities using radical substitution chemistry. On the other hand, by tuning the electron affinity of the substituents on phthalimide, we are able to predict the liberating groups after reduction and make good use of them. For example, *N*-chlorophthalimide has been reported to undergo reduction to yield the chloride anion and phthalimidyl radical, which is trapped by arenes, under photoredox catalysis.[61] In this reaction, *N*-iodo and *N*-bromophthalimide failed to be used in the same manner, presumably due to more facile formation of the phthalimide anion and halogen atom. Other moieties should be investigated that would yield radicals that may dimerize to form substrates for substitution.

4. Experimental details

4.1 General information

All chemicals were purchased from commercial sources and used without further purification, except where otherwise stated. Anhydrous ethyl acetate (EtOAc) was distilled from calcium hydride (10 % w/v) under positive pressure of nitrogen. All other anhydrous solvents were purchased from Fisher Chemicals, Sigma Aldrich or Acros Organics and used without further purification. All reactions were carried out under positive pressure of nitrogen using standard Schlenk technique, unless otherwise noted. Reactions were monitored by thin layer chromatography (TLC) with precoated silica gel plates from Merck Chemicals (TLC Silica gel 60 F254, 250 μm thickness) using UV light as the visualizing agent and/or iodine vapor, basic aqueous potassium permanganate ($KMnO_4$), or heat as developing agents. Flash column chromatography was performed over silica gel 60 (particle size 0.035- 0.07 mm) from Silicycle. NMR spectra were recorded on either Bruker AV-300, AV-400 or AV-600 unity plus spectrometers. Chemical shifts (δ) are quoted in parts per million (ppm) and were internally referenced to residual $CHCl_3$ (7.26 ppm for ^{1}H, 77.16 ppm for ^{13}C). Coupling constants (*J*) are reported in Hertz (Hz) to the nearest 0.1 Hz. The following abbreviations (or combinations thereof) were used for peak multiplicities: s = singlet, d = doublet, t = triplet, q = quartet, quintet, m = multiplet.

4.2 Preparation of *N*-perthiophthalimide and *N*-thiophthalimide derivatives

4.2.1 *N*-perthiophthalimide derivatives

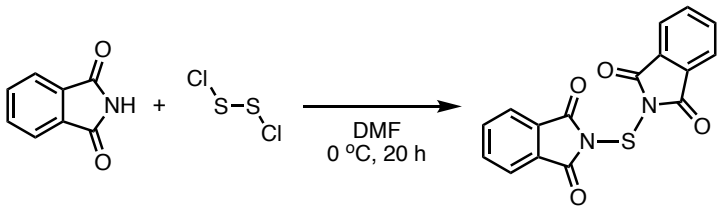

N-Perthiophthalimides was synthesized according to a reported procedure.[32] Briefly, phthalimide (7.36 g, 50 mmol) was dissolved in anhydrous DMF (40 mL) at 0 °C, and to the resulting solution, sulfur monochloride (4 mL, 50 mmol) was added dropwise. The reaction mixture was continuously stirred at 0 °C for 20 h. The precipitate was filtered and washed with Et_2O to obtain *N,N'*- thiobisphthalimide as white solid.

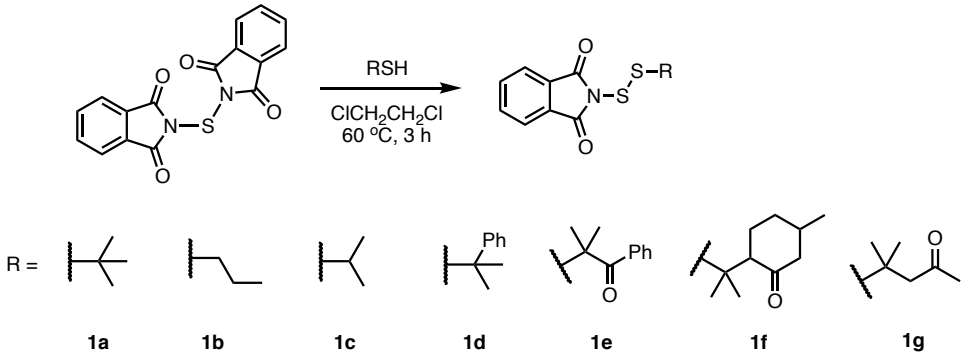

N,N'-Thiobisphthalimide (3.4 g, 10.5 mmol, 1.5 equiv.) was dissolved in dichloroethane (70 mL) to which was added thiol (7 mmol, 1 equiv) in one portion. The reaction mixture was stirred at 60 °C for 3h. The reaction was cooled to room temperature and filtered through a plug of celite. The crude mixture was concentrated under reduced pressure and purified by column chromatography (with hexane/EtOAc or hexane/DCM as eluent) to afford *N*-perthiophthalimide derivatives **1a** – **1g.**

4.2.2 *N*-thiophthalimides derivatives

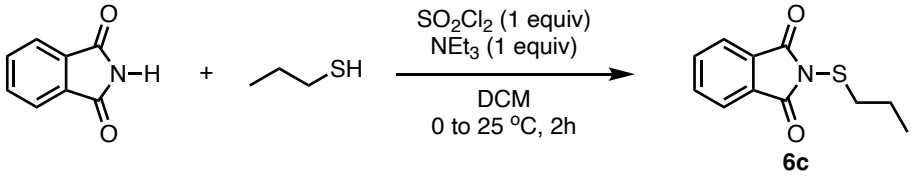

N-(*n*-Propylthio)phthalimide (PhthS^{n}Pr, **6c**) was synthesized according to a literature procedure.[62] Sulfuryl chloride (2.02 mL, 25 mmol) was added dropwise to an ice-chilled solution of *n*-propylthiol (2.27 mL, 25 mmol) and triethylamine (cat. amount, 3 drops) in dry dichloromethane (25 mL). After stirring for 30 mins at 0 °C, the mixture was warmed to rt. The mixture was then added by syringe to the ice-chilled suspension of phthalimide (3.68 g, 25 mmol) and triethylamine (4.6 mL, 33 mmol) in dry dichloromethane (25 mL). The reaction mixture was stirred for another 2h at rt. The solution was filtered, added to a separatory funnel, washed with water and brine, and dried over $MgSO_4$. The crude product was concentrated under reduced pressure and purified by column chromatography (hexane/DCM as eluent) to obtain *N*-(*n*-propylthio)phthalimide as white solid.

N-(Trifluoromethylthio)phthalimide (PhthSCF_3, **6d**)[63] and *N*-(phenylthio)phthalimide (PhthSPh, **6e**)[64] were prepared according to literature procedures.

4.3 General procedure for decarboxylative disulfuration

4.3.1 General information

The acridinium photocatalyst [Mes-Acr-Ph]$^{+}BF_4^{-}$ was prepared according to the reported procedure.[65] The light source was placed about 7 cm from the reaction vessel. A custom made

photoreactor was used with 4 LEDs (455 nm) arranged around the reaction vessel at room temperature as shown in Figure S1.

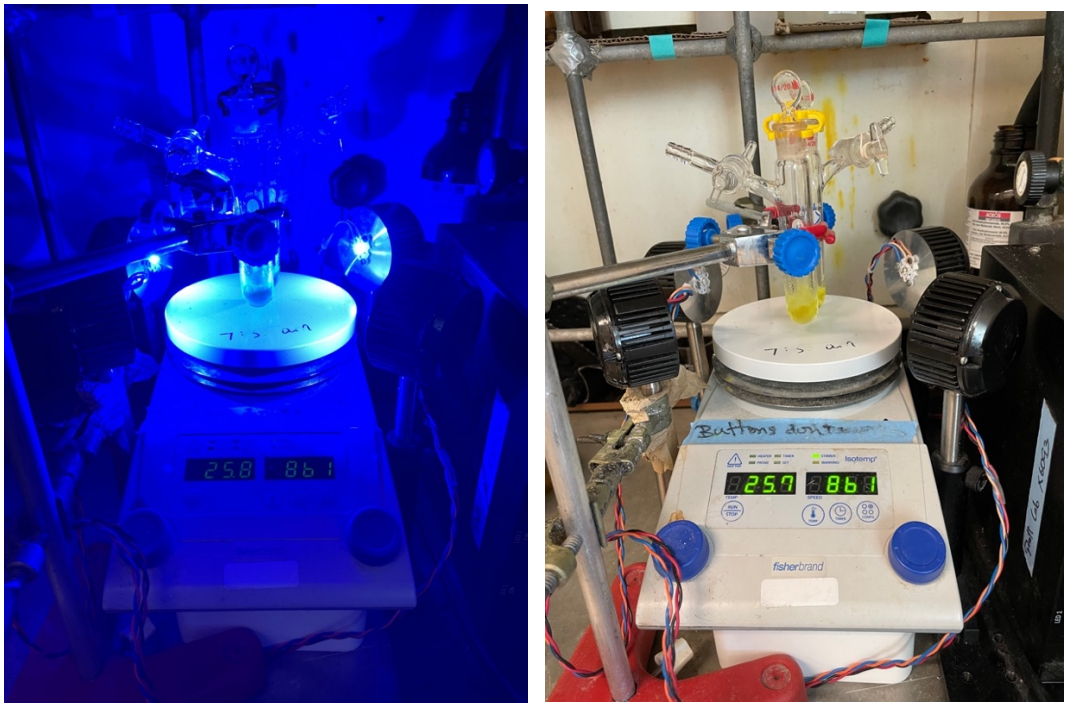

Figure S1. Reaction setup for decarboxylative disulfuration.

4.3.2 Synthesis procedure

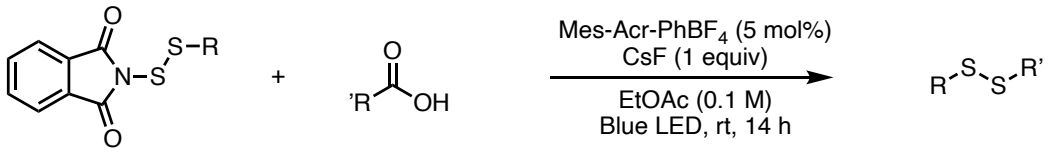

To an oven-dried Schlenk tube with a magnetic stirring bar was added carboxylic acid (0.2 mmol), *N*-perthiophthalimide (0.3 mmol), CsF (30.4 mg, 0.2 mmol), Mes-Acr-PhBF$_4$ (5.7 mg, 0.01 mmol) and anhydrous EtOAc (2 mL). The resulting solution was degassed by three freeze-

pump-thaw cycles. After backfilling with nitrogen, the tube was placed in the LEDs setup and stirred while being irradiated for 14 h. The reaction mixture was then filtered through a plug of celite and the solvent was removed under reduced pressure. The crude residue was purified by column chromatography with hexane/EtOAc as the eluent to afford the desired disulfide product. Characterization data for disulfide **3a** to **3w** was showing in section 6.1.

Example of NMR 'yield' determination (e.g. entry 1). After reaction work up and solvent removal, mesitylene (same equivalent as limiting reagent) was added to crude mixture as internal standard.

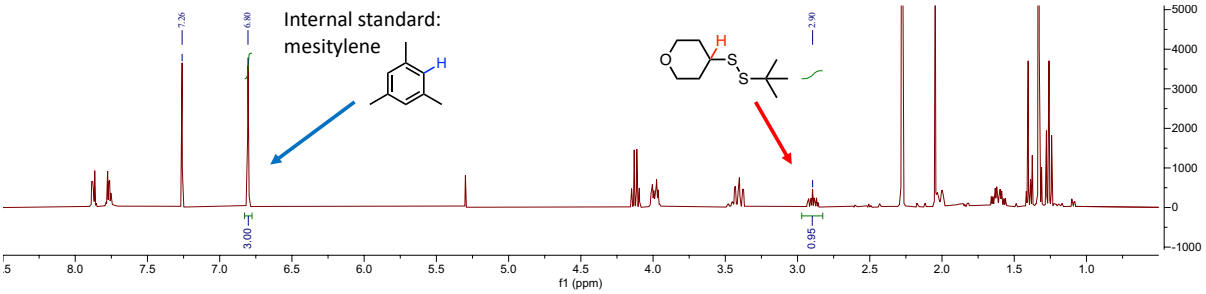

4.4 Mechanistic experiments for *N*-perthiophthalimide derivatives[1]

4.4.1 Radical clock experiment

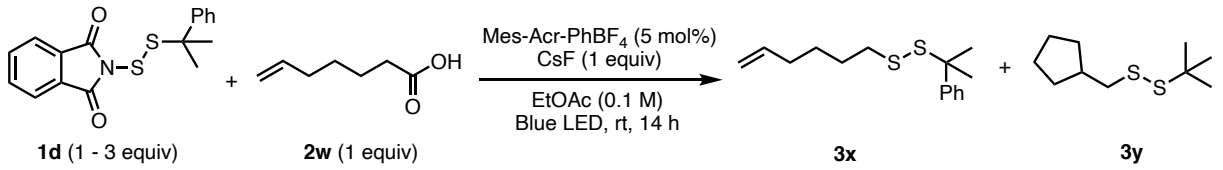

The reaction was carried out by the general procedure described above. Five samples were prepared with **1d** (0.10 mmol, 0.15 mmol, 0.20 mmol, 0.25 mmol, 0.30 mmol), **2w** (0.1 mmol), Mes-Acr-PhBF$_4$ (2.9 mg, 0.005 mmol), CsF (0.1 mmol) and anhydrous EtOAc (1 mL). The resulting solution was degassed by three freeze-pump-thaw cycles. After backfilling with nitrogen, the tube was placed in the LED setup and stirred while being irradiated for 14 h. The reaction mixture was then filtered through a plug of celite and the solvent was removed under reduced pressure. The yield was determined by crude NMR using mesitylene as internal standard.[36]

Entry	Equivalent of **1d**	Yield of **3x**	Yield of **3y**
1	1	10%	66%
2	1.5	10%	68%
3	2	10%	67%
4	2.5	10%	67%
5	3	10%	66%

[1] Out of concern for the volatility of the products, solvent was removed by rotary evaporator without heating. Thus, some EtOAc remain in crude NMR sample.

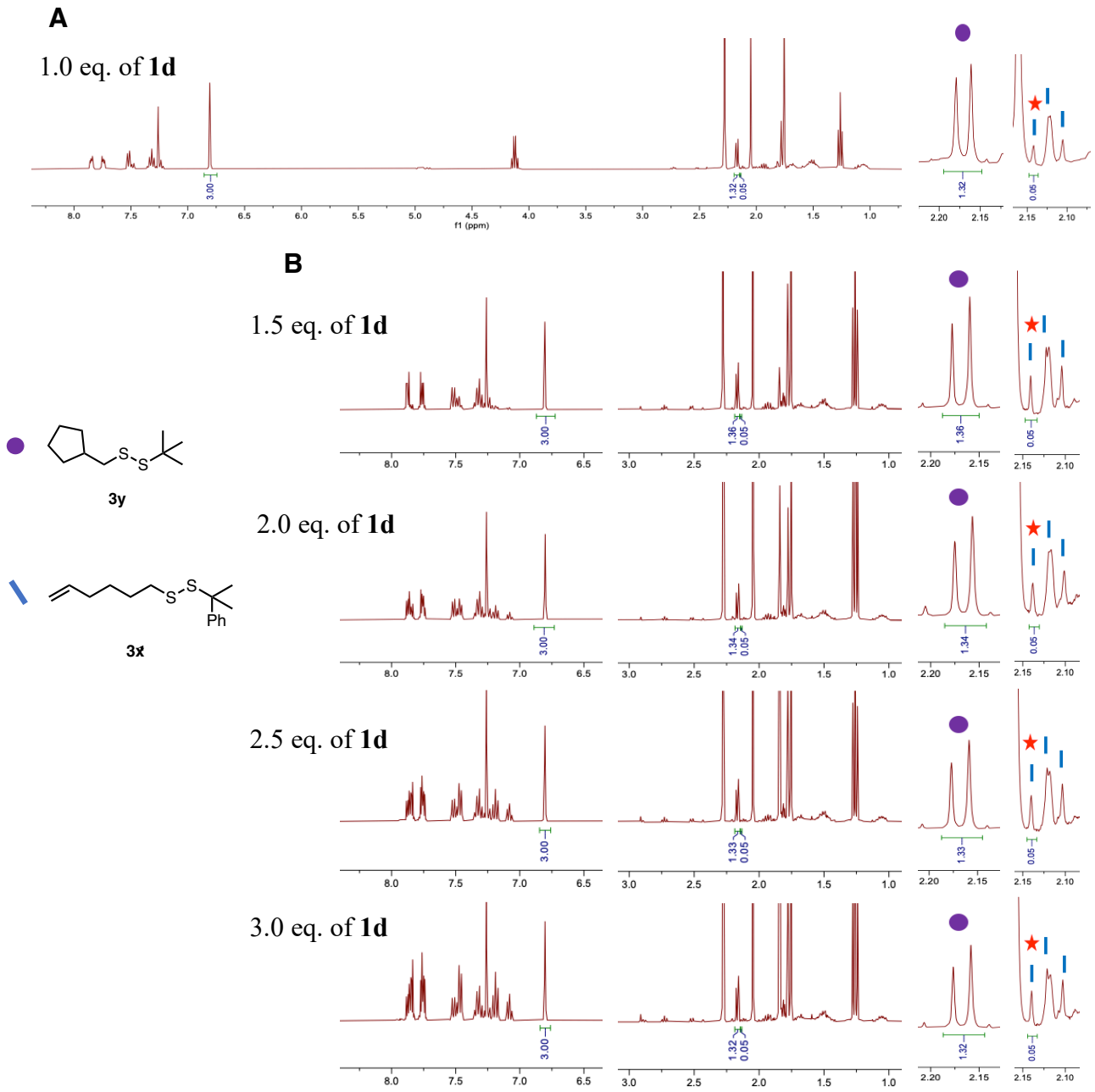
A
1.0 eq. of 1d
B
1.5 eq. of 1d
2.0 eq. of 1d
2.5 eq. of 1d
3.0 eq. of 1d
3y
3x
Ph

Figure S2. Representative ^{1}H NMR specta (400 MHz, $CDCl_3$) of disulfuration reactions carried out with various equivalents of initial Harpp reagent (**1d**) under standard conditions. A) Full spectrum shown for the reaction carried out using 1.0 eq. of **1d**, displaying integral of mesitylene at 6.8 ppm. To the right is an expanded spectrum showing peaks of **3y** and **3x**. Since the triplet from **3x** (labeled with blue lines) overlaps with something else in the mixture, only the integral labeled with the red star was used to estimate the yield. B) Key portions of spectra of reactions carried out with 1.5 to 3.0 eq. of **1d** and associated expanded spectra showing characteristic peaks of **3x** / **3y**.

4.4.2 Radical substitution under thermal conditions

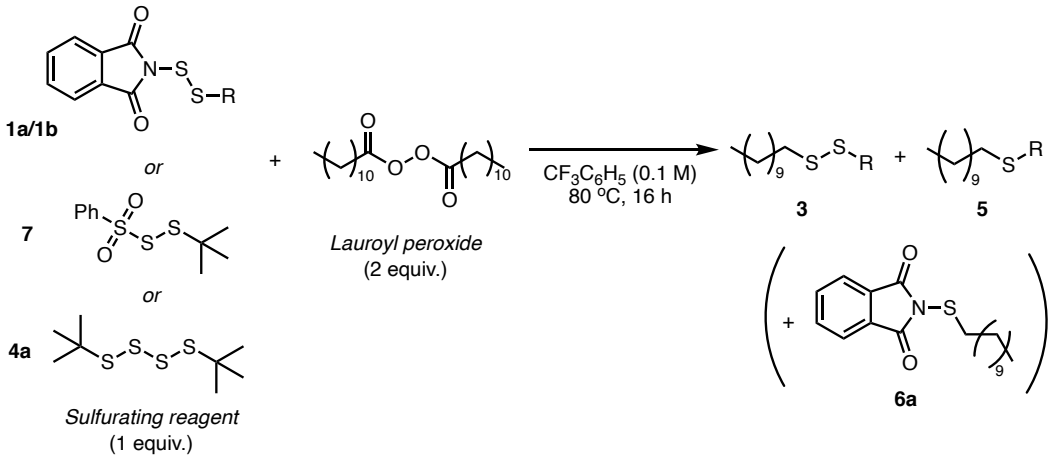

To an oven dried Schlenk tube with a magnetic stirring bar was added lauroyl peroxide (79.7 mg, 0.2 mmol), (di)sulfurating reagent (0.1 mmol) and 1.0 mL $CF_3C_6H_5$. The resulting solution was degassed by three freeze-pump-thaw cycles. After back filling with nitrogen, the tube was heated to 80 °C and stirred for 16 hours. The solvent was removed under reduced pressure.

The yield was determined by crude NMR with mesitylene as internal standard. NMR characterization data and spectra of **3ac**, **5b**, **6a** are shown in later sections.[2]

Entry	Starting Material (SM)		Remaining SM	Sulfide	Disulfide	**6a**
1	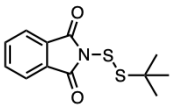	**1a**	< 73%	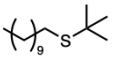 **5a**, trace	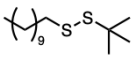 **3ac**, trace	30%
2	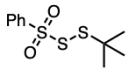	**7**	0%	**5a**, 0%	**3ac**, 62%	-
3	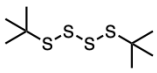	**4a**	0%	**5a**, 0%	**3ac**, 81%[2]	-
4	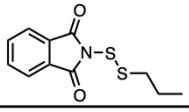	**1b**	31%	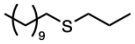 **5b**, 21%	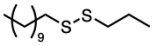 **3ad**, 0%	55%

[2] 1 eq of **4a** provides 1.62 eq of **3ac**

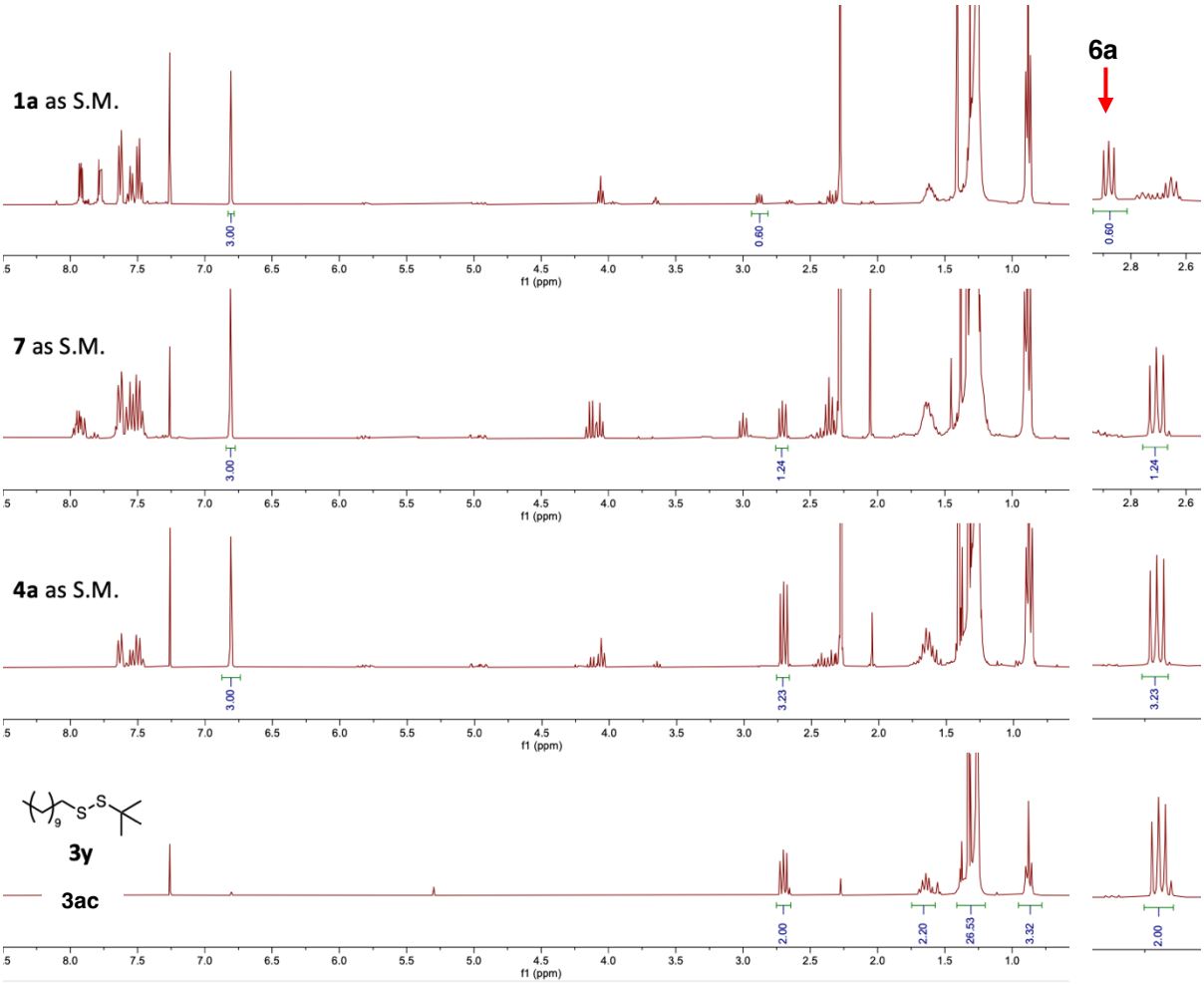

Figure S3. Representative ^{1}H NMR spectra (400 MHz, $CDCl_3$) of radical substitution reactions carried out under thermal conditions. Independent characterization of **5a** or **3ad** were consistent with reported data.[66]

4.4.3 Radical substitution under energy transfer photocatalysis conditions

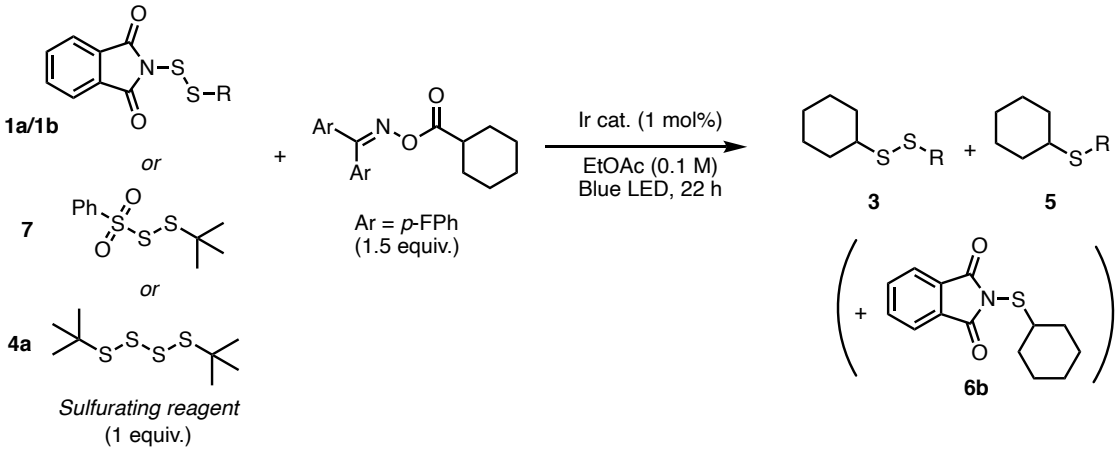

To an oven dried Schlenk tube with a magnetic stirring bar was added N-acyl oxime (0.15 mmol), (di)sulfurating reagent (0.1 mmol), $[Ir(dF(CF_3)ppy)_2(dtbbpy)]PF_6$ (0.001 mmol) and anhydrous EtOAc (1.0 mL). The resulting solution was degassed by three freeze-pump-thaw cycles. After backfilling with nitrogen, the tube was placed in the LED setup and stirred while being irradiated for 22 h. The solvent was removed under reduced pressure. The yield was determined by crude NMR with mesitylene as internal standard. NMR characterization data and spectra of **3aa**, **5d**, **6b** are shown in later sections.

Entry	Starting Material (SM)		Remaining SM	Sulfide	Disulfide	**6b**
1	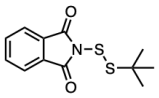	**1a**	~35%	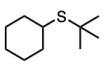 **5c**, trace	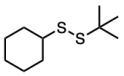 **3aa**, 0%	44%
2	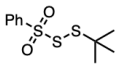	**7**	0%	**5c**, trace	**3aa**, ~85%	-
3	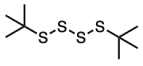	**4a**	-	**5c**, trace	**3aa**, quant.	-
4	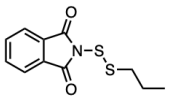	**1b**	31%	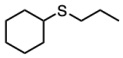 **5d**, 55%	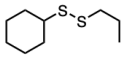 0%	50%

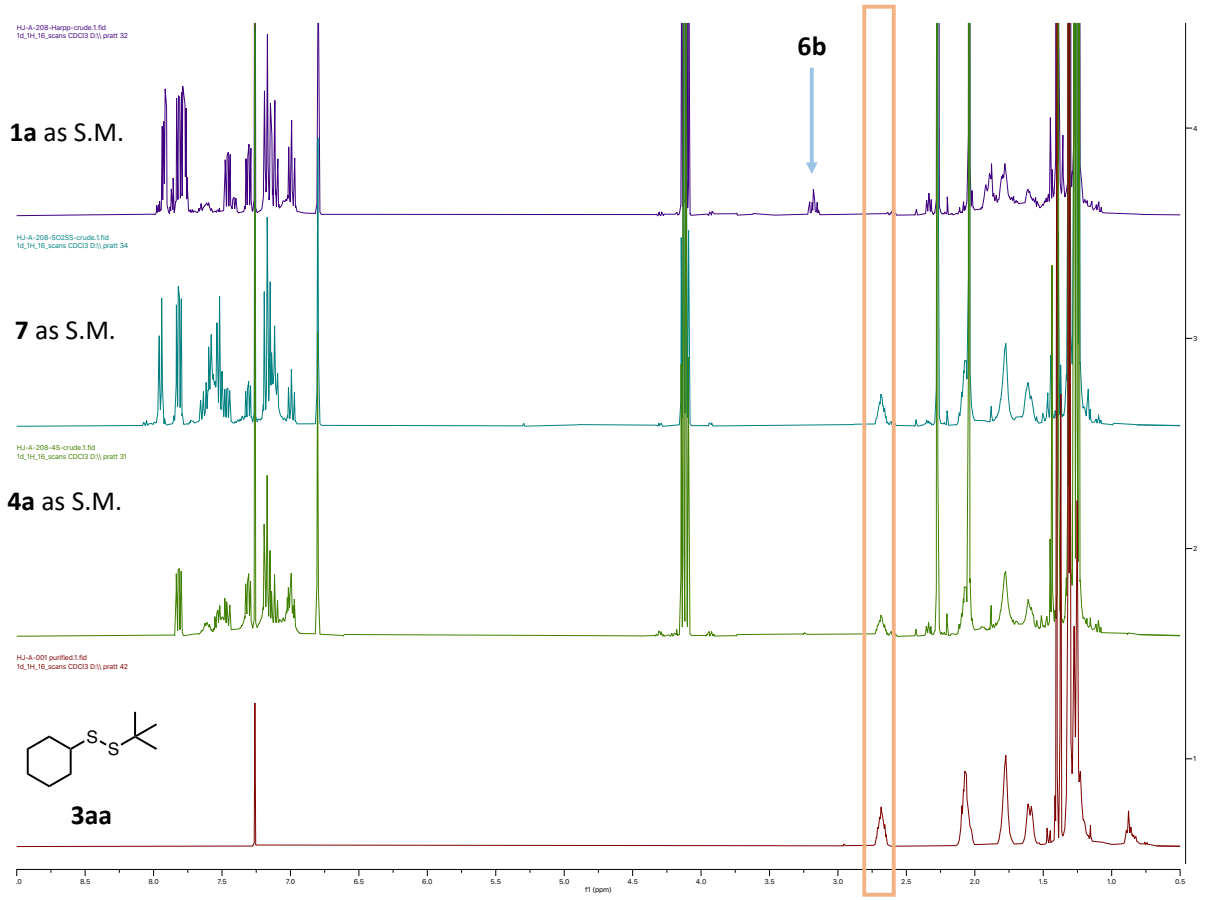

Figure S4. Representative ^{1}H NMR spectra (400 MHz, $CDCl_3$) of radical substitution reactions carried out under energy transfer photocatalytic conditions. Independent characterization of **5c** was consistent with reported data.[66]

4.4.4 Competition experiment

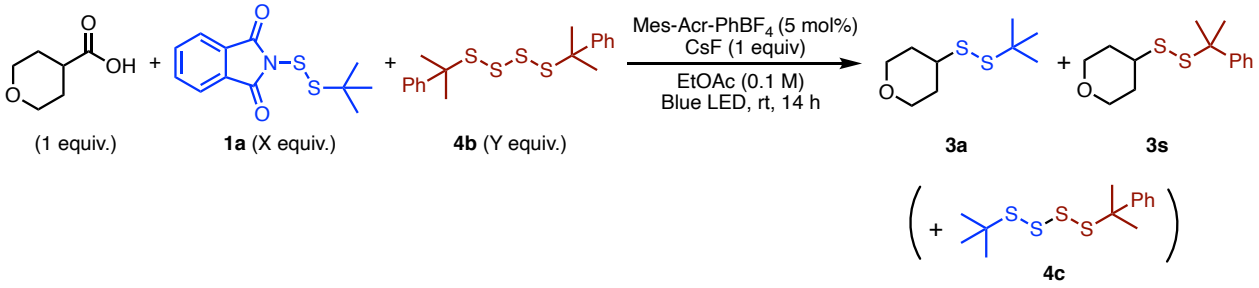

To an oven-dried Schlenk tube with a magnetic stirring bar was added carboxylic acid (0.2 mmol), *N*-(*t*-butylthio)phthalimide (0.2 mmol), dicumyltetrasulfide (0.05 mmol, 0.1 mmol, 0.15 mmol, 0.2 mmol), CsF (30.4 mg, 0.2 mmol) and Mes-Acr-$PhBF_4$ (5.7 mg, 0.01 mmol) and anhydrous EtOAc (2 mL). The resulting solution was degassed by three freeze-pump-thaw cycles. After backfilling with nitrogen, the tube was placed in the LED setup and stirred while being irradiated for 14 h. The reaction mixture was then filtered through a plug of celite and the solvent was removed under reduced pressure. The yields were determined by crude NMR with mesitylene as internal standard.

Starting materials		Yields from crude NMR:	
equiv. of **1a**	equiv. of **4b**	**3a**	**3s**
1	0.25	53	41
1	0.5	38	63
1	0.75	28	67
1	1	29	71
0.5	1	13	42

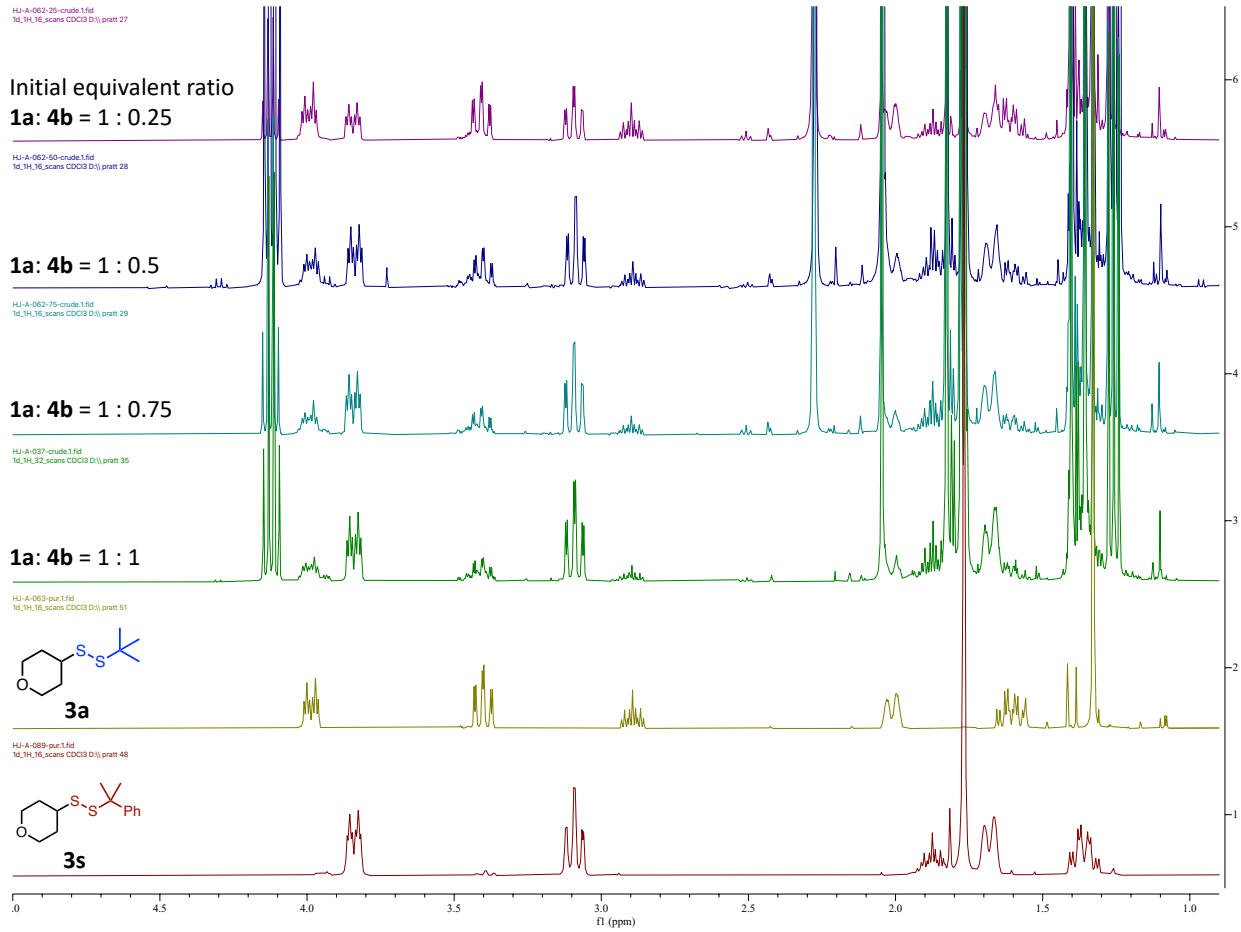

Figure S5. ^{1}H NMR spectra (400 MHz, $CDCl_3$) of disulfuration reactions carried out with different ratios of Harpp reagent (**1a**) and tetrasulfide (**4b**) carried out under otherwise standard conditions.

Cross coupled tetrasulfide (**4c**) was also detected and purified, which supported the formation of perthiyl radicals in situ. ^{1}H NMR (400 MHz, $CDCl_3$) δ 7.54 – 7.49 (m, 2H), 7.38 – 7.31 (m, 2H), 7.30 – 7.27 (m, 1H), 1.83 (s, 6H), 1.36 (s, 9H); ^{13}C NMR (101 MHz, $CDCl_3$) δ 144.12, 128.46, 127.52, 126.90, 54.25, 49.25, 30.34, 29.18; HRMS–EI (m/z) calcd for $C_{13}H_20S_4$ [M^+]: 304.0448, found 304.0479.

4.4.5 Addition of sub-stoichiometric tetrasulfide

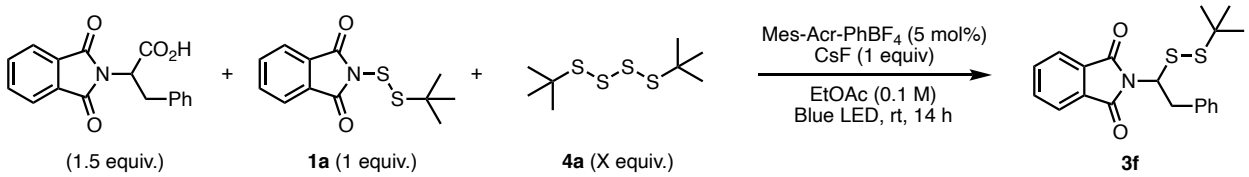

Four samples were prepared with carboxylic acid (0.15 mmol), **1a** (0.1 mmol), Mes-Acr-$PhBF_4$ (0.005 mmol), CsF (0.1 mmol) and varying concentrations of **4a** (0.0 mmol, 0.005 mmol, 0.01 mmol, 0.02 mmol) in anhydrous EtOAc (1 mL). The resulting solutions were degassed by three freeze-pump-thaw cycles. After backfilling with nitrogen, the tubes were placed in the LED setup and stirred while being irradiated for 14 h. The reaction mixtures were then filtered through plugs of celite and the solvents were removed under reduced pressure. The yields were determined by crude NMR with mesitylene as internal standard.

Entry	addition of **4a** (eq)	after irradiation: Yield of **3f** (%)	recovered **1a** (%)
1	0	4	95
2	0.05	13	92
3	0.1	16	73
4	0.2	74	14

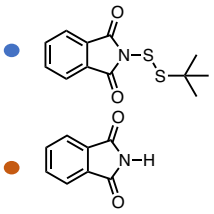

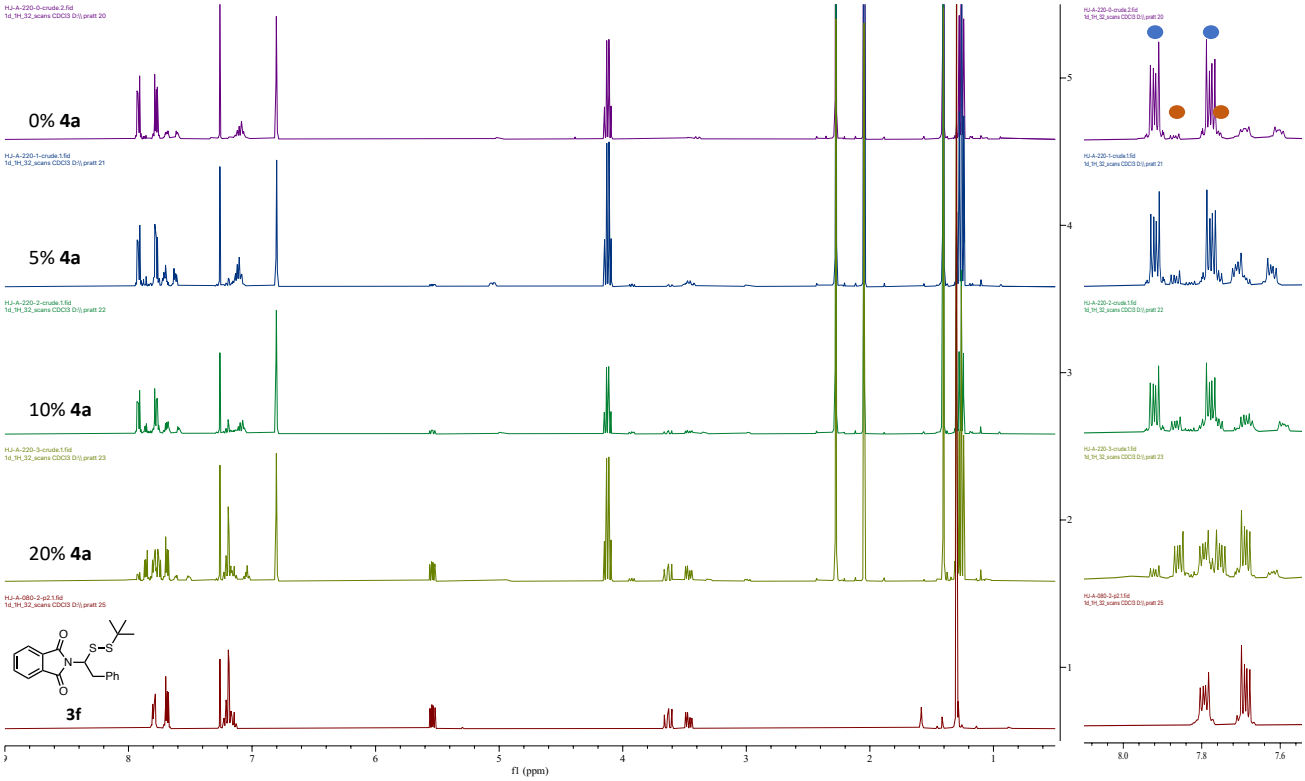

Figure S6. Representative ^{1}H NMR spectra (400 MHz, $CDCl_3$) of disulfuration reactions carried out with added tetrasulfide (**4a**) under otherwise standard conditions.

4.5 Mechanistic experiments for *N*-thiophthalimide derivatives

4.5.1 Radical substitution on *N*-thiophthalimide derivatives and disulfides under energy transfer photocatalysis conditions.

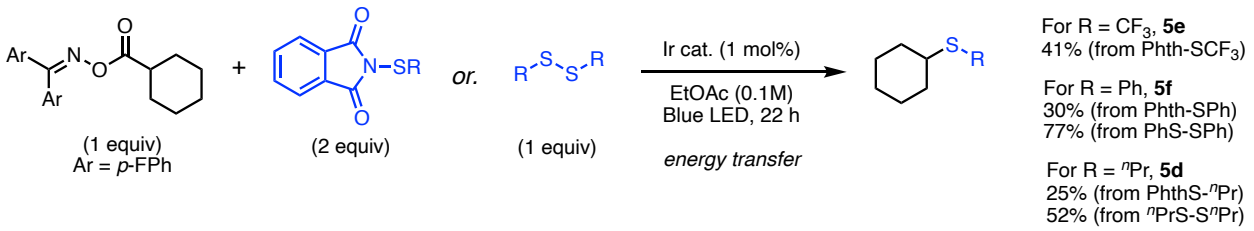

To an oven dried Schlenk tube with a magnetic stirring bar was added *N*-acyl oxime (0.1 mmol), (di)sulfurating reagent (0.2 mmol for *N*-thiophthalimide derivative; 0.1 mmol for disulfide), $[Ir(dF(CF_3)ppy)_2(dtbbpy)]PF_6$ (0.001 mmol) and anhydrous EtOAc (1.0 mL). The resulting solution was degassed by three freeze-pump-thaw cycles. After backfilling with nitrogen, the tube was placed in the LED setup and stirred while being irradiated for 22 h. The solvent was removed under reduced pressure and the crude residue was purified by column chromatography with hexane/EtOAc as the eluent to afford products for unambiguous characterization. The yield was determined by crude NMR with mesitylene as internal standard in order to provide the most accurate account of the chemistry unobscured by differences in efficiencies in purification. NMR characterization data and spectra of **5f, 5d** are shown in later sections.

For the reaction with *N*-(trifluoromethylthio)phthalimide ($PhthSCF_3$), ^{19}F NMR (283 MHz, $CDCl_3$) spectra of the crude mixtures were obtained without removal of the solvent. Yield of **5e** (δ = -39.21) [40] was determined by using trifluorotoluene as internal standard. The peak at δ = -45.84 is consistent with formation data of 1,2-bis-(trifluoromethyl)disulfide (CF_3SSCF_3).[67]

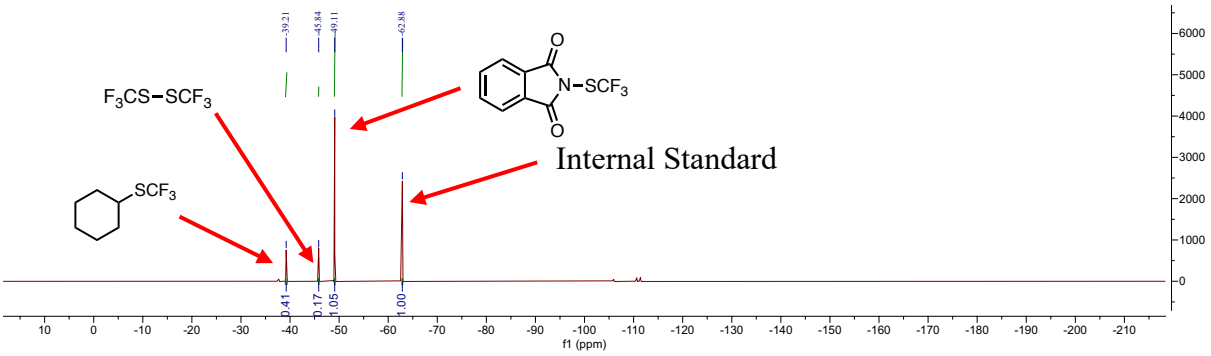

Figure S7. Representative ^{19}F NMR spectra (283 MHz, $CDCl_3$) of crude reaction mixture arising from radical substitution experiment with $PhthSCF_3$ under energy transfer photocatalysis conditions.

4.5.2 Radical substitution on *N*-thiophthalimide derivatives under photoredox conditions according to ref. 10.

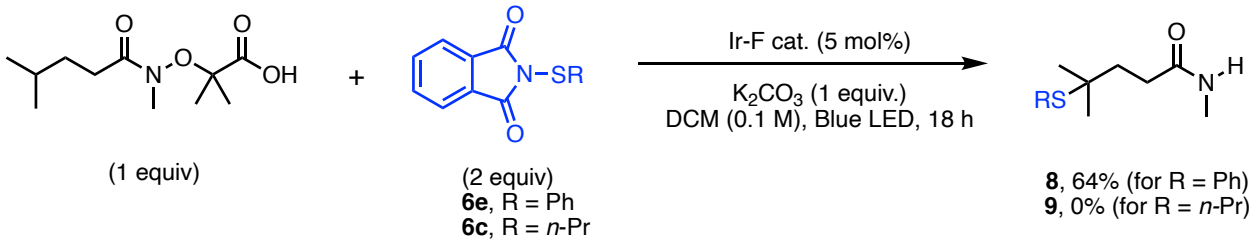

(1 equiv)

(2 equiv)
6e, R = Ph
6c, R = *n*-Pr

8, 64% (for R = Ph)
9, 0% (for R = *n*-Pr)

The reactions were carried out under similar conditions to those reported in the literature.[46] Briefly, to an oven-dried Schlenk tube with a magnetic stirring bar was added carboxylic acid (23.1 mg, 0.1 mmol), $[Ir(dF(CF_3)ppy)_2(dtbbpy)]PF_6$ (5.6 mg, 0.005 mmol), *N*-thiophthalimides derivative (0.2 mmol), K_2CO_3 (13.8 mg, 0.1 mmol) and anhydrous CH_2Cl_2 (1 mL). The resulting solution was degassed by three freeze-pump-thaw cycles. After backfilling with nitrogen, the tube was

placed in the LED setup and stirred while being irradiated for 18 h. The reaction mixture was then filtered through a plug of celite, the solvent was removed under reduced pressure and the crude residue was purified by column chromatography with hexane/EtOAc as the eluent.

8 was obtained as a colorless oil (64%).[46] ^{1}H NMR (400 MHz, $CDCl_3$) δ 7.52 – 7.46 (m, 2H), 7.38 – 7.29 (m, 3H), 5.58 (br, s, 1H), 2.81 (d, J = 4.1 Hz, 3H), 2.47 – 2.36 (m, 2H), 1.87 – 1.76 (m, 2H), 1.23 (s, 6H); HRMS–EI (m/z) calcd for $C_{13}H_{19}NOS$ [M+]: 237.1187, found 237.1180.

For reaction with *N*-(*n*-propylthio)phthalimide (PhthS^{n}Pr, **6c**), crude ^{1}H NMR spectra were collected after removal of the solvent and PTLC analysis was performed. A large amount of ^{n}PrSS^{n}Pr (58% based on converted **6c**) and oxidative cleavage of the substrate (**10**) were detected.

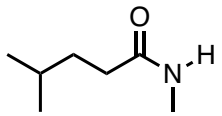

10

4.5.3 Radical substitution on N-thiophthalimide derivatives under photoredox conditions according to reference 8.

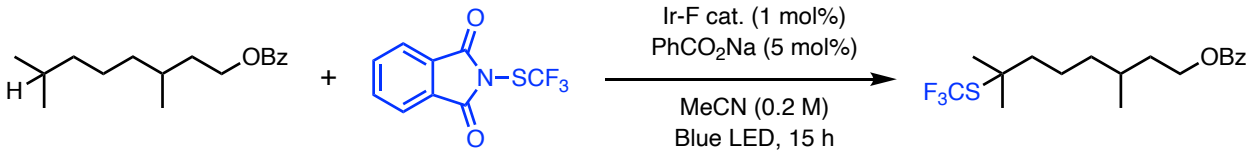

(1 equiv) (1.5 equiv) **11**, 76%

The reactions were carried out under similar conditions to those reported in the literature.[40] Briefly, to an oven-dried Schlenk tube with a magnetic stirring bar was added 3,7-dimethyloctyl benzoate (24.9 mg, 0.1 mmol), $[Ir(dF(CF_3)ppy)_2(dtbbpy)]PF_6$ (0.001 mmol), *N*-

(trifluoromethylthio)phthalimide (37 mg, 0.15 mmol), sodium benzoate (0.005 mmol), and anhydrous MeCN (0.2 M). The resulting solution was degassed by three freeze-pump-thaw cycles. After backfilling with nitrogen, the tube was placed in the LED setup and stirred while being irradiated for 15 h. The solvent was removed under reduced pressure and the crude residue was purified by column chromatography with hexane/EtOAc as the eluent.

11 was obtained as colorless oil (76%).[40] ^{1}H NMR (400 MHz, $CDCl_3$) δ 8.08 – 7.96 (m, 2H), 7.62 – 7.50 (m, 1H), 7.48 – 7.37 (m, 2H), 4.45 – 4.25 (m, 2H), 1.88 – 1.74 (m, 1H), 1.74 – 1.46 (m, 5H), 1.45 (s, 6H), 1.42 – 1.31 (m, 2H), 1.27 – 1.14 (m, 1H), 0.98 (d, J = 6.4 Hz, 3H); ^{13}C NMR (101 MHz, $CDCl_3$) δ 166.82, 133.00, 130.60, 129.67, 128.49, 63.54, 52.28, 43.55, 37.15, 35.66, 29.99, 29.57, 22.10, 19.64; ^{19}F NMR (377 MHz, $CDCl_3$) δ -35.63.

4.6 Procedure for C-H disulfuration using TBADT photocatalyst

TABDT photocatalst was prepared according literature.[68]

To an oven-dried Schlenk tube with a magnetic stirring bar was added Harpp reagent (0.2 mmol), C-H substrate (10 eq), TBADT (2 mol%), and MeCN (2 ml). The resulting solution was degassed by three freeze-pump-thaw cycles. After backfilling with nitrogen, the tube was placed in the kessil lamp setup (390 nm) and stirred while being irradiated for given time. Solvent was removed under reduced pressure. The yields were determined by ^{1}H NMR spectra.

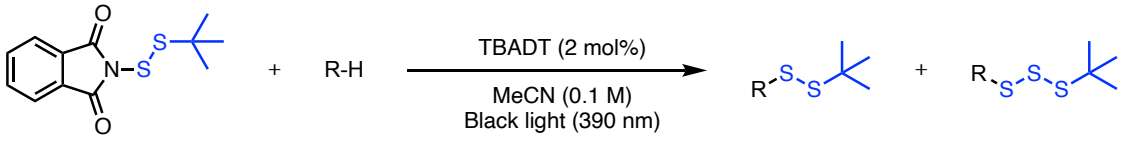

4.7 Reaction optimization of C-H disulfuration using Ir/quinuclidine system

Reaction setup was the same as described in section 4.3

DABCO-based HAT reagent was prepared according to literature.[60]

To an oven-dried Schlenk tube with a magnetic stirring bar was added *N*-perthiophthalimide, C-H substrate, K_2CO_3, Ir catalyst, and quinuclidine (or DABCO-based HAT reagent). The resulting solution was degassed by three freeze-pump-thaw cycles. After backfilling with nitrogen, the tube was placed in the LEDs setup and stirred while being irradiated for given time. The reaction mixture was then filtered through a plug of celite and the solvent was removed under reduced pressure. The yields were determined by ^{1}H NMR spectra.

1. With equivalent of THF as variant:

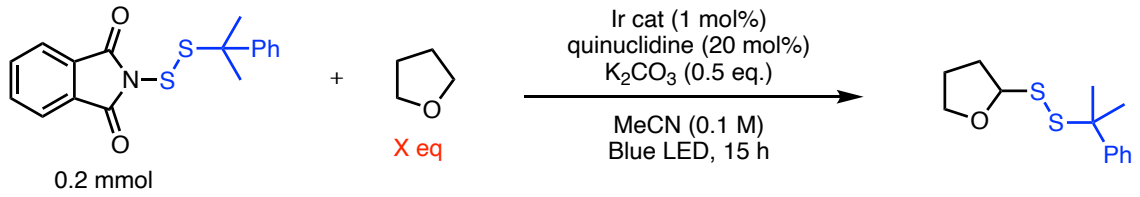

Entry	X eq of THF	NMR yield of T.M. (%)
1	0	0
2	2.5	0
3	5	60
4	7.5	68
5	10	65

2. With amount of quinuclidine as variant:

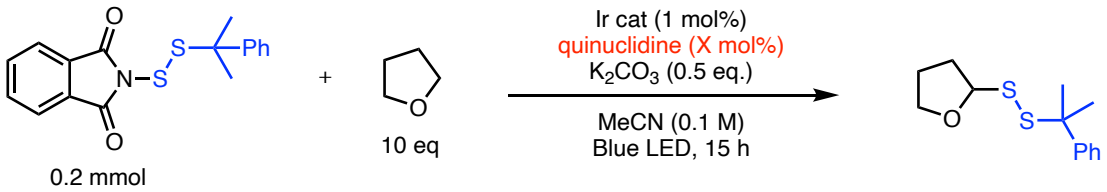

Entry	X mol% of quinuclidine	NMR yield of T.M. (%)
1	10%	68
2	20%	71
3	50%	56
4	100%	43

3. With base as variant:

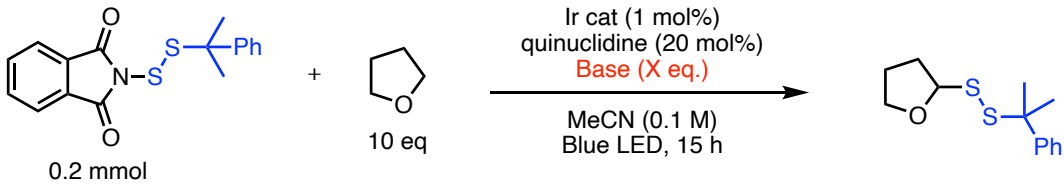

Entry	X eq / type of base	NMR yield of T.M. (%)
1	0 eq/ K2CO3	62
2	0.5 eq/K2CO3	71
3	1 eq/ K2CO3	77
4	1.5 eq/ K2CO3	73
5	1 eq/ tBuOK	0
6	1 eq/ Cs2CO3	69

4. With amount of Ir as variant:

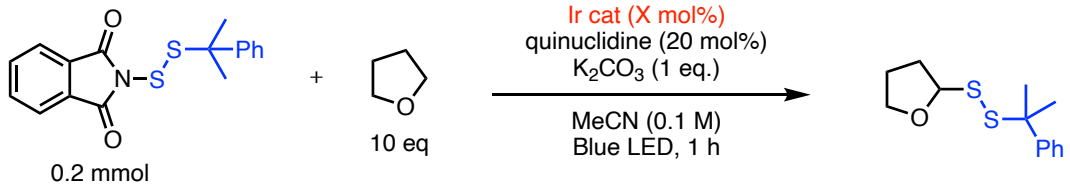

Entry	X mol% of quinuclidine	NMR yield of T.M. (%)
1	1%	80
2	2%	75
3	4%	78

5. With solvent as variant:

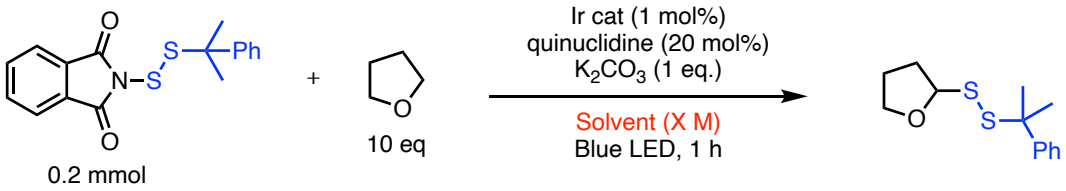

Entry	solvent	concentration	NMR yield of T.M. (%)
1	MeCN	0.05 M	78
2	MeCN	0.1 M	80
3	MeCN	0.2 M	7 (SM: 45%, messy crude)
4	EtOAc	0.1 M	23 (SM: 18%)
5	DCE	0.1 M	58

6. Other control experiments[a][b]:

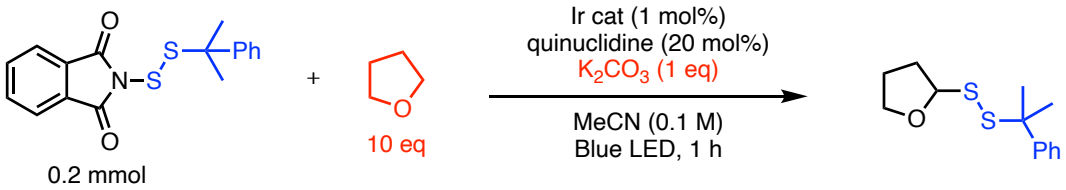

		+ THF - base	-THF -base (decomp)	- THF + base
1h	T.M	70	-	-
	Harpp	0	38	35
	Tetrasulfide (4S)	0	13	10
	Trisulfide (3S)	10	10	11
3h	T.M	72	-	-
	Harpp	0	20	17
	Tetrasulfide (4S)	0	13	14
	Trisulfide (3S)	10	10	12
7h	T.M	-	-	-
	Harpp	-	0	0
	Tetrasulfide (4S)	-	13	15
	Trisulfide (3S)	-	10	11
10h	T.M	60	-	-
	Trisulfide (3S)	10	-	-

[a] '+'indicates the experiment with addition of the component; '-'indicates reaction with absence of the component [b] Yields were determined by ^{1}H NMR spectrum of crude mixture

Noteworthy, the reaction completed (full consumption of Harpp reagent) in 1h and 7h with and without THF respectively. Meanwhile, the presence of base showed no influence to the decomposition rate of Harpp reagent. In all of the cases, trisulfide and tetrasulfide were generated in situ. But only with presence of THF, tetrasulfide was subsequently consumed.

4.8 Cyclic voltammetry of *N*-perthiophthalimide and *N*-thiophthalimide derivatives.

Cyclic voltammagrams were measured at 25 °C in dry acetonitrile containing $Bu_4N \cdot PF_6$ (0.1 M) as supporting electrolyte. Experiments were carried out with a potentiostat equipped with a glassy-carbon working electrode, a platinum auxiliary electrode, and a $Ag/AgNO_3$ (0.005 M) reference electrode. Each analyte was prepared as a 3 mM solution in 0.1 M electrolyte. The given E_{pc} were determined relative to ferrocene ($Fc^{+/0}$), and then converted to V vs. SCE using the conversion $E^{o}_{1/2}$ ($Fc^{+/0}$) = +0.400 V vs. SCE.[69]

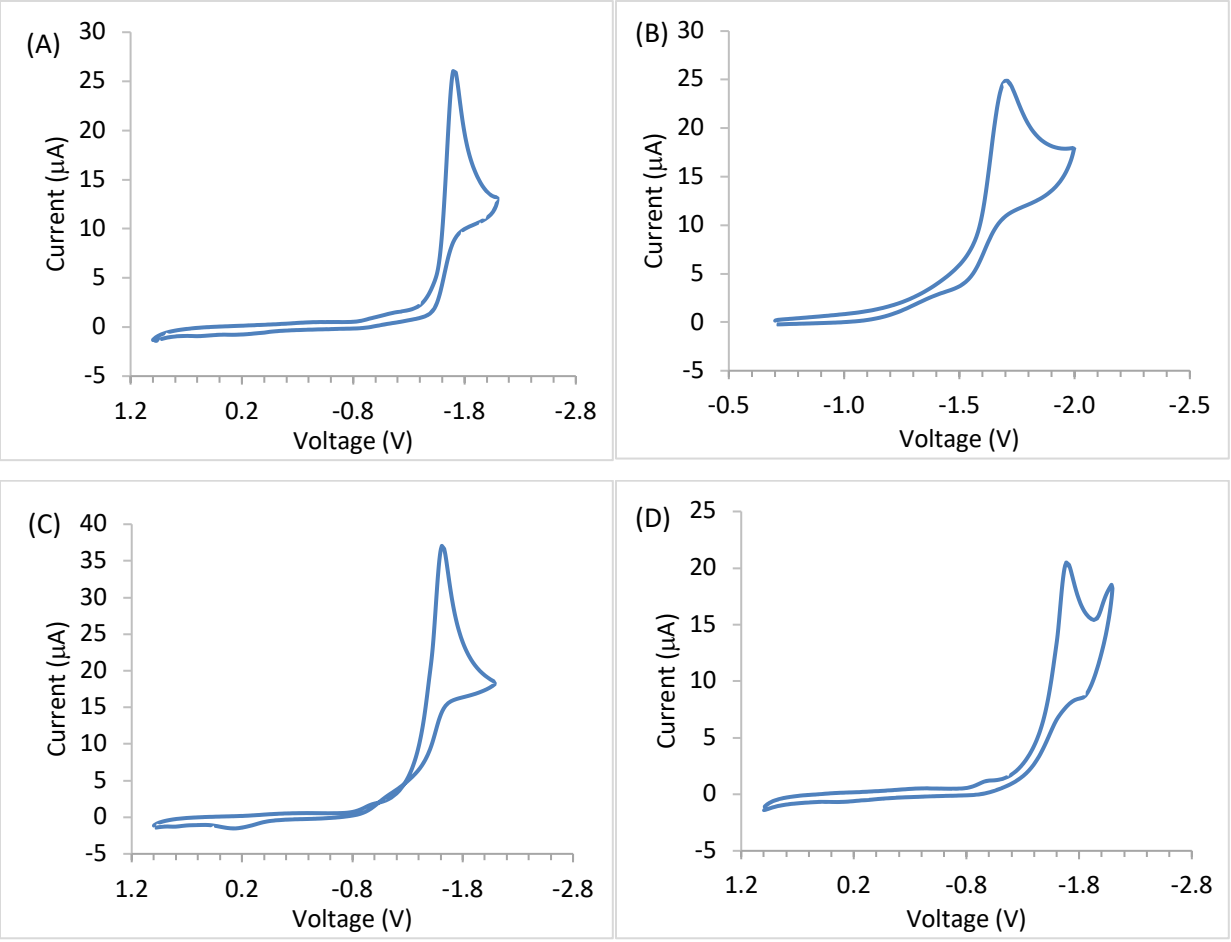

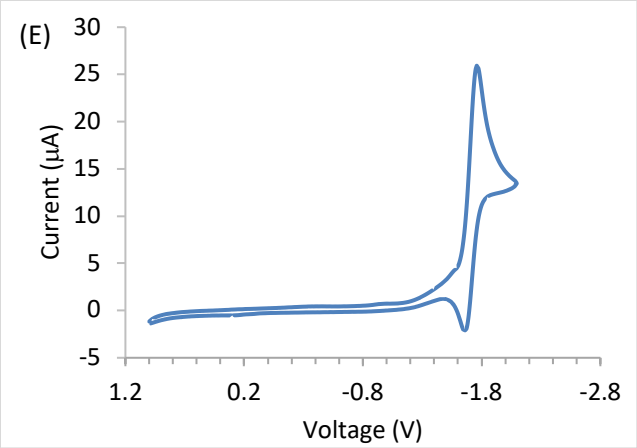

Figure S8, Representative cyclic voltammagrams of *N*-perthiophthalimide, *N*-thiophthalimide derivatives and tetrasulfides vs. Ag/Ag^+ (3 mM in 0.1M $Bu_4N{\cdot}PF_6$ electrolyte) (A) PhthSS^{t}Bu, E_{pc} = –1.67 V vs. Ag/Ag^+; E_{pc} = –1.36 V vs. SCE. (B) PhthSS-cumyl, E_{pc} = –1.70 V vs. Ag/Ag^+; E_{pc} = –1.40 V vs. SCE. (C) PhthSCF_3, E_{pc} = –1.63 V vs. Ag/Ag^+; E_{pc} = –1.34 V vs. SCE. (D) PhthSPh, E_{pc} = –1.66 V vs. Ag/Ag^+; E_{pc} = –1.37 V vs. SCE. (E) PhthS^{n}Pr, E_{pc} = –1.76 V vs. Ag/Ag^+; E_{pc} = –1.47 V vs. SCE.

Noteworthy, our CV measurements indicate that reduction of Harpp reagents, PhthSPh, and PhthSCF_3 are irreversible reaction, suggesting reduction of these species were followed by a very rapid fragmentation to form thiyl radical and phthalimide anion. As for PhthS^{n}Pr (Figure S8E), the small reversable oxidation peak indicates that the fragmentation is not as facile, probably due to the instability of *n*-propylthio radical comparing to perthio-radical and phenylthiol radical. However, the even more unstable trifluoromethylthio radical does not show the reversable curve as PhthS^{n}Pr. The reason behind this is still unclear.

4.9 Cyclic voltammetry of tetrasulfides.

Cyclic voltammagrams were measured by the same procedure as section 4.6. While measuring ^{t}BuSSSS^{t}Bu (Figure S9A), from –1.5 V to 2 V at 200 mV/s rate, an oxidation peak was observed around 1.58 V (vs. Ag/Ag^+), slightly before the limitation from the solvent (MeCN). Subsequently, a reduction peak at –1.09 V appeared while scanning back to –1.5 V. However, we found that directly scanning from 0 V to –1.5 V, without oxidation initially, the reduction peak at –1.09 would not show. This observation indicated that the reduction peak was related to fragments generated by fragmentation after oxidation of tetrasulfide (as shown below). Same observation was found in dicumyl-tetrasulfide (Figure S9B, C).

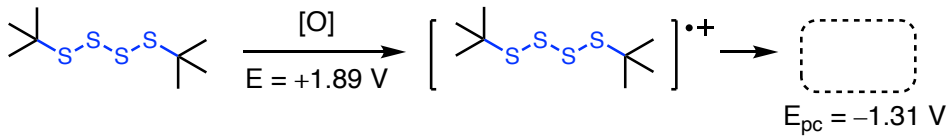

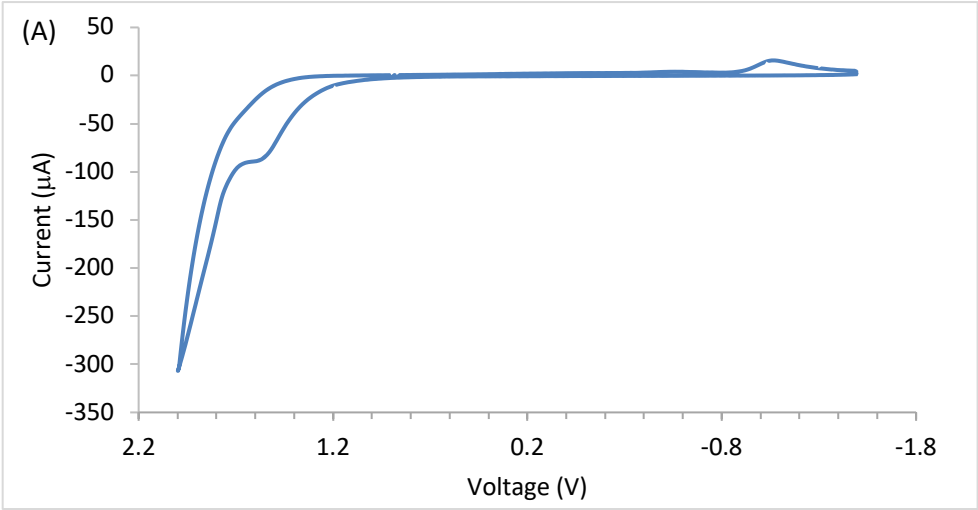

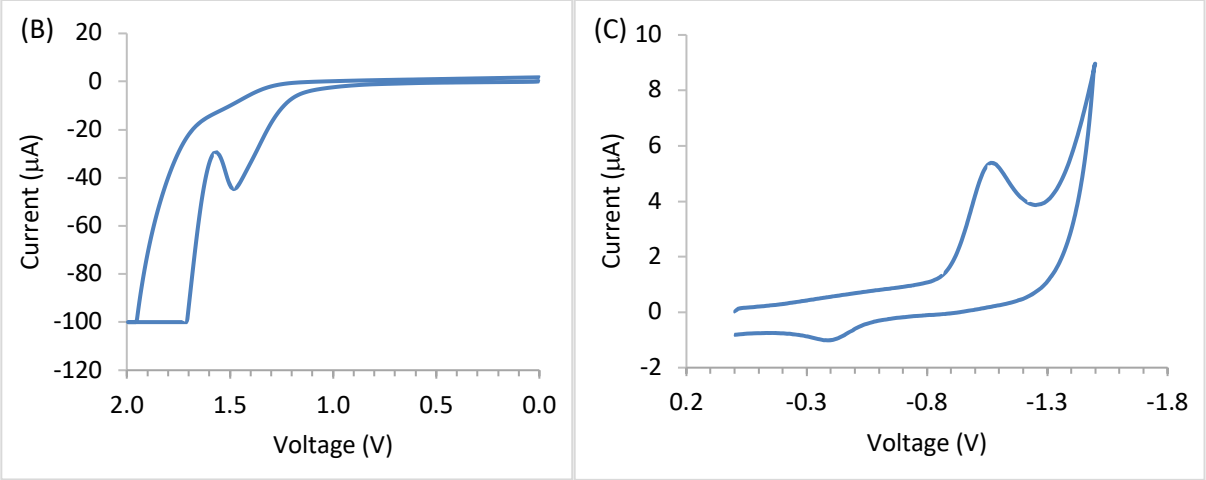

Figure S9, Cyclic voltammagrams of tetrasulfides vs. Ag/Ag^+ (3 mM in 0.1M $Bu_4N{\cdot}PF_6$ electrolyte) (A) ^{t}BuSSSS^{t}Bu, E_{pa} = 1.58 V vs. Ag/Ag^+; E_{pa} = 1.89 V vs. SCE. (B) dicumyl-tetrasulfide, scanning from 0 V to 2.0 V, found oxidation peak E_{pa} = 1.48 V vs. Ag/Ag^+; E_{pa} = 1.79 V vs. SCE. (C) dicumyl-tetrasulfide, reduction peak appeared in subsequent scanning from 0 V to –1.5 V after (B), which was –1.08 V vs. Ag/Ag^+; –0.77 V vs. SCE.

5. References

(1) Zhang, Y.; Glass, R. S.; Char, K.; Pyun, J. Recent Advances in the Polymerization of Elemental Sulphur, Inverse Vulcanization and Methods to Obtain Functional Chalcogenide Hybrid Inorganic/Organic Polymers (CHIPs). *Polym. Chem.* **2019**, *10* (30), 4078–4105. DOI: 10.1039/c9py00636b.

(2) Worthington, M. J. H.; Kucera, R. L.; Chalker, J. M. Green Chemistry and Polymers Made from Sulfur. *Green Chem.* **2017**, *19* (12), 2748–2761. DOI: 10.1039/c7gc00014f.

(3) Devendar, P.; Yang, G. F. Sulfur-Containing Agrochemicals. *Top. Curr. Chem.* **2017**, *375* (6), 1–44. DOI: 10.1007/s41061-017-0169-9.

(4) Feng, M.; Tang, B.; Liang, S. H.; Jiang, X. Sulfur Containing Scaffolds in Drugs: Synthesis and Application in Medicinal Chemistry. *Curr. Top. Med. Chem.* **2016**, *16* (11), 1200–1216. DOI: 10.2174/1568026615666150915111741.

(5) Scott, K. A.; Njardarson, J. T. Analysis of US FDA-Approved Drugs Containing Sulfur Atoms. *Top. Curr. Chem.* **2018**, *376* (1), 1–34. DOI: 10.1007/s41061-018-0184-5.

(6) Lesch, J. E. *The First Miracle Drugs: How the Sulfa Drugs Transformed Medicine.*; Oxford University Press, 2007.

(7) Williams, R. E. *Top 200 drugs Posters by Njardarson group*. https://sites.arizona.edu/njardarson-lab/top200-posters/.

(8) Bulaj, G. Formation of Disulfide Bonds in Proteins and Peptides. *Biotechnol. Adv.* **2005**, *23* (1), 87–92. DOI: 10.1016/j.biotechadv.2004.09.002.

(9) Jiang, C. S.; Müller, W. E. G.; Schröder, H. C.; Guo, Y. W. Disulfide- and Multisulfide-Containing Metabolites from Marine Organisms. *Chem. Rev.* **2012**, *112* (4), 2179–2207. DOI: 10.1021/cr200173z.

(10) Bhatwalkar, S. B.; Mondal, R.; Krishna, S. B. N.; Adam, J. K.; Govender, P.; Anupam, R. Antibacterial Properties of Organosulfur Compounds of Garlic (Allium Sativum). *Front. Microbiol.* **2021**, *12* (July), 1–20. DOI: 10.3389/fmicb.2021.613077.

(11) Caplin, M. E.; Pavel, M.; Ćwikła, J. B.; Phan, A. T.; Raderer, M.; Sedláčková, E.; Cadiot, G.; Wolin, E. M.; Capdevila, J.; Wall, L.; Rindi, G.; Langley, A.; Martinez, S.; Blumberg, J.; Ruszniewski, P. Lanreotide in Metastatic Enteropancreatic Neuroendocrine Tumors. *N. Engl. J. Med.* **2014**, *371* (3), 224–233. DOI: 10.1056/nejmoa1316158.

(12) Kornberg, H. L.; Krebs, H. A. Thiols, Disulphides and Thiosulphates: Some New Reactions and Possibilities in Peptide and Protein Chemistry. *Nature* **1957**, *180*, 756–757.

(13) Ren, S.; Luo, N.; Liu, K.; Liu, J. B. Synthesis of Unsymmetrical Disulfides via the Cross-Dehydrogenation of Thiols. *J. Chem. Res.* **2021**, *45* (5–6), 365–373. DOI: 10.1177/1747519820942872.

(14) Musiejuk, M.; Witt, D. Recent Developments in the Synthesis of Unsymmetrical Disulfanes (Disulfides). A Review. *Org. Prep. Proced. Int.* **2015**, *47* (2), 95–131. DOI: 10.1080/00304948.2015.1005981.

(15) Hitomi, S.; Sei-ichi, K.; Akira, N. Sodium Tellurite as a Mild and Selective Oxidizing Agent for Thiols: Its Use in the One-Pot Synthesis of Unsymmetrical Disulfides. *Bull. Chem. Soc. Japan* **1992**, *65*, 626–627.

(16) Parida, A.; Choudhuri, K.; Mal, P. Unsymmetrical Disulfides Synthesis via Sulfenium Ion. *Chem. - An Asian J.* **2019**, *14* (15), 2579–2583. DOI: 10.1002/asia.201900620.

(17) Marchand-Brynaert, J.; Bouchet, M.; Touillaux, R.; Beauve, C.; Fastrez, J. Design and Synthesis of a Bifunctional Label for Selection of β-Lactamase Displayed on Filamentous Bacteriophage by Catalytic Activity. *Tetrahedron* **1996**, *52* (15), 5591–5606. DOI: 10.1016/0040-4020(96)00197-4.
(18) Vandavasi, J. K.; Hu, W. P.; Chen, C. Y.; Wang, J. J. Efficient Synthesis of Unsymmetrical Disulfides. *Tetrahedron* **2011**, *67* (46), 8895–8901. DOI: 10.1016/j.tet.2011.09.071.
(19) Smith, R.; Zeng, X.; Müller-Bunz, H.; Zhu, X. Synthesis of Glycosyl Disulfides Containing an α-Glycosidic Linkage. *Tetrahedron Lett.* **2013**, *54* (39), 5348–5350. DOI: 10.1016/j.tetlet.2013.07.093.
(20) Ribeiro Morais, G.; Falconer, R. A. Efficient One-Pot Synthesis of Glycosyl Disulfides. *Tetrahedron Lett.* **2007**, *48* (43), 7637–7641. DOI: 10.1016/j.tetlet.2007.08.106.
(21) Huang, P.; Wang, P.; Tang, S.; Fu, Z.; Lei, A. Electro-Oxidative S−H/S−H Cross-Coupling with Hydrogen Evolution: Facile Access to Unsymmetrical Disulfides. *Angew. Chemie - Int. Ed.* **2018**, *57* (27), 8115–8119. DOI: 10.1002/anie.201803464.
(22) Qiu, X.; Yang, X.; Zhang, Y.; Song, S.; Jiao, N. Efficient and Practical Synthesis of Unsymmetrical Disulfides: Via Base-Catalyzed Aerobic Oxidative Dehydrogenative Coupling of Thiols. *Org. Chem. Front.* **2019**, *6* (13), 2220–2225. DOI: 10.1039/c9qo00239a.
(23) Arisawa, M.; Yamaguchi, M. Rhodium-Catalyzed Disulfide Exchange Reaction. *J. Am. Chem. Soc.* **2003**, *125* (22), 6624–6625. DOI: 10.1021/ja035221u.
(24) Wang, D.; Gao, Y.; Tong, Y.; Xiong, M.; Liang, X.; Zhu, H.; Pan, Y. Unsymmetrical Disulfides Synthesis via Cs2CO3-Catalyzed Three-Component Reaction in Water. *Adv. Synth. Catal.* **2020**, *362* (22), 4991–4995. DOI: 10.1002/adsc.202000851.
(25) Xiao, X.; Feng, M.; Jiang, X. Transition-Metal-Free Persulfuration to Construct Unsymmetrical Disulfides and Mechanistic Study of the Sulfur Redox Process. *Chem. Commun.* **2015**, *51* (20), 4208–4211. DOI: 10.1039/c4cc09633a.
(26) Chatterji, T.; Keerthi, K.; Gates, K. S. Generation of Reactive Oxygen Species by a Persulfide (BnSSH). *Bioorganic Med. Chem. Lett.* **2005**, *15* (17), 3921–3924. DOI: 10.1016/j.bmcl.2005.05.110.
(27) Xiao, X.; Feng, M.; Jiang, X. New Design of a Disulfurating Reagent: Facile and Straightforward Pathway to Unsymmetrical Disulfanes by Copper-Catalyzed Oxidative Cross-Coupling. *Angew. Chem. Int. Ed.* **2016**, *55* (45), 14121–14125. DOI: 10.1002/anie.201608011.
(28) Xiao, X.; Xue, J.; Jiang, X. Polysulfurating Reagent Design for Unsymmetrical Polysulfide Construction. *Nat. Commun.* **2018**, *9* (1), 2191. DOI: 10.1038/s41467-018-04306-5.
(29) Wang, W.; Lin, Y.; Ma, Y.; Tung, C. H.; Xu, Z. Cu-Catalyzed Electrophilic Disulfur Transfer: Synthesis of Unsymmetrical Disulfides. *Org. Lett.* **2018**, *20* (13), 3829–3832. DOI: 10.1021/acs.orglett.8b01418.
(30) Zou, J.; Chen, J.; Shi, T.; Hou, Y.; Cao, F.; Wang, Y.; Wang, X.; Jia, Z.; Zhao, Q.; Wang, Z. Phthalimide-Carried Disulfur Transfer to Synthesize Unsymmetrical Disulfanes via Copper Catalysis. *ACS Catal.* **2019**, *9* (12), 11426–11430. DOI: 10.1021/acscatal.9b04326.
(31) Harpp, D. N.; Steliou, K.; Chan, T. H. Synthesis and Reactions of Some New Sulfur Transfer Reagents. *J. Am. Chem. Soc.* **1978**, *505* (1977), 1222–1228. DOI: 10.1021/ja00472a032.
(32) Gao, W. C.; Tian, J.; Shang, Y. Z.; Jiang, X. Steric and Stereoscopic Disulfide Construction

for Cross-Linkage via N -Dithiophthalimides. *Chem. Sci.* **2020**, *11* (15), 3903–3908. DOI: 10.1039/d0sc01060j.

(33) Wang, D.; Li, W.; Shi, K.; Pan, Y. LiBr-Catalyzed C3-Disulfuration between Indole and N-Dithiophthalimide. *J. Org. Chem.* **2022**, *88* (4), 2550–2556. DOI: 10.1021/acs.joc.1c02556.

(34) Wu, Z.; Pratt, D. A. Radical Substitution Provides a Unique Route to Disulfides. *J. Am. Chem. Soc.* **2020**, *142* (23), 10284–10290. DOI: 10.1021/jacs.0c03626.

(35) Chauvin, J. P. R.; Haidasz, E. A.; Griesser, M.; Pratt, D. A. Polysulfide-1-Oxides React with Peroxyl Radicals as Quickly as Hindered Phenolic Antioxidants and Do so by a Surprising Concerted Homolytic Substitution. *Chem. Sci.* **2016**, *7* (10), 6347–6356. DOI: 10.1039/c6sc01434h.

(36) Wu, Z.; Pratt, D. A. A Divergent Strategy for Site-Selective Radical Disulfuration of Carboxylic Acids with Trisulfide-1,1-Dioxides. *Angew. Chem. Int. Ed.* **2021**, *60* (28), 15598–15605. DOI: 10.1002/anie.202104595.

(37) Tzirakis, M. D.; Lykakis, I. N.; Orfanopoulos, M. Decatungstate as an Efficient Photocatalyst in Organic Chemistry. *Chem. Soc. Rev.* **2009**, *38* (9), 2609–2621. DOI: 10.1039/b812100c.

(38) Schultz, D. M.; Lévesque, F.; DiRocco, D. A.; Reibarkh, M.; Ji, Y.; Joyce, L. A.; Dropinski, J. F.; Sheng, H.; Sherry, B. D.; Davies, I. W. Oxyfunctionalization of the Remote C−H Bonds of Aliphatic Amines by Decatungstate Photocatalysis. *Angew. Chemie - Int. Ed.* **2017**, *56* (48), 15274–15278. DOI: 10.1002/anie.201707537.

(39) Zhang, J.; Studer, A. Decatungstate-Catalyzed Radical Disulfuration Through Direct C-H Functionalization for the Preparation of Unsymmetrical Disulfides. *Nat. Commun.* **2022**, *13*, 3886. DOI: 10.1038/s41467-022-31617-5.

(40) Mukherjee, S.; Maji, B.; Tlahuext-Aca, A.; Glorius, F. Visible-Light-Promoted Activation of Unactivated C(Sp3)-H Bonds and Their Selective Trifluoromethylthiolation. *J. Am. Chem. Soc.* **2016**, *138* (50), 16200–16203. DOI: 10.1021/jacs.6b09970.

(41) Mukherjee, S.; Patra, T.; Glorius, F. Cooperative Catalysis: A Strategy to Synthesize Trifluoromethyl-Thioesters from Aldehydes. *ACS Catal.* **2018**, *8* (7), 5842–5846. DOI: 10.1021/acscatal.8b01519.

(42) Candish, L.; Pitzer, L.; Gómez-Suárez, A.; Glorius, F. Visible Light-Promoted Decarboxylative Di- A Nd Trifluoromethylthiolation of Alkyl Carboxylic Acids. *Chem. Eur. J.* **2016**, *22* (14), 4753–4756. DOI: 10.1002/chem.201600421.

(43) Schirmer, T. E.; Rolka, A. B.; Karl, T. A.; Holzhausen, F.; König, B. Photocatalytic C-H Trifluoromethylthiolation by the Decatungstate Anion. *Org. Lett.* **2021**, *23* (15), 5729–5733. DOI: 10.1021/acs.orglett.1c01870.

(44) Xu, W.; Ma, J.; Yuan, X. A.; Dai, J.; Xie, J.; Zhu, C. Synergistic Catalysis for the Umpolung Trifluoromethylthiolation of Tertiary Ethers. *Angew. Chem. Int. Ed* **2018**, *57* (32), 10357–10361. DOI: 10.1002/anie.201805927.

(45) Xu, W.; Wang, W.; Liu, T.; Xie, J.; Zhu, C. Late-Stage Trifluoromethylthiolation of Benzylic C-H Bonds. *Nat. Commun.* **2019**, *10*, 4867. DOI: 10.1038/s41467-019-12844-9.

(46) Morcillo, S. P.; Dauncey, E. M.; Kim, J. H.; Douglas, J. J.; Sheikh, N. S.; Leonori, D. Photoinduced Remote Functionalization of Amides and Amines Using Electrophilic Nitrogen Radicals. *Angew. Chem. Int. Ed.* **2018**, *57* (39), 12945–12949. DOI: 10.1002/anie.201807941.

(47) Mackenzie, I. A.; Wang, L.; Onuska, N. P. R.; Williams, O. F.; Begam, K.; Moran, A. M.; Dunietz, B. D.; Nicewicz, D. A.; Onuska, N. P. R. Discovery and Characterization of an Acridine Radical Photoreductant. *Nature* **2020**, *580*, 76–80. DOI: 10.1038/s41586-020-2131-1.
(48) K. Prier, C.; A. Rankic, D.; W. C. MacMillan, D. Visible Light Photoredox Catalysis with Transition Metal Complexes: Applications in Organic Synthesis. *Chem. Rev.* **2013**, *113* (7), 5322–5363. DOI: 10.1021/cr300503r.
(49) Montgomery, J. A.; Frisch, M. J.; Ochterski, J. W.; Petersson, G. A. A Complete Basis Set Model Chemistry. VI. Use of Density Functional Geometries and Frequencies. *J. Chem. Phys.* **1999**, *110* (2–12), 2822–2827. DOI: 10.1063/1.477924.
(50) Munavalli, S.; Rohrbaugh, D. K.; Rossman, D. I.; Berg, F. J.; Wagner, G. W.; Durst, H. D. Trifluoromethylsulfenylation of Masked Carbonyl Compounds. *Synth. Commun.* **2000**, *30* (16), 2847–2854. DOI: 10.1080/00397910008087435.
(51) Murarka, S. N-(Acyloxy)Phthalimides as Redox-Active Esters in Cross-Coupling Reactions. *Adv. Synth. Catal.* **2018**, *360* (9), 1735–1753. DOI: 10.1002/adsc.201701615.
(52) Parida, S. K.; Mandal, T.; Das, S.; Hota, S. K.; De Sarkar, S.; Murarka, S. Single Electron Transfer-Induced Redox Processes Involving N-(Acyloxy)Phthalimides. *ACS Catal.* **2021**, *11* (3), 1640–1683. DOI: 10.1021/acscatal.0c04756.
(53) Okada, K.; Okamoto, K.; Oda, M. A New and Practical Method of Decarboxylation: Photosensitized Decarboxylation of N-Acyloxyphthalimides via Electron-Transfer Mechanism. *J. Am. Chem. Soc.* **1988**, *110* (26), 8736–8738. DOI: 10.1021/ja00234a047.
(54) Joshi-Pangu, A.; Lévesque, F.; Roth, H. G.; Oliver, S. F.; Campeau, L. C.; Nicewicz, D.; DiRocco, D. A. Acridinium-Based Photocatalysts: A Sustainable Option in Photoredox Catalysis. *J. Org. Chem.* **2016**, *81* (16), 7244–7249. DOI: 10.1021/acs.joc.6b01240.
(55) Patra, T.; Bellotti, P.; Strieth-Kalthoff, F.; Glorius, F. Photosensitized Intermolecular Carboimination of Alkenes through the Persistent Radical Effect. *Angew. Chem. Int. Ed.* **2020**, *59* (8), 3172–3177. DOI: 10.1002/anie.201912907.
(56) Ravelli, D.; Fagnoni, M.; Fukuyama, T.; Nishikawa, T.; Ryu, I. Site-Selective C-H Functionalization by Decatungstate Anion Photocatalysis: Synergistic Control by Polar and Steric Effects Expands the Reaction Scope. *ACS Catal.* **2018**, *8* (1), 701–713. DOI: 10.1021/acscatal.7b03354.
(57) Xiao, W.; Wang, X.; Liu, R.; Wu, J. Quinuclidine and Its Derivatives as Hydrogen-Atom-Transfer Catalysts in Photoinduced Reactions. *Chinese Chem. Lett.* **2021**, *32* (6), 1847–1856. DOI: 10.1016/j.cclet.2021.02.009.
(58) Jeffrey, J. L.; Terrett, J. A.; MacMillant, D. W. C. O-H Hydrogen Bonding Promotes H-Atom Transfer from α C-H Bonds for C-Alkylation of Alcohols. *Science (80-.).* **2015**, *349* (6255), 1532–1536. DOI: 10.1126/science.aac8555.
(59) Leng, S.; Christner, J. A.; Carlson, S. K.; Jacobsen, M.; Vrieze, T. J.; Atwell, T. D.; McCollough, C. H. Handbook of Bond Energies. *American Journal of Roentgenology*. 2011, pp 1–1687.
(60) Matsumoto, A.; Yamamoto, M.; Maruoka, K. Cationic DABCO-Based Catalyst for Site-Selective C–H Alkylation via Photoinduced Hydrogen-Atom Transfer. *ACS Catal.* **2022**, *12* (3), 2045–2051. DOI: 10.1021/acscatal.1c05484.
(61) Kim, H.; Kim, T.; Gil Lee, D.; Weon Roh, S.; Lee, C. Nitrogen-Centered Radical-Mediated

C–H Imidation of Arenes and Heteroarenes via Visible Light Induced Photocatalysis. *Chem. Commun.* **2014**, *50* (66), 9273–9276. DOI: 10.1039/c4cc03905j.

(62) Sheppard, J. G.; Long, T. E. Allicin-Inspired Thiolated Fluoroquinolones as Antibacterials against ESKAPE Pathogens. *Bioorganic Med. Chem. Lett.* **2016**, *26* (22), 5545–5549. DOI: 10.1016/j.bmcl.2016.10.002.

(63) Xing, S.; Zhu, Y. Y.; Liu, W.; Liu, Y.; Zhang, J.; Zhang, H.; Wang, Y.; Ni, S. F.; Shao, X. C-H Fluoroalkylsulfinylation/Intramolecular Rearrangement for Precise Synthesis of Fluoroalkyl Sulfoxides. *Org. Lett.* **2022**. DOI: 10.1021/acs.orglett.2c01151.

(64) Saravanan, P.; Anbarasan, P. Palladium Catalyzed Aryl(Alkyl)Thiolation of Unactivated Arenes. *Org. Lett.* **2014**, *16* (3), 848–851. DOI: 10.1021/ol4036209.

(65) White, A. R.; Wang, L.; Nicewicz, D. A. Synthesis and Characterization of Acridinium Dyes for Photoredox Catalysis. *Synlett* **2019**, *30* (7), 827–832. DOI: 10.1055/s-0037-1611744.

(66) Gong, Y.; Zhu, Z.; Qian, Q.; Tong, W.; Gong, H. Zn- And Cu-Catalyzed Coupling of Tertiary Alkyl Bromides and Oxalates to Forge Challenging C−O, C−S, and C−N Bonds. *Org. Lett.* **2021**, *23* (3), 1005–1010. DOI: 10.1021/acs.orglett.0c04206.

(67) Koziakov, D.; Majek, M.; Jacobi von Wangelin, A. Radical Aromatic Trifluoromethylthiolation: Photoredox Catalysis vs. Base Mediation. *Eur. J. Org. Chem.* **2017**, *2017* (45), 6722–6725. DOI: 10.1002/ejoc.201701339.

(68) Perry, I. B.; Brewer, T. F.; Sarver, P. J.; Schultz, D. M.; DiRocco, D. A.; MacMillan, D. W. C. Direct Arylation of Strong Aliphatic C–H Bonds. *Nature* **2018**, *560* (7716), 70–75. DOI: 10.1038/s41586-018-0366-x.

(69) Connelly, N. G.; Geiger, W. E. Chemical Redox Agents for Organometallic Chemistry. *Chem. Rev.* **1996**, *96* (2), 877–910. DOI: 10.1021/cr940053x.

(70) Huttunen, K. M.; Mannila, A.; Laine, K.; Kemppainen, E.; Leppanen, J.; Vepsalainen, J.; Jarvinen, T.; Rautio, J. The First Bioreversible Prodrug of Metformin with Improved Lipophilicity and Enhanced Intestinal Absorption. *J. Med. Chem.* **2009**, *52* (14), 4142–4148. DOI: 10.1021/jm900274q.

6. Supporting Information

6.1 Characterization Data

Harpp reagents (**1a** – **1g**) were synthesized following the experimental procedure in Section 4.2.1

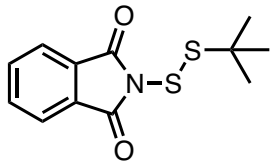

2-(tert-butyldisulfaneyl)isoindoline-1,3-dione (1a). **1a** was obtained as a white solid (87%). ^{1}H NMR (400 MHz, $CDCl_3$) δ 7.94 – 7.88 (m, 2H), 7.80 – 7.74 (m, 2H), 1.40 (s, 9H).; ^{13}C NMR (101 MHz, $CDCl_3$) δ 167.71, 134.82, 132.28, 124.10, 49.35, 29.98.; HRMS–EI (*m/z*) calcd for $C_{12}H_{13}NO_2S_2$ [M^+]: 267.0388, found 267.0396.

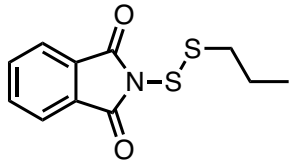

2-(propyldisulfaneyl)isoindoline-1,3-dione (1b). **1b** was obtained as a white solid (50%). ^{1}H NMR (400 MHz, $CDCl_3$) δ 7.96 – 7.90 (m, 2H), 7.82 – 7.76 (m, 2H), 3.03 (t, J = 7.44, 2H), 1.88 – 1.77 (m, 2H), 1.01 (t, J = 7.3 Hz, 3H).; ^{13}C NMR (101 MHz, $CDCl_3$) δ 167.97, 134.89, 132.39, 124.17, 43.10, 22.60, 13.16.; HRMS–EI (*m/z*) calcd for $C_{11}H_{11}NO_2S_2$ [M^+]: 253.0231, found 253.0228.

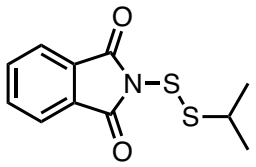

2-(isopropyldisulfaneyl)isoindoline-1,3-dione (1c). **1c** was obtained as a white solid (67%). ^{1}H NMR (400 MHz, $CDCl_3$) δ 7.95 – 7.89 (m, 2H), 7.81 – 7.75 (m, 2H), 3.36 (p, *J* = 6.8 Hz, 1H), 1.40 (d, *J* = 6.7 Hz, 6H).; ^{13}C NMR (101 MHz, $CDCl_3$) δ 167.96, 134.86, 132.39, 124.15, 43.21, 22.49; HRMS–EI (*m/z*) calcd for $C_{11}H_{11}NO_2S_2$ [M^+]: 253.0231, found 253.0620.

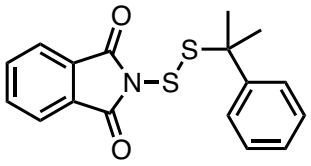

2-((2-phenylpropan-2-yl)disulfaneyl)isoindoline-1,3-dione (1d). **1d** was obtained as a white solid (89%). ^{1}H NMR (400 MHz, $CDCl_3$) δ 7.87 – 7.81 (m, 2H), 7.78 – 7.71 (m, 2H), 7.49 – 7.43 (m, 2H), 7.22 – 7.15 (m, 2H), 7.10 – 7.04 (m, 1H), 1.84 (s, 6H).; 13C NMR (101 MHz, $CDCl_3$) δ 167.30, 144.17, 134.68, 132.19, 128.35, 127.30, 126.81, 123.96, 54.38, 28.91.; HRMS–EI (m/z) calcd for $C_{17}H_{15}NO_2S_2$ [M^+]: 329.0544, found fragments [$C_8H_4NO_2S_2$ + H] (for PhthSS + H, calculated: 210.9762): 210.9772 and [C_9H_{12}] (for $C(CH_3)_2Ph$, calculated: 119.0861): 119.0874.

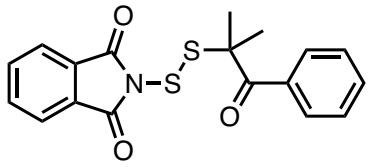

2-((2-methyl-1-oxo-1-phenylpropan-2-yl)disulfaneyl)isoindoline-1,3-dione (1e). **1e** was obtained as a white solid. ^{1}H NMR (400 MHz, $CDCl_3$) δ 7.96 – 7.85 (m, 2H), 7.85 – 7.62 (m, 4H), 7.22 – 7.06 (m, 3H), 1.77 (s, 6H).; ^{13}C NMR (101 MHz, $CDCl_3$) δ 198.58, 166.91, 135.17, 134.62, 131.88, 131.86, 129.70, 127.94, 123.95, 58.89, 26.65.; HRMS–EI (m/z) calcd for $C_{18}H_{15}NO_3S_2$ [M^+]: 357.0493, found fragments [$C_8H_4NO_2S_2$ + H] (for PhthSS + H, calculated: 210.9762): 210.9787.

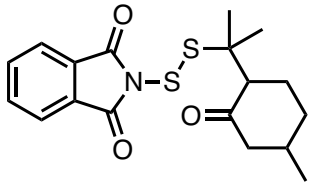

2-((2-(4-methyl-2-oxocyclohexyl)propan-2-yl)disulfaneyl)isoindoline-1,3-dione (1f). **1f** was obtained as white solid. ^{1}H NMR (400 MHz, $CDCl_3$) δ 7.95 – 7.89 (m, 2H), 7.82 – 7.75 (m, 2H), 2.98 (dd, J = 13.1, 4.7 Hz, 1H), 2.31 – 2.16 (m, 2H), 2.12 (m, 1H), 1.87 – 1.67 (m, 2H), 1.60 (s, 3H), 1.51 – 1.39 (m, 1H), 1.38 (s, 3H), 1.28 – 1.12 (m, 1H), 0.97 (d, J = 6.4 Hz, 3H).; ^{13}C NMR (101 MHz, $CDCl_3$) δ 210.68, 167.68, 134.98, 132.19, 124.10, 56.27, 54.32, 52.25, 36.72, 34.15, 29.73, 27.13, 23.23, 22.37.; HRMS–EI (m/z) calcd for $C_{18}H_{21}NO_3S_2$ [M^+]: 363.0963, found fragments [$C_8H_4NO_2S_2$ + H] (for PhthSS + H, calculated: 210.9762): 210.9769 and [$C_{10}H_{18}O$] (for $C(CH_3)_2C_7H_{11}O$, calculated: 153.1279): 153.1260.

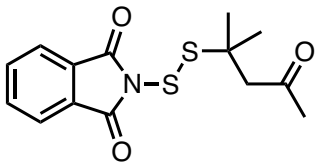

2-((2-methyl-4-oxopentan-2-yl)disulfaneyl)isoindoline-1,3-dione (1g). **1g** was obtained as white solid. ^{1}H NMR (400 MHz, $CDCl_3$) δ 7.98 – 7.87 (m, 2H), 7.87 – 7.70 (m, 2H), 2.94 (s, 2H), 2.12 (s, 3H), 1.48 (s, 6H); ^{13}C NMR (101 MHz, $CDCl_3$) δ 206.21, 167.69, 134.96, 132.19, 124.15, 53.02, 50.30, 31.96, 27.34; HRMS–EI (m/z) calcd for $C_{14}H_{15}NO_3S_2$ [M^+]: 309.0493, found fragments [$C_8H_4NO_2S_2$ + H] (for PhthSS + H, calculated: 210.9762): 210.9762 and [$C_6H_{11}O$] (for $C(CH_3)_2CH_2COCH_3$, calculated: 99.0810): 99.0822.

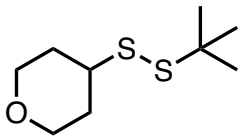

4-(tert-Butyldisulfaneyl)tetrahydro-2H-pyran (3a). Following the general procedure in section 4.3, **3a** was obtained as a colorless oil (29.6 mg, 72%). ^{1}H NMR (400 MHz, $CDCl_3$) δ 3.99 (m, 2H), 3.40 (ddd, *J* = 11.6, 10.7, 2.4 Hz, 2H), 2.89 (m, 1H), 2.07 – 1.94 (m, 2H), 1.67 – 1.50 (m, 2H), 1.33 (s, 9H); ^{13}C NMR (151 MHz, $CDCl_3$) δ 67.50, 47.63, 46.90, 32.93, 30.17; HRMS–EI (*m/z*) calcd for $C_9H_{18}OS_2$ [M+]: 206.0799, found 206.0807.

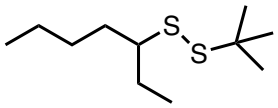

1-(tert-Butyl)-2-(heptan-3-yl)disulfane (3b). Following the general procedure in section 4.3, **3b** was obtained as a colorless oil (36.9 mg, 84%). ^{1}H NMR (400 MHz, $CDCl_3$) δ 2.66 (m, 1H), 1.72 – 1.52 (m, 4H), 1.47 – 1.26 (m, 4H), 1.32 (s, 9H), 0.97 (t, J = 7.4 Hz, 3H), 0.91 (t, J = 7.1 Hz, 3H); ^{13}C NMR (101 MHz, $CDCl_3$) δ 54.80, 47.49, 33.42, 30.18, 29.08, 26.87, 22.87, 14.17, 11.05; HRMS–EI (*m/z*) calcd for $C_{11}H_{24}S_2$ [M+]: 220.1319, found 220.1292

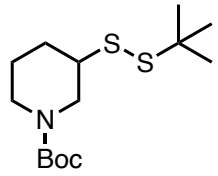

tert-Butyl 3-(tert-butyldisulfaneyl)piperidine-1-carboxylate (3c). Following the general procedure in section 4.3, **3c** was obtained as a colorless oil (34.3 mg, 64%). ^{1}H NMR (400 MHz, $CDCl_3$) δ 4.20 (m, 1H), 3.90 – 3.69 (m, 1H), 2.99 – 2.80 (m, 2H), 2.80 – 2.64 (m, 1H), 2.16 – 1.98 (m, 1H), 1.82 – 1.67 (m, 1H), 1.51-1.42 (m, 2H), 1.46 (s, 9H), 1.33 (s, 9H); ^{13}C NMR (151 MHz, $CDCl_3$) δ 154.69, 79.76, 49.51, 47.68, 43.99, 30.67, 30.12, 28.63, 28.58, 25.03; HRMS–EI (*m/z*) calcd for $C_{14}H_{20}OS_2$ [M+]: 268.0956, found 268.0949.

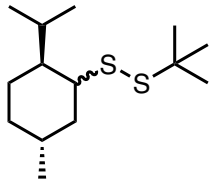

1-(tert-Butyl)-2-((2S,5R)-2-isopropyl-5-methylcyclohexyl)disulfane (3d). Following the general procedure in section 4.3, **3d** was obtained as a colorless oil (35.9 mg, 69%). ^{1}H NMR (400 MHz, $CDCl_3$) δ 3.36 – 3.30 (m, 0.6H), 2.64 – 2.54 (m, 0.4H), 2.48 – 2.39 (m, 0.4H), 2.39 – 2.28 (m, 1H), 1.93 – 1.61 (m, 3H), 1.39 – 1.36 (m, 0.6H), 1.34 – 1.31 (m, 9H), 1.28 – 1.22 (m, 0.4H), 1.21 – 1.09 (m, 1.6H), 1.05 – 0.99 (m, 2H), 0.95 – 0.80 (m, 9H); ^{13}C NMR (101 MHz, $CDCl_3$) δ 53.49, 53.13, 49.22, 48.12, 47.49, 43.11, 39.63, 35.61, 34.79, 33.42, 30.33, 30.22, 29.96, 27.49, 26.17, 25.31, 24.86, 22.42, 22.39, 21.51, 21.49, 21.34, 15.80; HRMS–EI (*m/z*) calcd for $C_{14}H_{28}S_2$ [M+]: 260.1632, found 260.1627.

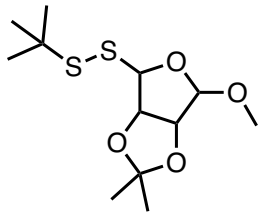

4-(tert-Butyldisulfaneyl)-6-methoxy-2,2-dimethyltetrahydrofuro[3,4-d][1,3]dioxole (3e). Following the general procedure in section 4.3, **3e** was obtained as a colorless oil (38.2 mg, 65%). ^{1}H NMR (400 MHz, $CDCl_3$) δ 5.19 (s, 1H), 5.04 (s, 1H), 4.97 (d, *J* = 5.7 Hz, 1H), 4.65 (d, *J* = 5.7 Hz, 1H), 3.41 (s, 3H), 1.45 (s, 3H), 1.36 (s, 9H), 1.31 (s, 3H); ^{13}C NMR (101 MHz, $CDCl_3$) δ 112.97, 110.40, 98.63, 86.55, 84.50, 55.46, 48.07, 29.99, 26.49, 25.18. NMR data are consistent with literature data.[36]

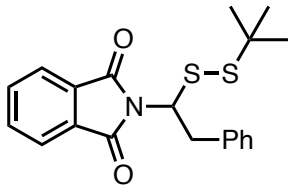

2-(1-(tert-Butyldisulfaneyl)-2-phenylethyl)isoindoline-1,3-dione (3f). Following the general procedure in section 4.3 with DMF as solvent, **3f** was obtained as a while solid (43.7 mg, 59%). ^{1}H NMR (400 MHz, $CDCl_3$) δ 7.82 – 7.76 (m, 2H), 7.72 – 7.65 (m, 2H), 7.24 – 7.10 (m, 5H), 5.54 (dd, *J* = 10.5, 6.0 Hz, 1H), 3.63 (dd, *J* = 14.1, 10.6 Hz, 1H), 3.47 (dd, *J* = 14.1, 6.0 Hz, 1H), 1.30 (s, 9H); ^{13}C NMR (101 MHz, $CDCl_3$) δ 167.39, 136.99, 134.23, 131.67, 129.01, 128.74, 127.09, 123.60, 62.84, 48.38, 38.57, 29.98. NMR data are consistent with literature data.[36]

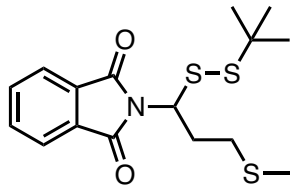

2-(1-(tert-Butyldisulfaneyl)-3-(methylthio)propyl)isoindoline-1,3-dione (3g). Following the general procedure in section 4.3 with DMF as solvent, **3g** was obtained as a white solid (39.1 mg, 55%). ^{1}H NMR (400 MHz, $CDCl_3$) δ 7.89 – 7.82 (m, 2H), 7.77 – 7.70 (m, 2H), 5.46 (dd, *J* = 8.6, 6.2 Hz, 1H), 2.67 – 2.50 (m, 3H), 2.50 – 2.38 (m, 1H), 2.07 (s, 3H), 1.31 (s, 9H); ^{13}C NMR (101 MHz, $CDCl_3$) δ 167.43, 134.37, 131.79, 123.69, 60.61, 48.29, 31.75, 31.40, 29.97, 15.55. NMR data are consistent with literature data.[36]

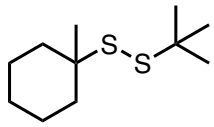

1-(tert-Butyl)-2-(1-methylcyclohexyl)disulfane (3h). Following the general procedure in section 4.3, **3h** was obtained as a colorless oil (32.7 mg, 75%). ^{1}H NMR (400 MHz, $CDCl_3$) δ 1.75 – 1.58 (m, 4H), 1.52 – 1.34 (m, 6H), 2.30 (s, 9H), 1.28 (s, 3H); ^{13}C NMR (101 MHz, $CDCl_3$) δ 50.23, 46.22, 38.20, 30.80, 30.33, 25.83, 22.92; HRMS–EI (*m/z*) calcd for $C_{11}H_{22}S_2$ [M+]: 218.1163, found 218.1153.

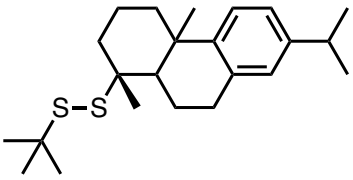

1-(tert-butyl)-2-((1R)-7-isopropyl-1,4a-dimethyl-1,2,3,4,4a,9,10,10a-octahydrophenanthren-1-yl)disulfane (3i). Following the general procedure in section 4.3, **3i** was obtained as a colorless oil (39.8 mg, 53%). ^{1}H NMR (400 MHz, $CDCl_3$) δ 7.20 – 7.12 (m, 1H), 7.03 – 6.97 (m, 1H), 6.93 – 6.88 (m, 1H), 2.96 – 2.76 (m, 3H), 2.39 – 2.22 (m, 2H), 1.91 – 1.69 (m, 6H), 1.53 – 1.40 (m, 1H), 1.34 (s, 3H), 1.31 (s, 9H), 1.25 (s, 3H), 1.23 (s, 3H), 1.23 – 1.20 (m, 3H); ^{13}C NMR (101 MHz, $CDCl_3$) δ 146.82, 145.82, 135.14, 127.13, 124.31, 123.94, 55.51, 47.74, 46.55, 40.56, 39.23, 38.03, 33.58, 30.80, 30.29, 25.50, 24.13, 24.11, 20.51, 20.21, 19.92. NMR data are consistent with literature data.[36]

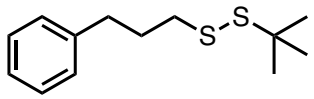

1-(tert-Butyl)-2-(3-phenylpropyl)disulfane (3j). Following the general procedure in section 4.3, **3j** was obtained as a colorless oil (30.8 mg, 65%). ^{1}H NMR (400 MHz, $CDCl_3$) δ 7.32 – 7.26 (m, 2H), 7.22 – 7.15 (m, 3H), 2.75 – 2.67 (m, 4H), 2.05 – 1.94 (m, 2H), 1.32 (s, 9H); ^{13}C NMR (151 MHz, $CDCl_3$) δ 141.56, 128.65, 128.51, 126.06, 47.89, 40.01, 34.57, 30.82, 30.10; HRMS–EI (*m/z*) calcd for $C_{13}H_{20}S_2$ [M+]: 240.1006, found 240.1004.

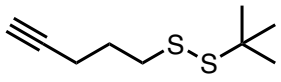

1-(tert-Butyl)-2-(pent-4-yn-1-yl)disulfane (3k). Following the general procedure in section 4.3, **3k** was obtained as a colorless oil (16.5 mg, 44%). ^{1}H NMR (400 MHz, $CDCl_3$) δ 2.79 (t, J = 7.2 Hz, 2H), 2.36 – 2.27 (m, 2H), 1.98 – 1.94 (m, 1H), 1.94 – 1.84 (m, 2H), 1.33 (s, 9H); ^{13}C NMR (101 MHz, $CDCl_3$) δ 83.53, 69.10, 47.94, 39.15, 30.09, 27.94, 17.37; HRMS–EI (*m/z*) calcd for $C_9H_{16}S_2$ [M+]: 188.0693, found 188.0685.

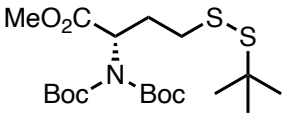

(S)-Methyl 2-((di(tert-butoxycarbonyl))amino)-4-(tert-butyldisulfanyl)butanoate (3m). Following the general procedure in section 4.3, **3m** was obtained as a colorless oil (49.8 mg, 57%). ^{1}H NMR (400 MHz, $CDCl_3$) δ 5.01 – 4.95 (m, 1H), 3.71 (s, 3H), 2.84 – 2.66 (m, 2H), 2.66 – 2.44

(m, 1H), 2.31 – 2.14 (m, 1H), 1.49 (s, 18H), 1.32 (s, 9H); ^{13}C NMR (101 MHz, $CDCl_3$) δ 171.04, 151.96, 83.46, 57.03, 52.39, 48.00, 37.09, 30.11, 30.03, 28.12; HRMS–EI (*m/z*) calcd for $C_{19}H_{35}NO_6S_2$ [M+]: 437.1906, found 437.1918.

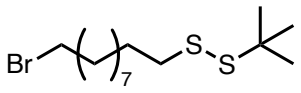

1-(10-Bromodecyl)-2-(tert-butyl)disulfane (3n). Following the general procedure in section 4.3, **3n** was obtained as a colorless oil (34.6 mg, 51%). ^{1}H NMR (400 MHz, $CDCl_3$) δ 3.41 (t, *J* = 6.9 Hz, 2H), 2.75 – 2.64 (m, 2H), 1.92 – 1.79 (m, 2H), 1.70 – 1.59 (m, 2H), 1.47 – 1.34 (m, 4H), 1.33 (s, 9H), 1.31 – 1.23 (m, 8H); ^{13}C NMR (101 MHz, $CDCl_3$) δ 47.81, 41.10, 34.20, 32.96, 30.10, 29.49, 29.43, 29.29, 28.87, 28.67, 28.30; HRMS–EI (*m/z*) calcd for $C_{14}H_{29}BrS_2$ [M+]: 340.0894, found 340.0922.

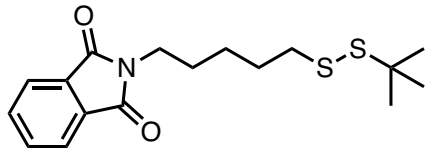

2-(5-(tert-Butyldisulfaneyl)pentyl)isoindoline-1,3-dione (3p). Following the general procedure in section 4.3, **3p** was obtained as a white solid (37.2 mg, 55%). ^{1}H NMR (400 MHz, $CDCl_3$) δ 7.85 – 7.80 (m, 2H), 7.72 – 7.67 (m, 2H), 3.67 (t, *J* = 7.2 Hz, 2H), 2.73 – 2.62 (m, 2H), 1.73 – 1.65 (m, 4H), 1.48 – 1.38 (m, 2H), 1.30 (s, 9H); ^{13}C NMR (101 MHz, $CDCl_3$) δ 168.42, 133.89, 132.14,

123.20, 47.72, 40.48, 37.84, 29.95, 28.87, 28.22, 25.81. NMR data are consistent with literature data.[36]

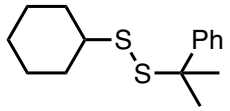

4-((2-Phenylpropan-2-yl)disulfaneyl)tetrahydro-2H-pyran (3q). Following the general procedure in section 4.3 with **1d** as starting material, **3q** was obtained as a colorless oil (38.8 mg, 73%). ^{1}H NMR (400 MHz, $CDCl_3$) δ 7.55 – 7.49 (m, 2H), 7.36 – 7.28 (m, 2H), 7.27 – 7.21 (m, 1H), 1.87 – 1.77 (m, 3H), 1.76 (s, 6H), 1.69 – 1.57 (m, 2H), 1.54 – 1.45 (m, 1H), 1.17 – 0.94 (m, 5H); ^{13}C NMR (101 MHz, $CDCl_3$) δ 145.76, 128.09, 127.00, 126.79, 51.94, 48.79, 32.82, 28.52, 26.17, 25.81; HRMS–EI (*m/z*) calcd for $C_{15}H_{22}S_2$ [M+]: 266.1163, found 266.1142.

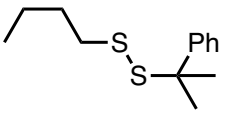

1-Butyl-2-(2-phenylpropan-2-yl)disulfane (3r). Following the general procedure in section 4.3 with **1d** as starting material, **3r** was obtained as a colorless oil (24.2 mg, 50%). ^{1}H NMR (400 MHz, $CDCl_3$) δ 7.58 – 7.46 (m, 2H), 7.37 – 7.28 (m, 2H), 7.26 – 7.19 (m, 1H), 2.22 – 2.08 (m, 2H), 1.76 (s, 6H), 1.47 – 1.37 (m, 2H), 1.29 – 1.19 (m, 2H), 0.82 (t, *J* = 7.3 Hz, 3H); ^{13}C NMR (101 MHz, $CDCl_3$) δ 145.53, 128.16, 127.05, 126.76, 52.15, 38.77, 31.23, 28.60, 21.74, 13.75; HRMS–EI (*m/z*) calcd for $C_{13}H_{20}S_2$ [M^+]: 240.1006, found 240.1025.

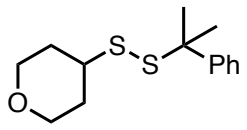

4-((2-Phenylpropan-2-yl)disulfaneyl)tetrahydro-2H-pyran (3s). Following the general procedure in section 4.3 with **1d** as starting material, **3s** was obtained as a colorless oil (39.6 mg, 74%). ^{1}H NMR (400 MHz, $CDCl_3$) δ 7.57 – 7.46 (m, 2H), 7.32 (m, 2H), 7.28 – 7.21 (m, 1H), 3.84 (dt, *J* = 11.6, 3.7 Hz, 2H), 3.09 (td, *J* = 11.3, 2.3 Hz, 2H), 1.93 – 1.83 (m, 1H), 1.77 (s, 6H), 1.72 – 1.63 (m, 2H), 1.45 – 1.28 (m, 2H); ^{13}C NMR (101 MHz, $CDCl_3$) δ 145.65, 128.11, 127.09, 126.78, 67.47, 51.97, 45.03, 32.63, 28.42; HRMS–EI (*m/z*) calcd for $C_{14}H_{20}OS_2$ [M+]: 268.0956, found 268.0949.

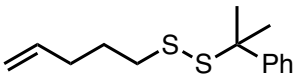

1-(Pent-4-en-1-yl)-2-(2-phenylpropan-2-yl)disulfane (3t). Following the general procedure in section 4.3 with **1d** as starting material, **3t** was obtained as a colorless oil (28.3 mg, 56%). ^{1}H NMR (400 MHz, $CDCl_3$) δ 7.55 – 7.48 (m, 2H), 7.35 – 7.28 (m, 2H), 7.26 – 7.20 (m, 1H), 5.68 (ddt, *J* = 16.9, 10.2, 6.7 Hz, 1H), 5.02 – 4.88 (m, 2H), 2.18 – 2.06 (m, 2H), 2.02 – 1.93 (m, 2H), 1.75 (s, 6H), 1.61 – 1.47 (m, 2H); ^{13}C NMR (101 MHz, $CDCl_3$) δ 145.39, 137.71, 128.08, 126.98, 126.65, 115.15, 52.08, 38.12, 32.44, 28.49, 28.15; HRMS–EI (*m/z*) calcd for $C_{14}H_{20}S_2$ [M+]: 252.1006, found 252.0998.

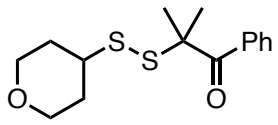

2-Methyl-1-phenyl-2-((tetrahydro-2H-pyran-4-yl)disulfaneyl)propan-1-one (3u). Following the general procedure in section 4.3 with **1e** as starting material, **3u** was obtained as a colorless oil (30.8 mg, 52%). ^{1}H NMR (400 MHz, $CDCl_3$) δ 8.13 – 8.05 (m, 2H), 7.54 – 7.44 (m, 1H), 7.44 – 7.36 (m, 2H), 3.89 – 3.80 (m, 2H), 3.20 – 3.09 (m, 2H), 2.80 – 2.65 (m, 1H), 1.88 – 1.81 (m, 2H), 1.64 (s, 6H), 1.55 – 1.40 (m, 2H); ^{13}C NMR (101 MHz, $CDCl_3$) δ 200.20, 136.46, 132.05, 129.58, 128.21, 67.16, 56.11, 45.46, 32.74, 26.34; HRMS–EI (*m/z*) calcd for $C_{15}H_{20}O_2S_2$ [M+]: 296.0905, found 296.0883.

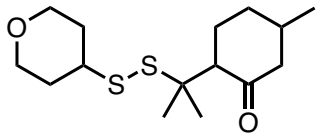

5-Methyl-2-(2-((tetrahydro-2H-pyran-4-yl)disulfaneyl)propan-2-yl)cyclohexan-1-one (3v). Following the general procedure in section 4.3 with **1f** as starting material, **3v** was obtained as a colorless oil (39.8 mg, 66%). ^{1}H NMR (400 MHz, $CDCl_3$) δ 4.04 – 3.91 (m, 2H), 3.45 – 3.31 (m, 2H), 3.00 – 2.77 (m, 1H), 2.66 – 2.56 (m, 1H), 2.52 – 2.37 (m, 1H), 2.34 – 3.23 (m, 1H), 2.16 – 1.80 (m, 5H), 1.65 – 1.42 (m, 3H), 1.50 (s, 3H), 1.41 – 1.31 (m, 1H), 1.34 (s, 3H), 1.01 (d, J = 6.3 Hz, 3H); ^{13}C NMR (101 MHz, $CDCl_3$) δ 210.99, 67.43, 67.34, 56.98, 52.57, 52.47, 46.58, 36.97, 34.67, 32.87, 32.79, 29.83, 27.51, 22.96, 22.39; HRMS–EI (*m/z*) calcd for $C_{15}H_{26}O_2S_2$ [M+]: 302.1374, found 302.13945.

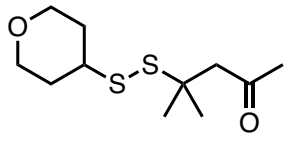

4-Methyl-4-((tetrahydro-2H-pyran-4-yl)disulfaneyl)pentan-2-one (3w). Following the general procedure in section 4.3 with **1g** as starting material, **3w** was obtained as a colorless oil (25.3 mg, 51%). ^{1}H NMR (400 MHz, $CDCl_3$) δ 3.98 (dt, *J* = 11.7, 3.8 Hz, 2H), 3.40 (ddd, *J* = 11.7, 10.7, 2.4 Hz, 2H), 2.98 – 2.86 (m, 1H), 2.75 (s, 2H), 2.17 (s, 3H), 2.06 – 1.93 (m, 2H), 1.67 – 1.53 (m, 2H), 1.42 (s, 6H); ^{13}C NMR (101 MHz, $CDCl_3$) δ 206.74, 67.38, 53.59, 49.03, 46.95, 32.86, 32.30, 27.35; HRMS–EI (*m/z*) calcd for $C_{11}H_{20}O_2S_2$ [M+]: 248.0905, found 248.0929.

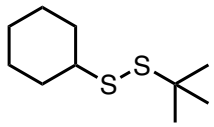

1-(tert-Butyl)-2-cyclohexyldisulfane (3aa). In the mechanistic experiment described in section 4.4.3, **3aa** was obtained as a colorless oil. ^{1}H NMR (400 MHz, $CDCl_3$) δ 2.83 – 2.55 (m, 1H), 2.16 – 1.96 (m, 2H), 1.83 – 1.71 (m, 2H), 1.64 – 1.56 (m, 1H), 1.31 (s, 9H), 1.30 – 1.22 (m, 5H). ^{1}H NMR data are consistent with literature data.[36]

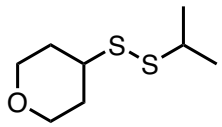

4-(iso-Propyldisulfaneyl)tetrahydro-2H-pyran (3ab). In the mechanistic experiment shown in Scheme 18. **3ab** was obtained as a colorless oil. ^{1}H NMR (400 MHz, $CDCl_3$) δ 4.04 – 3.93 (m, 2H), 3.45 – 3.34 (m, 2H), 3.06 – 2.76 (m, 2H), 2.04 – 1.89 (m, 2H), 1.74 – 1.60 (m, 2H), 1.30 (d, J = 6.7 Hz, 6H); ^{13}C NMR (101 MHz, $CDCl_3$) δ 67.56, 46.44, 41.73, 32.86, 22.71; HRMS–EI (*m/z*) calcd for $C_8H_{16}OS_2$ [M+]: 192.0643, found 192.0627.

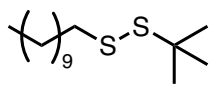

1-(tert-Butyl)-2-undecyldisulfane (3ac). In the mechanistic experiment described in Section 4.4.2, **3ac** was obtained as a colorless oil. ^{1}H NMR (300 MHz, $CDCl_3$) δ 2.75 – 2.62 (m, 2H), 1.71 – 1.57 (m, 2H), 1.43 – 1.21 (m, 16H), 1.33 (s, 9H), 0.91 – 0.84 (m, 3H); ^{13}C NMR (151 MHz, $CDCl_3$) δ 47.80, 41.15, 32.06, 30.10, 29.76, 29.74, 29.64, 29.48, 29.47, 29.37, 28.75, 22.84, 14.27; HRMS–EI (*m/z*) calcd for $C_{15}H_{32}S_2$ [M+]: 276.1945, found 276.1925.

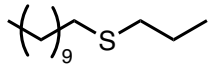

n-Propyl(undecyl)sulfane (5b). In the mechanistic experiment described in section 4.4.2, **5b** was obtained as a colorless oil. ^{1}H NMR (600 MHz, $CDCl_3$) δ 2.67 – 2.36 (m, 4H), 1.65 – 1.58 (m, 4H), 1.40 – 1.33 (m, 2H), 1.31 – 1.22 (m, 14H), 0.99 (t, J = 7.3 Hz, 3H), 0.88 (t, J = 6.9 Hz, 3H);

^{13}C NMR (101 MHz, $CDCl_3$) δ 34.50, 32.41, 32.06, 29.88, 29.76, 29.69, 29.49, 29.42, 29.12, 23.15, 22.84, 14.27, 13.70; HRMS–EI (*m/z*) calcd for $C_{14}H_{30}S$ [M+]: 230.2068, found 230.2045.

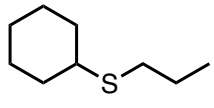

Cyclohexyl(propyl)sulfane (5d). In the mechanistic experiment described in sections 4.5, **5d** was obtained as a colorless oil. ^{1}H NMR (400 MHz, $CDCl_3$) δ 2.71 – 2.57 (m, 1H), 2.52 (t, *J* = 7.4 Hz, 2H), 2.09 – 1.87 (m, 2H), 1.84 – 1.69 (m, 2H), 1.66 – 1.53 (m, 3H), 1.41 – 1.19 (m, 5H), 0.98 (t, *J* = 7.3 Hz, 3H); ^{13}C NMR (101 MHz, $CDCl_3$) δ 43.69, 33.88, 32.45, 26.31, 26.02, 23.51, 13.80. NMR data are consistent with literature data.[36]

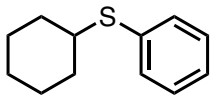

Cyclohexyl(phenyl)sulfane (5f). In the mechanistic experiment described in section 4.5, **5f** was obtained as a colorless oil. ^{1}H NMR (300 MHz, $CDCl_3$) δ 7.44 – 7.36 (m, 2H), 7.33 – 7.24 (m, 2H), 7.24 – 7.17 (m, 1H), 3.35 – 2.89 (m, 1H), 1.99 – 2.07 – 1.89 (m, 2H), 1.89 – 1.68 (m, 2H), 1.68 – 1.51 (m, 1H), 1.48 – 1.15 (m, 5H); ^{13}C NMR (76 MHz, $CDCl_3$) δ 135.30, 131.98, 128.87, 126.70, 46.69, 33.48, 26.19, 25.90; HRMS–EI (*m/z*) calcd for $C_{12}H_{16}S$ [M+]: 192.0973, found 192.0985.

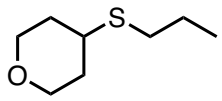

4-(*n*-Propylthio)tetrahydro-2*H*-pyran (5g). In the mechanistic experiment shown in Section 2.3. **5g** was obtained as a colorless oil. ^{1}H NMR (400 MHz, $CDCl_3$) δ 3.97 (dt, *J* = 11.9, 3.9 Hz, 2H), 3.46 – 3.38 (m, 2H), 2.88 – 2.77 (m, 1H), 2.55 – 2.49 (m, 2H), 1.94 – 1.83 (m, 2H), 1.71 – 1.52 (m, 4H), 0.99 (t, *J* = 7.4 Hz, 3H); ^{13}C NMR (101 MHz, $CDCl_3$) δ 67.62, 40.20, 33.74, 32.03, 23.42, 13.75; HRMS–EI (*m/z*) calcd for $C_8H_{16}OS$ [M+]: 160.0922, found 160.0948.

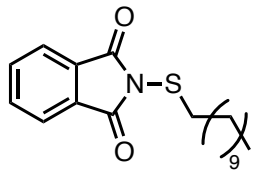

2-(Undecylthio)isoindoline-1,3-dione (6a). In the mechanistic experiment described in section 4.4.2, **6a** was obtained as a white solid. ^{1}H NMR (400 MHz, CDCl3) δ 7.93 (dd, J = 5.5, 3.1 Hz, 2H), 7.78 (dd, J = 5.5, 3.1 Hz, 2H), 2.96 – 2.75 (m, 2H), 1.63 – 1.53 (m, 2H), 1.45 – 1.34 (m, 2H), 1.31 – 1.19 (m, 14H), 0.87 (t, J = 6.9 Hz, 3H); ^{13}C NMR (101 MHz, $CDCl_3$) δ 168.70, 134.70, 132.24, 124.01, 38.81, 32.04, 29.71, 29.69, 29.58, 29.45, 29.26, 28.60, 28.29, 22.82, 14.26; HRMS–EI (*m/z*) calcd for $C_{19}H_{27}NO_2S$ [M+]: 333.1762, found 333.1749.

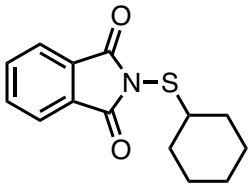

2-(Cyclohexylthio)isoindoline-1,3-dione (6b). In the mechanistic experiment described in section 4.4.3, **6b** was obtained as a white solid. ^{1}H NMR (400 MHz, $CDCl_3$) δ 7.95 – 7.89 (m, 2H), 7.81 – 7.74 (m, 2H), 3.23 – 3.12 (m, 1H), 1.96 – 1.85 (m, 2H), 1.84 – 1.71 (m, 2H), 1.65 – 1.55 (m, 1H), 1.42 – 1.20 (m, 5H); HRMS–EI (*m/z*) calcd for C14H15NO2S [M+]: 261.0823, found 261.07. ^{1}H NMR data are consistent with literature data.[70]

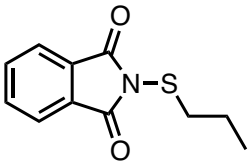

2-(propylthio)isoindoline-1,3-dione (6c)**. 6c** was synthesized following procedure in section 4.2.2, as a white solid (59%). ^{1}H NMR (400 MHz, $CDCl_3$) δ 7.98 – 7.81 (m, 2H), 7.81 – 7.63 (m, 2H), 2.81 (t, J = 7.3 Hz, 2H), 1.57 (q, J = 7.3 Hz, 2H), 0.99 (t, J = 7.3 Hz, 3H).; ^{13}C NMR (101 MHz, $CDCl_3$) δ 168.59, 134.64, 132.10, 123.89, 40.70, 21.72, 13.05.; HRMS–EI (m/z) calcd for $C_{11}H_{11}NO_2S$ [M^+]: 221.0510, found 221.0499.

6.2 Calculation Data

Optimized structures and CBS-QB3 Energies

Me•

CBS-QB3 Enthalpy = -39.740781

CBS-QB3 Free Energy = -39.763940

0 2

C	0.00000000	0.00000000	0.00000100
H	0.00000000	0.00000000	1.08045400
H	0.00000000	-0.93569900	-0.54022900
H	0.00000000	0.93569900	-0.54022900

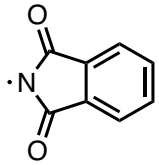

CBS-QB3 Enthalpy = -511.602296

CBS-QB3 Free Energy = -511.645563

0 2

C	2.51898400	-0.70237600	-0.00015200
C	1.32677300	-1.42435900	0.00905900
C	0.14280100	-0.69791100	0.01291000
C	0.14280100	0.69791100	0.01290900
C	1.32677300	1.42435800	0.00905800
C	2.51898400	0.70237600	-0.00015300
H	3.46578900	-1.22985700	-0.01061800
H	1.31611400	-2.50750300	0.00808500
H	1.31611400	2.50750300	0.00808300
H	3.46578900	1.22985600	-0.01061900
C	-1.27972600	-1.15104500	0.01169900
C	-1.27972500	1.15104500	0.01169800

O	-1.71134200	-2.26981600	-0.12322900
O	-1.71134100	2.26981600	-0.12322800
N	-2.09833300	0.00000000	0.22493700

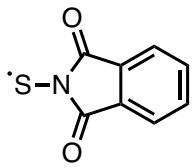

CBS-QB3 Enthalpy = -909.398804

CBS-QB3 Free Energy = -909.444574

0 2

C	3.16644000	-0.70018700	0.00000300
C	1.97112800	-1.42106900	-0.00000200
C	0.78780400	-0.69680900	-0.00000200
C	0.78780400	0.69680900	-0.00000300
C	1.97112800	1.42106900	0.00000400
C	3.16644000	0.70018700	0.00000700
H	4.11152500	-1.23057500	0.00000700
H	1.95825700	-2.50406600	-0.00000100
H	1.95825700	2.50406600	0.00000200
H	4.11152600	1.23057500	0.00001100
C	-0.61136900	-1.19111100	0.00001000
C	-0.61136900	1.19111100	-0.00002100
O	-1.02220600	-2.31517800	-0.00001300
O	-1.02220600	2.31517800	-0.00000500
N	-1.43664200	0.00000000	-0.00000300
S	-3.09348900	0.00000000	0.00001000

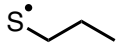

CBS-QB3 Enthalpy = -515.962795

CBS-QB3 Free Energy = -515.998330

0 2

C	-0.21519600	0.83017400	0.30763300
H	-0.12652900	0.87337500	1.39990700
H	-0.62053200	1.80577500	0.00930300
C	1.13927600	0.56765500	-0.35505500
H	1.00081100	0.51856100	-1.43949100
H	1.78404100	1.43332700	-0.15856600
C	1.82553800	-0.70634900	0.14085600
H	2.78751800	-0.85371800	-0.35589900
H	2.00978500	-0.66253600	1.21912900
H	1.20719400	-1.58557600	-0.05998400
S	-1.53375000	-0.35488000	-0.07343800

CBS-QB3 Enthalpy = -555.194003

CBS-QB3 Free Energy = -555.232290

0 2

C	0.66638000	0.00007700	1.49506700
H	1.75702800	0.00009500	1.59943300
H	0.27760100	0.88737100	1.99956100
H	0.27761500	-0.88717400	1.99964300
C	0.31152200	0.00000100	-0.00659900
C	0.85999700	1.26522600	-0.68387800
H	0.57911900	1.30208100	-1.73919600
H	0.47875300	2.16631100	-0.20028400
H	1.95438600	1.27525100	-0.62681600
C	0.85995700	-1.26531900	-0.68373700
H	0.47867500	-2.16633800	-0.20005100
H	0.57909600	-1.30227600	-1.73905600
H	1.95434500	-1.27537400	-0.62665800

S	-1.53273500	0.00000900	-0.07448100

• SCF_3

CBS-QB3 Enthalpy = -735.020381

CBS-QB3 Free Energy = -735.055202

0 2

S	1.48421000	-0.04347400	0.00001900
C	-0.32815000	-0.00456500	0.00000200
F	-0.71197700	1.28432500	-0.00024100
F	-0.85390500	-0.60219900	-1.07898100
F	-0.85394600	-0.60179500	1.07918700

• SPh

CBS-QB3 Enthalpy = -628.910084

CBS-QB3 Free Energy = -628.947151

0 2

S	-0.00002000	2.29995700	0.00000000
C	0.00000600	0.57708400	0.00000000
C	0.00000900	-0.14939000	-1.21798400
C	0.00000900	-0.14939000	1.21798400
C	0.00000900	-1.53450300	-1.21270900
H	0.00001000	0.40352600	-2.14899700
C	0.00000900	-1.53450300	1.21270900
H	0.00001000	0.40352600	2.14899700
C	0.00000400	-2.23139000	0.00000000
H	0.00001400	-2.07917500	-2.14990300
H	0.00001400	-2.07917500	2.14990300
H	-0.00001200	-3.31547300	0.00000000

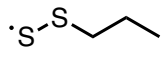

CBS-QB3 Enthalpy = -913.744243

CBS-QB3 Free Energy = -913.784694

0 2

S	1.86440700	-0.71718200	0.08723600
C	-0.72089000	0.80793800	0.73969600
H	-1.25821200	1.73112300	0.49721100
H	-0.29600600	0.90774800	1.73971000
C	-1.63220900	-0.41530900	0.63684900
H	-1.03219400	-1.31369500	0.81071500
H	-2.34636500	-0.35768600	1.46647700
C	-2.38962300	-0.52898200	-0.68800000
H	-3.04249200	-1.40495700	-0.68590500
H	-3.01472100	0.35178600	-0.86522200
H	-1.70459500	-0.62856100	-1.53372000
S	0.70752500	0.81295400	-0.43476900

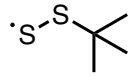

CBS-QB3 Enthalpy = -952.978966

CBS-QB3 Free Energy = -953.021731

0 2

C	-0.98123900	0.11913600	-0.00000100
C	-2.11286300	-0.91716600	0.00000000
H	-2.07539200	-1.55564100	-0.88644600
H	-2.07539500	-1.55563800	0.88644700
H	-3.07759500	-0.40069800	-0.00000300
C	-1.00918100	0.97909900	1.26471700
H	-1.92560900	1.57834000	1.27894000
H	-0.99021400	0.36369900	2.16729700
H	-0.15706500	1.66086500	1.29412500
S	0.59123600	-0.93896400	-0.00000200
S	2.16182400	0.27303400	0.00000100
C	-1.00918200	0.97910300	-1.26471500

H	-0.15706200	1.66086600	-1.29412300
H	-0.99022000	0.36370700	-2.16729700
H	-1.92560600	1.57835000	-1.27893200

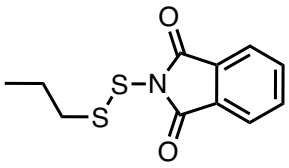

CBS-QB3 Enthalpy = -1425.460955

CBS-QB3 Free Energy = -1425.522490

0 1

C	4.36494300	0.23900400	0.78641400
C	3.40754800	-0.77135200	0.90728400
C	2.18978800	-0.57486900	0.27520000
C	1.92522600	0.58291700	-0.45138800
C	2.86808200	1.59130500	-0.57687400
C	4.09940700	1.40223600	0.05551700
H	5.32992600	0.12220000	1.26587700
H	3.60131000	-1.67598500	1.47066500
H	2.65080700	2.48760300	-1.14500500
H	4.86296500	2.16778400	-0.01957500
C	0.99284000	-1.46070300	0.22548900
C	0.54313900	0.50376000	-1.00199200
O	0.82643000	-2.53588300	0.73146900
O	-0.04838600	1.31454600	-1.66631000
N	0.03786200	-0.75326500	-0.57021800
S	-1.49238100	-1.40248700	-1.00417500
C	-3.67935800	0.57255400	0.01019600
H	-4.58302900	0.54374500	0.63063400
H	-3.98740900	0.42187500	-1.02503300
C	-2.93592500	1.89563900	0.18542400
H	-2.04791100	1.89591200	-0.45110400

H	-3.59152300	2.68182700	-0.20982100
C	-2.56213100	2.22710000	1.63187100
H	-2.06176400	3.19692400	1.68979700
H	-3.44874900	2.27155000	2.27279900
H	-1.88700900	1.47733000	2.05187600
S	-2.79564100	-0.95956100	0.54519300

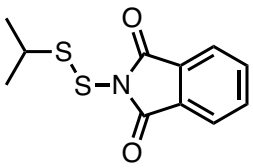

CBS-QB3 Enthalpy = -1425.465932

CBS-QB3 Free Energy = -1425.527639

0 1

C	-4.60375600	-0.28420900	0.65311100
C	-3.70430900	0.78374700	0.60010600
C	-2.42251100	0.51615700	0.14615000
C	-2.04067600	-0.76547000	-0.24218800
C	-2.92475200	-1.83189000	-0.19123200
C	-4.22011100	-1.57196100	0.26313500
H	-5.61565300	-0.11492800	1.00261200
H	-3.98922800	1.78456400	0.90093900
H	-2.61586300	-2.82488200	-0.49438400
H	-4.94109400	-2.37949700	0.31600200
C	-1.26148100	1.43733500	-0.01561400
C	-0.61342400	-0.73504600	-0.66757600
O	-1.18913600	2.61099500	0.22409100
O	0.08488400	-1.64703800	-1.02887400
N	-0.21127500	0.62116400	-0.53661600
S	1.34644200	1.21688400	-0.95673600
S	2.55025500	0.84084500	0.68053700
C	3.23161900	-0.87148100	0.37823100

C	4.10750900	-0.92920500	-0.86788700
H	4.47133100	-1.95129300	-1.01717800
H	3.54549600	-0.64436100	-1.75868500
H	4.97200700	-0.26635500	-0.77274000
C	3.98803400	-1.24880500	1.65462800
H	3.33840100	-1.23100200	2.53262900
H	4.39189000	-2.26031200	1.55260900
H	4.82870000	-0.57211100	1.83504700
H	2.36295100	-1.51831500	0.25171400

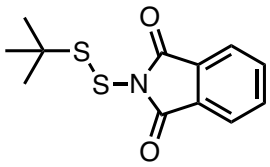

CBS-QB3 Enthalpy = -1464.695468

CBS-QB3 Free Energy = -1464.759332

0 1

C	-4.75946100	-0.06685600	0.84748200
C	-3.79119100	0.93382000	0.73199800
C	-2.56891700	0.57826200	0.18384300
C	-2.31043200	-0.72392100	-0.23555000
C	-3.26406000	-1.72383700	-0.12512300
C	-4.49998200	-1.37536400	0.42539300
H	-5.72828600	0.17199000	1.27066100
H	-3.98026200	1.95020400	1.05533100
H	-3.05142900	-2.73340000	-0.45516300
H	-5.27190700	-2.12920600	0.52833700
C	-1.36054800	1.41436500	-0.06490200
C	-0.92120800	-0.79301100	-0.76987000
O	-1.18864400	2.58039500	0.16088700
O	-0.33403800	-1.74566400	-1.21416100
N	-0.40451000	0.52453000	-0.64503800

S	1.13773500	1.03293500	-1.21684600
S	2.40670800	1.07040300	0.41140100
C	3.32025600	-0.58235000	0.48173600
C	3.94537300	-0.90797800	-0.87525300
H	4.51968100	-1.83759200	-0.79890800
H	3.17815400	-1.05231100	-1.63815100
H	4.62007300	-0.11433100	-1.20396400
C	2.38549800	-1.70196300	0.94482800
H	2.96229500	-2.62319500	1.08501400
H	1.90933300	-1.45316300	1.89628900
H	1.61056900	-1.90482900	0.20471700
C	4.40523000	-0.30567700	1.53550900
H	3.97058300	-0.03469100	2.50152400
H	5.00195200	-1.21163400	1.68046900
H	5.07781200	0.49625100	1.22188200

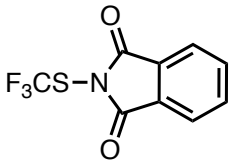

CBS-QB3 Enthalpy = -1246.761804

CBS-QB3 Free Energy = -1246.817852

0 1

C	-4.13016900	0.69968100	0.50824000
C	-2.97294600	1.42100400	0.20600600
C	-1.82893800	0.69654800	-0.09154100
C	-1.82894500	-0.69655000	-0.09153200
C	-2.97296000	-1.42099200	0.20602400
C	-4.13017600	-0.69965400	0.50824800
H	-5.04440100	1.23042800	0.74699500
H	-2.96089500	2.50404300	0.20243700
H	-2.96092000	-2.50403100	0.20246700

H	-5.04441300	-1.23038900	0.74701000
C	-0.47082300	1.18794100	-0.44816500
C	-0.47084000	-1.18796100	-0.44815300
O	-0.07434600	2.31232700	-0.56968500
O	-0.07436300	-2.31234500	-0.56966500
N	0.30999300	-0.00000900	-0.63763800
S	1.93029300	-0.00001900	-1.13351500
C	2.74504700	0.00000800	0.50538300
F	4.06611400	-0.00000400	0.26579100
F	2.43973500	1.07796700	1.23867300
F	2.43972400	-1.07792800	1.23870600

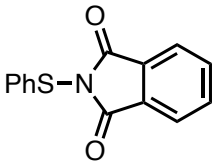

CBS-QB3 Enthalpy = -1140.639349

CBS-QB3 Free Energy = -1140.698694

0 1

C	4.37585500	-0.69946400	1.08745200
C	3.29978200	-1.42060200	0.56331600
C	2.23882900	-0.69619600	0.04359600
C	2.23882900	0.69619600	0.04359300
C	3.29978200	1.42060300	0.56331100
C	4.37585500	0.69946700	1.08744900
H	5.22510600	-1.23035400	1.50188900
H	3.28766300	-2.50377100	0.55922400
H	3.28766300	2.50377300	0.55921600
H	5.22510600	1.23036000	1.50188500
C	0.96776700	-1.17850400	-0.56932800
C	0.96776700	1.17850100	-0.56933100
O	0.58711100	-2.30869300	-0.72368500

O	0.58711100	2.30869000	-0.72369300
N	0.26194700	-0.00000200	-0.93738900
S	-1.25386100	-0.00000300	-1.74985300
C	-2.40949000	-0.00000100	-0.37878300
C	-2.87822600	-1.21341000	0.13428500
C	-2.87822200	1.21341100	0.13428400
C	-3.81224800	-1.20869400	1.16725800
H	-2.50078100	-2.14362400	-0.27184600
C	-3.81224400	1.20870000	1.16725700
H	-2.50077400	2.14362300	-0.27184800
C	-4.27893600	0.00000400	1.68208700
H	-4.17602400	-2.14783900	1.56835100
H	-4.17601600	2.14784600	1.56834900
H	-5.00816500	0.00000500	2.48450500

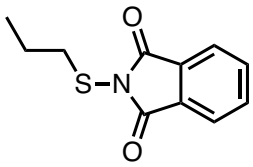

CBS-QB3 Enthalpy = -1027.699980

CBS-QB3 Free Energy = -1027.758414

0 1

C	-4.17552200	0.87757100	-0.38920000
C	-2.95585800	1.52549700	-0.17665300
C	-1.83868400	0.73145300	0.02869500
C	-1.92237000	-0.65814600	0.02181400
C	-3.12654000	-1.31047600	-0.19093600
C	-4.25957900	-0.51889500	-0.39620500
H	-5.07231100	1.46422100	-0.55180800
H	-2.87796900	2.60593200	-0.17011200
H	-3.17880400	-2.39246500	-0.19518600
H	-5.22017100	-0.99209900	-0.56404000

C	-0.42252200	1.12919400	0.27319800
C	-0.56428000	-1.22457100	0.26174400
O	0.05073300	2.23253800	0.32815600
O	-0.22507900	-2.37710800	0.30315700
N	0.28862100	-0.09586600	0.42213200
S	1.95060700	-0.19887000	0.81390800
C	2.69247600	-0.31644000	-0.86610600
H	2.41577900	0.58059000	-1.42443700
H	2.26601500	-1.19543700	-1.35134200
C	4.21619600	-0.44645700	-0.76087000
H	4.46429800	-1.31349400	-0.13885000
H	4.58712100	-0.67911900	-1.76495000
C	4.92910500	0.80342300	-0.23300900
H	4.63398500	1.04101000	0.79167400
H	6.01263400	0.66137200	-0.24241300
H	4.69960100	1.67611700	-0.85133300

$F_3CS-SCF_3$

CBS-QB3 Enthalpy = -1470.152078

CBS-QB3 Free Energy = -1470.201548

0 1

S	-0.77407700	-0.99233800	0.68242500
S	0.77407700	-0.99233800	-0.68242500
C	-1.93490000	0.23477000	-0.05220200
C	1.93490000	0.23477000	0.05220200
F	-2.29302500	-0.07870700	-1.30091800
F	-1.44954000	1.47789200	-0.06441400
F	-3.02770200	0.20845900	0.72815400
F	1.44954100	1.47789200	0.06441400
F	2.29302500	-0.07870700	1.30091800
F	3.02770200	0.20845800	-0.72815400

PhS−SPh

CBS-QB3 Enthalpy = -1257.905506

CBS-QB3 Free Energy = -1257.961565

0 1

C	-2.90048100	0.62658100	0.48071200
C	-1.83711100	0.39294000	-0.39824000
C	-1.70084600	-0.85771600	-1.00939500
C	-2.62231700	-1.86758900	-0.73942900
C	-3.67636300	-1.63498500	0.14124400
C	-3.81353900	-0.38776800	0.75106000
H	-3.00441900	1.59973800	0.94486100
H	-0.87728800	-1.03086000	-1.69111900
H	-2.51461400	-2.83529100	-1.21633300
H	-4.39227900	-2.42186500	0.35027900
H	-4.63619600	-0.20352400	1.43280200
S	-0.68536300	1.70392900	-0.80430500
S	0.68535600	1.70392600	0.80431600
C	1.83711000	0.39294300	0.39824200
C	1.70087000	-0.85770500	1.00941700
C	2.90045900	0.62658300	-0.48073600
C	2.62234500	-1.86757300	0.73944600
H	0.87732600	-1.03084800	1.69115900
C	3.81352000	-0.38776200	-0.75109000
H	3.00437800	1.59973400	-0.94490100
C	3.67637000	-1.63497100	-0.14125300
H	2.51466100	-2.83526900	1.21636600
H	4.63616000	-0.20352000	-1.43285300
H	4.39228800	-2.42184700	-0.35029200

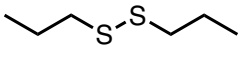

CBS-QB3 Enthalpy = -1032.028681

CBS-QB3 Free Energy = -1032.081181

0 1

C	1.83478400	-0.02611300	1.06086700
H	2.60107500	-0.61777300	1.57507500
H	1.11030900	0.29332700	1.81180100
C	2.45763200	1.17168800	0.34308900
H	1.67840000	1.68252900	-0.23129300
H	2.78595000	1.88200000	1.11206700
C	3.63750100	0.81883500	-0.56500800
H	4.04219300	1.71460600	-1.04279600
H	4.44747000	0.34993200	0.00310300
H	3.33648800	0.12496500	-1.35308900
S	1.01276100	-1.26926400	-0.02875000
S	-0.65400600	-0.26839500	-0.76400600
C	-1.94713800	-0.62412900	0.51057700
H	-1.63511600	-0.18000000	1.45858700
H	-1.99238600	-1.70705000	0.62921100
C	-3.30551400	-0.06672300	0.07154200
H	-3.56496100	-0.47730600	-0.91029600
H	-4.05464300	-0.45457600	0.77132300
C	-3.38730000	1.46304100	0.03893600
H	-2.69271000	1.89130100	-0.68754100
H	-4.39436700	1.79157300	-0.23002800
H	-3.14758200	1.88942200	1.01793400

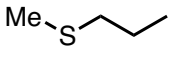

CBS-QB3 Enthalpy = -555.820603

CBS-QB3 Free Energy = -555.860661

0 1

C	0.31210200	-0.37440900	0.93968700
H	0.72213600	-1.36718200	1.14734300
H	-0.13123600	-0.00951800	1.87043900
C	1.42121100	0.56729300	0.45666900
H	0.98977400	1.53907800	0.19404100
H	2.08755400	0.75542600	1.30785100
C	2.23602500	0.02518200	-0.71933600
H	3.01235800	0.73440300	-1.01791400
H	2.72871200	-0.91589000	-0.45453100
H	1.59837200	-0.16474700	-1.58549700
S	-1.05328600	-0.68712100	-0.24446700
C	-1.93079000	0.90858100	-0.17893000
H	-1.31869500	1.72604400	-0.56209800
H	-2.81035800	0.80468300	-0.81552200
H	-2.25734000	1.13174600	0.83882300

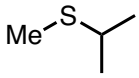

CBS-QB3 Enthalpy = -555.823964

CBS-QB3 Free Energy = -555.863708

0 1

C	-2.10100800	0.37017300	0.29826800
H	-3.04011500	-0.10480100	0.01143600
H	-2.06624300	0.44672500	1.38688100
H	-2.06354200	1.36466500	-0.14794500
S	-0.77029900	-0.70787400	-0.32217800
C	1.91166300	-0.82366200	0.16156800
H	2.82177700	-0.38234800	0.57830300
H	1.74201000	-1.78520400	0.65038400
H	2.08663800	-1.00755700	-0.90259800
C	0.98297000	1.49687400	-0.26029000

H	0.14277800	2.17841300	-0.11128700
H	1.86667200	1.96014000	0.19228900
H	1.15694800	1.40335100	-1.33540500
C	0.72813100	0.12542000	0.36595300
H	0.54732200	0.23977100	1.43979100

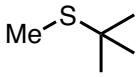

CBS-QB3 Enthalpy = -595.053089

CBS-QB3 Free Energy = -595.095454

0 1

C	-0.81050900	0.94511500	1.26304300
H	-1.78864800	1.43885200	1.27993000
H	-0.71804000	0.33564800	2.16430000
H	-0.05009300	1.72885100	1.30017900
C	-0.68166700	0.08426400	0.00000000
C	-1.75494600	-1.01518100	-0.00000300
H	-1.67263400	-1.64990400	-0.88579200
H	-1.67263200	-1.64991000	0.88578200
H	-2.74991400	-0.55912600	0.00000000
C	-0.81050800	0.94512000	-1.26304000
H	-0.05009400	1.72885800	-1.30017100
H	-0.71803400	0.33565600	-2.16429900
H	-1.78864800	1.43885300	-1.27992800
S	0.93220500	-0.85628900	0.00000000
C	2.19895100	0.45272000	0.00000000
H	2.14388200	1.07430100	0.89448700
H	3.15775900	-0.06798600	0.00000400
H	2.14388600	1.07429700	-0.89449000

$Me-SCF_3$

CBS-QB3 Enthalpy = -774.888685

CBS-QB3 Free Energy = -774.927673

0 1

C	-0.66290900	-0.04334400	0.00000000
F	-1.66057700	0.85315000	0.00000000
F	-0.81353900	-0.83655600	-1.07986500
F	-0.81353900	-0.83655600	1.07986500
S	0.90797900	0.85350100	0.00000000
C	2.03562000	-0.58153200	0.00000000
H	3.04268600	-0.16477800	0.00000000
H	1.89114000	-1.18116700	0.89714300
H	1.89114000	-1.18116600	-0.89714300

Me−SPh

CBS-QB3 Enthalpy = -668.758372

CBS-QB3 Free Energy = -668.800883

0 1

C	0.12440700	-0.00000300	-0.27048500
C	-0.56915100	-1.20806700	-0.14796900
C	-0.56914800	1.20806400	-0.14797800
C	-1.93856400	-1.20606300	0.10813000
H	-0.03266800	-2.14273300	-0.26030300
C	-1.93856100	1.20606700	0.10812200
H	-0.03266300	2.14272800	-0.26031800
C	-2.62453500	0.00000300	0.23798700
H	-2.46973000	-2.14678900	0.20105500
H	-2.46972400	2.14679500	0.20104100
H	-3.69085700	0.00000500	0.43387900
S	1.88211700	-0.00000700	-0.63450000
C	2.57753300	0.00000900	1.05949100
H	2.27362000	-0.89395400	1.60430200

H	3.66265100	0.00000800	0.94427300
H	2.27362000	0.89398300	1.60428500

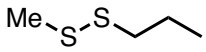

CBS-QB3 Enthalpy = -953.578788

CBS-QB3 Free Energy = -953.623753

0 1

C	-1.01568000	0.50276600	0.93882500
H	-1.58735000	1.41928400	1.12523300
H	-0.42170700	0.30224300	1.83218300
C	-1.94538400	-0.66669900	0.61356200
H	-1.33761900	-1.53595700	0.34332000
H	-2.47041000	-0.93652900	1.53827900
C	-2.96632700	-0.37303600	-0.48766100
H	-3.60355500	-1.24220500	-0.66895900
H	-3.61582800	0.46401700	-0.21180000
H	-2.47222700	-0.11732900	-1.42767100
S	0.13898400	1.00327100	-0.41177800
S	1.45627000	-0.59918100	-0.56452000
C	2.74951100	-0.19668800	0.66733600
H	2.34860100	-0.20980300	1.68037500
H	3.50682900	-0.97869700	0.57082800
H	3.19648500	0.77148100	0.44660300

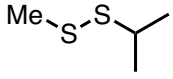

CBS-QB3 Enthalpy = -953.582489

CBS-QB3 Free Energy = -953.627124

0 1

S	-0.06250100	-0.60600400	0.75307000

C	-2.54677100	-0.88532600	-0.31504500
H	-3.32825500	-0.56947100	-1.01244700
H	-2.29005600	-1.92308200	-0.53909900
H	-2.96645600	-0.84608800	0.69448600
C	-1.68160500	1.50303500	-0.18505100
H	-0.79526700	2.13703900	-0.24515600
H	-2.40174000	1.85652900	-0.93107100
H	-2.12562100	1.62581900	0.80648600
C	-1.33436300	0.04108700	-0.44474400
H	-0.90108400	-0.06973500	-1.44178200
S	1.64786900	0.50496400	0.36012700
C	2.47432800	-0.44845500	-0.96690200
H	1.88231100	-0.44790000	-1.88148000
H	3.42374500	0.06003500	-1.15260700
H	2.66699600	-1.46855500	-0.63804300

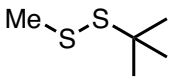

CBS-QB3 Enthalpy = -992.812899

CBS-QB3 Free Energy = -992.859844

0 1

C	-1.30897800	0.16238400	0.07553000
C	-2.48429600	-0.08693200	-0.88208800
H	-2.28391100	0.31597700	-1.87806600
H	-2.70332800	-1.15342000	-0.97886500
H	-3.38066300	0.40563300	-0.49210200
C	-1.60513800	-0.41461100	1.46222000
H	-2.44985300	0.11709000	1.91447800
H	-1.85861400	-1.47508100	1.40201600
H	-0.74451200	-0.30449200	2.12548600
S	0.10193500	-0.79252900	-0.73112000

S	1.77293900	-0.50485900	0.46756500
C	2.65115300	0.89513600	-0.32392800
H	3.60062300	0.98592100	0.20979700
H	2.84700700	0.67291500	-1.37180900
H	2.09190400	1.82457600	-0.23031600
C	-0.98373100	1.65514900	0.15988400
H	-0.12955800	1.83370000	0.81668000
H	-0.76136700	2.07031900	-0.82561500
H	-1.83975300	2.19830800	0.57548300

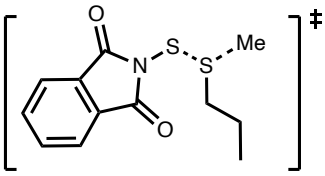

TS Freq.: -294.46 cm^{-1}

CBS-QB3 Enthalpy = -1465.195220

CBS-QB3 Free Energy = -1465.264707

0 2

C	4.57926000	-0.06790600	1.11028600
C	3.58787600	-1.03837700	0.94343200
C	2.44654800	-0.67139500	0.24807900
C	2.28800500	0.61315600	-0.26423900
C	3.26502100	1.58324100	-0.10381500
C	4.42037100	1.22292400	0.59446300
H	5.48707500	-0.31673200	1.64764200
H	3.69922500	-2.04092000	1.33822500
H	3.13031000	2.57937800	-0.50746600
H	5.20762400	1.95350600	0.74034000
C	1.23712800	-1.47580500	-0.08345700
C	0.96807700	0.70065400	-0.94917800
O	0.99113200	-2.61692400	0.19601500
O	0.46976500	1.64922200	-1.49772100

N	0.38879900	-0.59214200	-0.82167600
S	-1.10856400	-1.07070700	-1.49298500
C	-3.36870500	0.84346400	-0.44664700
H	-4.37834500	0.80628800	-0.02851700
H	-3.46054100	0.80804500	-1.53214900
C	-2.63259900	2.10740700	-0.00402100
H	-1.64193000	2.12457700	-0.46363100
H	-3.17933000	2.95724100	-0.43265000
C	-2.52216400	2.28937200	1.51106200
H	-2.00314900	3.22059500	1.75168000
H	-3.50950900	2.33003900	1.98310600
H	-1.96308100	1.46949800	1.96941300
S	-2.61581100	-0.77173200	0.06364100
C	-4.16349600	-1.22645000	1.86764000
H	-4.02175000	-0.34741900	2.48355300
H	-5.09378100	-1.31147800	1.32007200
H	-3.72353000	-2.14868600	2.22363200

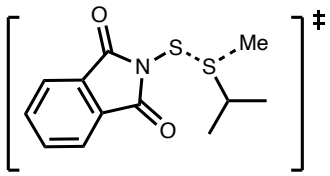

TS Freq.: -298.93

CBS-QB3 Enthalpy = -1465.198408

CBS-QB3 Free Energy = -1465.267072

0 2

C	3.24527900	0.89157600	0.51052700
S	2.58154700	-0.81309200	0.09871800
S	1.18847500	-0.49742700	-1.54769800
C	3.64419100	-1.87976200	1.98692700
H	4.67796300	-1.83822500	1.66585300
H	3.15542100	-2.84316400	1.92512300

H	3.35224300	-1.24149400	2.81180100
C	3.59966300	1.70204400	-0.73332700
H	4.10941400	2.62211800	-0.42937700
H	4.26356200	1.14677100	-1.39895300
H	2.70287500	1.98284700	-1.28763200
C	2.33739600	1.65711500	1.47143300
H	2.07516300	1.05657400	2.34501400
H	2.85025500	2.55955200	1.82190600
H	1.41949400	1.97007200	0.97123500
N	-0.35597400	-0.26303100	-0.85019300
C	-0.92476100	1.00403000	-0.55413500
C	-1.25309400	-1.32930500	-0.53184300
C	-2.29230100	0.71528600	-0.03888100
C	-2.48585600	-0.66333900	-0.02371900
O	-0.38417600	2.07174100	-0.69253000
O	-1.02642700	-2.50132700	-0.65725900
C	-3.67497300	-1.22313700	0.41569700
H	-3.81338600	-2.29745300	0.42362900
C	-3.28051000	1.59064100	0.38341700
H	-3.11840200	2.66153900	0.36661700
C	-4.48406300	1.03623800	0.82684000
H	-5.28162900	1.68801700	1.16427800
C	-4.67818200	-0.34916200	0.84297100
H	-5.62301400	-0.74871600	1.19289800
H	4.16959300	0.61441300	1.02550900

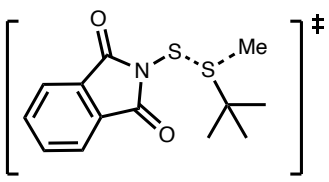

TS Freq.: -315.89 cm^{-1}

CBS-QB3 Enthalpy = -1504.423947

CBS-QB3 Free Energy = -1504.494401

0 2

C	-4.87059200	0.17396500	0.97102000
C	-3.92756800	1.10186500	0.52070600
C	-2.73410100	0.60667900	0.02002900
C	-2.47869000	-0.76096700	-0.03283300
C	-3.40648500	-1.68936000	0.41245200
C	-4.61415100	-1.20023800	0.91751500
H	-5.81676500	0.52228600	1.36879400
H	-4.11438000	2.16821900	0.55760100
H	-3.19637800	-2.75102400	0.36659700
H	-5.36580500	-1.89484700	1.27433100
C	-1.55491900	1.33897100	-0.52316100
C	-1.12221400	-0.97449100	-0.61011600
O	-1.38514200	2.52273000	-0.62726200
O	-0.53573100	-2.01274700	-0.78582100
N	-0.62799500	0.32158000	-0.90820500
S	2.31152800	0.89356900	-0.02000100
C	3.08215700	-0.82714900	0.31139900
C	3.09717100	-1.65362500	-0.97713900
H	3.61953600	-2.59514500	-0.77494600
H	2.09086900	-1.89117400	-1.31868000
H	3.63002100	-1.13739400	-1.77911100
C	2.28500500	-1.54569000	1.40477100
H	2.78114900	-2.48969500	1.65780600
H	2.21892200	-0.94726400	2.31593600
H	1.27647400	-1.78184600	1.06424100
C	4.52549400	-0.56078300	0.76540600
H	4.57226600	-0.02023700	1.71101200
H	5.02872300	-1.52276200	0.91023800
H	5.08225700	0.00295200	0.01381100

S	0.87889900	0.63992100	-1.65295300
C	3.00910600	2.11778500	1.94534000
H	4.03971000	2.34872000	1.70685100
H	2.29733800	2.92593400	1.83554900
H	2.83088800	1.43473400	2.76699000

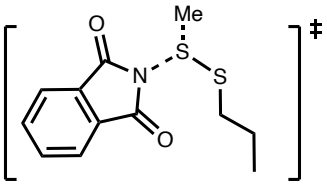

TS Freq.: -338.30 cm^{-1}

CBS-QB3 Enthalpy = -1465.188136

CBS-QB3 Free Energy = -1465.256868

0 2

C	-4.61856200	-0.18559300	-0.66745200
C	-3.49267700	-0.92690400	-1.03820100
C	-2.29787800	-0.63266400	-0.40176000
C	-2.21566100	0.36225100	0.56845700
C	-3.32445500	1.10409500	0.94228200
C	-4.53580900	0.81397700	0.30748200
H	-5.57239800	-0.38690600	-1.14155000
H	-3.54444300	-1.70305600	-1.79224500
H	-3.24800700	1.87609900	1.69849900
H	-5.42686600	1.37106700	0.57355100
C	-0.93996200	-1.23926700	-0.57094500
C	-0.80007200	0.43746800	1.05146200
O	-0.61224400	-2.14634900	-1.29432100
O	-0.34191800	1.17215300	1.89386100
N	-0.09476800	-0.52259800	0.30193800
S	1.66960200	-1.07672200	0.66829300
C	3.36078500	1.32432200	-0.28396900

H	4.06301900	1.61697200	-1.07414500
H	3.94729100	1.08436500	0.60405200
C	2.35367500	2.43856900	-0.00274300
H	1.65632700	2.11036300	0.77249000
H	2.91894700	3.27329600	0.43052700
C	1.58874800	2.92658900	-1.23458400
H	0.90603100	3.73697000	-0.96794400
H	2.26981300	3.30377500	-2.00457900
H	0.99682400	2.12301500	-1.67901800
S	2.68329100	-0.25873500	-0.94994200
C	3.19153400	-2.62543000	1.10912200
H	3.32258500	-3.16160400	0.17730500
H	2.70811200	-3.18956700	1.89998700
H	4.03514100	-2.02018600	1.42466000

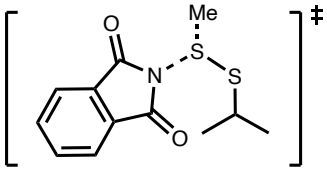

TS Freq.: -337.43

CBS-QB3 Enthalpy = -1465.191115

CBS-QB3 Free Energy = -1465.259469

0 2

C	4.75279600	0.01669700	-0.86225900
C	3.63261400	0.80739300	-1.13541500
C	2.46057200	0.50709600	-0.46065800
C	2.39494900	-0.54067500	0.45352200
C	3.49813800	-1.33170800	0.73047800
C	4.68666100	-1.03615700	0.05623400
H	5.68907200	0.22089000	-1.36903500
H	3.67160800	1.62503500	-1.84508300
H	3.43454700	-2.14481000	1.44358800

H	5.57275100	-1.63087700	0.24674300
C	1.11409700	1.15741700	-0.52917100
C	1.00147000	-0.60784700	0.99807800
O	0.77974800	2.11490800	-1.18118200
O	0.56248500	-1.37772000	1.81900700
N	0.28980900	0.41144000	0.33853200
S	-1.43929700	0.98793800	0.82261700
S	-2.54122300	0.36204100	-0.81910600
C	-3.27397500	-1.26854400	-0.28983100
C	-2.22899700	-2.36223000	-0.10312000
H	-2.72488100	-3.29483100	0.18775200
H	-1.68451300	-2.54292500	-1.03415800
H	-1.51071700	-2.10936100	0.67756000
C	-4.30687300	-1.61280600	-1.36812400
H	-3.82992500	-1.75435000	-2.34235600
H	-4.80724600	-2.54897700	-1.10439200
H	-5.06877500	-0.83646800	-1.46762700
C	-2.88409400	2.53869900	1.47156900
H	-2.34954000	3.00832500	2.29081800
H	-3.73666500	1.93472800	1.76455600
H	-3.03152400	3.16538700	0.60067700
H	-3.78655300	-1.07304100	0.65463700

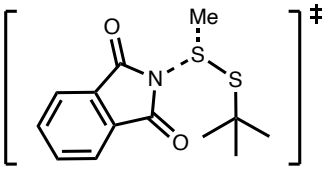

TS Freq.: -337.20 cm^{-1}

CBS-QB3 Enthalpy = -1504.422565

CBS-QB3 Free Energy = -1504.493449

0 2

C	4.97698800	-0.09441800	-0.78774300

C	3.89216300	0.73775500	-1.07983300
C	2.69546400	0.47569200	-0.43301000
C	2.57214000	-0.57447800	0.47235900
C	3.63998400	-1.40615300	0.76819300
C	4.85291700	-1.14965400	0.12198100
H	5.93095500	0.07900600	-1.27252800
H	3.97614100	1.55791000	-1.78268700
H	3.53170000	-2.22043100	1.47455600
H	5.71273700	-1.77693000	0.32786500
C	1.37491300	1.17493800	-0.52573600
C	1.16548900	-0.59364200	0.98621000
O	1.09130400	2.15037100	-1.17517800
O	0.68185700	-1.35009600	1.79484200
N	0.50450300	0.45187900	0.31598100
S	-1.21091400	1.09149000	0.77956500
S	-2.31180800	0.54471600	-0.88665400
C	-3.07478800	-1.13490200	-0.48754900
C	-3.94407400	-1.04395400	0.76788500
H	-4.41908800	-2.01287800	0.95589500
H	-3.34350800	-0.79452800	1.64510500
H	-4.73086700	-0.29460900	0.65464200
C	-1.99011100	-2.20278800	-0.33389000
H	-2.46256800	-3.18188100	-0.19594600
H	-1.35689400	-2.25308700	-1.22253200
H	-1.35710500	-2.01299800	0.53431900
C	-3.93586400	-1.40216400	-1.73283500
H	-3.32873300	-1.44358500	-2.64076400
H	-4.43594600	-2.36901900	-1.61973500
H	-4.70607300	-0.63805300	-1.86515500
C	-2.58635800	2.70966100	1.43278000
H	-2.71436100	3.33541500	0.55814600

H	-3.46058100	2.14441100	1.73794200
H	-2.02223700	3.16122300	2.24224000

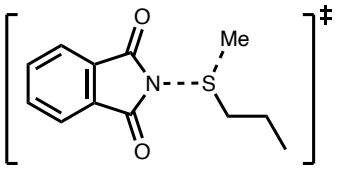

TS Freq.: -292.21 cm^{-1}

CBS-QB3 Enthalpy = -1067.432608

CBS-QB3 Free Energy = -1067.496888

0 2

C	-4.22995300	0.42639000	0.86598900
C	-2.99438200	0.29808500	1.50740100
C	-1.89465300	0.00089800	0.71878000
C	-2.00926400	-0.16323900	-0.65862400
C	-3.22802000	-0.03610100	-1.30463600
C	-4.34488200	0.26224900	-0.51822300
H	-5.11466800	0.65615400	1.44866600
H	-2.89309900	0.42285000	2.57877000
H	-3.30452500	-0.16577900	-2.37747300
H	-5.31680700	0.36790000	-0.98646000
C	-0.46356500	-0.19779800	1.09933600
C	-0.65497800	-0.46846700	-1.21700800
O	0.03244600	-0.15269400	2.19959300
O	-0.35483900	-0.69492100	-2.36109000
N	0.22411000	-0.43470500	-0.10805100
S	1.94060800	-1.02986300	-0.18281700
C	2.71597300	0.55127400	0.34298600
H	3.77328500	0.30519900	0.45687200
H	2.32011100	0.79488900	1.33056300
C	2.53314900	1.69862500	-0.64853200

H	1.46663000	1.88311000	-0.80237700
C	3.73179400	-2.33932400	0.52219600
H	4.48685300	-2.02835600	-0.19331400
H	3.89687800	-2.05740000	1.55534400
H	3.32592600	-3.33200000	0.36952600
C	3.21006200	2.98409200	-0.15759400
H	3.06754700	3.79613200	-0.87499300
H	2.79677900	3.31035500	0.80138500
H	4.28722300	2.84346600	-0.02518300
H	2.94081400	1.40503700	-1.62036100

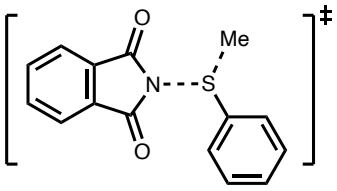

TS Freq.: -301.77 cm^{-1}

CBS-QB3 Enthalpy = -1180.370720

CBS-QB3 Free Energy = -1180.436580

0 2

C	4.61293500	-1.05581700	-0.62341700
C	3.42648400	-0.85682500	-1.33561800
C	2.38107000	-0.23537100	-0.67217400
C	2.50117700	0.17526900	0.65253800
C	3.67101700	-0.01941600	1.36841800
C	4.73326900	-0.64369900	0.70768100
H	5.45450600	-1.53722400	-1.10829100
H	3.32112700	-1.17279600	-2.36650900
H	3.75191900	0.30326300	2.39944500
H	5.66619200	-0.81226200	1.23338500
C	1.00714300	0.11084900	-1.15137000
C	1.20766300	0.79892500	1.07640300

O	0.52672000	-0.08225000	-2.24254800
O	0.92410900	1.27204500	2.14774100
N	0.36348500	0.70877600	-0.05277800
S	-1.29335700	1.50062300	-0.15715700
C	-2.25802200	0.00980100	0.10618000
C	-2.54599300	-0.84905700	-0.95835400
C	-2.72285100	-0.27599100	1.39173200
C	-3.30762700	-1.99188100	-0.73037300
H	-2.15111900	-0.63018300	-1.94241800
C	-3.48990700	-1.41919100	1.60876100
H	-2.47599900	0.39008200	2.20934200
C	-3.78354800	-2.27530100	0.54964700
H	-3.52761000	-2.66264600	-1.55320300
H	-3.85292800	-1.64112700	2.60586300
H	-4.37872300	-3.16510300	0.72130900
C	-3.03777500	2.58415800	-1.13769900
H	-3.28271000	1.99875400	-2.01519200
H	-3.75470400	2.54536200	-0.32413400
H	-2.59746600	3.55539400	-1.33131300

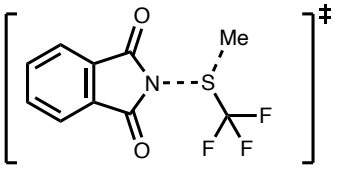

TS Freq.: -275.64 cm^{-1}

CBS-QB3 Enthalpy = -1286.492537

CBS-QB3 Free Energy = -1286.555220

0 2

C	-4.41165800	0.86470900	0.29028800
C	-3.18148100	1.51204300	0.14712500
C	-2.06650500	0.71998800	-0.07611400
C	-2.16275900	-0.66711900	-0.15516000

C	-3.37757500	-1.31869100	-0.01404200
C	-4.50813500	-0.52868800	0.21111200
H	-5.30713400	1.44960700	0.46586600
H	-3.09441600	2.59011000	0.20714100
H	-3.43986600	-2.39830200	-0.07692400
H	-5.47681300	-1.00107000	0.32668800
C	-0.63895100	1.11321700	-0.26581000
C	-0.80149100	-1.23232600	-0.39934700
O	-0.15529000	2.21526800	-0.28481800
O	-0.47858400	-2.38040100	-0.54896500
N	0.06389200	-0.10571900	-0.42333500
S	1.80773000	-0.19592800	-0.89105400
C	2.44002400	-0.11564800	0.84137200
F	3.62061500	-0.75521600	0.90540100
F	2.63959900	1.14275800	1.26176700
F	1.60062300	-0.70387900	1.69511600
C	3.77031200	0.56635400	-1.66644100
H	3.96998600	1.45539100	-1.08044400
H	3.51145500	0.74856900	-2.70289000
H	4.41865800	-0.28436100	-1.48741000

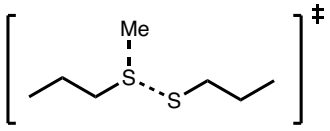

TS Freq.: -298.86 cm^{-1}

CBS-QB3 Enthalpy = -1071.760586

CBS-QB3 Free Energy = -1071.820918

0 2

C	-1.50667000	-0.43697200	0.97901500
H	-2.33760100	0.04105100	1.50353100
H	-0.68292700	-0.53737000	1.68686100

C	-1.92377600	-1.79975000	0.42421700
H	-1.09527800	-2.21475600	-0.15730300
H	-2.06472400	-2.47193300	1.28007200
C	-3.19991200	-1.77184900	-0.41955300
H	-3.44898500	-2.77228400	-0.78232500
H	-4.05290300	-1.40850600	0.16309600
H	-3.08313900	-1.12034200	-1.28878900
S	-0.98193800	0.79241200	-0.30255100
S	0.96479100	-0.02659300	-0.85169900
C	2.07280800	0.72421300	0.41896300
H	1.79061600	0.34493100	1.40458100
H	1.90325900	1.80151400	0.40104100
C	3.54468900	0.40941300	0.12640800
H	3.79338000	0.75623700	-0.88214500
H	4.14769600	1.01205600	0.81594800
C	3.92430700	-1.06666800	0.28061000
H	3.38472600	-1.69833000	-0.42896500
H	4.99420900	-1.21209200	0.11043500
H	3.69444000	-1.42801800	1.28788900
C	-2.63419000	2.43082000	0.26497300
H	-3.53336700	1.87243500	0.03175400
H	-2.43909300	2.63796000	1.31012400
H	-2.35950400	3.20908900	-0.43559400

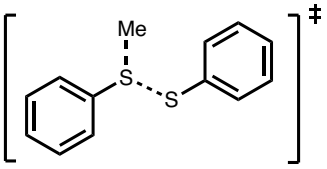

TS Freq.: -266.12 cm^{-1}

CBS-QB3 Enthalpy = -1297.641044

CBS-QB3 Free Energy = -1297.704855

0 2

C	2.76384600	-0.06075500	-0.90342100
C	1.73058700	0.12839800	0.01988300
C	1.45396300	-0.86478900	0.96489800
C	2.20777800	-2.03639900	0.98494600
C	3.23655200	-2.22294500	0.06370800
C	3.51244400	-1.23419200	-0.88010300
H	2.97127500	0.71067000	-1.63501000
H	0.64945000	-0.71634700	1.67471800
H	1.98923800	-2.80347900	1.71949400
H	3.82213100	-3.13519000	0.08097700
H	4.31227800	-1.37596200	-1.59829600
S	0.78028400	1.64945400	0.01037600
S	-0.78213700	1.17796700	-1.48743100
C	-1.97750100	0.21351100	-0.58473800
C	-1.92465200	-1.18597800	-0.62999900
C	-3.00256800	0.84177800	0.13498200
C	-2.88445200	-1.94340500	0.03682900
H	-1.13396200	-1.66880600	-1.19078400
C	-3.95545900	0.07978400	0.80328400
H	-3.04423000	1.92379800	0.16246800
C	-3.89885500	-1.31327500	0.75541800
H	-2.83976400	-3.02598300	-0.00589700
H	-4.74629600	0.57268900	1.35770700
H	-4.64549700	-1.90470400	1.27334200
C	2.09433600	2.61807800	1.86993000
H	3.06890300	2.56529400	1.40273100
H	1.61326600	3.58603900	1.91574400
H	1.87673800	1.91437000	2.66197700

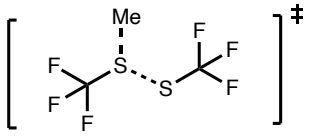

TS Freq.: -245.81 cm^{-1}

CBS-QB3 Enthalpy = -1509.887386

CBS-QB3 Free Energy = -1509.944461

0 2

S	0.76047200	0.69361900	-0.69830400
S	-1.09256000	-0.28836800	-1.23358400
C	2.34187400	2.30474500	0.25809000
H	3.20338000	2.07974000	-0.35625400
H	1.78154200	3.20186400	0.03027500
H	2.35613900	1.98060500	1.29043900
C	-2.09978400	0.08764800	0.24507600
C	1.64348100	-0.70694500	0.13495400
F	-2.21338300	1.40261600	0.48280100
F	-1.62425000	-0.48102800	1.36179200
F	-3.32933400	-0.40420500	0.01314800
F	1.40194200	-0.74280800	1.45335500
F	2.96705300	-0.53373000	-0.03123200
F	1.31563100	-1.89183600	-0.37797200

6.3 NMR Spectra

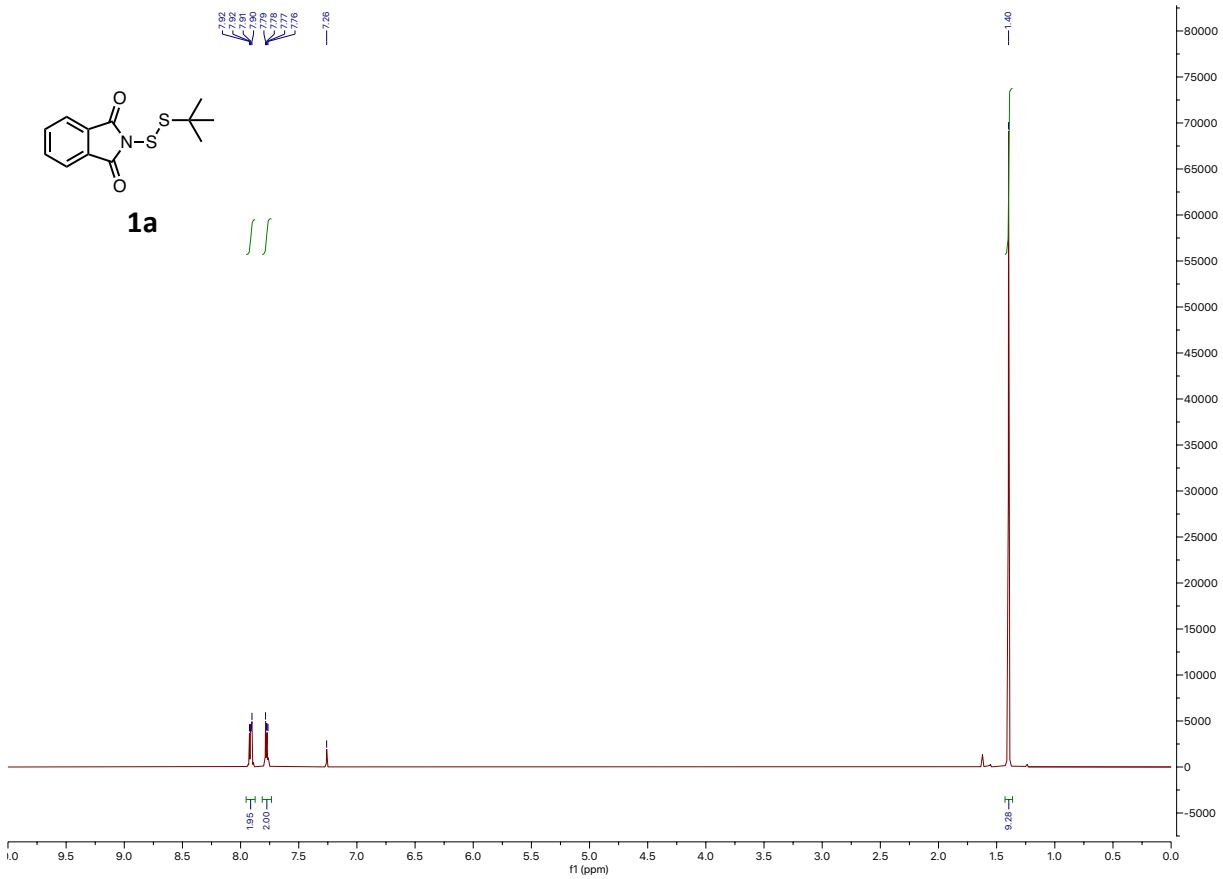
7.92
7.92
7.91
7.90
7.90
7.79
7.78
7.77
7.76
7.26
1.40
1.95
2.00
9.28
f1 (ppm)

1a

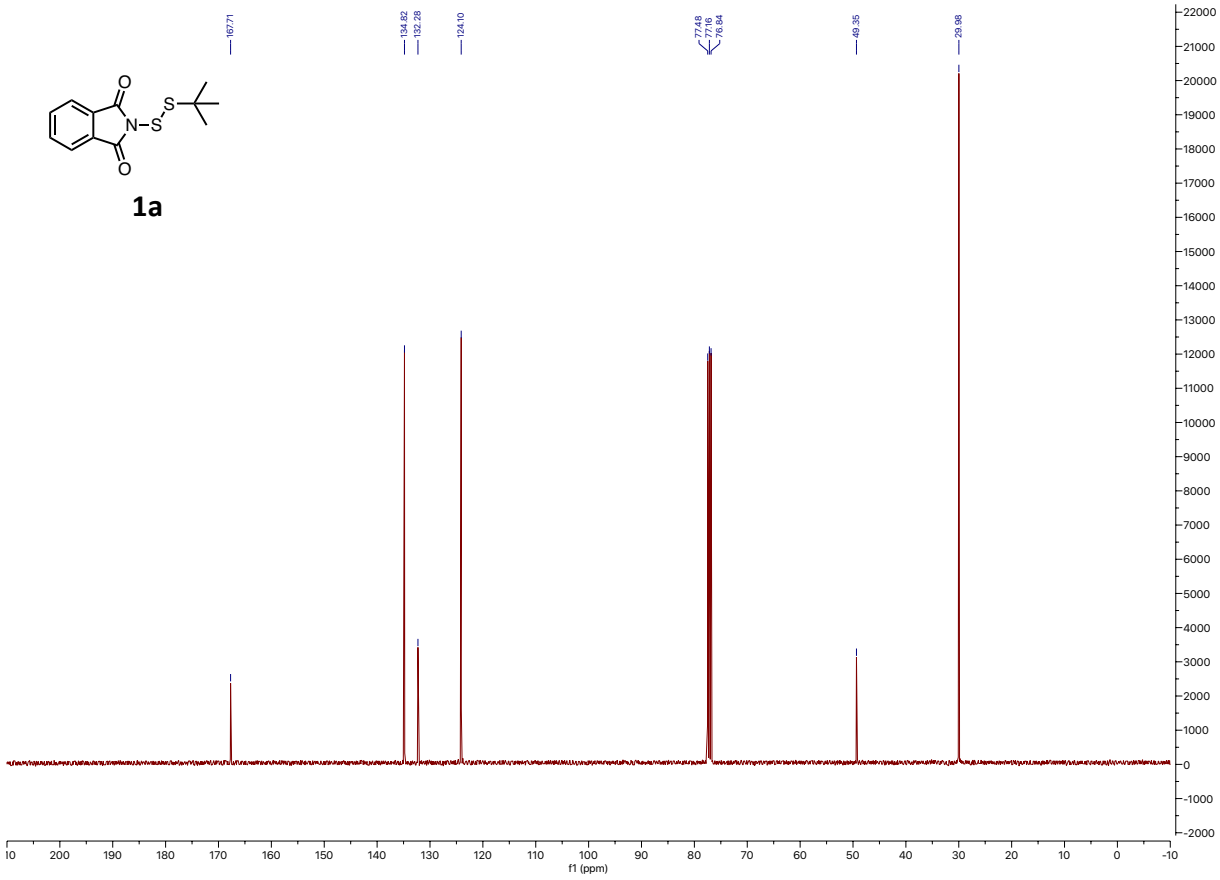
167.71
134.82
132.28
124.10
77.48
77.16
76.84
49.35
29.98
f1 (ppm)

1a

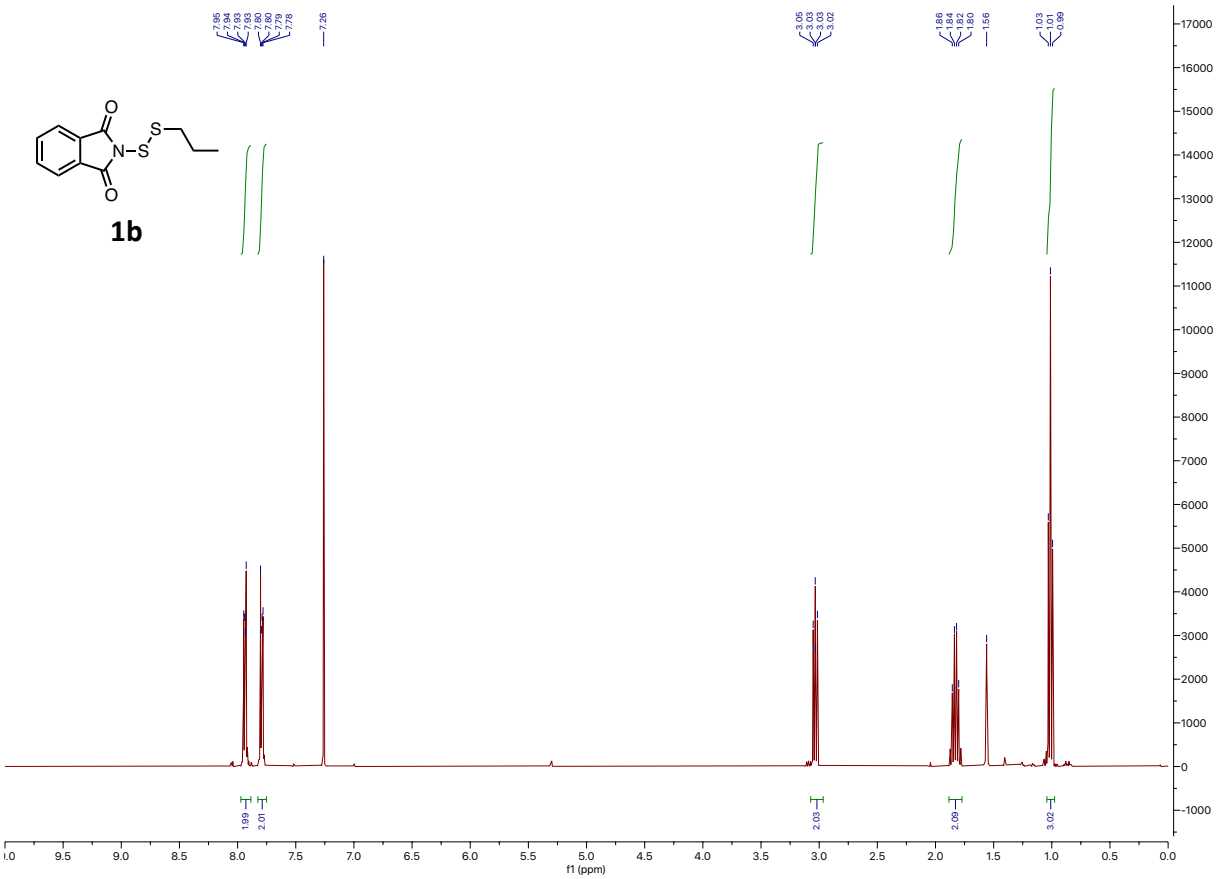
7.96
7.94
7.93
7.80
7.80
7.79
7.78
7.26
2.05
3.03
3.03
3.02
1.86
1.84
1.82
1.80
1.56
1.03
1.01
0.99
1b
1.99
2.01
2.03
2.09
3.02
f1 (ppm)

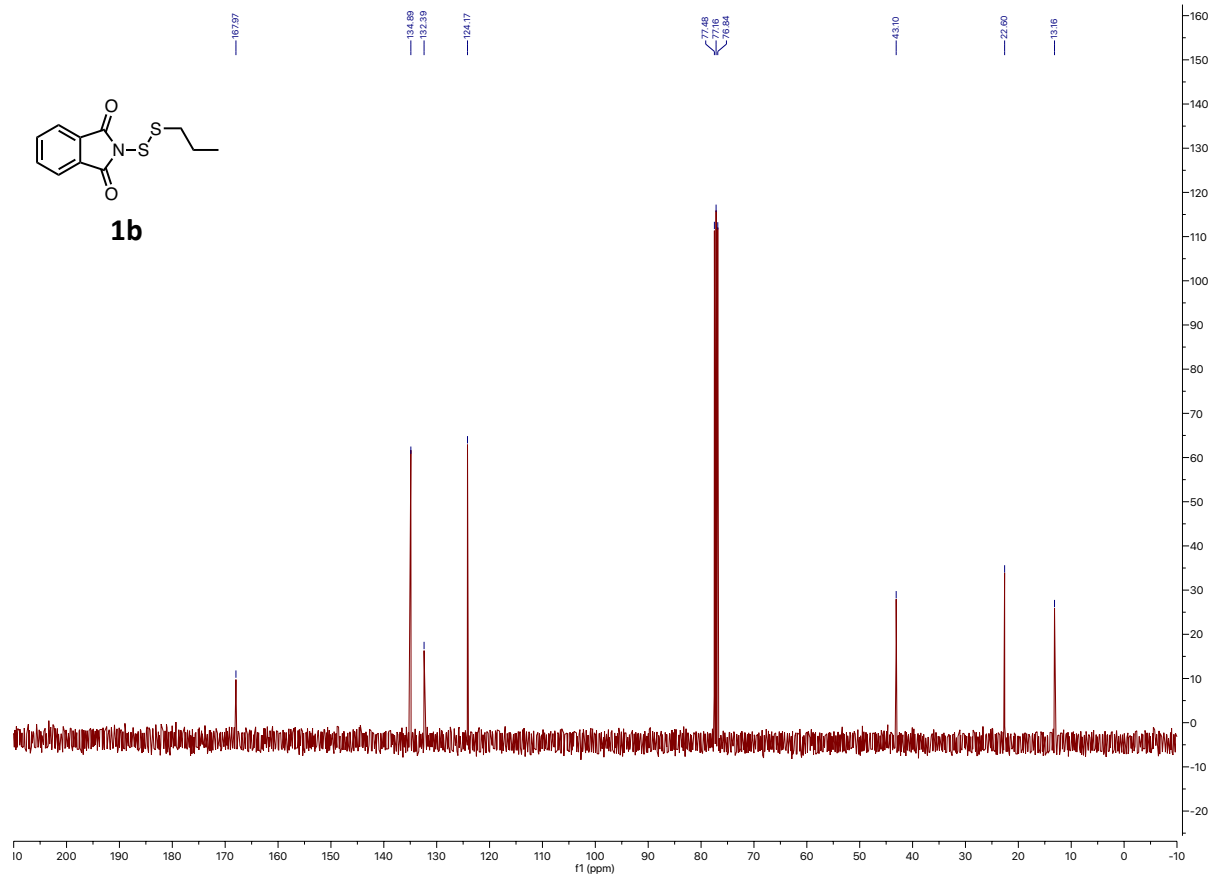
167.97
134.89
132.39
124.17
77.48
77.16
76.84
43.10
22.60
13.16
1b
f1 (ppm)

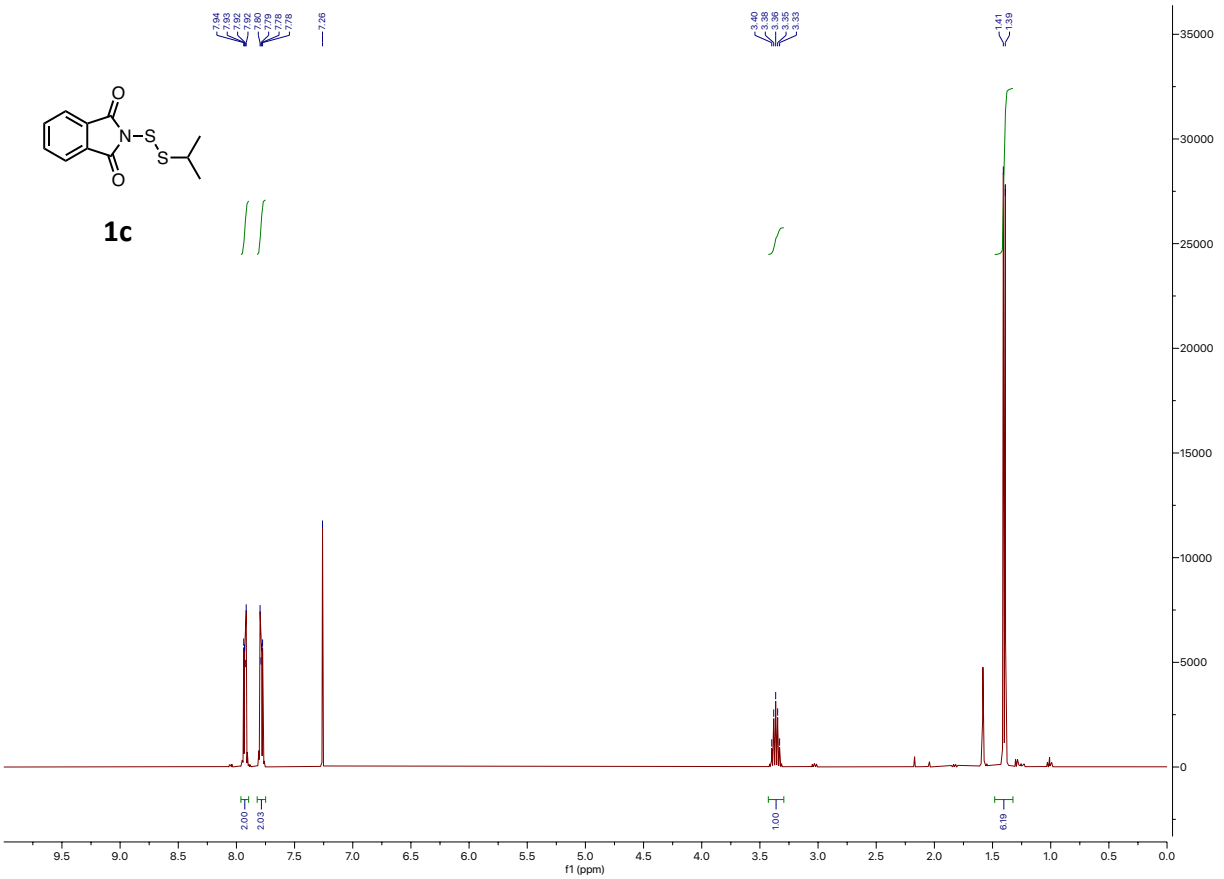
7.94
7.93
7.92
7.92
7.80
7.79
7.78
7.78
7.26
3.40
3.38
3.36
3.35
3.33
1.41
1.39
1c
2.00
2.03
1.00
6.19
f1 (ppm)

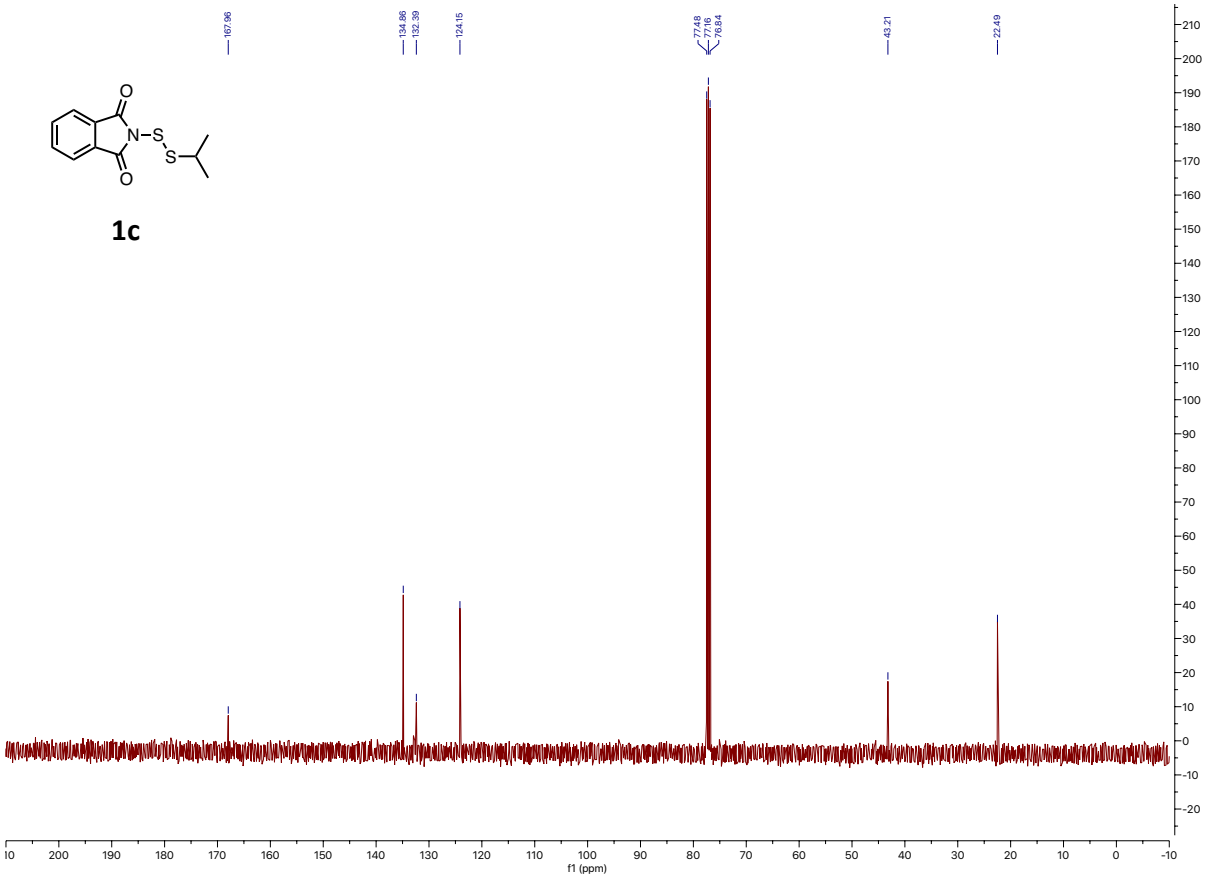
167.96
134.86
132.39
124.15
77.48
77.16
76.84
43.21
22.49
1c
f1 (ppm)

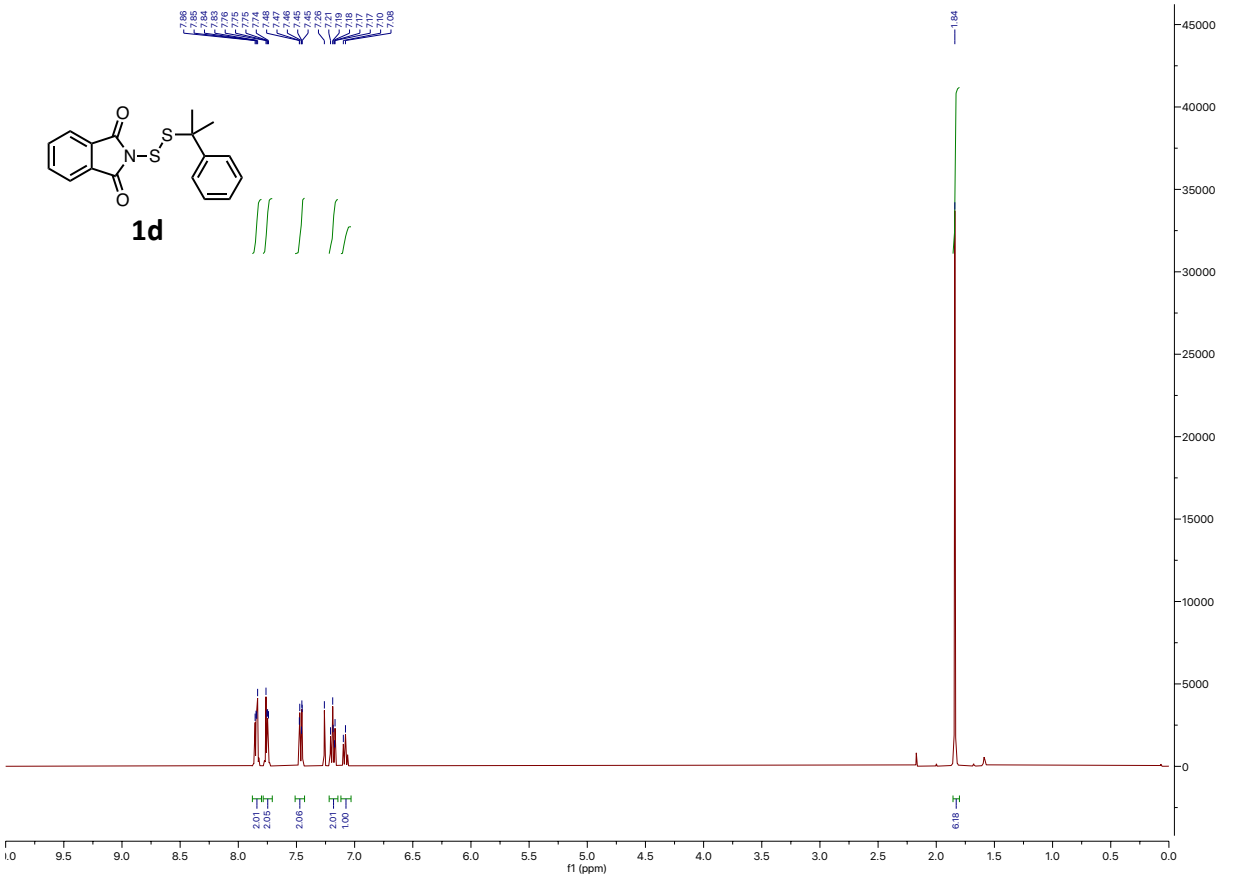
7.86
7.85
7.84
7.83
7.76
7.75
7.75
7.74
7.48
7.47
7.46
7.45
7.45
7.25
7.21
7.19
7.18
7.17
7.17
7.10
7.08
1.84
1d
2.01
2.05
2.06
2.01
1.00
6.18
f1 (ppm)

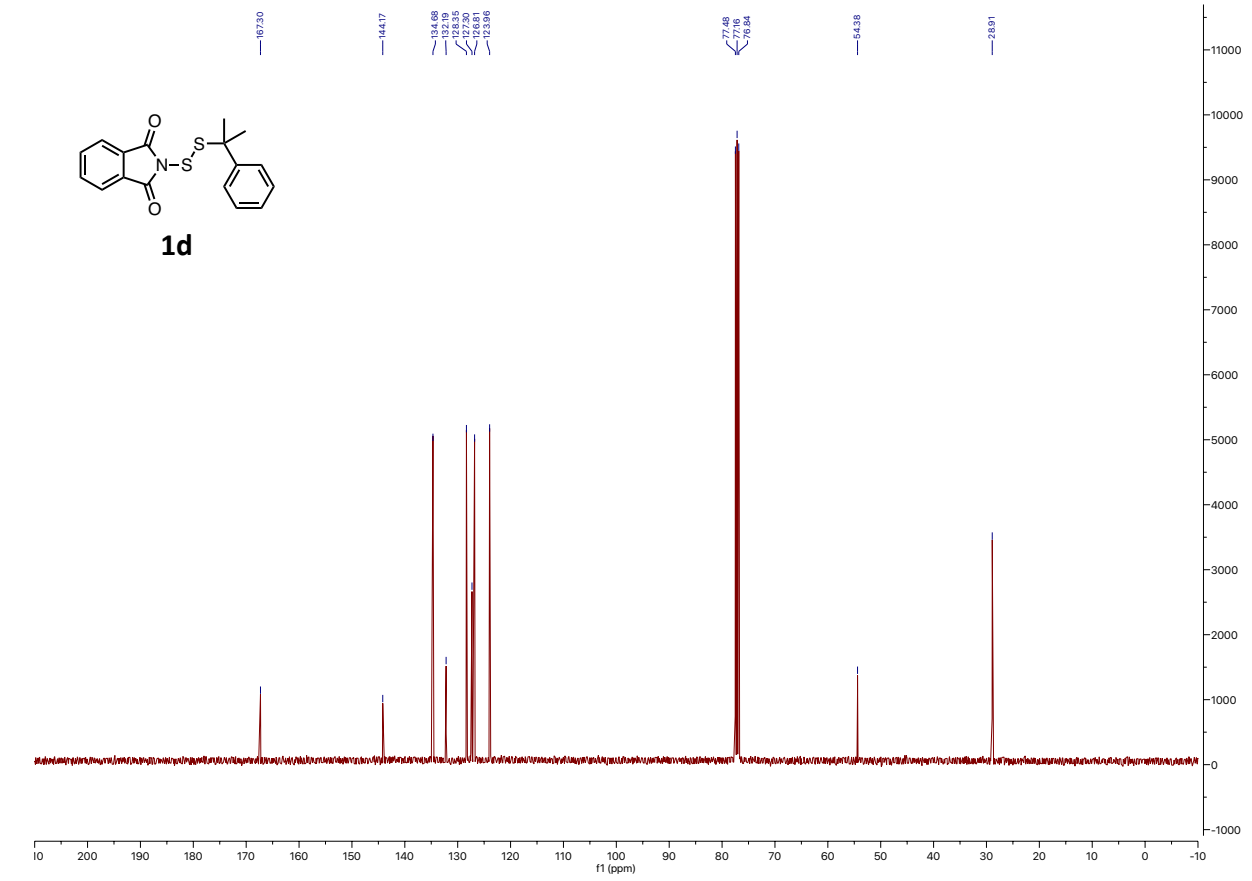
167.30
144.17
134.68
132.19
129.35
127.30
126.81
123.96
77.48
77.16
76.84
54.38
28.91
1d
f1 (ppm)

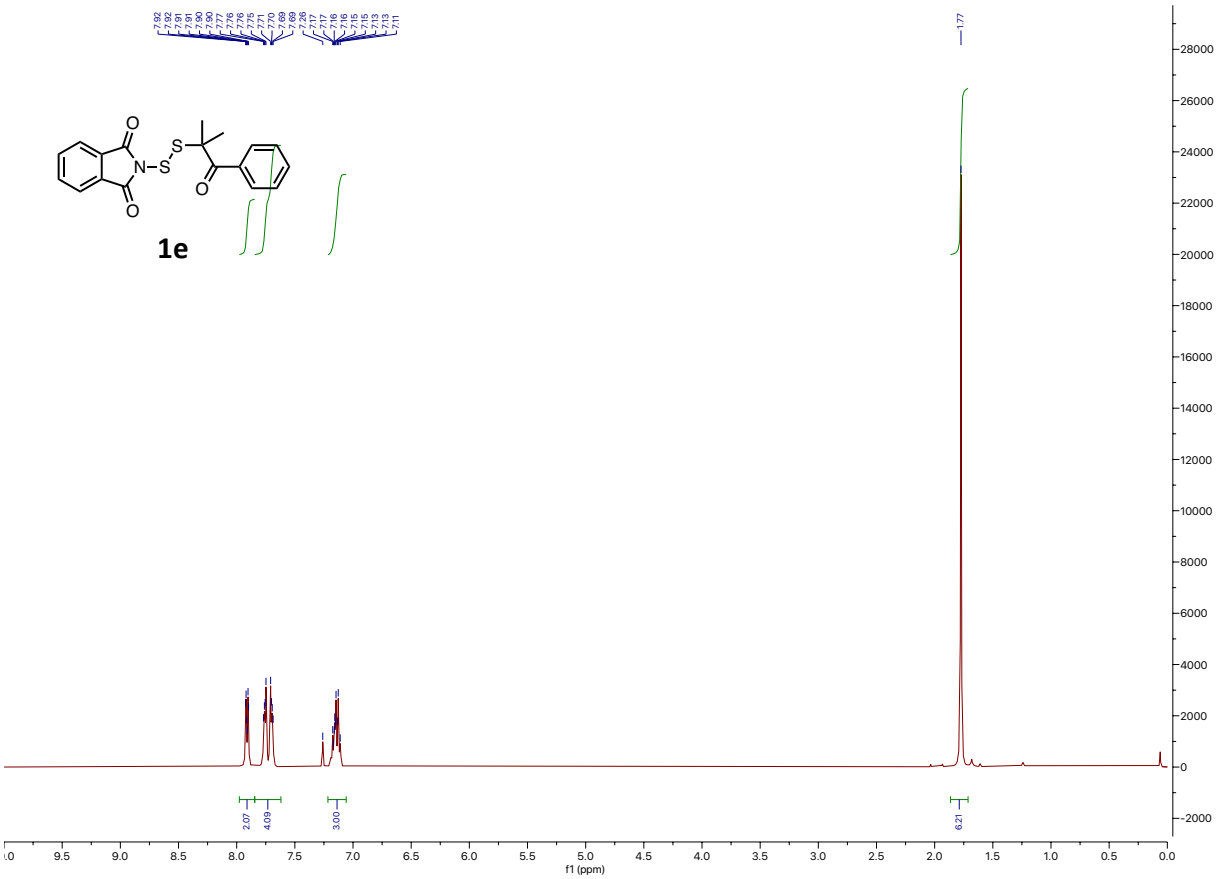
1e
f1 (ppm)

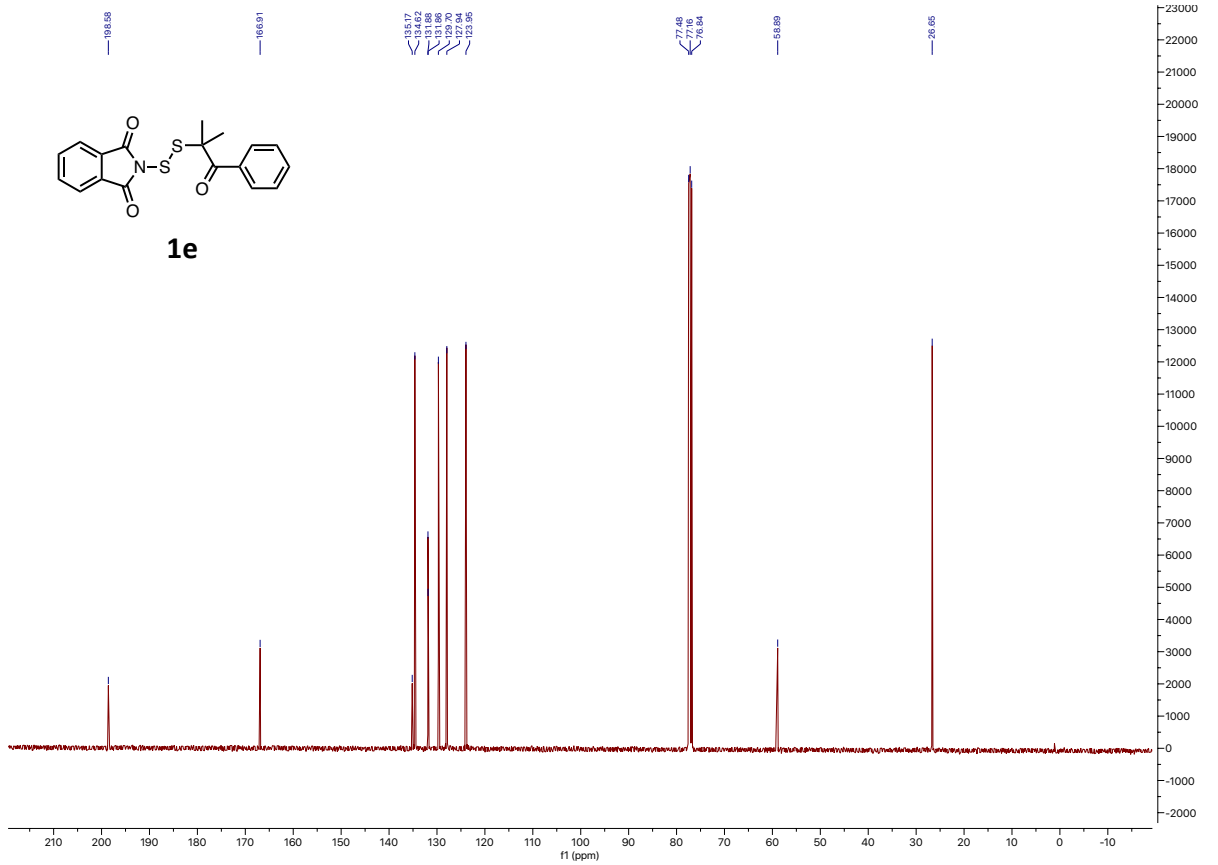
1e
f1 (ppm)

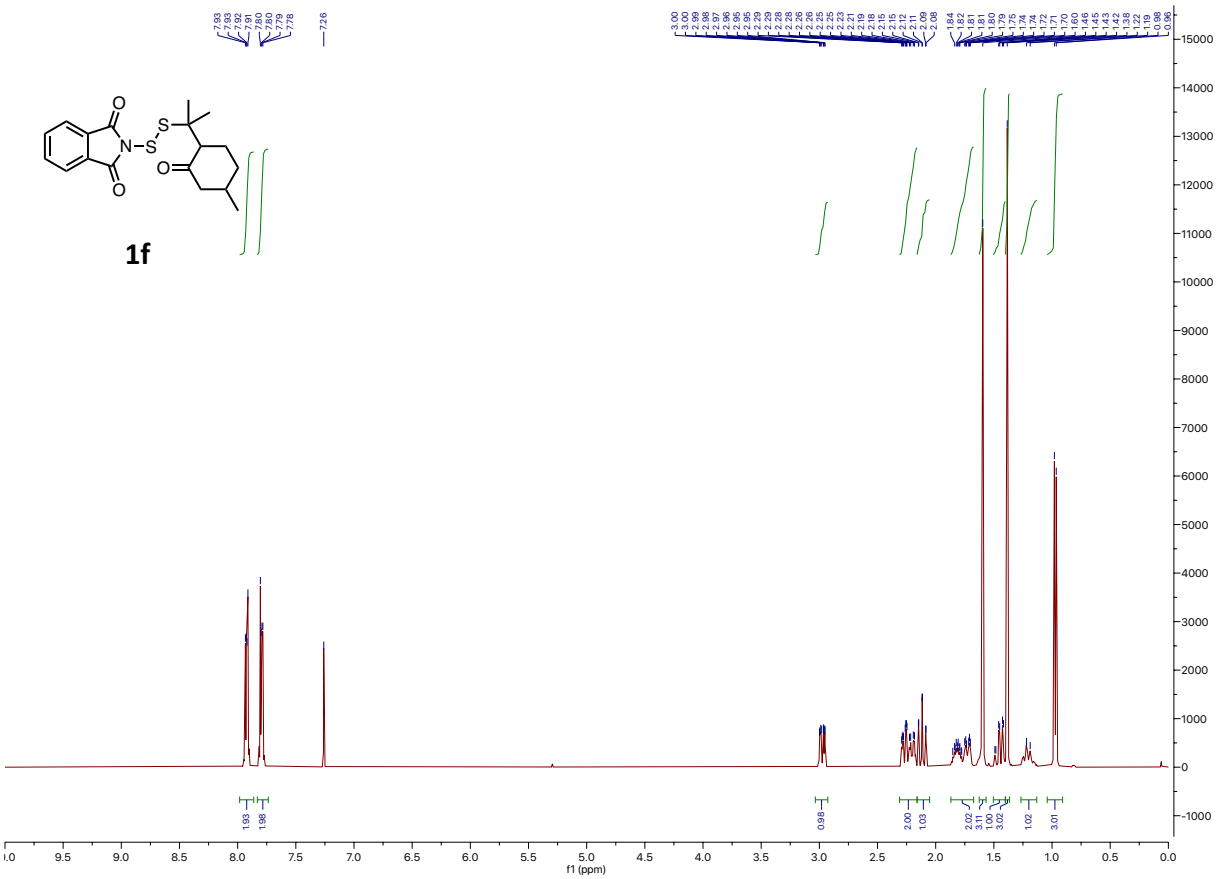
1f
f1 (ppm)

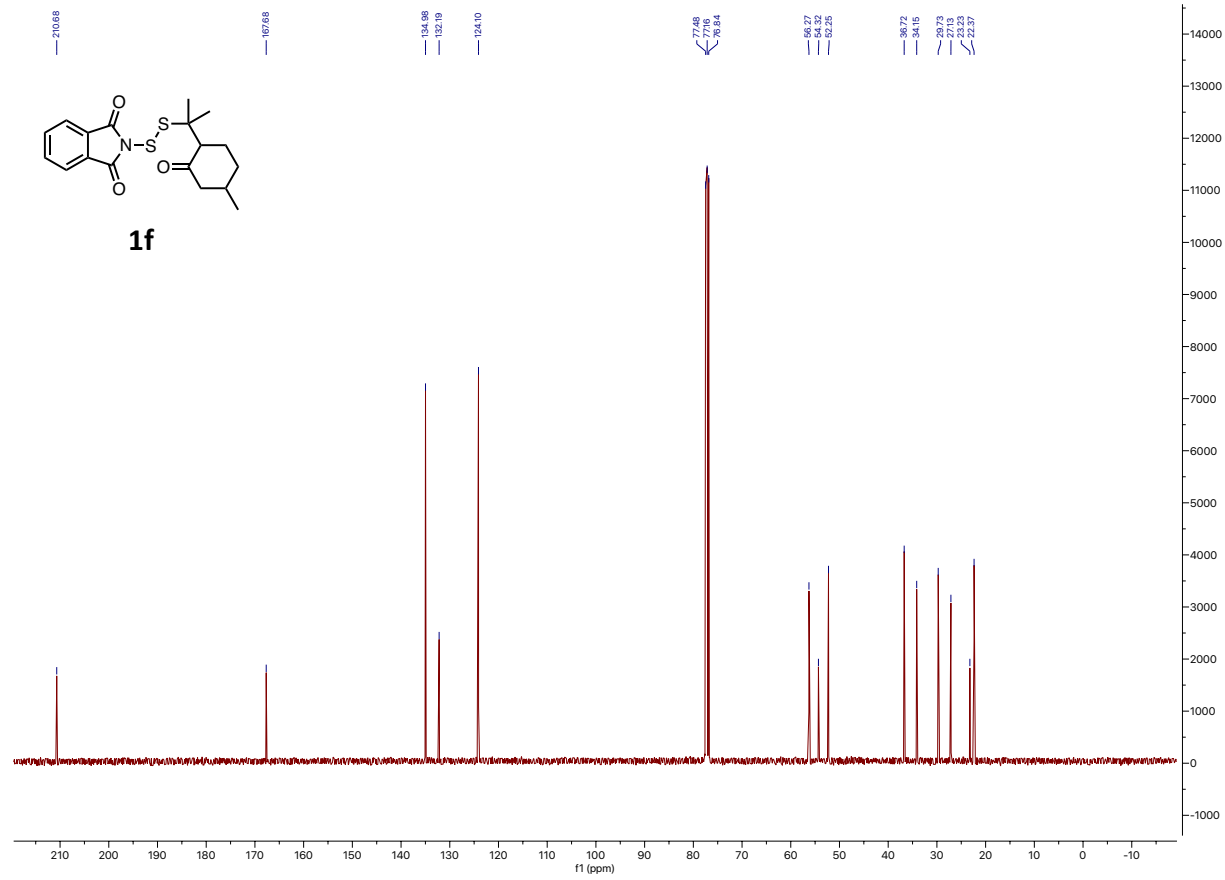
1f
f1 (ppm)

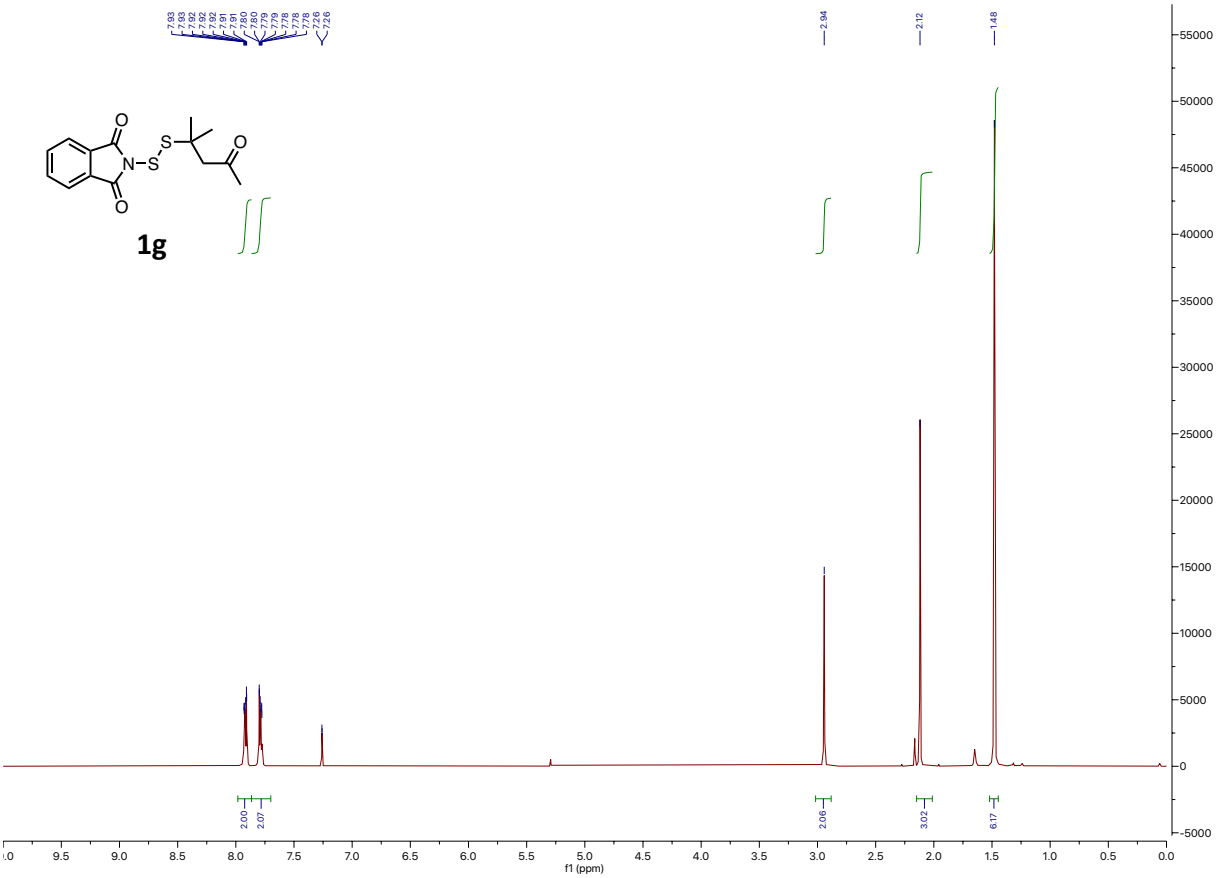
7.93
7.93
7.92
7.92
7.92
7.92
7.91
7.91
7.80
7.80
7.79
7.79
7.78
7.78
7.78
7.78
7.26
7.26
2.94
2.12
1.48
O
N
S
S
O
O
1g
55000
50000
45000
40000
35000
30000
25000
20000
15000
10000
5000
0
-5000
2.00
2.07
2.06
3.02
6.17
9.5
9.0
8.5
8.0
7.5
7.0
6.5
6.0
5.5
5.0
4.5
4.0
3.5
3.0
2.5
2.0
1.5
1.0
0.5
0.0
f1 (ppm)

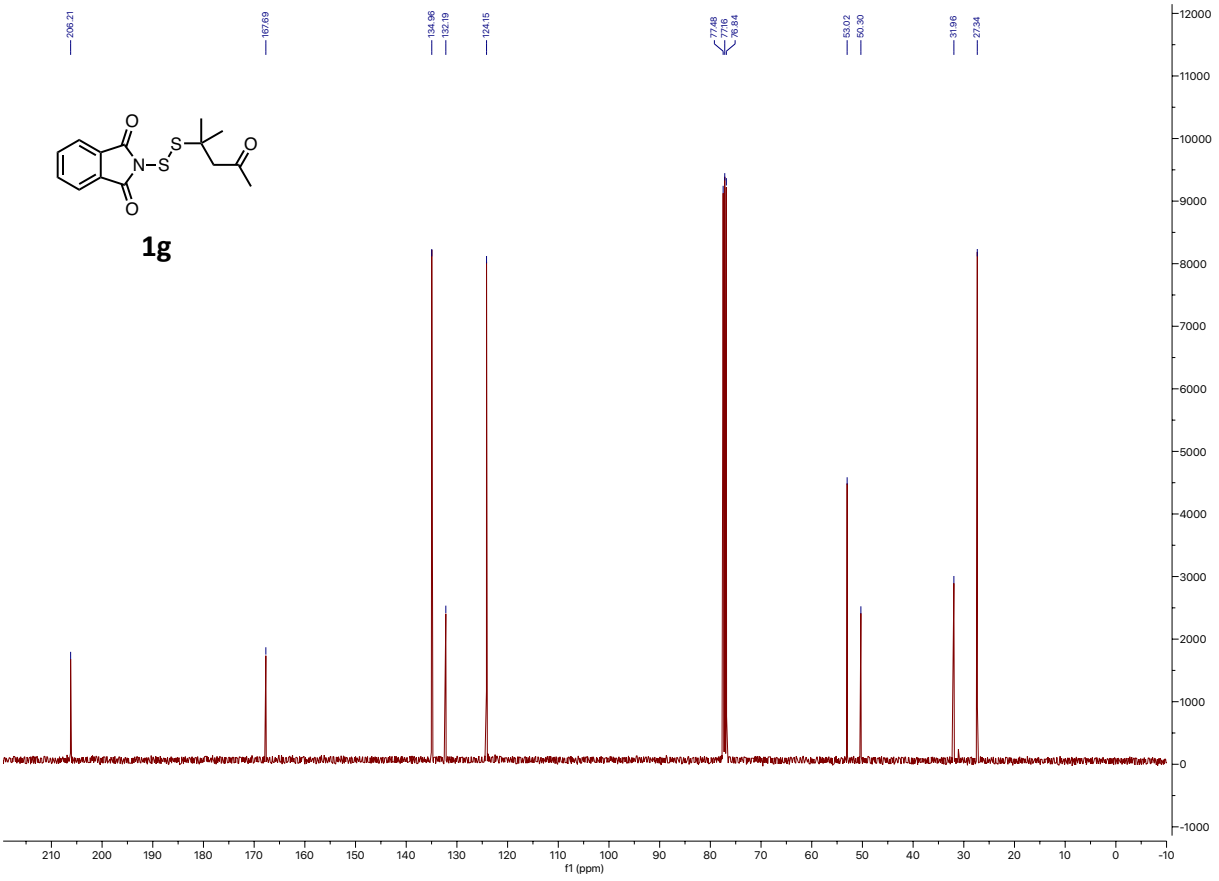
206.21
167.69
134.96
132.19
124.15
77.48
77.16
76.84
53.02
50.30
31.96
27.34
O
N
S
S
O
O
1g
12000
11000
10000
9000
8000
7000
6000
5000
4000
3000
2000
1000
0
-1000
210
200
190
180
170
160
150
140
130
120
110
100
90
80
70
60
50
40
30
20
10
0
-10
f1 (ppm)

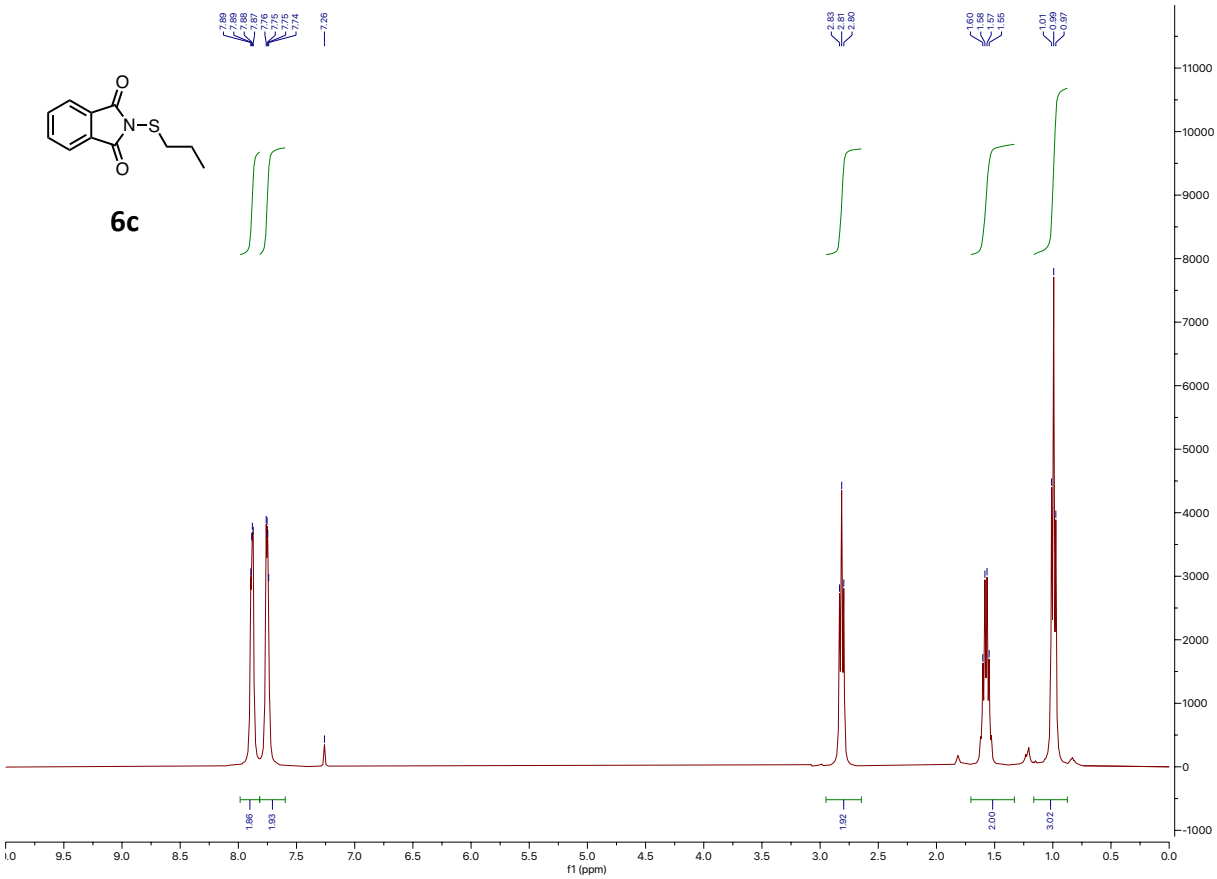
7.89
7.88
7.88
7.87
7.76
7.75
7.75
7.74
7.26
2.83
2.81
2.80
1.60
1.58
1.57
1.55
1.01
0.99
0.97
6c
1.86
1.93
1.92
2.00
3.02
f1 (ppm)

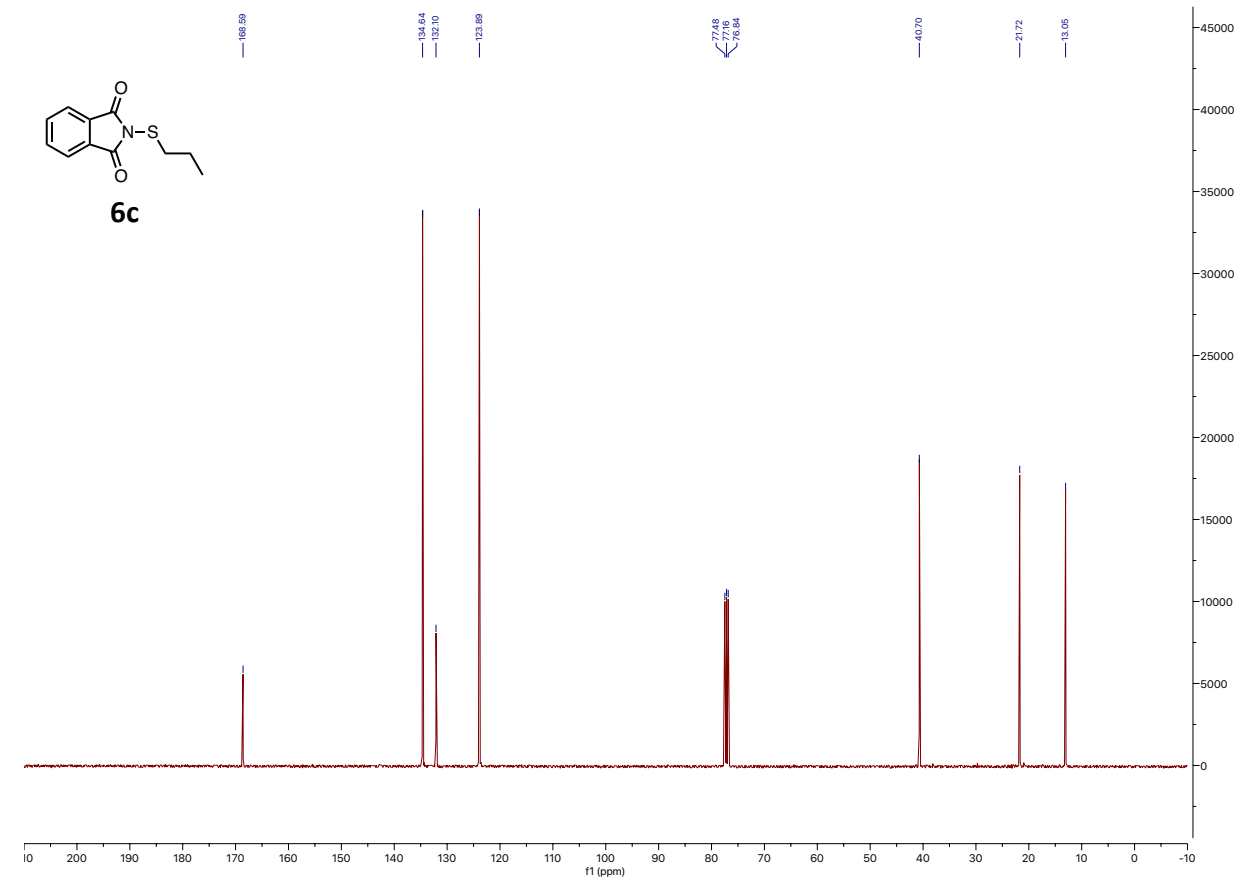
168.59
134.64
132.10
123.89
77.48
77.16
76.84
40.70
21.72
13.05
6c
f1 (ppm)

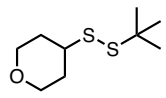

3a

7.26
4.00
3.97
3.43
3.42
3.41
3.40
3.40
3.39
3.38
3.37
2.99
2.04
2.03
2.03
2.02
2.02
2.01
2.00
2.00
2.00
1.99
1.98
1.99
1.63
1.62
1.60
1.42
1.39
1.33
1.32
2.00
2.02
0.99
2.06
2.28
8.79
f1 (ppm)

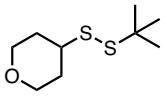

3a

77.37
77.16
76.96
67.50
47.63
46.90
32.93
30.17
f1 (ppm)

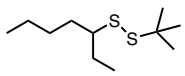

3b

7.26
2.68
2.66
2.64
1.67
1.66
1.65
1.65
1.63
1.59
1.58
1.57
1.56
1.55
1.40
1.40
1.38
1.37
1.35
1.33
1.32
1.31
0.99
0.97
0.96
0.93
0.91
0.89
1.00
4.18
13.27
3.17
3.14
f1 (ppm)

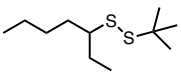

3b

77.48
77.16
76.84
54.80
47.49
33.42
30.18
29.08
26.87
22.87
14.17
11.05
f1 (ppm)

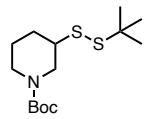
S
S
N
Boc

3c

7.26
4.21
4.18
3.83
3.82
3.82
3.82
3.81
3.81
3.79
3.78
3.78
3.77
2.92
2.89
2.88
2.87
2.86
2.79
2.77
2.76
2.75
2.74
2.73
2.07
2.06
2.04
2.04
1.77
1.76
1.75
1.74
1.73
1.73
1.72
1.51
1.50
1.49
1.48
1.46
1.33
1.00
1.04
1.91
1.03
1.03
1.05
11.25
8.86
f1 (ppm)

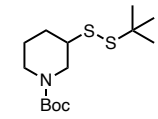
S
S
N
Boc

3c

154.69
79.76
77.37
77.16
76.95
49.51
47.68
43.99
30.67
30.12
28.63
28.58
25.03
f1 (ppm)

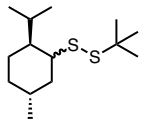

3d

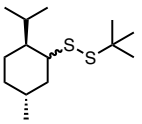

3d

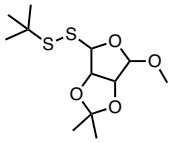

3e

7.26
5.19
5.19
5.04
4.98
4.96
4.66
4.64
3.41
1.45
1.45
1.36
1.31
1.31
0.97
0.99
1.00
0.99
3.00
3.03
9.05
3.03
f1 (ppm)

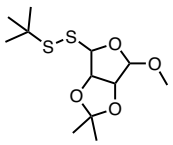

3e

112.97
110.40
98.63
86.55
84.50
77.48
77.16
76.84
55.46
48.07
29.99
29.49
29.16
f1 (ppm)

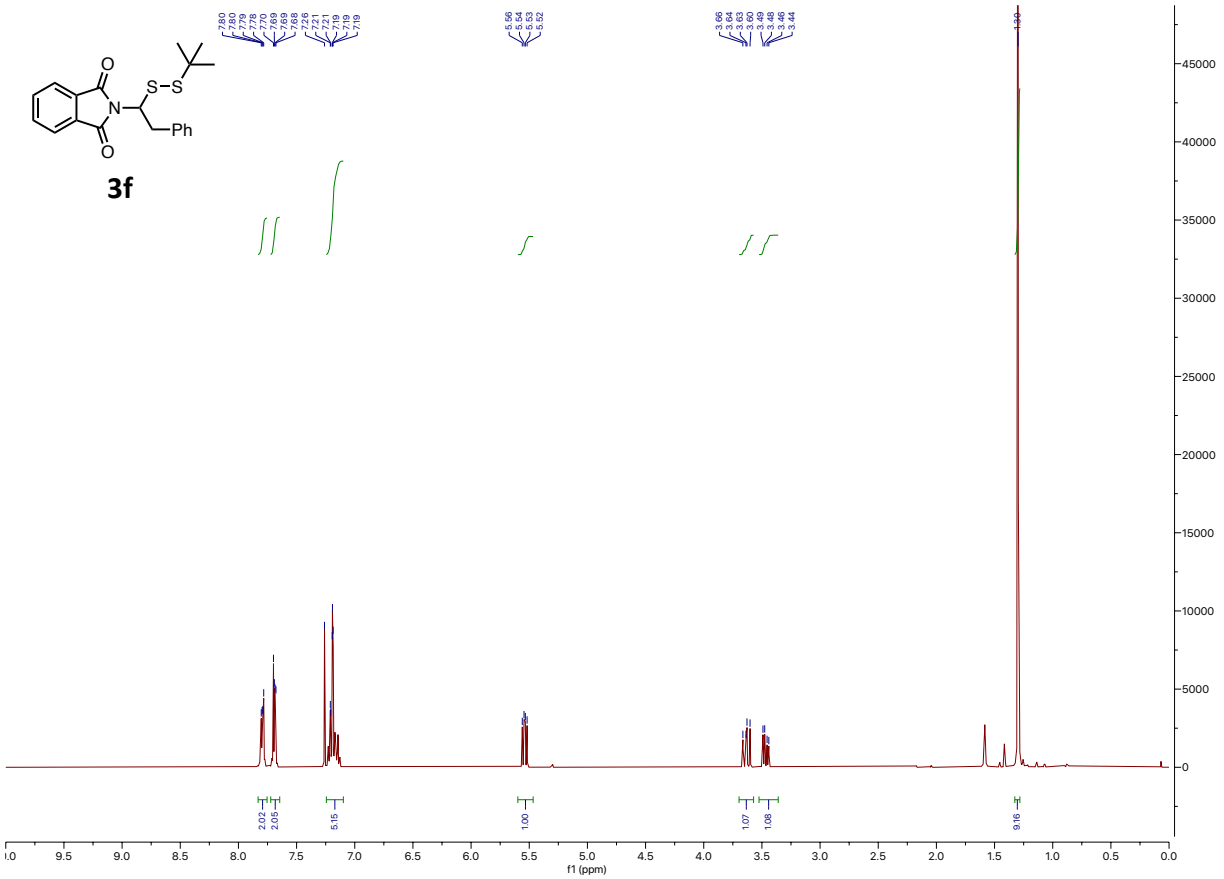
3f
f1 (ppm)

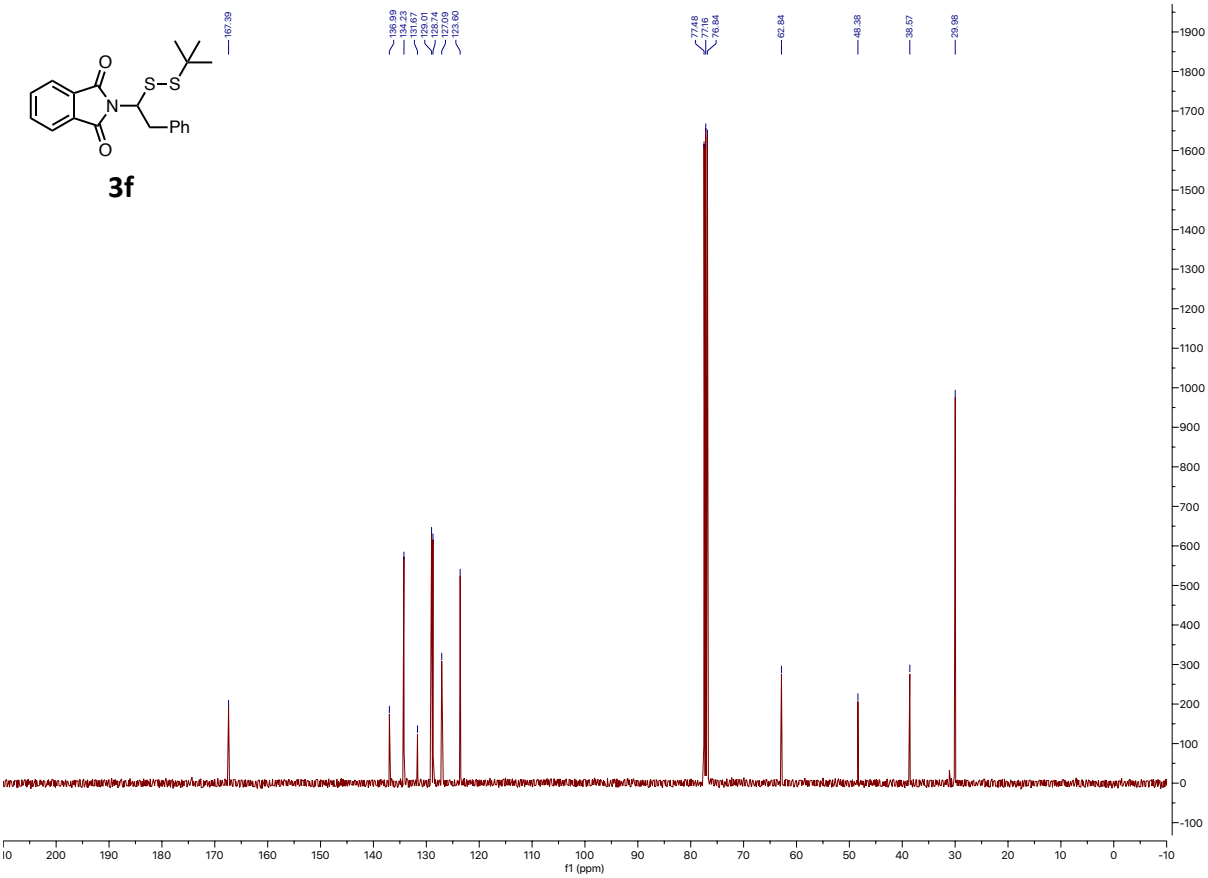
3f
f1 (ppm)

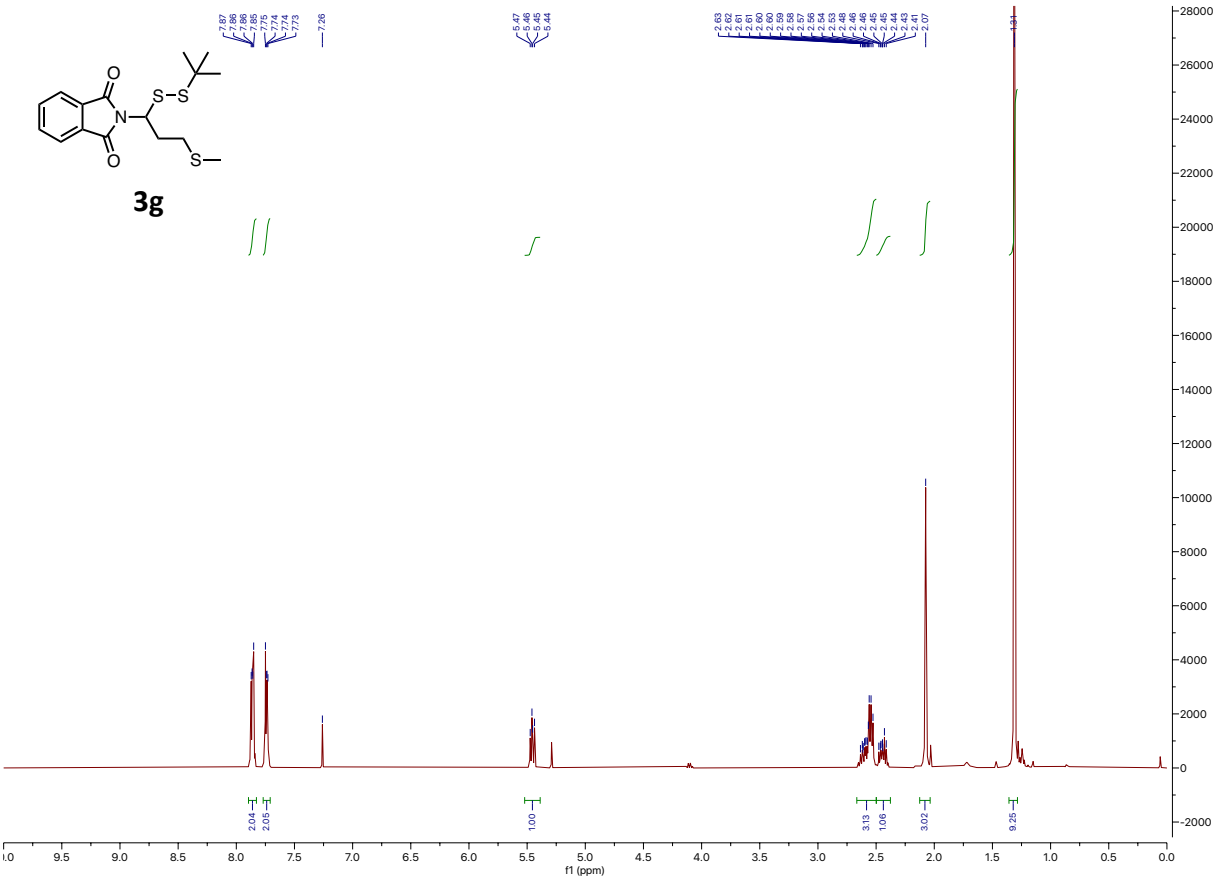
3g
f1 (ppm)

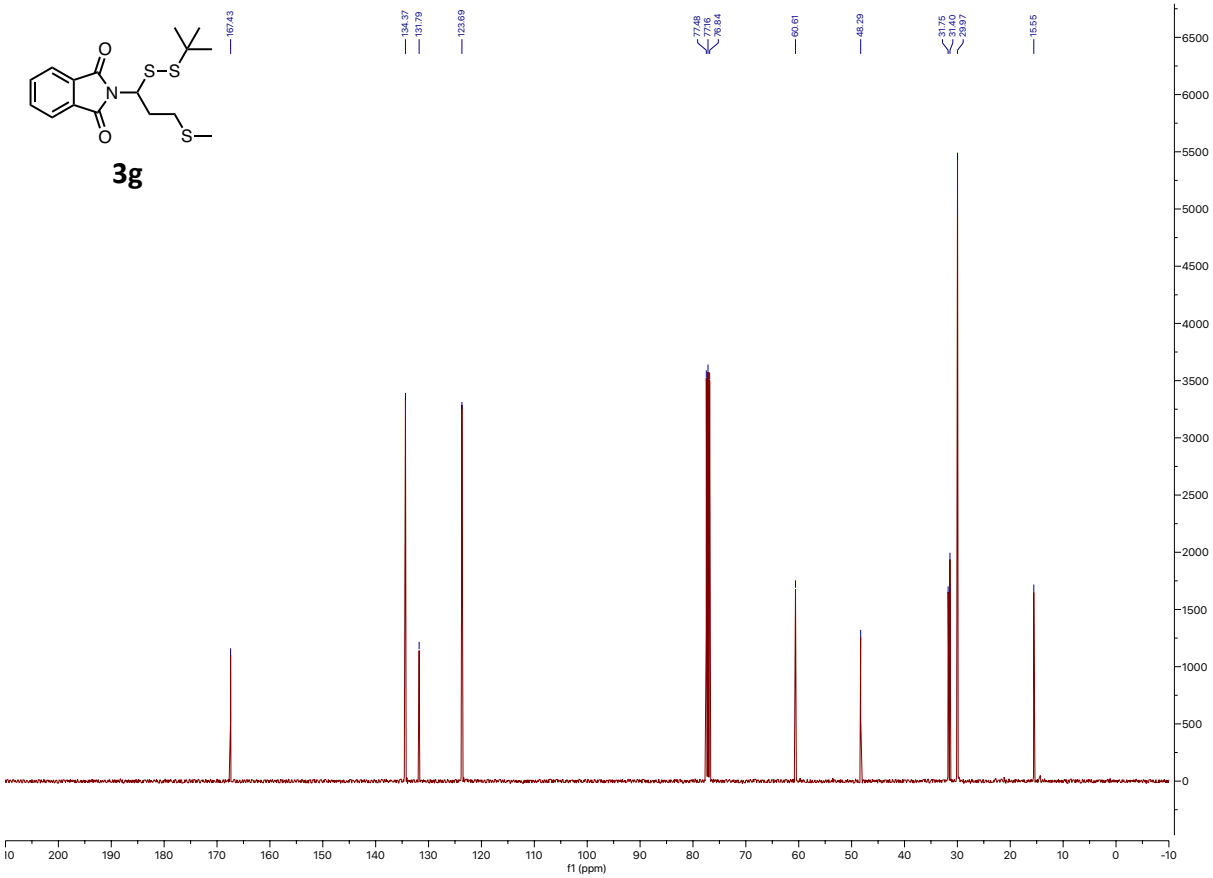
3g
f1 (ppm)

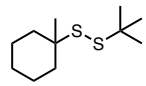

3h

7.26
4.00
6.00
8.75
3.08
f1 (ppm)

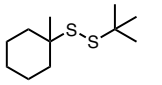

3h

77.48
77.16
76.84
50.23
46.22
38.20
30.80
30.33
25.83
22.92
f1 (ppm)

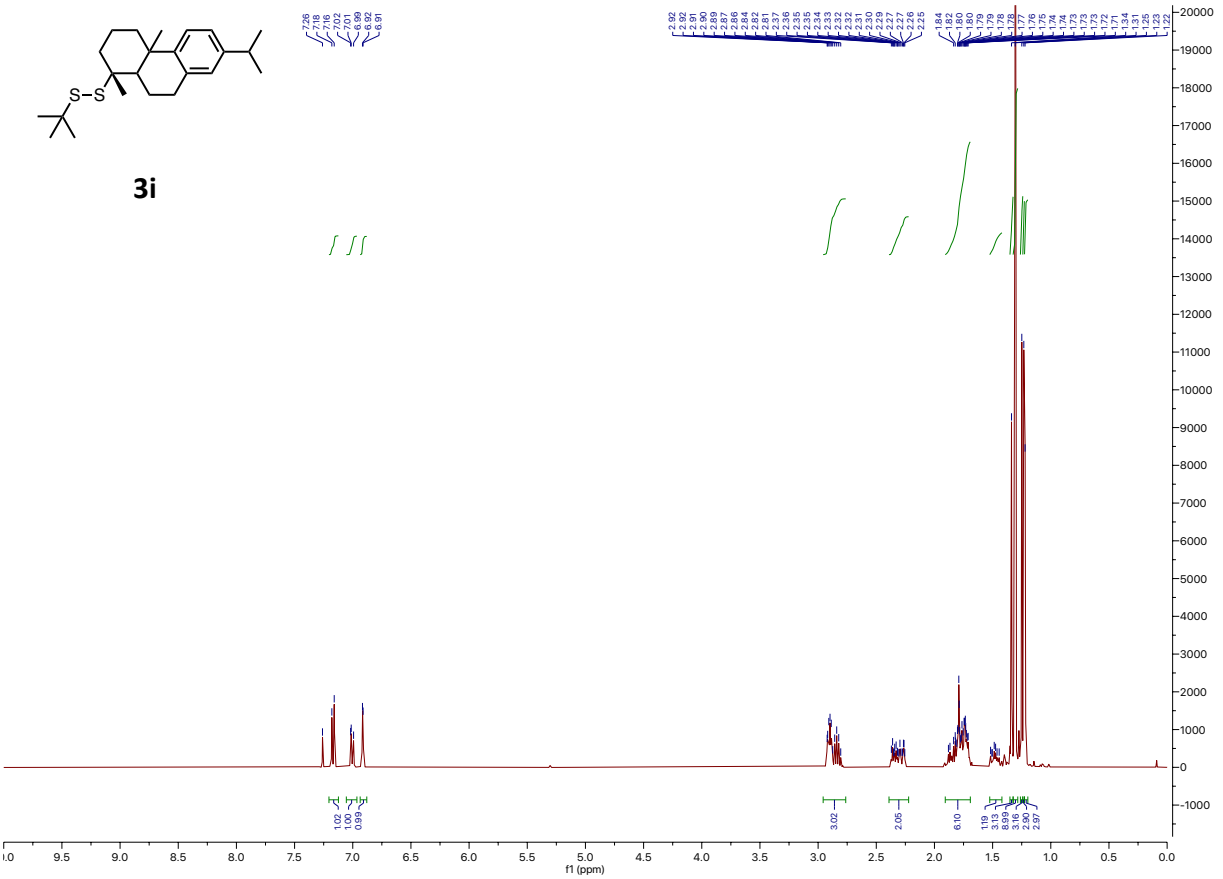
3i
f1 (ppm)

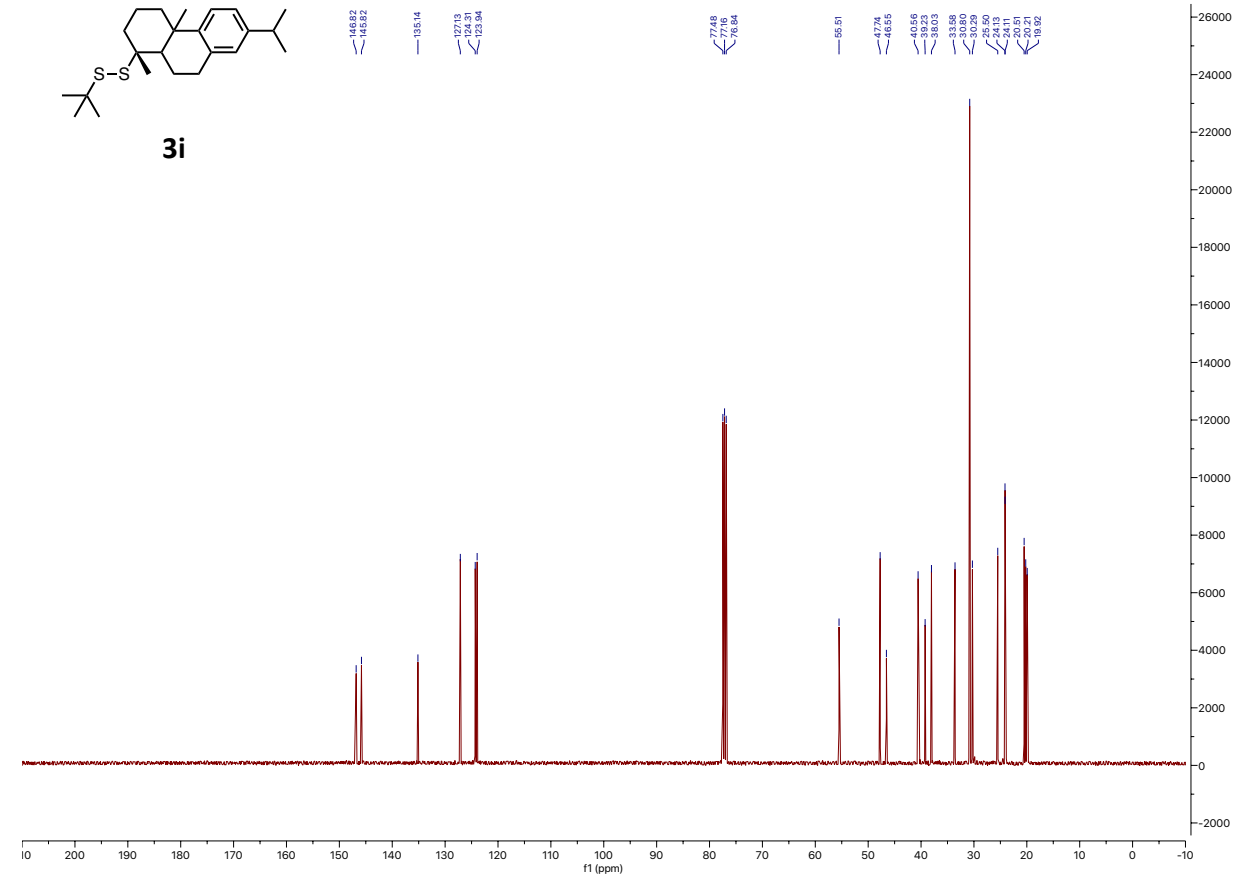
3i
f1 (ppm)

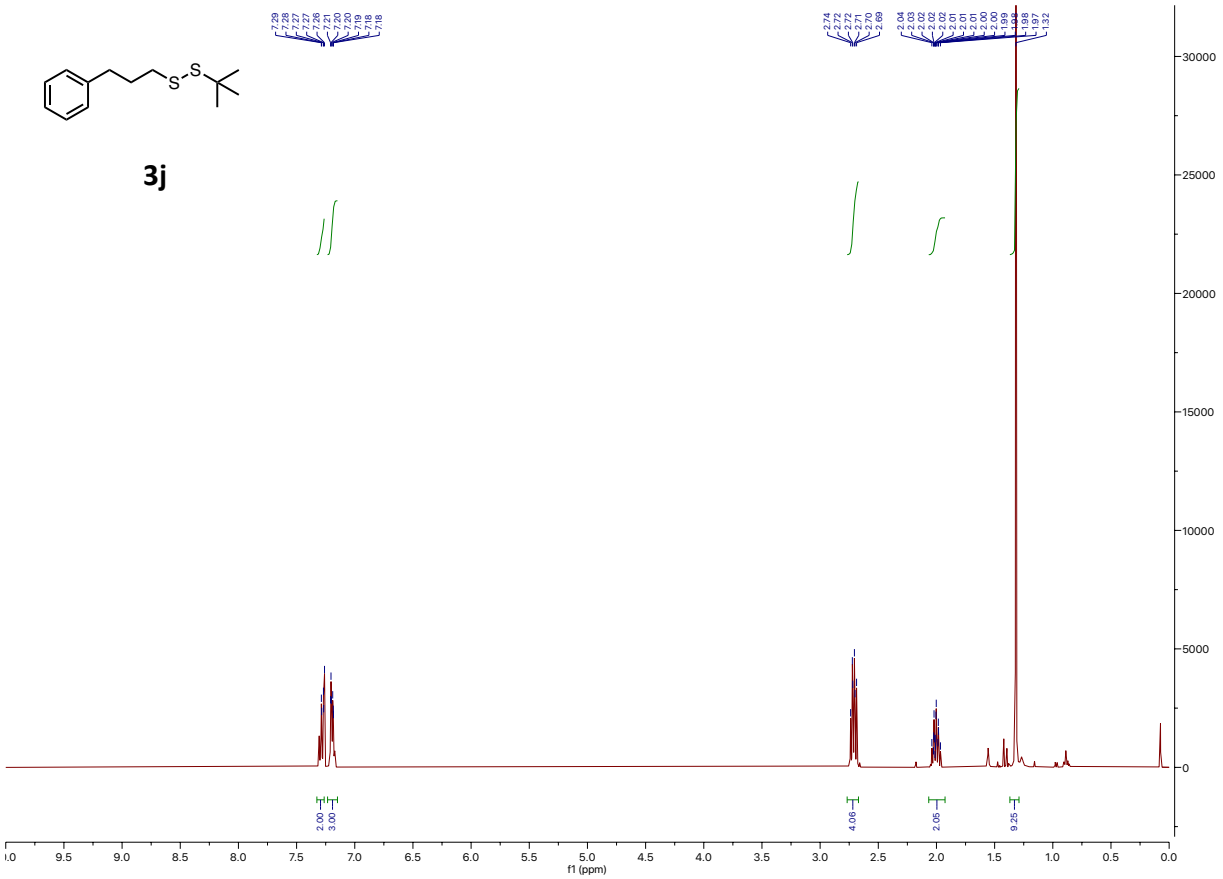
3j
f1 (ppm)

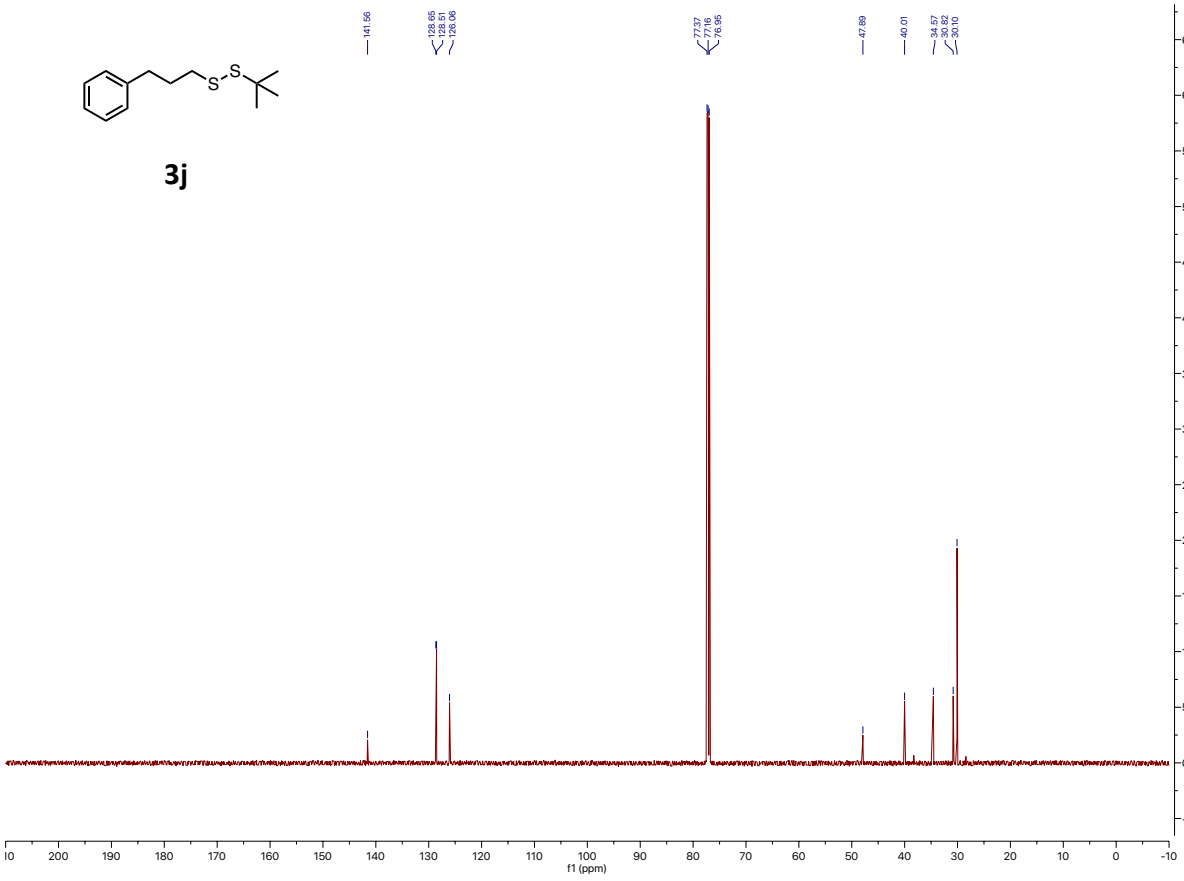
3j
f1 (ppm)

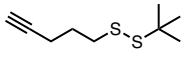

3k

7.26
2.81
2.79
2.78
2.34
2.33
2.32
2.31
2.30
1.97
1.96
1.92
1.90
1.88
1.33
1.32
2.00
2.02
0.93
2.00
9.17
f1 (ppm)

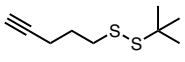

3k

83.53
77.48
77.16
76.84
69.10
47.94
39.15
30.09
27.94
17.37
f1 (ppm)

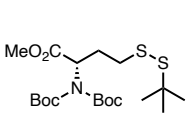

3m

7.26
5.01
4.99
4.98
4.97
3.71
2.75
2.75
2.73
2.73
2.71
2.66
2.65
2.55
2.53
2.51
2.34
2.23
2.21
2.04
1.49
1.32
1.00
3.15
1.99
1.04
1.00
18.81
9.49
f1 (ppm)

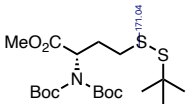

3m

171.04
151.96
83.46
77.48
77.16
76.84
57.03
52.39
48.00
37.09
30.11
30.03
28.12
f1 (ppm)

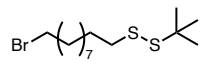
Br
S
S
7

3n

7.26
3.42
3.40
3.39
2.71
2.70
2.68
1.88
1.87
1.85
1.84
1.83
1.81
1.66
1.65
1.64
1.62
1.60
1.44
1.42
1.40
1.38
1.36
1.34
1.33
1.32
1.29
1.28
2.00
1.99
2.02
2.03
4.02
9.24
7.85
f1 (ppm)

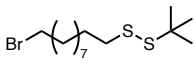
Br
S
S
7

3n

77.48
77.16
76.84
47.81
41.10
39.00
32.96
30.10
29.49
29.43
29.29
28.87
28.67
28.50
f1 (ppm)

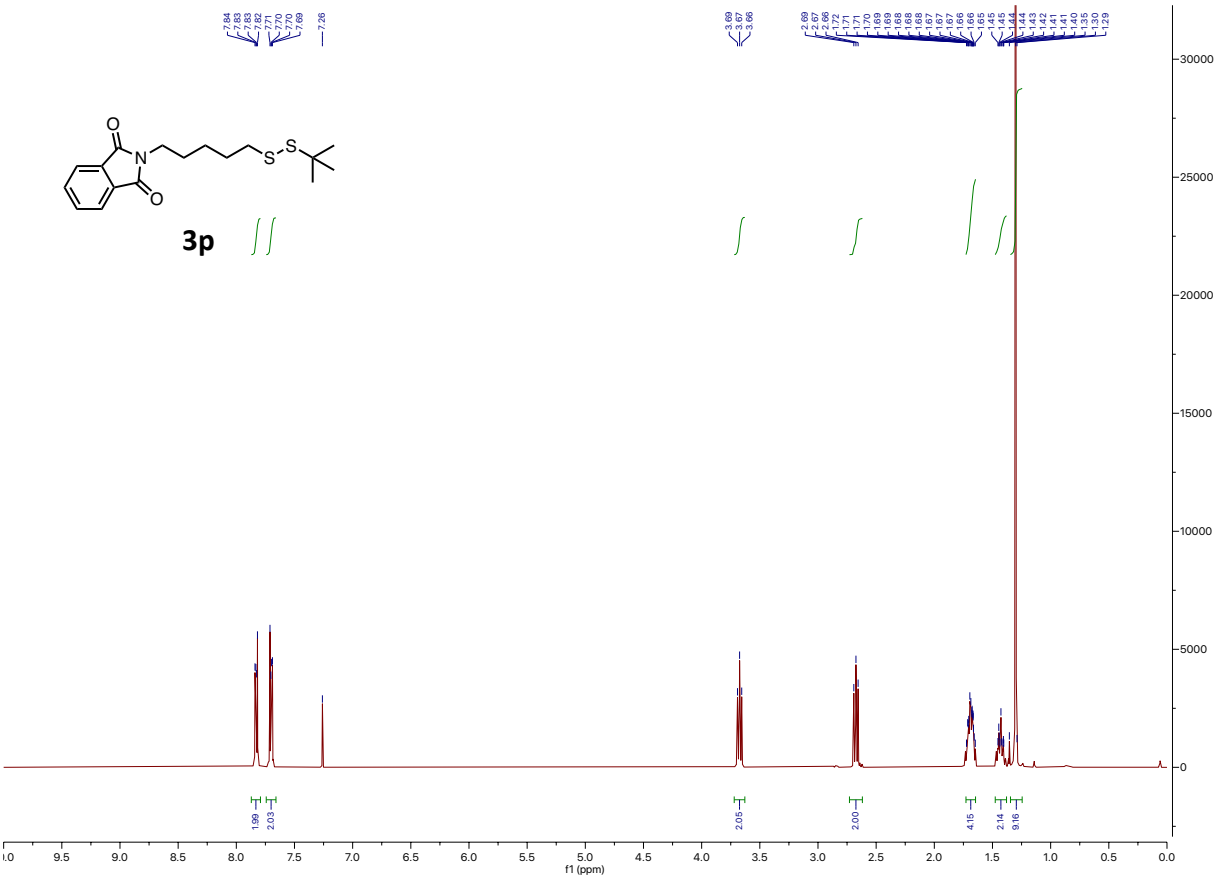
7.84
7.83
7.83
7.82
7.72
7.71
7.70
7.70
7.69
7.26
3.69
3.67
3.66
2.69
2.67
2.66
1.72
1.71
1.71
1.70
1.69
1.69
1.68
1.68
1.67
1.67
1.67
1.66
1.66
1.65
1.45
1.44
1.44
1.43
1.42
1.41
1.41
1.40
1.35
1.30
1.29
O
N
O
S
S
3p
1.99
2.03
2.05
2.00
4.15
2.14
9.16
f1 (ppm)

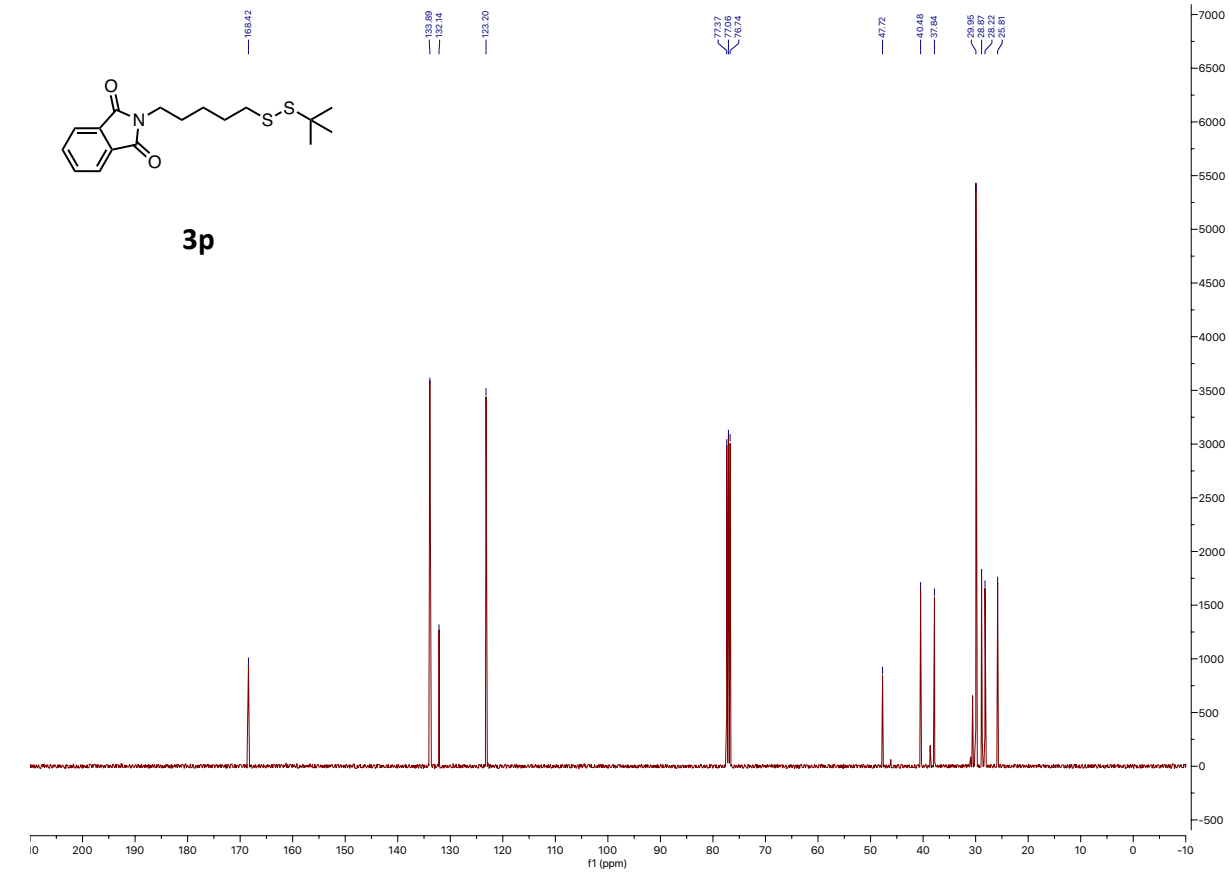
168.42
133.89
132.14
123.20
77.37
77.06
76.74
47.72
40.48
37.84
29.95
28.87
28.22
25.81
O
N
O
S
S
3p
f1 (ppm)

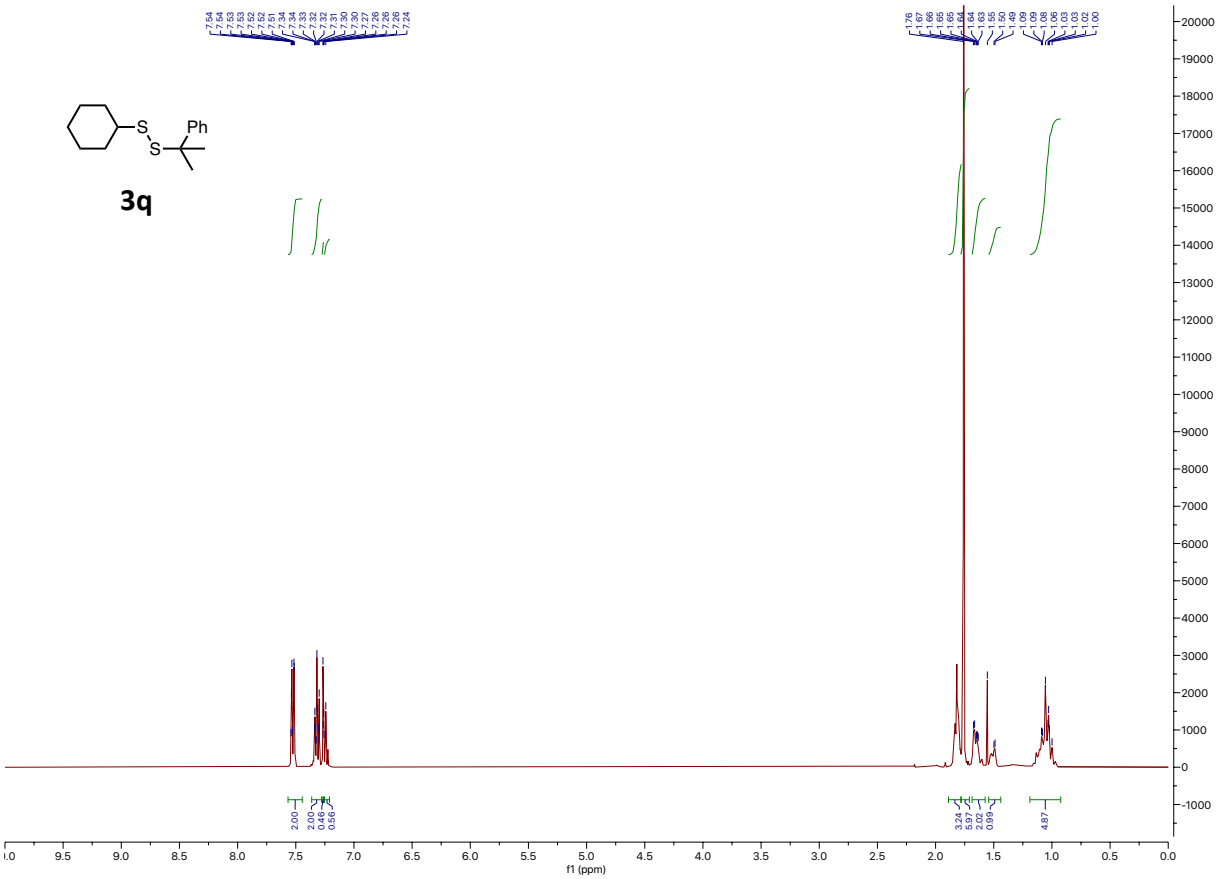
3q
f1 (ppm)

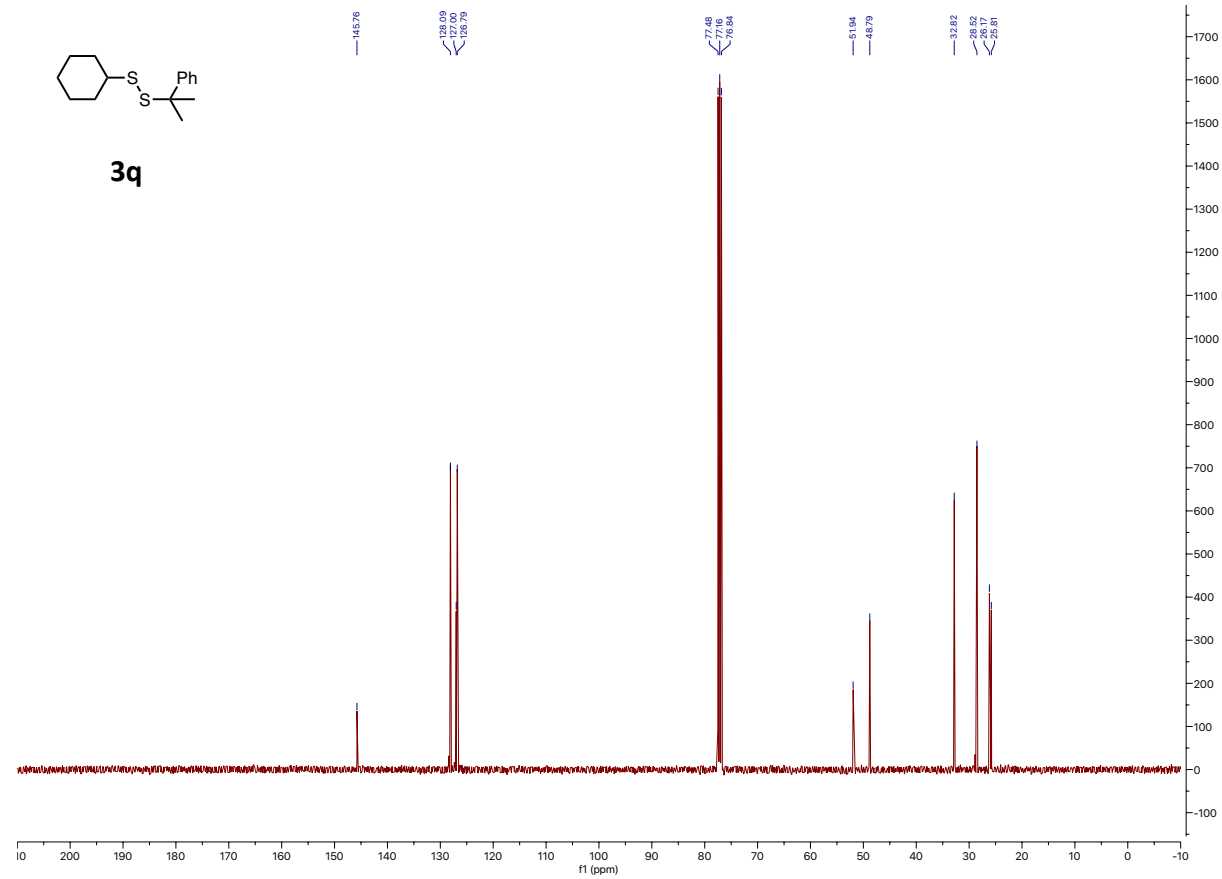
3q
f1 (ppm)

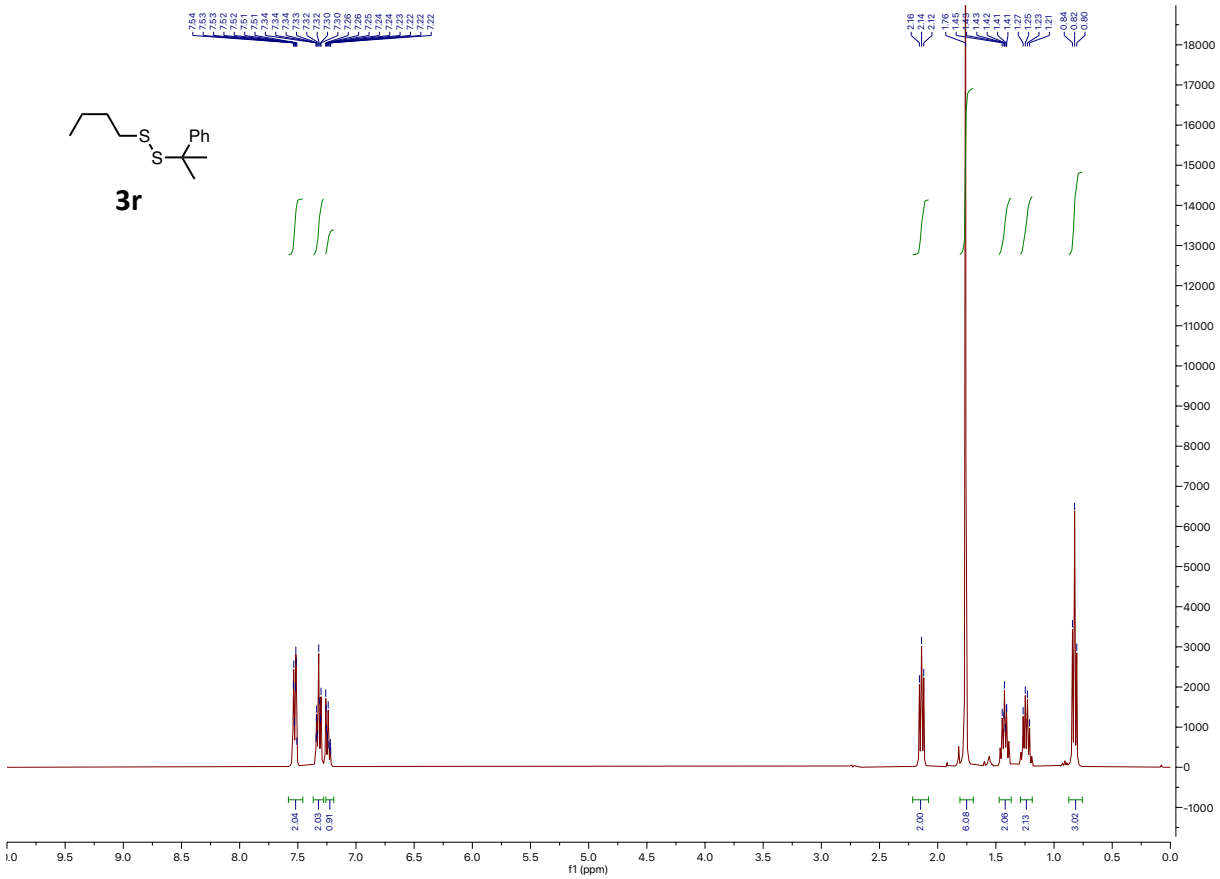
3r
f1 (ppm)

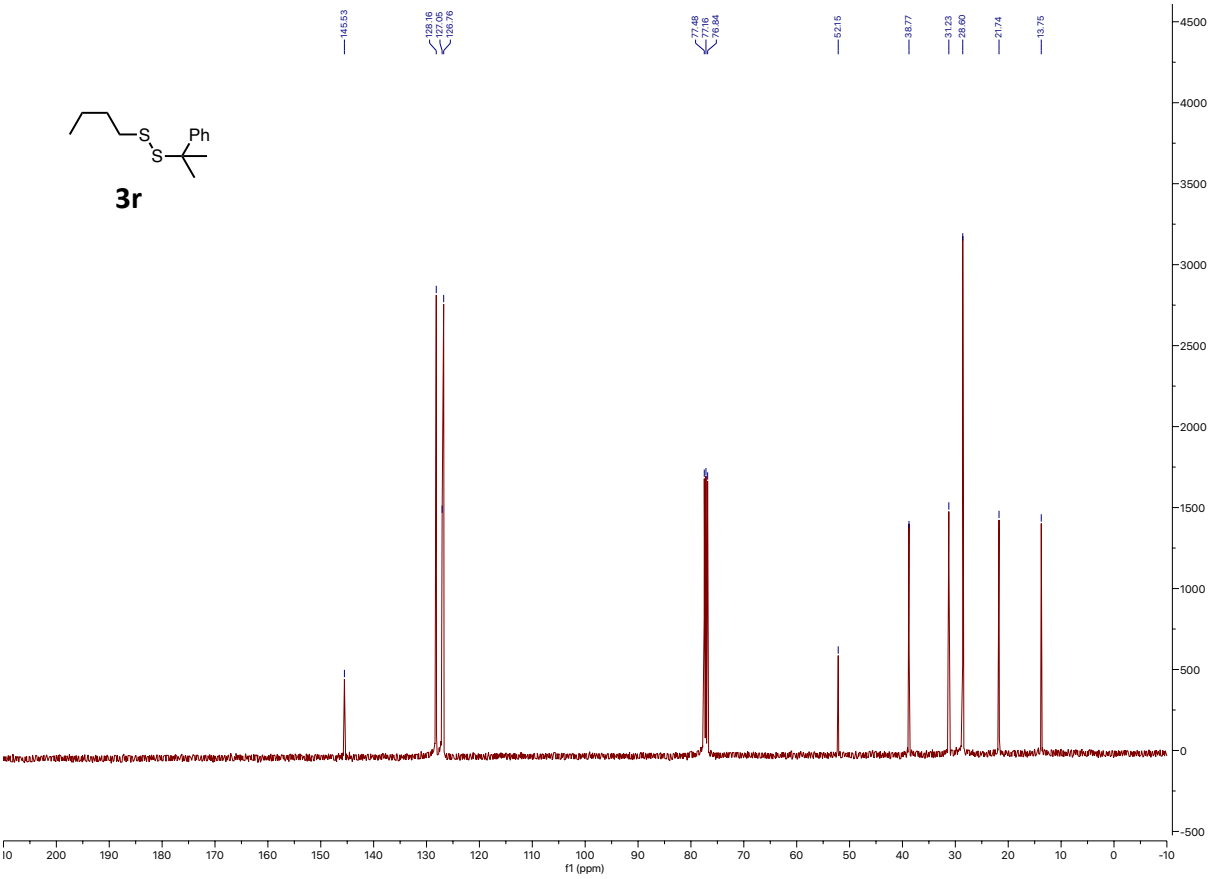
3r
f1 (ppm)

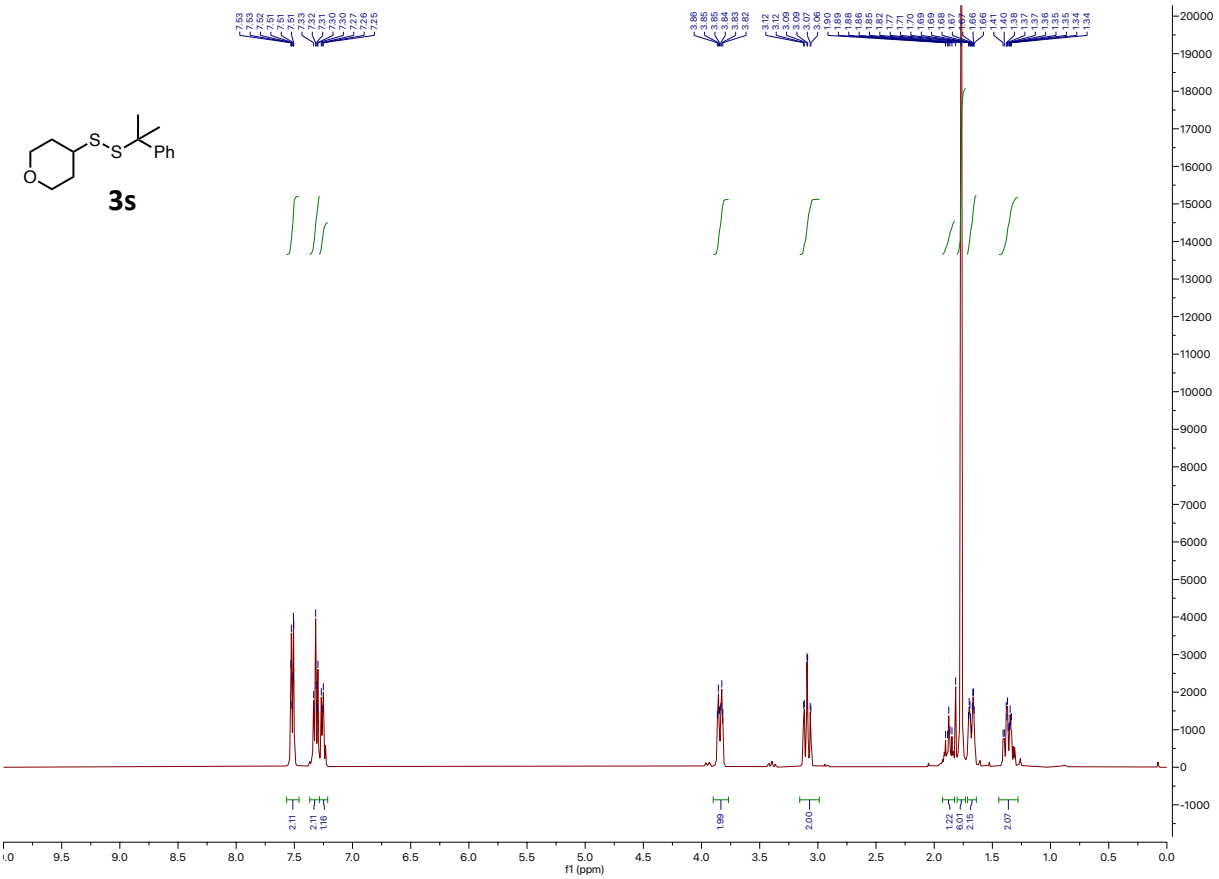
3s
f1 (ppm)

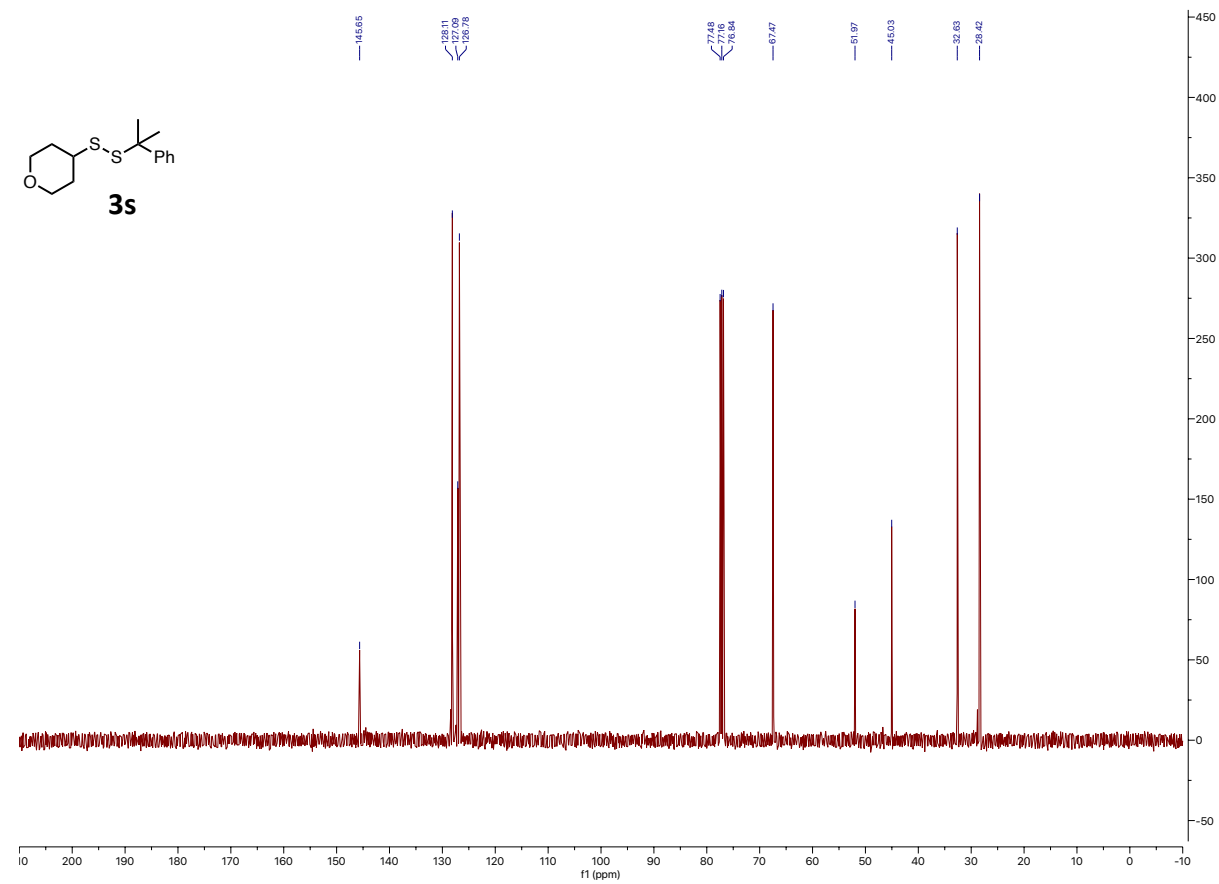
3s
f1 (ppm)

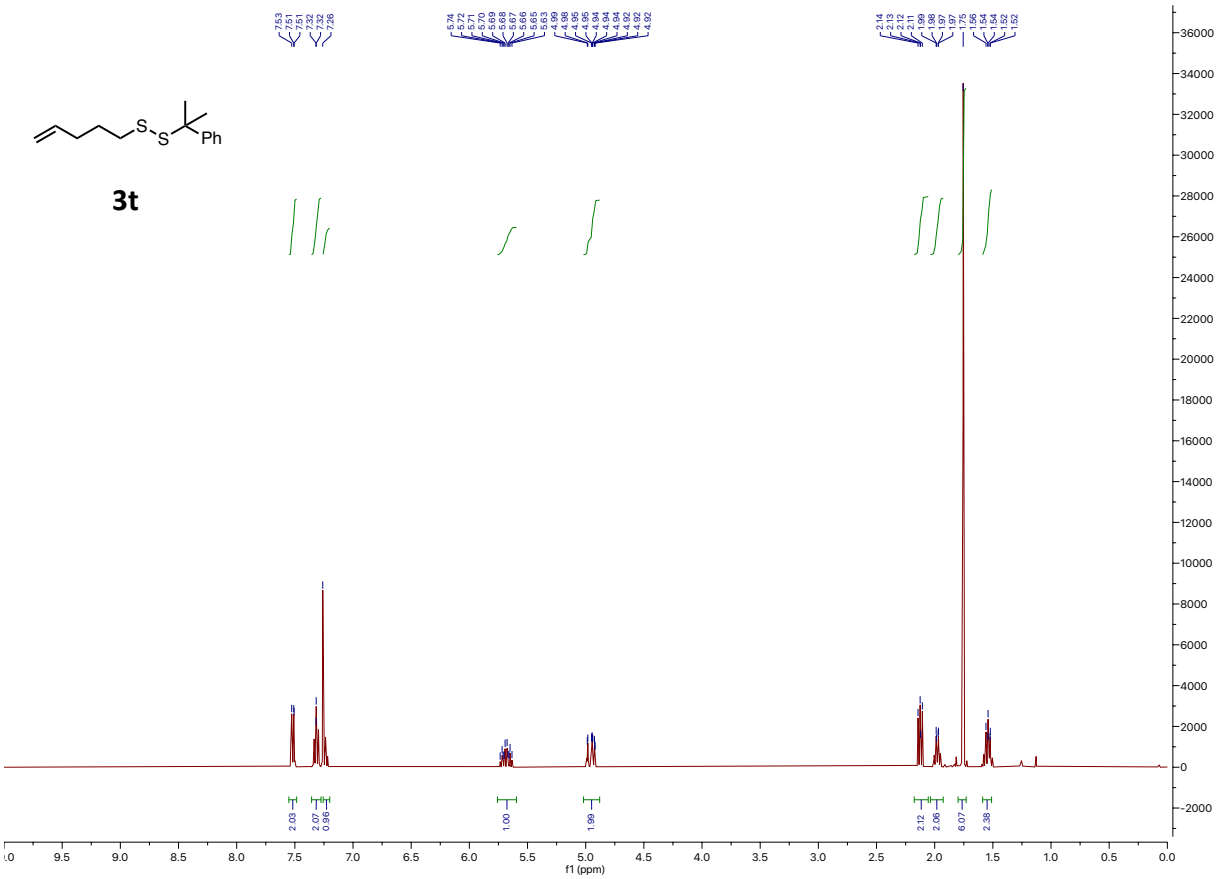
3t
f1 (ppm)

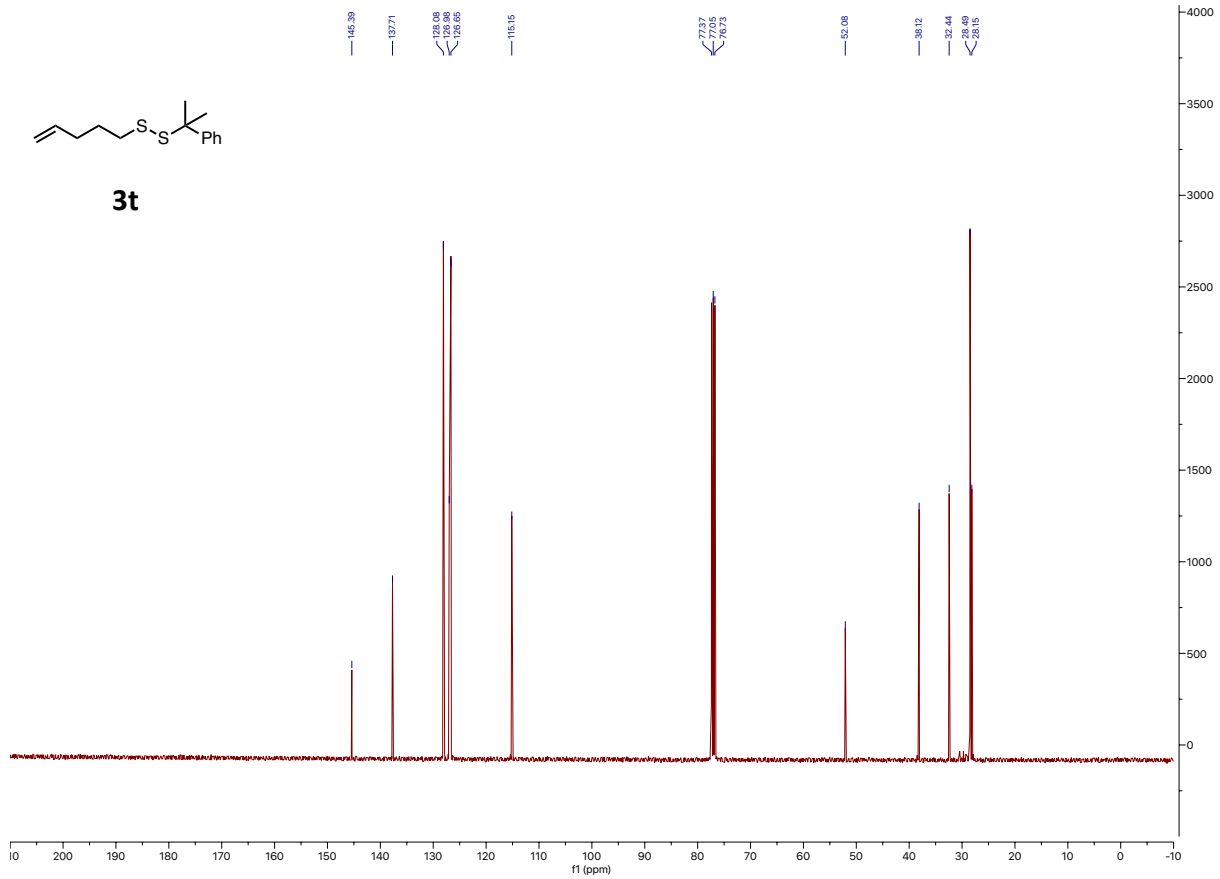
3t
f1 (ppm)

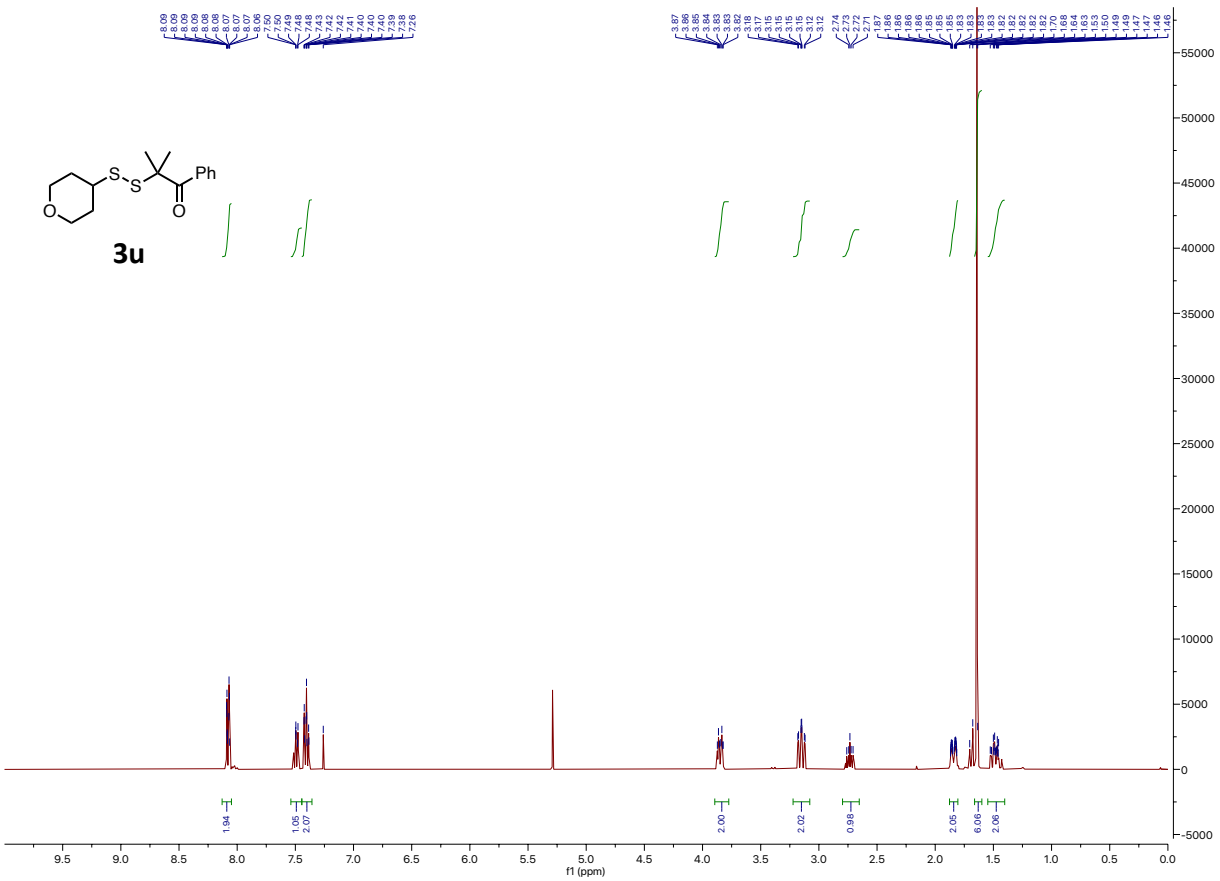
S
S
Ph
O
O
3u
f1 (ppm)

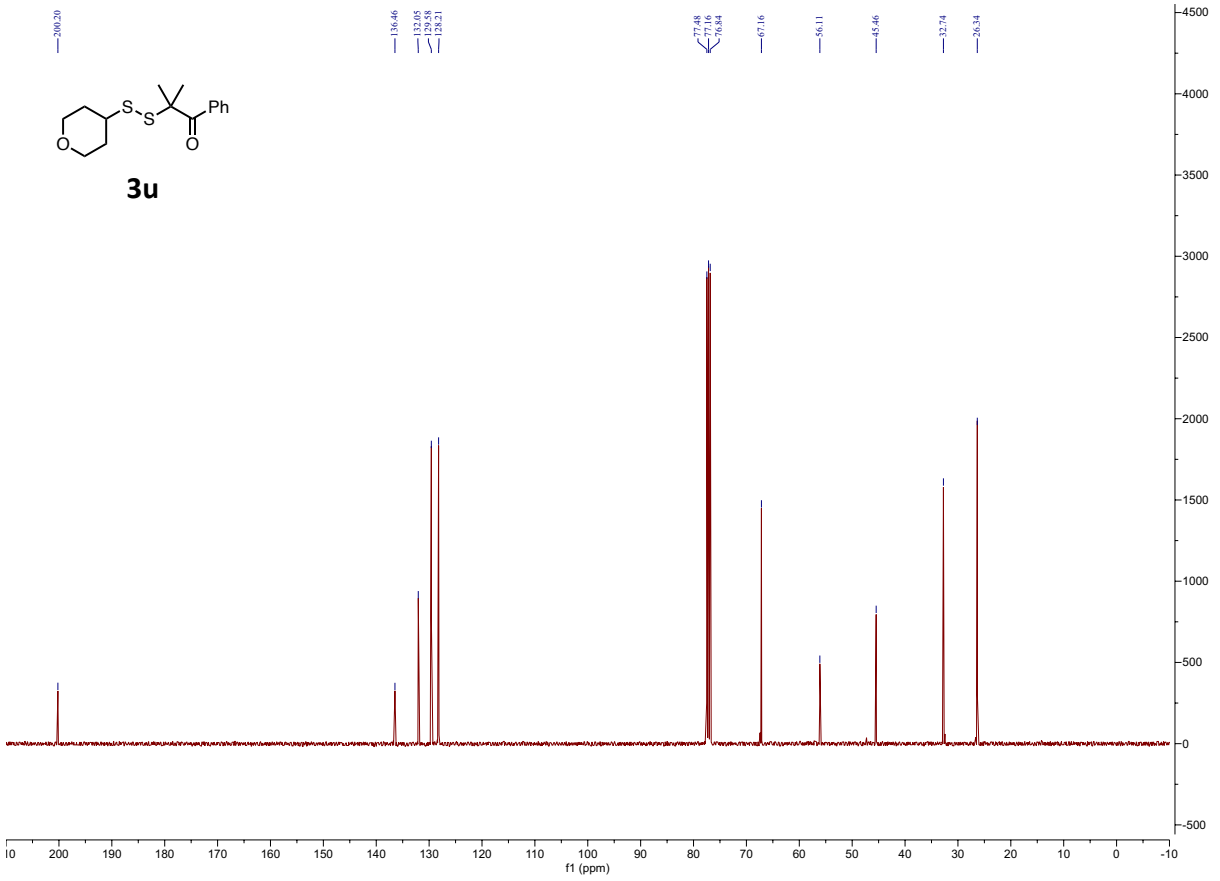
S
S
Ph
O
O
3u
f1 (ppm)

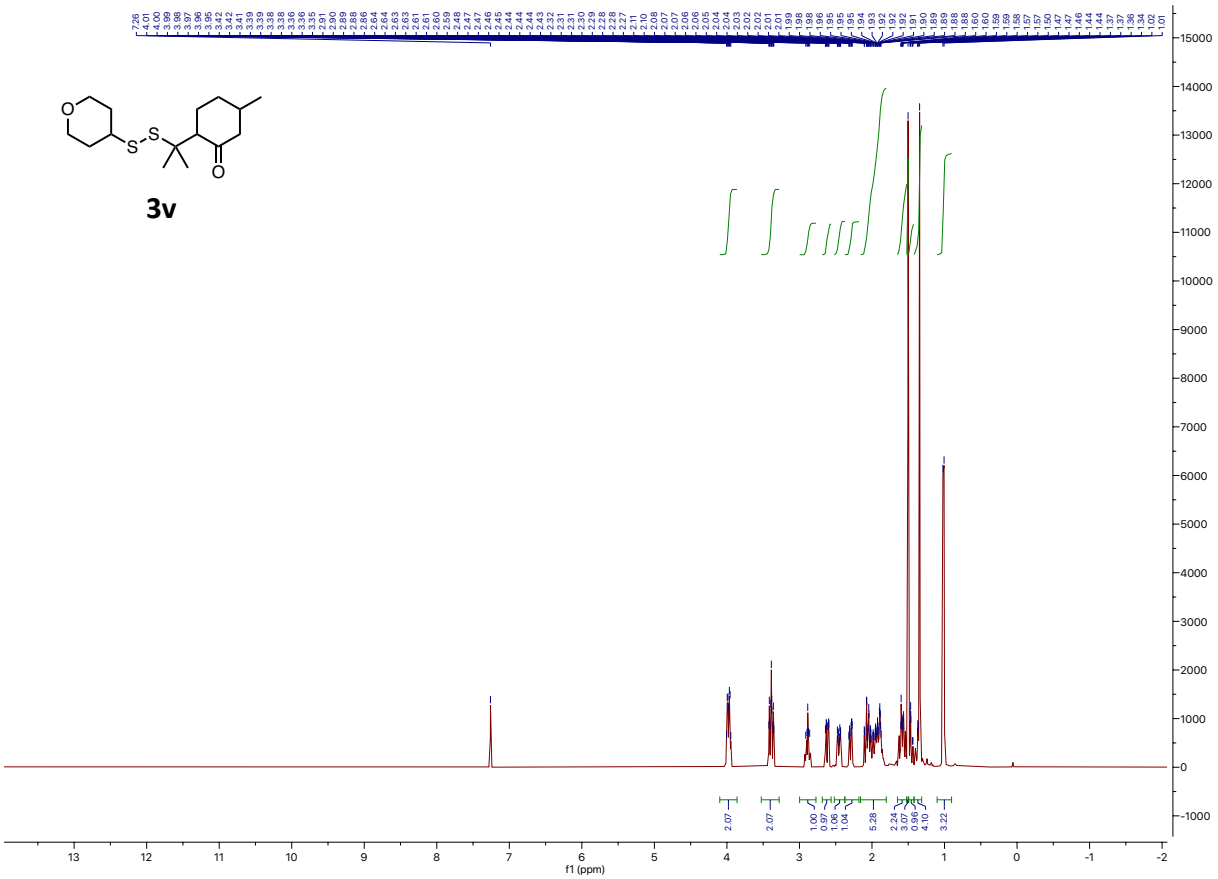
3v
f1 (ppm)

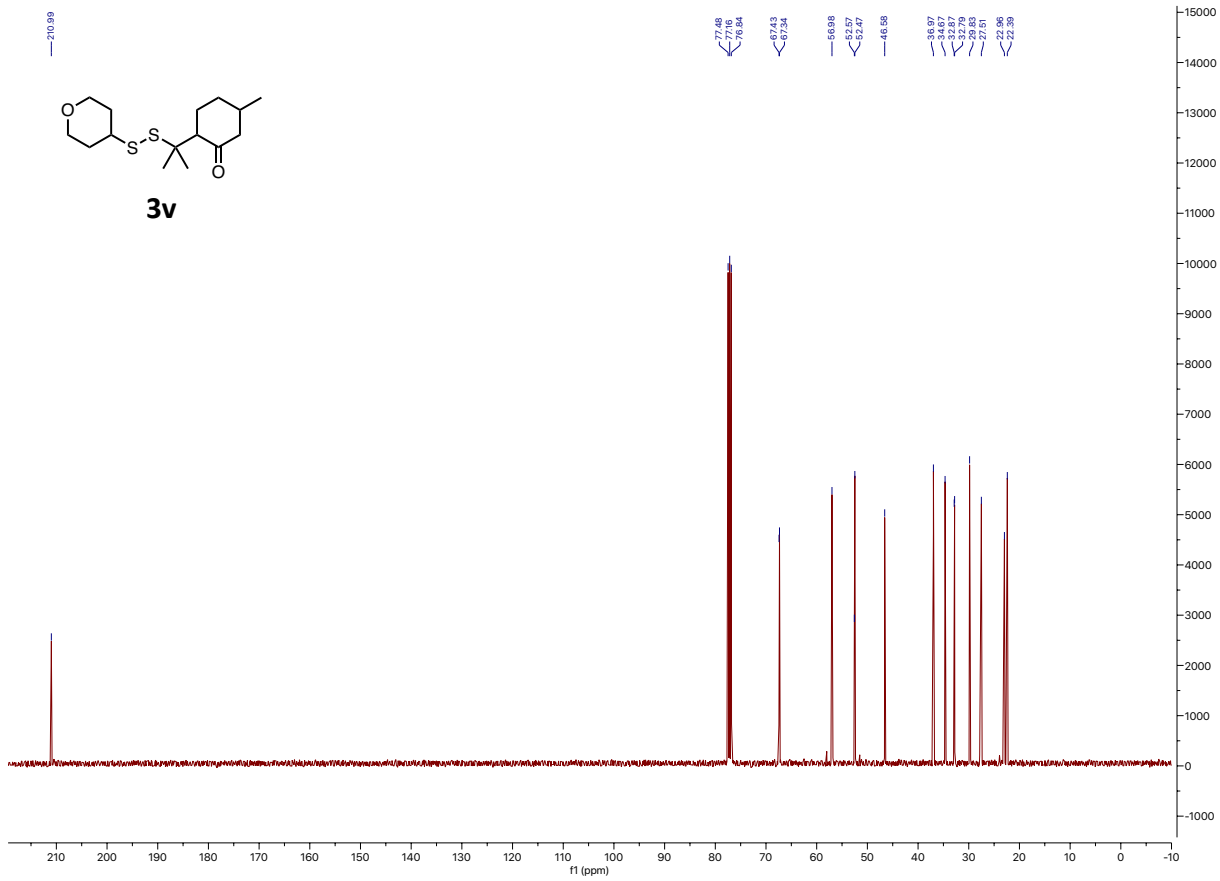
3v
f1 (ppm)

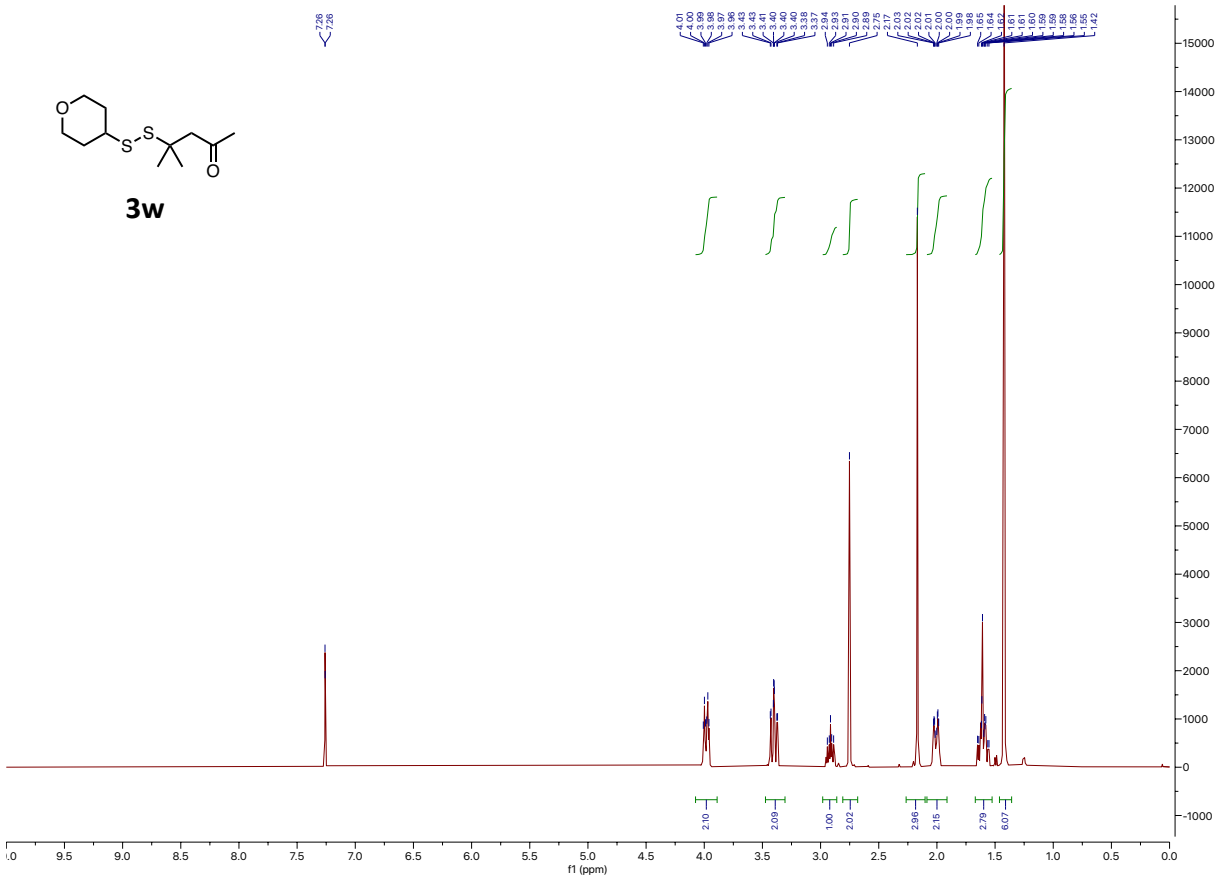
3w
f1 (ppm)

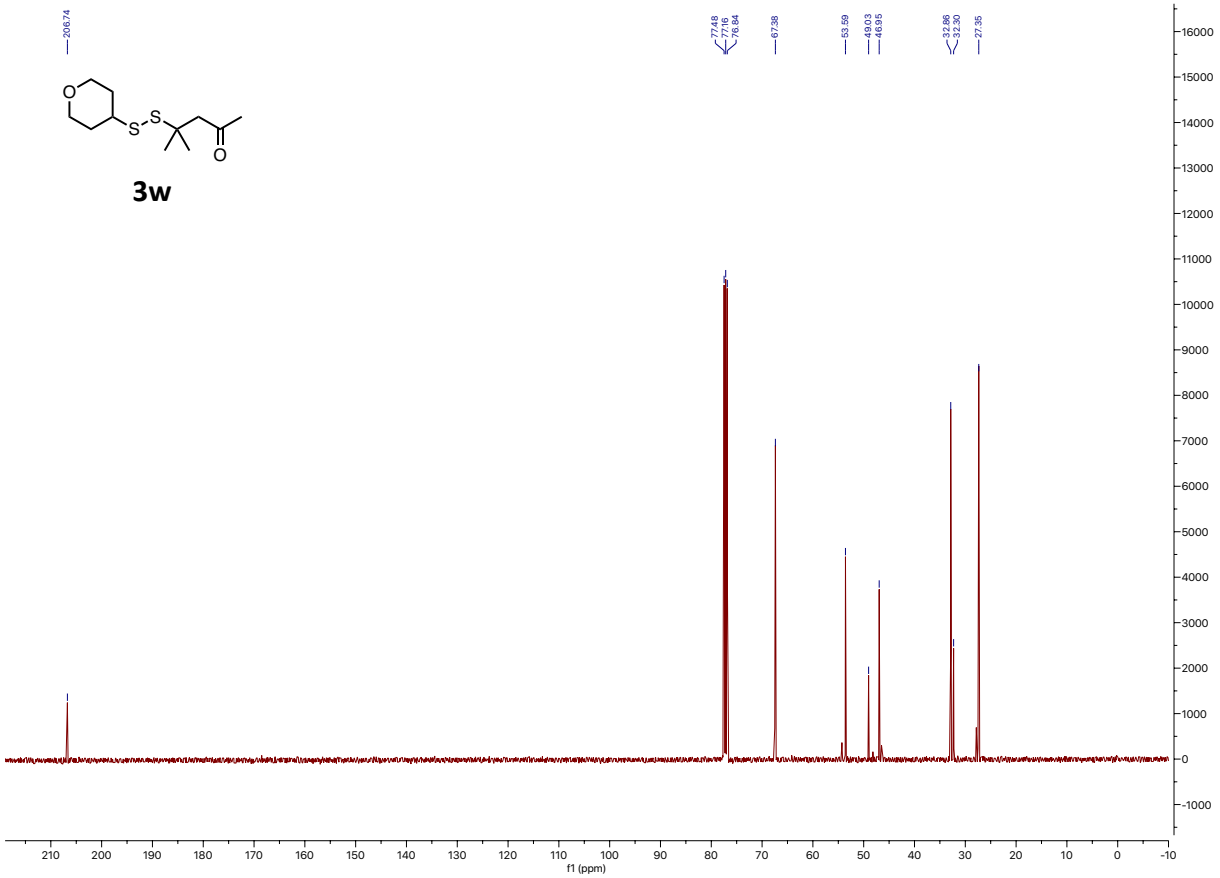
3w
f1 (ppm)

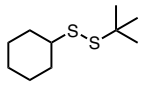

3aa

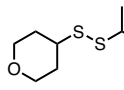

3ab

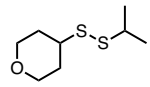

3ab

77.48
77.16
76.84
67.56
46.44
41.73
32.86
22.71
f1 (ppm)

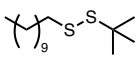

3ac

7.26
2.72
2.72
2.70
2.70
2.67
2.67
1.99
1.37
1.37
1.33
1.33
1.33
1.32
1.32
1.32
1.31
1.31
1.30
1.26
0.90
0.88
0.88
0.86
2.00
2.10
26.22
3.08
f1 (ppm)

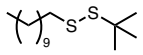

3ac

77.37
76.95
47.80
41.15
32.06
30.10
29.76
29.74
29.64
29.46
29.47
29.37
28.75
22.84
14.27
f1 (ppm)

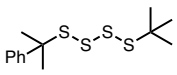

4c

7.53
7.52
7.51
7.50
7.35
7.35
7.33
7.27
7.26
1.83
1.36
2.00
2.05
1.15
6.00
8.93
f1 (ppm)

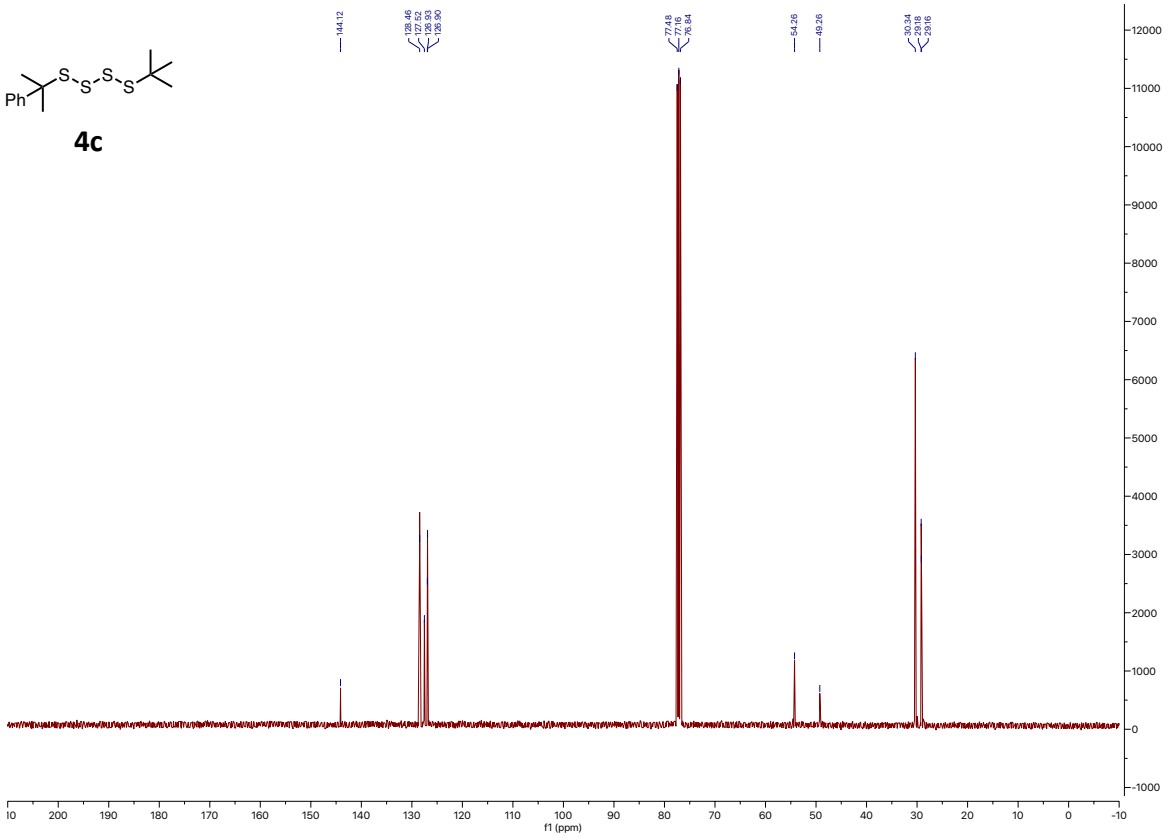
144.12
138.46
127.52
126.93
125.90
77.48
77.16
76.84
54.26
49.26
30.34
29.18
29.16
Ph
S
S
S
S
f1 (ppm)

4c

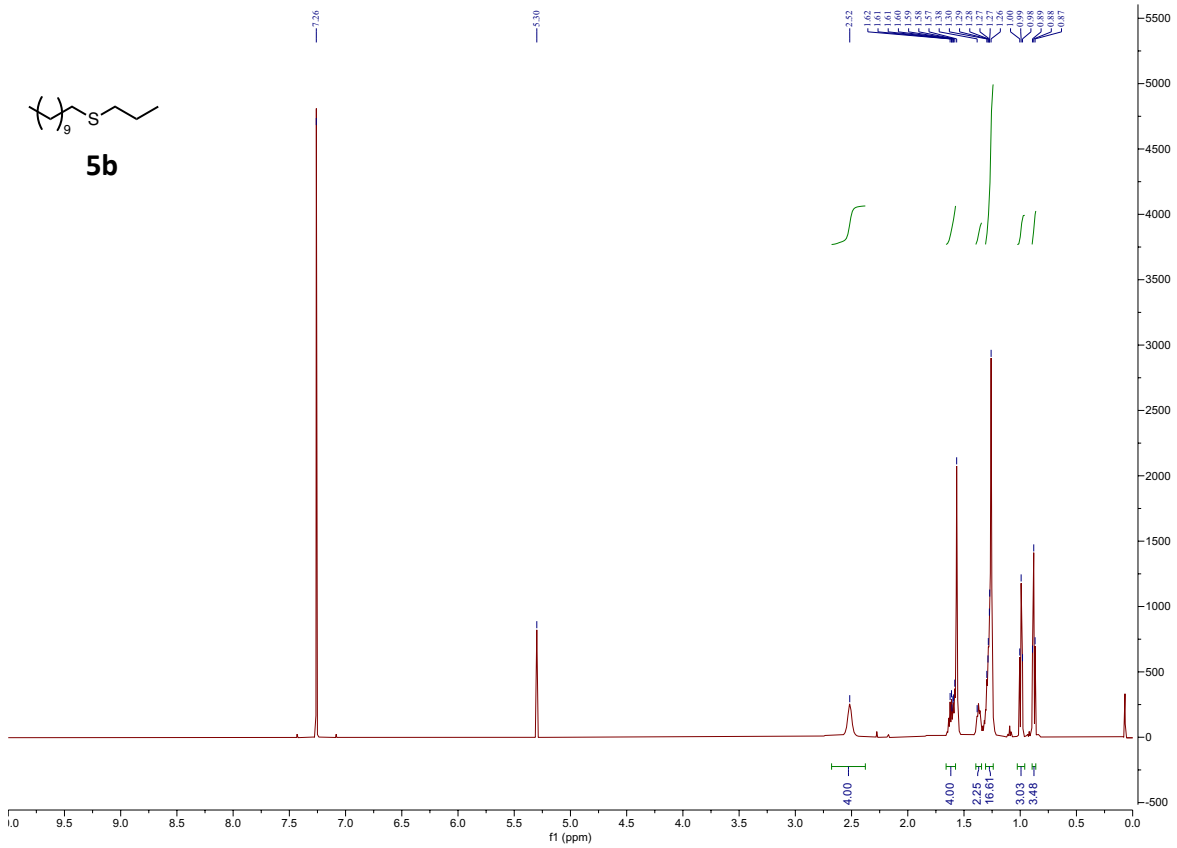
7.26
5.30
2.52
1.62
1.61
1.60
1.59
1.58
1.57
1.56
1.30
1.29
1.28
1.27
1.26
1.00
0.99
0.98
0.89
0.88
0.87
4.00
4.00
2.25
16.61
3.03
3.48
g
S
f1 (ppm)

5b

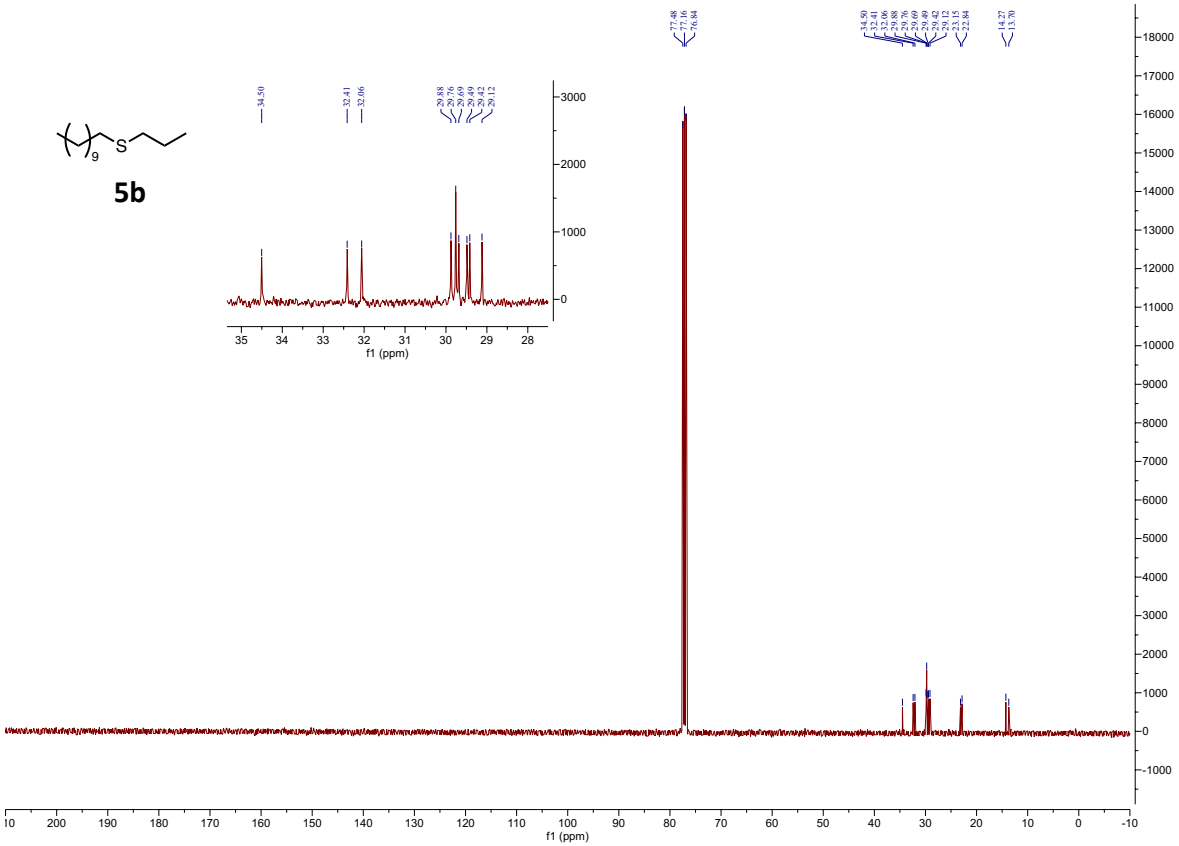
5b
77.48
77.16
76.84
14.50
13.41
13.06
29.88
29.76
29.69
29.49
29.42
29.12
23.15
22.84
14.27
13.70
34.50
32.41
32.06
29.88
29.76
29.69
29.49
29.42
29.12
f1 (ppm)

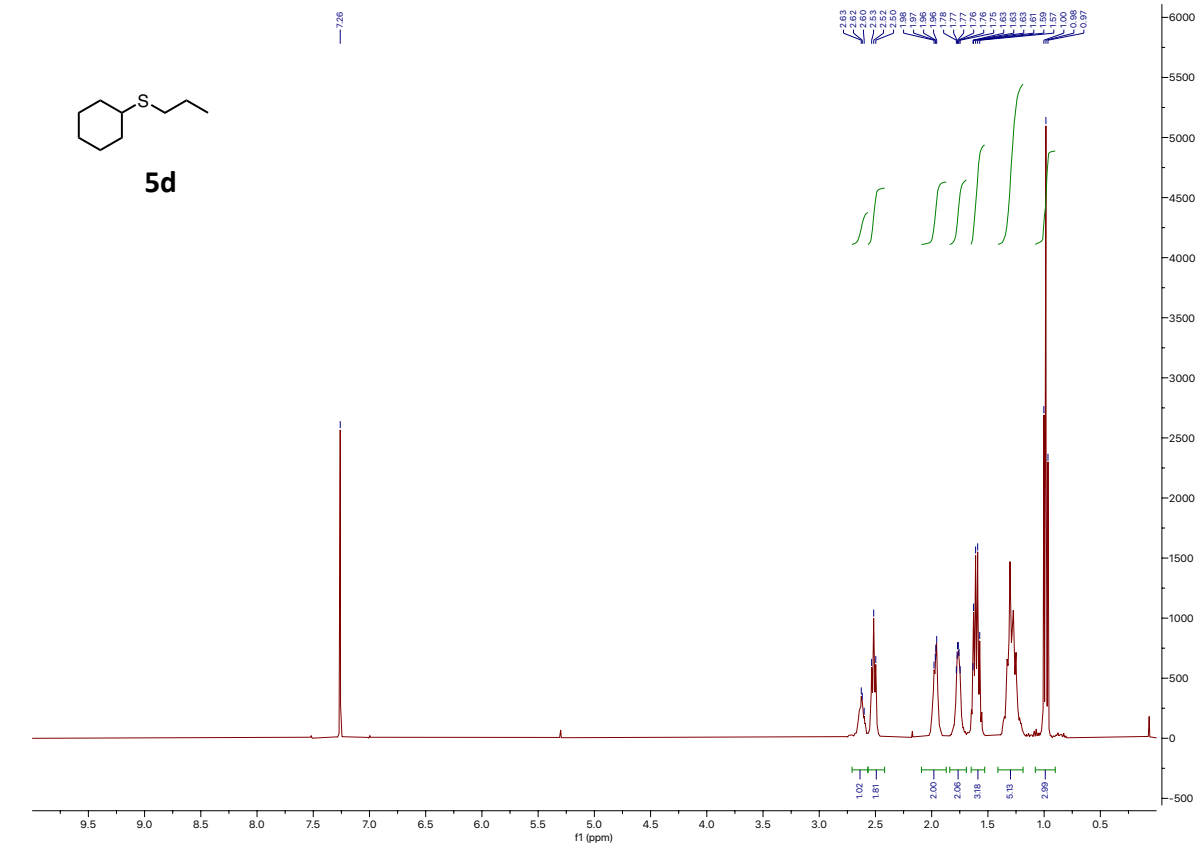
5d
7.26
2.63
2.62
2.60
2.53
2.53
2.50
1.98
1.97
1.96
1.96
1.78
1.77
1.77
1.76
1.75
1.75
1.63
1.63
1.63
1.61
1.59
1.57
1.00
0.98
0.97
1.02
1.81
2.00
2.06
3.18
5.13
2.99
f1 (ppm)

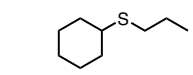

5d

77.48
77.16
76.84
43.69
33.88
32.45
26.31
26.02
23.51
13.80
f1 (ppm)

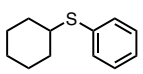

5f

1.84
1.96
0.90
0.96
2.00
2.03
1.11
5.08
f1 (ppm)

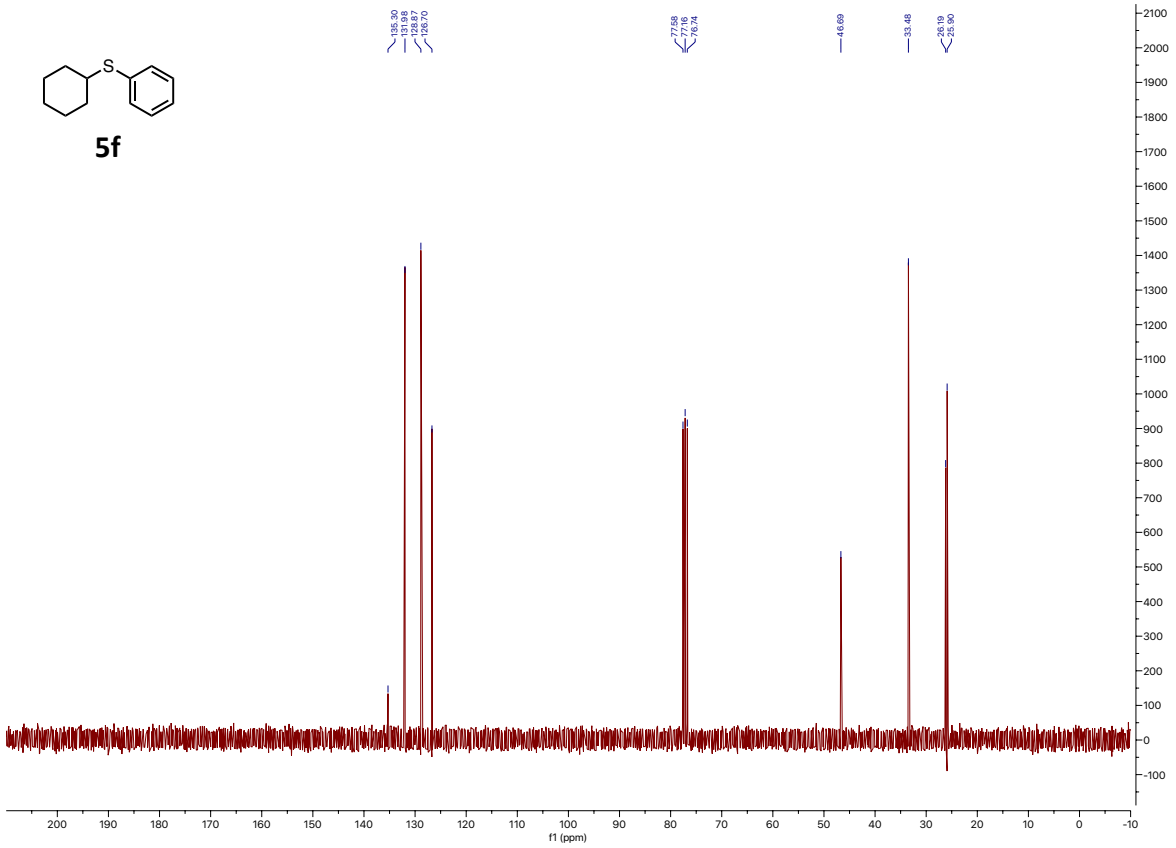
5f
135.30
131.98
128.87
126.70
77.58
77.16
76.74
46.69
33.48
26.19
25.90
f1 (ppm)

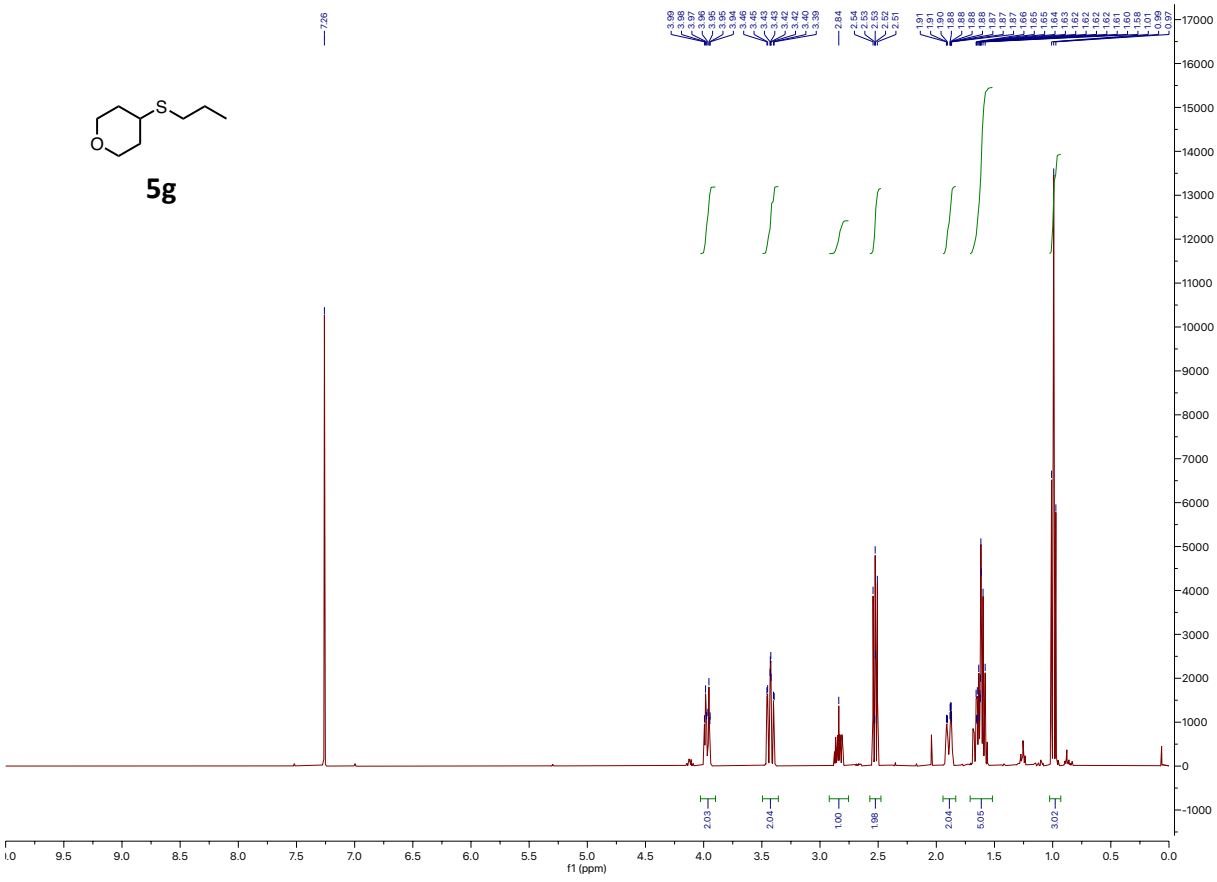
5g
7.26
3.99
3.98
3.97
3.96
3.95
3.95
3.94
3.46
3.45
3.45
3.43
3.42
3.42
3.40
3.39
2.84
2.54
2.53
2.53
2.52
2.51
1.91
1.91
1.90
1.88
1.88
1.88
1.88
1.87
1.87
1.87
1.66
1.65
1.65
1.64
1.63
1.62
1.62
1.62
1.62
1.61
1.61
1.60
1.58
1.01
0.99
0.97
2.03
2.04
1.00
1.98
2.04
5.05
3.02
f1 (ppm)

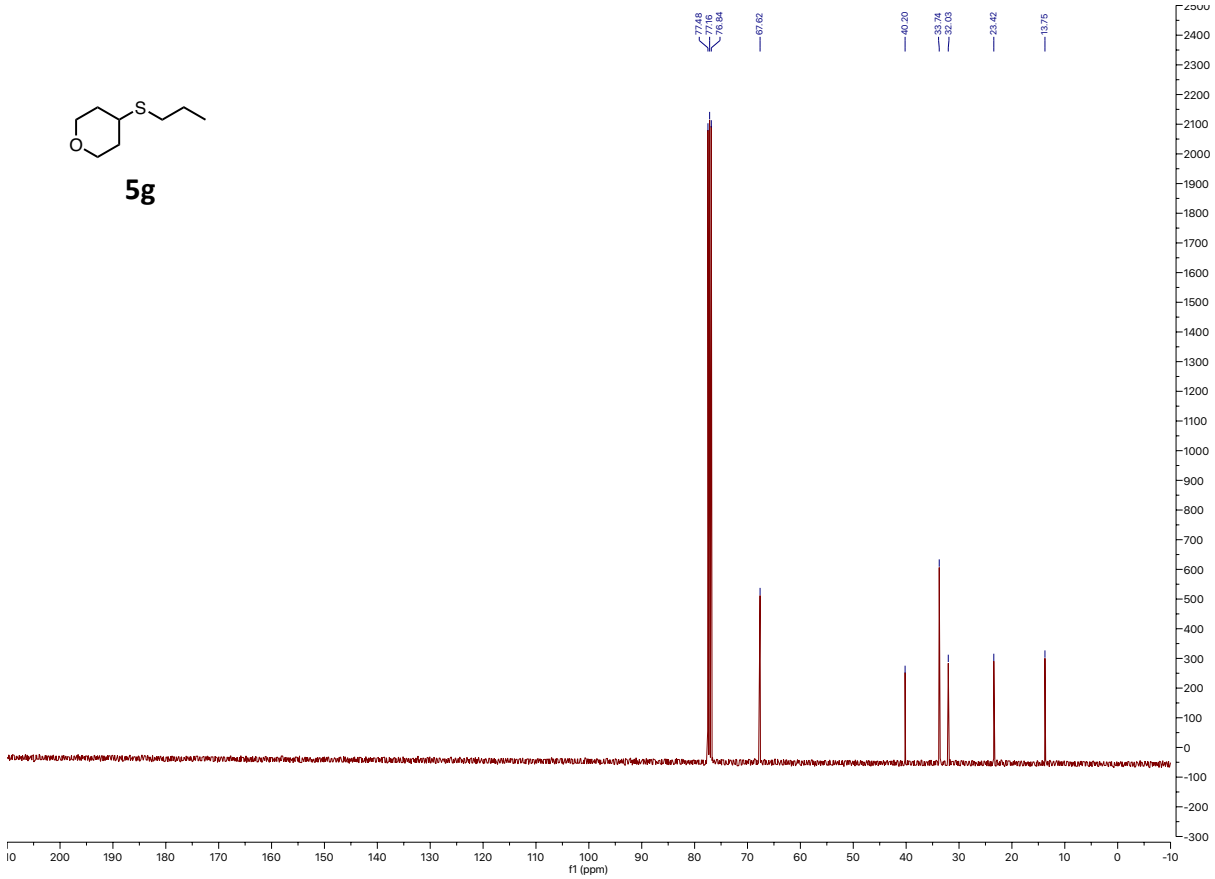
77.48
77.16
76.84
67.62
40.20
33.74
32.03
23.42
13.75
f1 (ppm)

5g

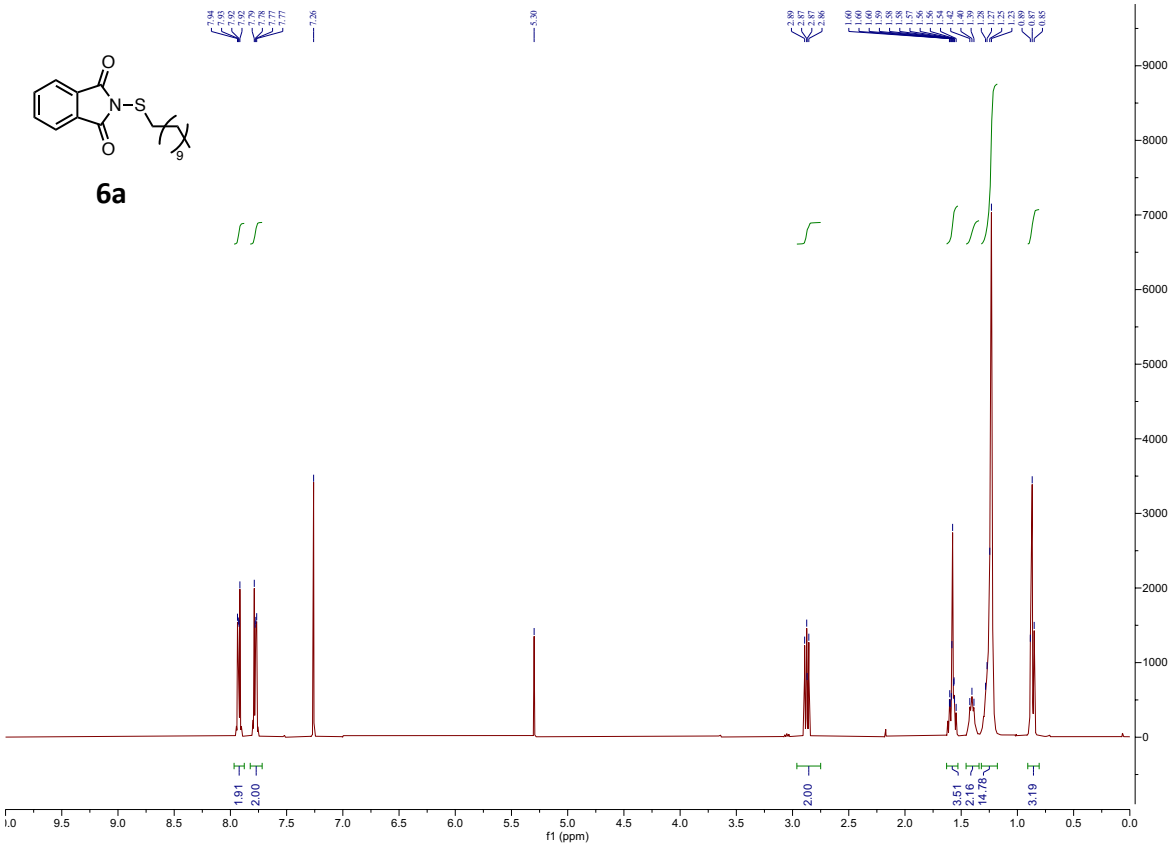
7.94
7.93
7.92
7.92
7.79
7.78
7.77
7.77
7.26
5.30
2.89
2.87
2.87
2.86
1.60
1.60
1.60
1.60
1.59
1.58
1.58
1.57
1.56
1.56
1.54
1.42
1.40
1.39
1.25
1.23
0.88
0.87
0.85
1.91
2.00
2.00
3.51
2.16
14.78
3.19
f1 (ppm)

6a

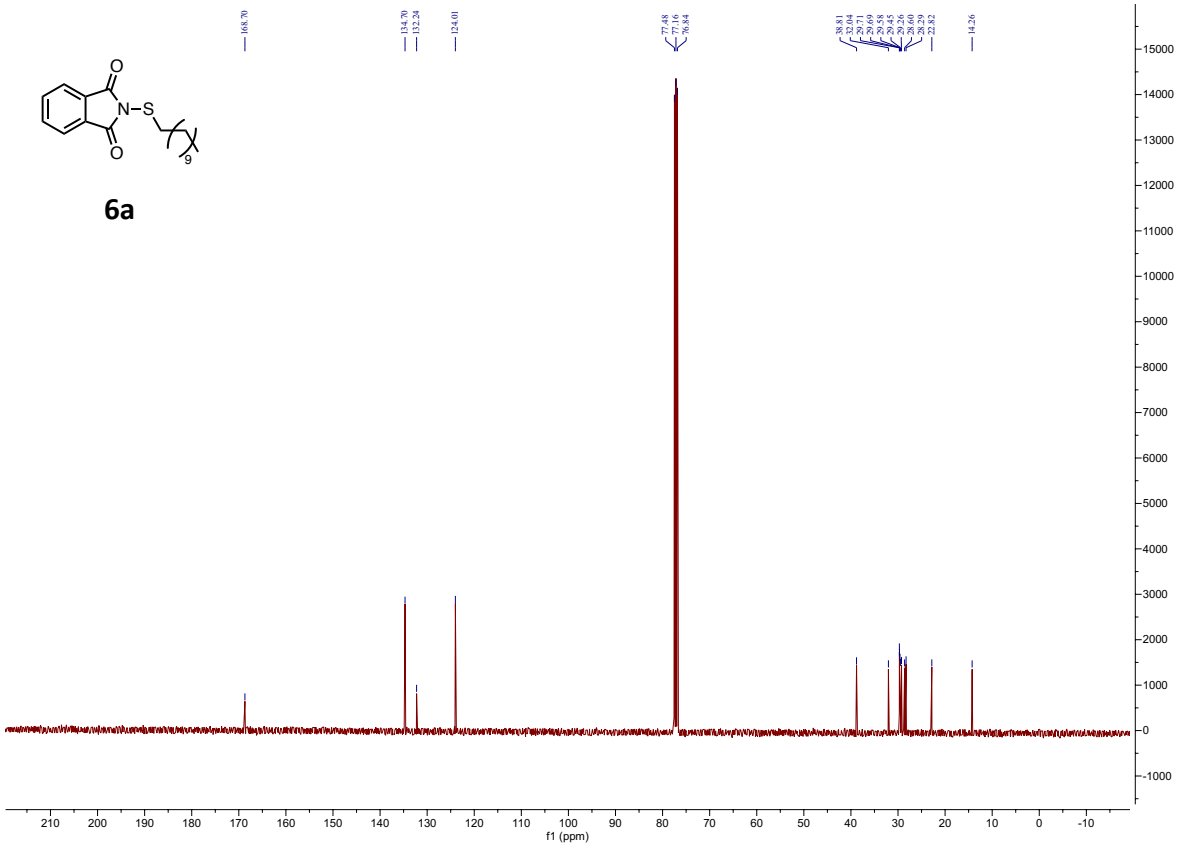
6a
168.70
134.70
132.24
124.01
77.48
77.16
76.84
38.81
32.04
29.71
29.69
29.58
29.45
29.26
29.00
28.29
22.82
14.26
f1 (ppm)

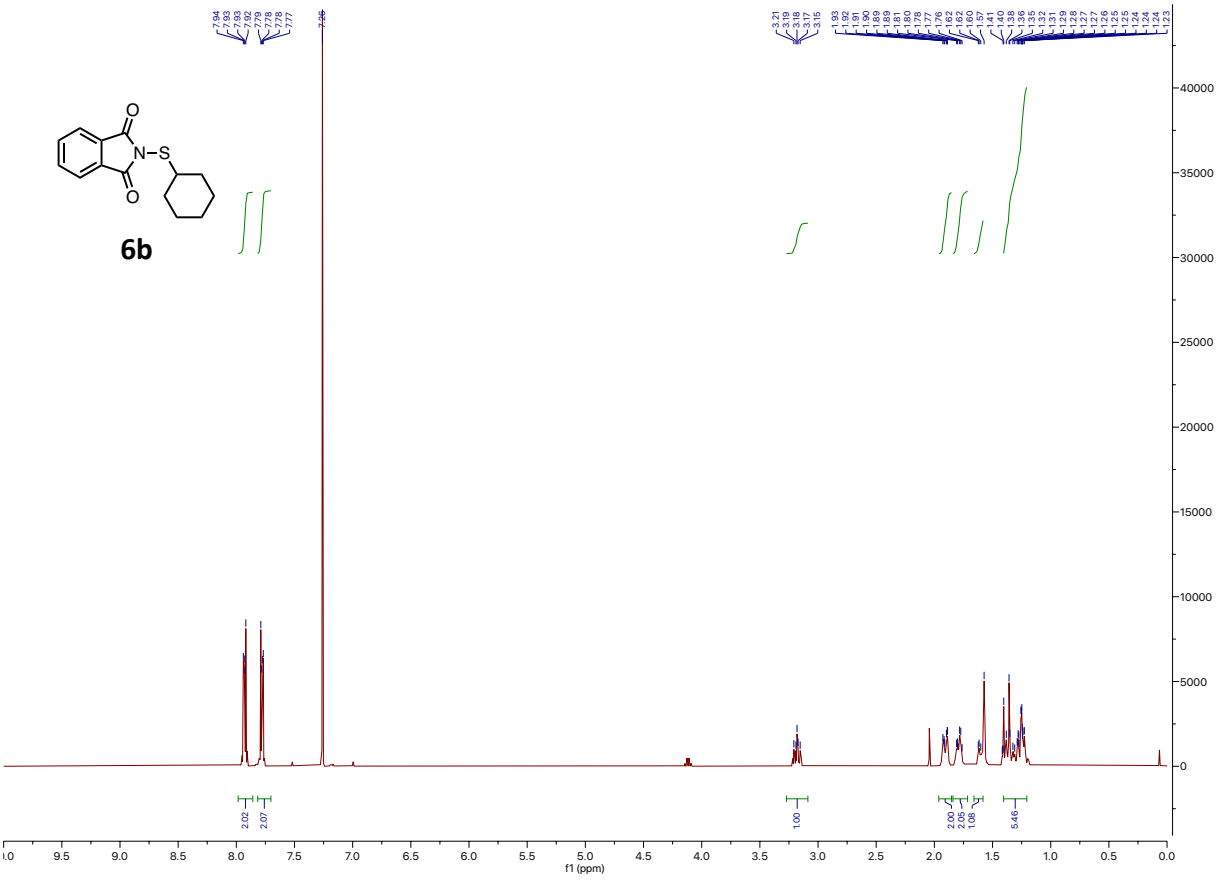
6b
7.94
7.93
7.93
7.92
7.79
7.79
7.78
7.78
7.77
7.26
3.21
3.19
3.18
3.17
3.16
1.93
1.92
1.91
1.90
1.89
1.89
1.88
1.81
1.80
1.78
1.77
1.76
1.62
1.62
1.60
1.57
1.41
1.40
1.38
1.36
1.35
1.32
1.31
1.29
1.28
1.27
1.27
1.26
1.25
1.25
1.24
1.24
1.24
2.02
2.07
1.00
2.00
2.06
1.08
5.46
f1 (ppm)